

SUPERIOR STRUCTURAL DESIGN THROUGH AUTOMATED TOPOLOGY OPTIMIZATION AND ADVANCED MANUFACTURING

By Martin James Muir

University of Leeds

School of Mechanical Engineering

March 2018

Submitted in accordance with the requirements for the degree of Doctor of Philosophy

Intellectual Property and Publication Statement

The right of Martin James Muir to be identified as Author of this work has been asserted by Martin James Muir in accordance with the Copyright, Designs and Patents Act 1988.

This copy has been supplied on the understanding that it is copyright material and that no quotation from the thesis may be published without proper acknowledgement.

The candidate confirms that the work submitted is his/her/their own and that appropriate credit has been given where reference has been made to the work of others.

The work contained within this thesis contains information related to Airbus, its products and its methods which together are regarded as background IP belonging to Airbus. The research developed during this PhD has been supported by Airbus and thus constitutes foreground IP which belongs, at least in part to Airbus and its partners. The developed research should not be publicly disclosed without the express permission of the author and/or Airbus where the two are not the same.

Publications and Conference Proceedings

Civil Aerospace Mass Reduction Through Automated Topology Optimization and Advanced Manufacturing – ASMO UK, Cork, Ireland, July 2012

The Use of MDO and Advanced Manufacturing to Demonstrate Rapid, Agile Construction of a Mission Optimized UAV – 10th AIAA MDO, Boston, USA, April 2013

Airbus PhD Conference Days – Filton, Bristol, England, March 2013

Multidisciplinary Optimisation of Business Jet MED Hinge for Production by Additive Manufacturing – European Altair Technology Conference, Turin, Italy, June 2013

SUPERIOR STRUCTURAL DESIGN THROUGH AUTOMATED TOPOLOGY OPTIMIZATION AND ADVANCED MANUFACTURING - 4th Annual University of Leeds Postgraduate Research Conference, Leeds, England, December 2013 (winner of best research student award)

Rules, Precursors and Parameterization Methodologies for Topology Optimized Structural Designs Realized Through Additive Manufacturing – SciTech 2014, National Harbor, USA, January 2014

Additive Manufacture of Multi-Disciplinary Optimised Aero-Structures and Systems – Altair ATCX, Coventry, England, October 2015

Multi-Disciplinary Optimization and Additive Manufacture of Airbus Main Landing Gear Manifolds – 6th International Workshop on Aircraft System Technologies, Hamburg, Germany, February 2017

Enablement of Next Generation Hybrid Structures through Optimization and Advanced Manufacturing – Altair ATC, Gaydon, England, October 2017.

Acknowledgements

I would very much like to thank the University of Leeds, particularly, professors, Querin, Neville and Morina for their continued support, funding and patience throughout the long duration of this part-time PhD. In addition, I would like to thank Airbus Central Research and Technology for their support and guidance particularly in areas related to design, certification and stress for which I had little initial understanding and for which there is little published material. Without this, the research may not have been as applicable as it eventually became.

In addition to the support from the projects direct sponsors, I would also like to thank Professor Vassili Toropov (Queen Mary University London) and Dr Robert Hewson (Imperial College London) for their advice and guidance regarding the structure and content of the PhD as it approached completion. Their advice has been invaluable in reaching this stage.

Last, but most certainly not least, I would to express my everlasting thanks my wife, Dr Kate Muir, for all her help, understanding and support, particularly in the last year as the research approached completion. Without her understanding, support and sacrifice, I would never have completed the research.

Abstract

Challenging times lie ahead for commercial aerospace, facing regulatory pressure to reduce emissions on one side and the potential of increased competition on the other, a continuation of the business and engineering philosophies which led to such a healthy orderbook in the past, cannot be guaranteed for the future – substantial, disruptive change is required. Additive Manufacturing (AM) and Topology Optimization (TO) are two technologies under investigation by Airbus and others which have promised to deliver such change. Problematically, both are expert level technologies with enormous complexities and thus their application is commonly applied only where justification of such skills for such lengths of time can be considered to be economically viable. However, whilst there are indeed gains to be had in such large, complex structures, their numbers on commercial aircraft are few. Conversely, there are literally thousands of small, heavy, metallic components which would benefit from the application of these technologies if the cost of technology application could be reduced. The aim of this research is to deskill the application of TO and AM by automating the process of TO specific to manufacturing via AM and thus reduce the cost of its implementation and increase the practicality of its application. Through a survey of the Airbus user community, a standardised series of tools, inputs, outputs and process was developed, culminating in an analysis of time consumed during a series of optimization tasks. From this list of tasks and the time lost to each, a series of targets for automation were identified and researched. Using a series of interconnected codes and scripts, pre-processing phases such as design space creation, meshing and loading application were automated and applied to a common FEM template. Within this template, generic material and geometric capability figures for AM Ti64 Grade 5 were established via bespoke testing on a range of AM platforms under common parameters and builds. After this, methods for automated design extraction back to parametric CAD were investigated and performed, establishing a direct link between the FEM and the output CAD to enable rapid design development. The combined series of automation steps leads to an almost 75% reduction in total non-recurring cost for optimization and design of small components. Whilst not, as yet, wholly industrialised and implemented within Airbus, research from the early phases is now in use for MDO tools within Airbus and Airbus Group.

Table of Contents

1	Introduction: Commercial Aerospace Design – Past, Present and Future.....	1
1.1	Challenges Facing Commercial Aerospace Manufacturers.....	1
1.2	Industrial Context of Research.....	1
1.3	Research Aim	3
1.4	Key Research Objectives	3
1.5	Secondary Research Objectives	4
1.6	Principal Research Challenges.....	4
1.7	Projected Impact of Undertaken Research.....	5
1.8	Challenges of Research in an Industrial Environment	6
1.9	Thesis Layout.....	7
1.9.1	Chapter 2 – Literature Review	7
1.9.2	Chapter 3 – Understanding the Current Process	7
1.9.3	Chapter 4 – Automation of Pre-processing.....	8
1.9.4	Chapter 5 – The Mapped Manual Process.....	8
1.9.5	Chapter 6 – Automation of Post Processing	8
1.9.6	Chapter 7 – General Results, Discussion, Conclusions and Future work.....	8
1.9.7	Chapter 8 – Discussion, Conclusions, Future Works and Concluding Remarks	8
2	Literature Review.....	9
2.1	Civil Aerospace Design and Manufacturing	9
2.1.1	Fundamental Aspects of Commercial Aerospace Design.....	9
2.1.2	Conventional Methods of Civil Aerospace Component Manufacturing.....	14
2.1.3	Advanced Manufacturing Techniques	19
2.1.4	Additive Manufacturing and its use in Commercial Aerospace.....	21
2.1.5	Design for Additive Manufacturing.....	50
2.2	Optimization and its use in Commercial Aerospace and Component Design	56
2.2.1	History, Principles and Design Optimization.....	56
2.2.2	Approaches to Design Optimization	59
2.2.3	Applications of Design Optimization in Airbus.....	61
2.2.4	Design Optimization vs. Structural Optimization.....	64
2.3	Structural Optimization.....	65
2.3.1	Fundamentals of Structural Optimization.....	66
2.3.2	The Finite Element Method and its use in Structural Optimization	67
2.3.3	The Finite Element Method and its use in Structural Optimization	70
2.4	Topology Optimization – An Introduction	72

2.4.1	Topology Optimization – Methods and Comparisons	73
2.4.2	Implementation of Topology Optimization.....	76
2.4.3	Use and Applications of Topology Optimization in Aerospace.....	77
2.4.4	Limitations of Topology Optimization for Design and Development.....	79
2.4.5	Manufacturability of Topology Optimised Structural Designs.....	79
2.4.6	Additive Manufacturing and Topology Optimization.....	79
2.4.7	Combinatory Benefits of Technology Pairing.....	79
2.4.8	Optimization Driven Design for Enhanced Concept Generation	81
2.4.9	Material Problems Arising from the Combination of Topology Optimization and Additive Manufacturing	84
2.5	Reducing the Cost of Complex Design	85
2.5.1	Conceptual Design vs. Detail Design	86
2.5.2	Difficulties in Extracting Complex Designs from Topology Optimised Results	87
2.5.3	Available Methods for Design Extraction.....	90
2.5.4	Difficulties of Safety and Certification for Complex Designs	95
2.5.5	The Total Design Cycle and its Non-Recurring Cost	97
2.6	Processes Automation as a Means of Cost Reduction.....	98
2.6.1	Fundamentals of Process Automation	101
2.6.2	Historical Use of Automation in Design Optimization	102
2.6.3	Automated Structural Optimization – Methods and Limitations	103
2.6.4	Automation of Structural Topology Optimization and Design Extraction	104
2.7	Summary of the State of the Art	105
3	The Automation of Structural Topology Optimization and its Recreation into Parametric Design Data	107
3.1	Research Motivation and Context – Why is the Research Project Required.....	107
3.2	Baseline Establishment – What is the Current Process for the use of Structural Optimization in Airbus	108
3.2.1	Current TO Process Applications within Airbus	108
3.2.2	Primary Work Breakdown Structure for Airbus TO Processes.....	109
3.2.3	Evaluation of Baseline Topology Optimization Process	110
3.2.4	Standardization of Tools and Processes.....	117
3.3	Targets for Automation – Application and Survey of Optimization as Applied to the Candidate Parts	118
3.3.1	Experimental Methodology for the Survey of Topology User in Airbus	119
3.4	Results of Baseline Optimization Trials.....	121
3.4.1	Results - Performance vs. Cost of Design.....	121
3.4.2	Results - Time Required for Process Phases	122

3.4.3	Engineer Satisfaction/Value Add of Each Optimization Task.....	122
3.5	Identification of Primary Targets for Automation of the Design Process.....	125
3.6	Summary of Automation Targets.....	126
4	The Development and Application of Robust Material Data into the Pre-Process Automation Phases	127
4.1	Automation of Pre-Process Parameterization Phases	127
4.1.1	Feature Recognition – Introduction.....	127
4.1.2	Feature Recognition – State of the Art.....	128
4.1.3	Methodology for Automation of CAD Feature-Recognition	129
4.1.4	Results of Automated Feature Recognition.....	130
4.1.5	De-featuring - Introduction,.....	130
4.1.6	De-Featuring – State of the Art.....	130
4.1.7	Results of Defeaturing Trials	132
4.1.8	Automation of De-Featuring in Preparation for Meshing.....	133
4.1.9	Results of Automated Defeaturing	135
4.1.10	Conclusions for Pre-Process Automation of Recognition and Defeaturing	135
4.2	Domain Separation into Design and Non-Design Space – Introduction	135
4.2.1	Methods for the Separation of the Structural Domain.....	136
4.2.2	Methodology for the Separation of the Structural Domain	137
4.3	Automated Loading Perturbation for Simple Load Case Topology Optimization.....	137
4.4	Conclusion of Robust Design Methods.....	139
4.5	The Application of Constant Mesh Density Topology Optimization.....	140
4.5.1	Methodology for the Implementation of Mesh Refinement.....	141
4.5.2	Results of Constant Mesh Refinement.....	141
4.5.3	Conclusions of Mesh Refinement	141
4.6	Determination Optimization Constraints in Relation to Mechanical Performance and Geometric Capability Data for Powder Bed Additive Manufacturing.....	142
4.6.1	Material: Additive Manufacturing and the Effects of Orientation upon Material Properties.....	143
4.6.2	Determining the Effects of Build Orientation on Material Properties.....	143
4.6.3	Test Methodology for Determining the Effects of Orientation on Mechanical Performance.....	144
4.6.4	Manufacture and Test of Mechanical Specimens.....	145
4.6.5	Results of Mechanical Testing.....	146
4.6.6	Conclusion of Mechanical Performance Trials:.....	149
4.7	Definition of the Processing Limits of AM Platforms.....	149
4.7.1	Conclusions of Design Constraints	150

4.7.2	Manufacture and Economics: The Constraints of Layer-wise Production and their Inclusion within the Templates.....	151
4.8	Summary of the Automation of the Pre-processing Phase.....	153
5	Development of the Mapped Manual Process for Airbus and the Effects of Automation on its Implementation.....	154
5.1	Introduction to the Mapped Manual Process.....	154
5.2	Methodology for the Development of the Mapped Manual Process	156
5.2.1	Requirements Capture	157
5.2.2	Analysis Pre-process Parameterization Phase	159
5.2.3	Optimization Problem Formulation	161
5.2.4	Interrogation and Initial Extraction of Concept Design	163
5.2.5	Design Extraction Methodology.....	164
5.3	The Mapped Manual Process for the Application of Topology Optimization	165
5.4	Methodology for Testing the Effectiveness of the Mapped Manual Process.....	168
5.5	Results of Using the Mapped Manual Process.....	168
5.6	Conclusions of the use of the Mapped Manual Process.....	170
5.7	Application of Automation to Mapped Manual Process	170
5.7.1	Feature Recognition and CAD Parameterization Automation in the Mapped Manual Process.....	171
5.7.2	CAD De-Featuring in Preparation for Meshing	171
5.7.3	Grid Generation for Analysis and Optimization	172
5.7.4	Load Application and Perturbation.....	173
5.7.5	Summary of Automation for the Mapped Manual Process.....	173
5.8	Methodology for Testing of the Semi-Automated Mapped Manual Process.....	173
5.9	Results of Automation Implementation	174
5.10	Summary of The Effects of the Combined Automated Processes on the Time Required for Topology Optimization	176
6	Automation of Parametric Design Extraction	178
6.1	Introduction to Design Extraction.....	178
6.2	Establishment of Baseline Inputs and Benchmarks	180
6.2.1	Baseline Results for Design Extraction.....	183
6.3	Early and Abandoned Methods of Design Extraction Automation . Error! Bookmark not defined.	
6.3.1	Direct Smoothing/Modification of the STL Output from Topology Optimization	184
6.3.2	Skeletal Modelling Approach - Introduction.....	193
6.4	Problems with Investigated Methods for Design Extraction	207

6.5	Problem Formulation for New Extraction Method	209
6.6	Parametric Linking of the CAD to the FEM	211
6.6.1	Creation of Key Parametric CAD based on Recognised Commonality between the Input CAD and the TO Results	211
6.6.2	Automation of Common Reconstruction Features - Planes, Control Points and Curve Reconstruction	212
6.6.3	Automated Surface Generation and Intersection Computation	220
6.7	Results of Design Extraction Methodology on the 5 Candidate Parts	225
6.8	Discussion of the Design Extraction Results	227
6.9	Summary of Automated Design Extraction	229
7	The Effects of Full Automation Implementation into the Design Process	230
7.1	Introduction	230
7.2	Methodology for Establishing Baseline Costing for Conventional and Optimization Driven Design in Airbus	230
7.3	Results – The cost of Design and Manufacturing without Automation	231
7.4	Discussion of Conventional Design Costs	232
7.5	Does Automation Reduce the Cost of Optimization Driven Design?	232
7.6	Methodology for Testing if Design Automation Reduces Component Cost	232
7.7	Results of Automated Design Processes	235
7.8	General Discussion	236
7.8.1	Introduction and Overview of Results	236
8	Discussion, Conclusions and Future Work	238
8.1	Technical Accomplishments	238
8.1.1	Introduction and Integration	238
8.1.2	Identification of Primary Targets for Optimization	238
8.1.3	Airbus Specific Feature Recognition and Design Space Separation	238
8.1.4	Forces Splitter and Loading Perturbation	239
8.1.5	Hyperworks Optimization Template	239
8.1.6	The Mapped Manual Process	239
8.1.7	Automated FEA Linked Parametric CAD Extraction Methods	239
8.1.8	Skinned Point Cloud Methodology	240
8.1.9	Material and Geometric capabilities for AM platforms	240
8.2	Conclusions – Research Strengths and Limitations	240
8.2.1	Cost implications for Automation	240
8.2.2	Robustness and Variation	241
8.2.3	Structure Types	241

8.2.4	Software Limitations	242
8.2.5	Automated Meshing	243
8.2.6	Material and Production Data for Hyperworks Template	243
8.2.7	Expert Level Process.....	244
8.3	Impact - Applicability and Use	244
8.3.1	Direct use on Aerospace Componentry	244
8.3.2	Use in on-going and Future Research	244
8.3.3	Indirect use in Training and Development.....	245
8.4	Future work.....	245
8.4.1	Constant Mesh Density Topology Iteration	246
8.4.2	Integration of Toolsets.....	246
8.4.3	Skinned Point Cloud Surface Reconstruction.....	247
8.4.4	Multi-Disciplinary Optimization Research	247
8.5	Concluding Statement.....	247
9	References.....	249
10	Appendices.....	263
10.1	Appendix A – Background Material	263
10.1.1	Additive Manufacturing Standards	263
10.2	Appendix B – Design Work.....	263
10.2.1	T-spline Modelling Trials	263
10.2.2	STR1 Design Extraction.....	264
10.2.3	STR2 Design Extraction.....	265
10.2.4	STR3 Design Extraction.....	266
10.2.5	STR4 Design Extraction.....	267
10.2.6	STR5 Design Extraction.....	268
10.2.7	Geometric Sample Build Setup	269
10.3	Appendix C – Coding and Scripting	270
10.3.1	Feature Recognition and Domain Segregation Script.....	270
10.3.2	Thickness Calculation Script.....	274
10.3.3	Design Extraction Script	277
10.4	Appendix D – Calculations.....	290
10.4.1	Aircraft Small Part Numbers	290
10.4.2	Forces Perturbation Calculations	290
10.4.3	Additional Material Data from Concept Laser	291

List of Figures

Figure 1 - Safety criticality table for Airbus Structure.....	12
Figure 2 - Near-net shape forging (top) and the machined part extracted from the forging (bottom).....	17
Figure 3 – Showing incredible design complexity of a Ferrari Engine block casting after machining and assembly.....	17
Figure 4 - Complex machining of A380 Rib from billet material at GKN.....	19
Figure 5 - A coarse representation of a 3D CAD part sliced into 2D planar profiles.....	22
Figure 6 - EBM deposited AM parts showing introductory support structures (left and right) and build errors (top right)	27
Figure 7 - Distortion of a component due to residual stress	31
Figure 8 - Similar component stress, relieved on its own build plate and tooling - now almost completely flat	32
Figure 9 - Irepa Laser test wall from AMAZE showing residual stress fracture due to part length	35
Figure 10 - Airbus Demonstrator component made by Norsk Titanium	39
Figure 11 - Cracks in as deposited samples (InSiGen Project) which occurred after build completion.	40
Figure 12 - AM Manufacturing flow process showing the digital (top) material (middle) and platform (bottom) process stages.....	44
Figure 13 - Uniform micro-lattice by PBF AM	49
Figure 14 - HYPER pins embedded into CFRP leading edge wing skins	50
Figure 15 - Showing the effects of altering orientation on both build economics (numbers on the plate) and scan area (red lines).....	51
Figure 16 - Overheating of the deposit caused by a combination of inadequate thermal dissipation and fast scan and recoating strategies	52
Figure 17 - Analysis of existing part (left) expansion of design space with consideration of manufacturing and assembly (centre) and allocation of non-design areas (right)	54
Figure 18-A350 Outboard wing rib complex design	55
Figure 19 - Showing the different branches of optimization and the pathways to their application.....	62
Figure 20 - A400M Bulkhead Seals - Original (right) and design for AM (left).....	63
Figure 21 - Safety Collar for MRO - Design optimization for cost and AM – red arrow indicates flow of design from left to right.....	64
Figure 22 - A380 DN ribs : design and manufacture (Krog et al, 2002)	65
Figure 23- Brunel's suspension bridge in Clifton, Bristol	66
Figure 24 – Aircraft rib development in-line with loading and performance requirements and the development of better analytical techniques	67
Figure 25 - A 2x2x2 cube showing a tetrahedral volume mesh with an element size of 1	68
Figure 26 - Showing the effect of variable mesh density and higher order functions to represent geometry.....	69
Figure 27 - An example of sizing optimization (Bendsoe and Sigmund, 2003).....	71
Figure 28 - An example of shape optimization (Bendsoe and Sigmund, 2003).....	71
Figure 29 - An example of topology optimization (Bendsoe and Sigmund, 2003)	72

Figure 30 - VTS when compared to SIMP and two scale lattice.....	75
Figure 31 - The effects of mesh refinement and STO on the quality of the resulting design output with a low density mesh shown on the left and a high density mesh on the right.	76
Figure 32 - Parameterized design space for Airbus A350 rear fuselage	78
Figure 33 - EADS A320 hinge - Optimised using compliance based STO	78
Figure 34 - Unconstrained TO applied to an aerospace bracket - note the poor seating of the bolts - image courtesy of Nottingham university at the Farnborough Airshow in 2012	80
Figure 35 - showing the resulting optimised design (white) from an original design space (green) and the erosion of the original surface topology.....	88
Figure 36 - Extracted design showing misalignment of triangle surface normals in close proximity to one another	88
Figure 37 - Showing substantially greater detail revealed through use of a high definition FE mesh.....	89
Figure 38 - Typical notch impact damage and the subsequent creation of a fatigue initiator.....	96
Figure 39 - Fully Stressed Design through optimization and AM.....	97
Figure 40 - Typical process for the design and manufacture of an Airbus designed, supplier manufactured part	99
Figure 41 - Analysis driven design cycle without complex supplier engagement shown in Figure 40	100
Figure 42 - Coarse work breakdown structure for concept design using Dassault 3D-Experience Software in Airbus.....	109
Figure 43 - Conventional approach to the redesign of components using an analysis inspired design approach.....	110
Figure 44 - Full WBS for the manual TO Process within Airbus Group	112
Figure 45 - Software selections for future progression within the project	116
Figure 46 - Percentage mass reduction vs time required (hours) for each of the user on the five candidate parts.	121
Figure 47 - Chart showing the time required for each task within the optimization cycle as a percentage of the whole task	122
Figure 48 - Perceived satisfaction/value add time as a percentage of the whole task undertaken	123
Figure 49 - features recognized by commercial codes in preparation for CNC machining	129
Figure 50 – The results of adapted CATIA FR for bolts and radii – note the removed fillets and highlighted bolts in without the centre pressure channels being selected (right).....	130
Figure 51 - an example of fillet removal from within Hyperworks.....	131
Figure 52 - Figure showing the effects of de-featuring on complex geometry through the removal and adaptation of proximate geometric features and their removal (dashed lines) from the mesh seeding process.....	132
Figure 53 - Effects of line suppression on mesh size: without line suppression (middle) the mesh is ~1m elements, with line suppression, the mesh reduces in size to ~0.3m elements.....	133
Figure 54 - Wall thickness analysis from Materialise Magics showing some areas of almost negligible thickness (red) due to problems with the triangle mesh normal.....	133
Figure 55 - the selectable and modifiable elements of the feature suppression aspect of Hyperworks.	135
Figure 56 - The effectiveness of the implemented de-featuring on mesh sizing and quality	135

Figure 57 - Showing the automated design space progression after feature recognition	137
Figure 58 - Single loadcase optimization of STR1 on a high definition mesh using an expanded design space.....	138
Figure 59 – Depiction of perturbed single loadcase optimization of STR1 using an expanded design space.....	139
Figure 60 - Topology change when applying perturbed loadcase application to STR1.....	140
Figure 61 - STR2 optimised using an iterative mesh refinement technique - note the detail revealed in optimisation	142
Figure 62 - demonstrates the effects of orientation alteration on multiple optimized versions of STR3. On the left, scan areas are minimised, but build height is increased (400 layers vs. 135). By assuming a vertical orientation more parts can be built at once, thus offsetting build cost against a higher number of parts.....	143
Figure 63 - Build setup #1 showing fatigue crack growth and tensile specimens in multiple orientations and chamber locations	145
Figure 64 - Build setup #2 showing axial fatigue specimens in multiple locations and orientations	145
Figure 65 – Example of geometric sample builds designed to test minimal features on a range of different platforms.....	150
Figure 66 - Aspects of additive manufacturing which are affected by changes in orientation ..	151
Figure 67 - Opticontrol modification script and its effects.....	153
Figure 68 - Flowprocess for design optimization showing major areas and their sub-processes	155
Figure 69 – Automated recognition and separation of NDS (left) followed by uniform meshing of NDS (centre) and application of rigid elements (RBE3) for loading transfer (right).....	161
Figure 70 - Typical results from a Mass Objective optimization problem (left) vs Compliance (right).	162
Figure 71 - Graph showing the total time required to reach optimal mass fraction using conventional methods and duo approach.....	163
Figure 72 - Variation in topology through modification of density parameters – 40%+ density shown in blue (left) and 70%+ density shown in orange (right).	164
Figure 73 - Flow process for the MMP.....	167
Figure 74 - Results of using the MMP when compared to the original approach.....	168
Figure 75 - Comparison of the variation between operators before and after implementation of the MMP	169
Figure 76 - Showing the before (left) and after (right) depiction of the automated defeaturing process on STR3.	172
Figure 77 - Proposed design process after MMP and automation	175
Figure 78 - Effectiveness of the partially automated Mapped Manual Process at reducing the required time for design optimization.....	176
Figure 79 - Current Design Process in Airbus showing manual tasks (blue) validation phases (purple) input documents (green)	179
Figure 80 - New design process for AM concept generation showing how design space creation, parameterization and concept generation are now performed in a single software environment.	180
Figure 81 - Baseline topology output for extractions trials	181

Figure 82 - Direct STL Output from the Optistruct via Hyperview.....	181
Figure 83 - STL output from Optistruct after completion of OSSmooth at fine limits.....	182
Figure 84 - design extraction from CATIA using advanced surfacing techniques.....	182
Figure 85 - Validation of final design showing a reserve factor >1.5.....	183
Figure 86 - Comparison of a well-defined optimization result (left) to a poorly defined one (right)	186
Figure 87 - A coarse grid definition has revealed a highly tessellated structure.....	187
Figure 88 - Baseline topology output using the unperturbed result of STR1 at moderate mesh density.....	185
Figure 89 - Non-design space of STR1 indicating feature which must be preserved intact and in conformance with the Airbus Design Rules.....	187
Figure 90 - Results of best practice methods for mesh smoothing of STR2 within Geomagics.	188
Figure 91 - Showing the significant loss of detail through use of aggressive smoothing techniques and poor application.	189
Figure 92 - Showing the effects of Magics local smoothing with combined feature preservation at bespoke settings	190
Figure 93 - Showing damage to converging areas during STL repair/smoothing.to size topology directly off the resul.....	191
Figure 94 - 2D Optimization problem with representative skeletal approach.	193
Figure 95 – Optimised and sliced 2D representation of STR 2 with vector plots based upon slice zone averaged centroid locations.....	194
Figure 96 - Confusing pattern of vector intersections in areas of complex geometry even after boundary trimming	195
Figure 97 - Showing the offset line profiles designed to impart thickness to the trusses resulting from the optimization.....	196
Figure 98 - Output of STR2 showing complex geometry and shape of irregular truss members	197
Figure 99 - TO output of STR3 showing truss style connections in some locations	198
Figure 100 - Differences in centroid location determination based upon two different slice directions	199
Figure 101 - Advanced surfacing extracted design of STR1.....	200
Figure 102 - Sliced STL of STR 1 Design Extraction showing individual areas within the slice....	200
Figure 103 - Showing the sliced profile of STR1 along with the extracted extremum points of one contour and their axial (along X or y axis) measurements	201
Figure 104 - Showing the computed centroid locations and the spline curves created through them and their previous slice profile centroid locations	201
Figure 105 - Surface reconstruction using sliced FEM for profile sizing and centroid locations - note the bump/discontinuity in the structure due to the tessellated attributes of the underlying FEM TO.....	202
Figure 106 - Modified spine for control of discontinuities within the structure	203
Figure 107 - Computed spline curve for surface reconstruction	204
Figure 108 - Full Surface reconstruction using parametric CATIA functions fed by interrogation of the STL.....	204
Figure 109 - Presence of non-cylindrical cross sections in the output from the slicer from the optimisation of STR2	206

Figure 110 - Stress hotspots in the extracted design after local smoothing whilst attempting to maintain Non-modifiable design features.	208
Figure 111 - Detailed extraction process showing common steps in design extraction and those which're unique to the design being extracted.	210
Figure 112 - Point clusters where DS and NDS meet as identified by scripting.....	213
Figure 113 - Intermediate slice plane (orange) and contours (black) for use in spline drafting	215
Figure 114 - STR1 and STR3 at the end of automated transfer of DS (top) and creation of parametric construction geometry (bottom)	215
Figure 115 - Manually demonstrated next steps for design extraction on STR 1.....	216
Figure 116 - Showing the effects of kinematic factors included as NDS (tool access – orange) on the load paths (Black) of TO results (Green).....	216
Figure 117 – Showing changes in spline curves (left original, right new) as a result of additional mapped sections and planes at centre profiles (orange)	218
Figure 118 – Imported IGES slice/line data (black contours) for CATIA based upon slicing and analysis.....	220
Figure 119 - Failure of manual sweep operations due to complex curvature (Red)	222
Figure 120 - Effects of multiplane slicing of STR2	223
Figure 121 - Results of the skinned point cloud method of surface reconstruction method using CATIA QSR on STR3 the creation of the new surface (blue) can be seen to almost perfectly overlap the output topology.....	224
Figure 122 - STR1 TO output (left) and Design extraction enabled by research (right).....	225
Figure 123 - STR2 TO output (left) and Design extraction (penalised for AM) (right)	225
Figure 124 – STR3 TO output (left) and Design extraction without intersection (right)	226
Figure 125 – STR4 TO output (left) and Design extraction without intersection (right)	226
Figure 126 – STR5 TO output (left) and Design extraction without intersection (right)	226
Figure 127 - Final flow-process showing the semi-automated approach to topology optimized design.	234

List of Tables

Table 1 - Comparison of costs/Kg and predicted B2F ratios for typical titanium components.....	15
Table 2 - Table of General Additive Manufacturing Terminology.....	23
Table 3 - Comparison of material cost and availability (assuming stock availability.....	35
Table 4 - showing the down-selected list of candidate parts for use during the investigations	113
Table 5 - List of toolsets for primary phases of optimization process	114
Table 6 - Excerpt from the results of the software selection trials for pre, solve and post-processing. Blue shows highest capability, green shows the selected software.....	115
Table 7 - Results of CAD export>Import trials between CATIA and Hyperworks	117
Table 8 - Version control for all software used during the PhD.....	117
Table 9 - Survey template for optimization responses	120
Table 10 - cross compared rankings for time required vs. task satisfaction (value add) - Higher is worst in both columns	123
Table 11 - Time reduction through the use of partial automation in the defeaturing phase	135
Table 12 - Table showing processing capabilities of each platform under investigation	146
Table 13 – Showing the results of tensile testing with outliers (more than 2 SD from the mean) noted in red and lowest values in green.....	148
Table 14 – Summary of material results showing derived design variables for Ti64 produced using Powder Bed Fusion AM	149
Table 15 - Tabulated features showing design allowables attained from geometric testing.....	150
Table 16 - Showing the average mass reduction and stress value for each structure optimized manually and using the MMP	169
Table 17 – Results of Design Extraction in respect of time taken to complete the task vs manual methods for each structure	227
Table 18 - Breakdown of time required for the design, assessment and validation of ST1 and STR3 using manual methods and the most skilled CAD operators.....	231
Table 19 - Showing the costing of each process using equations and base input costs found in Appendix D - Calculations	231
Table 20 - Final calculated costs and times of each of the 3 processes when tasked with optimization and design of STR1 and STR3 and showing the dramatic reduction in NRC stemming from optimisation and design.....	235

List of Acronyms

ADR	Airbus Design Rules
AiMS	Airbus Material Specification
AiPS	Airbus Process Specification
ALM	Additive Layer Manufacturing
AM	Additive Manufacturing
ASD	Advanced Surfacing Design
ASO	Automated Structural Optimization
ATO	Automated Topology Optimization
B2F	Buy-2-Fly
BHS	Bulkhead Seals
BP	Blown Powder
CAD	Computer Aided Design
CAE	Computer-Aided Engineering
CSG	Constructive Solid Geometry
DED	Directed Energy Deposition
DFM	Design for Manufacture
DMLS	Direct Metal Laser Sintering
DO	Design Optimization
EBM	Electron Beam Melting
EDS	Expanded Design Space
ESO	Evolutionary Structural Optimization
FEM	Finite Element Method
FR	Feature Recognition
FSM	Freeform Surface Modelling
GDR	Global Design Rules
HIP	Hot Isostatic Pressing
M&P	Material and Processes
MDO	Multi-Disciplinary Optimization
NRC	Non-Recurring Cost
PAS	Process Automation System
PBF	Powder Bed Fusion
PCP	Profile Centred Point

PPR	Photo-Polymerizing Resin
RF	Reserve Factor
RS	Reserve Factor
SAM	Space Allocation Model
SCADA	Supervisory Control and Data Acquisition
SLA	Stereolithography
SLM	Selective Laser Melting
SMM	Solid Modelling Methods
SO	Structural Optimization
SPCM	Skinned Point Cloud Method
SR	Surface Roughness
SS	Support Structures
STL	Stereolithography (file type)
STO	Structural Topology Optimization
TO	Topology Optimization
TRL	Technology Readiness Level
UTS	Ultimate Tensile Strength
VTS	Variable Thickness Sheet
WBS	Work Breakdown Structure
WF	Wire Fed
YS	Yield Strength

1 Introduction: Commercial Aerospace Design – Past, Present and Future

1.1 Challenges Facing Commercial Aerospace Manufacturers.

Throughout the history of aviation, mass, due to its significant effects upon myriad aircraft performance attributes, has often been a key factor in deciding the success or failure of many aircraft programmes. Indeed, it was weight reduction which finally allowed the Wright Brothers to succeed where others had failed, achieving the first powered flight in 1903 through the development of a bespoke, lightweight engine for the Wright Flyer. This same, light weight approach was applied to not only the engine, but also the structure and was employed industry wide within a few years (Smithsonian, 1999) of its unveiling. Historically, commercial aviation has built upon past success, employing a largely iterative process of structural evolution through experience, with each subsequent aircraft program building on the achievements of the last. Problematically, the majority of modern aircraft designs are now approaching a state in which intuitive iteration can offer only minimal savings. As such, performance benefits (and subsequent fuel reduction) derived through mass reduction for future aircraft programs must be attained through non-derivative, non-intuitive solutions.

Challengingly, recently imposed environmental legislation has further compounded the already substantial economic pressures affecting the airline industry; in response, aircraft operators require markedly greater efficiency savings from new aircraft designs in order to remain not only commercially competitive (Mahashabde et al., 2011), but environmentally compliant with future legislation. Conventionally either design, material or manufacturing changes have been used to affect reductions in airframe mass properties. Of these, material and manufacturing changes are the techniques most widely employed (Greenhalgh and Hiley, 2003) as they are the easiest to implement and are employed only after substantial incremental development. Problematically, material change (steel>titanium) is now, more than at any other time, becoming a very expensive proposition for airframers due to both alloy cost and fabrication complexity. The economic vice formed by these challenges has forced airframers to embrace previously lightly used or even shunned emergent technologies in order to address marketplace demands for greater performance.

1.2 Industrial Context of Research

In a search for emergent technologies, two candidates are foremost in the minds of leading industrialists and researchers: additive manufacturing (AM - aka 3D printing) and design optimization (DO). AM in particular (Gibson, 2010, Sachs et al., 1993) has been identified as a potential game changer for high-tech manufacture and fabrication and is currently being heavily researched by Airbus Group Innovations and the larger Airbus Group for myriad aspects of the

business. Capable of producing complex parts with little or no material waste, AM is capable of producing metallic structural components with previously impossible to manufacture geometric complexity whilst still demonstrating comparable material properties (Al-Bermani et al., 2010). The ability to manufacture highly complex structural components with little or no increase in cost over a conventionally designed component, removes one of the great inhibitors to the application of the second identified technology; Design Optimization (DO)

DO in its various forms has found extensive use in many engineering sectors as a means of design enhancement and mass reduction (Chiandussi et al., 2004, Yang and Chahande, 1995, Cavazzuti et al., 2011) but has so far found limited use in commercial aerospace structures (Deaton and Grandhi, 2013, Tomlin and Meyer, 2011, Krog et al., 2002). Confusingly, and despite many exemplary case studies demonstrating attractive incentives (Krog et al., 2004), DO (in its truest form) has been met with scepticism and concern, the former in respect of economics and the latter, at least in part, due to the uncertainties introduced (structural failure modes, longevity, maintenance and repair, etc) and their potential effects in a safety-focused industry. As such, and despite demonstrated performance and cost advantages, regulatory problems/costs surrounding its application to primary and secondary structure remain plentiful, meaning that examples of primary structure design optimization for commercial aircraft remain few. These concerns are due at least in part, to the uncertainties introduced and their potential effects when considering a safety-focused industry. Furthermore, economic factors including manufacturing (Chang and Tang, 2001), certification (Georgiadis et al., 2008) and most notably, design expedience, all combine to provide significant barriers to the application of the technique on parts of lower criticality.

Of all the DO techniques applied to structural components, it is widely acknowledged that Structural Topology Optimization (STO) offers the most attractive percentage mass savings, especially when coupled with the relatively unconstrained design for manufacture offered by AM (Yang et al., 2015). Problematically, whilst STO can, on a part-by-part basis, offer a substantial mass reduction (in percentage terms), it often comes at the expense of analysis and design complexity. As such, STO can only be economically applied when cost of design AND manufacture are summated and enacted as a constraint. Additionally, due to the novel nature of both the design and manufacturing process, the pathway to certification is a both a tortuous and expensive one. These inherent non-recurring costs (NRC) stemming from design, analysis and certification can, and often do, limit the application of novel technologies to those applications which offer the greatest potential savings in mass or cost, i.e. large structures and assemblies.

For civil aircraft, there exists but a few large structural components to which topology optimization could be applied in the hope of achieving either a mass or cost reduction. Of these components exactly, none could be manufactured using the current AM processing techniques which are approaching technical maturity. These issues show an almost inverse relationship between design cost and mass (in Kg) saved; indeed, one would expect that smaller parts (and thereby smaller mass savings) would require substantially reduced design and analytics in order to achieve it, sadly this is not the case. In effect, this often-equivalent required time (and thus cost) to optimize and design small parts, often precludes their inclusion within mass reduction studies for aircraft development programs. Viewed individually, and contrasted, the optimization of large parts over small ones is, as such, an obvious choice for program leaders as it reduces the required NRC to the minimal required to affect a mass saving. However, large, un-optimized parts on an aircraft are uncommon at best; furthermore, the novel manufacturing technologies offered by AM are limited in scale and unable to produce large parts. In order to surmount this impasse, a change in approach must be undertaken in order to either reduce costs for small parts or increase manufacturing scale for larger ones. However, as previously noted, there exists little potential for the optimization of large parts, and so small parts must be the focus.

Cumulatively, small parts number into the thousands on even smaller aircraft such as A320 with tens of thousands of opportunities available across the entire aircraft catalogue. However, in order to cost effectively optimize such a vast array of parts, a means of speeding the optimization and design process whilst maintaining commonality with current design and analysis systems must be sought.

1.3 Research Aim

The aim of this research project is to provide a new means of employing the emergent technologies of additive manufacturing and topology optimization in a cost-effective manner, suitable for the design optimization of large numbers of small, metallic aerospace components.

1.4 Key Research Objectives

In order to facilitate the accomplishment of the research aim and to control the scope of the investigation, the following research objectives have been identified:

1. Comprehensive Literature Review intended for use during subsequent staff training – topics to be covered include:
 - I. Commercial aerospace design and manufacturing
 - II. Additive manufacturing
 - III. Design optimization

- IV. Topology optimization
 - V. Design extraction
 - VI. Process automation
 - VII. Automated component optimization and design generation
2. Automation Targets - Survey of TO users to determine which of the previously identified categories are the most time consuming and user intensive processes.
 3. Automation of Pre-processing - Development of independent automated processes for the inefficient stages of topology optimization pre-processing
 4. Automation of Post-processing - Development, validation and benchmarking of an approach intended to automate, or at least simplify, the process of design extraction for 3D TO structures.

1.5 Secondary Research Objectives

5. TO Process Discretization - Investigation of conventionally employed methods for TO and the discretization of the steps required to achieve a result followed by the development of robust Process for Manual Topology Optimization, culminating in a complete mapping of the manual process.
6. Collection of required input data used to parameterize and eventually test any developed processes including:
 - i. Gathering of current aerospace design rules for metallic parts
 - ii. Identification of component geometry, material data, loading conditions, together suitable to demonstrate the effectiveness of the developed process
 - iii. identification of current manufacturing limitations of AM and the elicitation of any missing data required for inclusion into the parameterization
7. Toolset investigation - determination of the effectiveness of commercial toolsets and their applicability to the project
8. Cross Comparison - determination of suitable targets for automation
9. Benchmarking - Performance test of developed automated process vs established benchmark
10. Automation Validation - Validation of automated pre- processes against manual methods

1.6 Principal Research Challenges

Perhaps the most notable challenge in attempting this research is the requirement to weave a complex fabric of emergent research in design, optimization and manufacturing with established methods and processes for the creation of commercial aerospace componentry. Currently, each of the techniques defined requires specialized skills and a wealth of experience for correct

implementation, thus limiting their appeal and use; simplification of those techniques whilst maintaining or hopefully increasing their applicability to commercial aerospace design, will thus be of critical importance. Research suggests that perhaps the most complex task, and the one for which there is almost no published research, revolves around the expedient and linked extraction of topology optimised results into new component designs, and perhaps more importantly, to do so in a manner deemed to be compatible with aerospace design and certification rules and for safety and traceability. Crucially, circumstance provides for an ideal situation in which experience of aerospace design, analysis, optimization and manufacture is provided on an almost daily basis. This allows for (relatively) simplified gathering, quantification and digitization of contextual data to serve as the foundation of this research.

1.7 Projected Impact of Undertaken Research

Through investigation of Airbus programme documentation, it is estimated that there are several thousand small, metallic, structural components on each aircraft programme within the Airbus product portfolio. These were identified as metallic structural/systems components with overall dimensions suitable for processing within the confines of most AM build platforms (<250x250x300mm). The components were identified from current aircraft programmes (A320CEO/NEO, A330CEO/NEO/Voyager/MRTT, A350, A380 and A400M) based upon an initial analysis of the A380 and A350 digital small parts catalogues.

Based on experience as to the effectiveness of optimization and additive manufacturing (Muir, 2013), it has been shown that mass savings in excess of 20% are highly probable. If one allows for the consideration of material change or pre-design optimization analysis, those savings can increase substantially with some examples eliciting savings in excess of 50% (Muir, 2017).

Economically, if one were to optimise those parts using conventional methods for analysis and redesign, it is estimated that the total hourly commitment to the task would be in excess of 300,000 working hours (excluding test, certification and paperwork) or over 35 years of continuous work. At an hourly rate of €93/h (correct as of 2018) this equates to over €30m of labour. Assuming complete industrialisation and integration of the research, the total cost reduction could be in excess of 50%. If the developed methods and tools were to be licensed the net positive result would be even higher.

Environmentally, assuming applicability of the technique to all of the ~9300 identified parts (a summary of the identified parts can be found in Appendix A – Background Material and that an average mass reduction of 30% were achievable and if one were to assume an average original part mass of 1kg (based upon the gathered data), the total mass saving would be 2.3t. This would

equate to a potential reduction in fuel burn of almost 11.5m litres from a fleet consisting of 3xA320, 2xA330, 1xA350 and 1xA380 in service for 25 years. This in turn would equate to a total operational cost saving of almost €6m over a similar timespan and asset register. Environmentally, each kg of mass saved is equal to around 0.4t of CO₂ per year (European Commission 2016). Assuming a conservative mass saving of 400kg over an aircraft's 25 year lifespan, this equates to a saving of 4000 tonnes of CO₂ for every aircraft sold. If it were assumed that this topic could be applied to even 2/3 of Airbus' 7000 aircraft order book, this would equate to 9.4m tonnes of CO₂ over the fleets lifetime.

1.8 Challenges of Research in an Industrial Environment

Whilst it is acknowledged that all research projects are challenging, the additional constraints placed upon this project through the bounds, both regulatory and budgetary, of commercial aerospace, create additional difficulties in terms of development and integration.

The research undertaken in this project was initially proposed by EADS Innovation Works on behalf of Airbus Commercial Aircraft and was based upon results achieved in undergraduate research projects at the University of Leeds. Three such projects were demonstrated, the first used structural optimization to demonstrate that even lightweight structures could be optimized to reduce mass. The second considered the combined effects of additive manufacturing and structural optimization to further reduce mass. The final project considered the effects of scripting to perform automation of complex optimization tasks in order to speed convergence of aerodynamic optimization on variable complex aerofoil shapes. Combined these research topics presented an opportunity.

EADS Innovation Works Provided initial funding to the research in partnership with the University of Leeds, with an agreement that Airbus would continue funding of the research once the initial two-year period ended. Regrettably and in part due to shifting commercial priorities within the group, Airbus did not continue funding beyond the two year period, but did agree to provide support to the project through the provision of data, resources, software and manufacturing facilities up to early 2014. However, due to resource commitments and the part-time nature of the research project, the research was not completed in time for the A320 NEO programme and thus was retargeted for A350-2000 and A380 NEO. Again, shifting priorities within Airbus Commercial and the reorganization of EADS Innovation Works into Airbus Central Research meant that little time was devoted to the research goals and support for the project was terminated with the cancellation of both the A350 and A380 upgrade programs at the end of 2015. Funding was provided by Airbus to wrap-up the research in such a way as to allow for its best integration from Airbus Toolsets.

During both the data gathering activities of Chapter 3 and the wrap-up activities of Chapter 5, it was noted that, in part as a response to the regulatory effects noted in Chapter 2, but also due to the difficulties of keeping large, interconnected and complex software tools working together, that there was a reluctance to adopt and integrate new tools into the design process. Acknowledging these difficulties and reluctancies, it was decided that all future research would focus, wherever possible, on the enhanced application of existing tools rather than the integration of new tools into the design process. Furthermore, the development of any new tools or methodology for the implementation of STO and AM must be robust both in terms of stability, but also in terms of variability both computationally and between operators.

During the initial period of research five candidate parts were identified. Initially these were five structural brackets and thus represented only a limited candidate pool of geometries, limited to structural applications. Later, STR5 was replaced with a systems manifold candidate part in order to expand the capabilities of the developed automation. When identifying targets for automation, all five candidate parts were assessed by 23 Airbus engineers, 2 of those parts were also optimized by the researcher – STR1 and STR3. Later, when Airbus support for the project was rescinded, further optimization and automation trials were conducted on those two parts only as they were the only parts upon which uniformity of research could be guaranteed.

1.9 Thesis Layout

1.9.1 Chapter 2 – Literature Review

In this section a comprehensive literature review is undertaken detailing the current state of design, manufacture and certification in commercial aerospace, their limitations and their dependencies. The review then focusses upon emergent and combinatory technologies such as optimisation and additive manufacturing looking specifically at their advantages and difficulties of their use in a safety focussed industry. The review concludes with a consideration of automation methods suitable for the reduction in extended design time common with advanced design and analysis tools. (Objective 1)

1.9.2 Chapter 3 – Understanding the Current Process

Chapter 3 begins where Chapter 2 left off identifying, in context, the use of structural optimization and additive manufacturing within commercial aerospace, establishing a baseline against which improvements derived from the research can be compared. During this section, standardised tools, operators and work-flows are detailed before being surveyed in order to find suitable initial targets for automation. (Objectives 2, 5, 6, 7 and 8)

1.9.3 Chapter 4 – Automation of Pre-processing

With targets identified in Chapter 3, Chapter 4 begins with attempts to automate those processes which occur prior to main optimization phase. In this section, the primary targets such as import, defeaturing and design space separation are individually automated and tested. During this phase, the limits and capabilities of additive manufacturing are evaluated with parameters defined for mechanical performance and geometric constraint during the optimisation phase. (Objective 3)

1.9.4 Chapter 5 – The Mapped Manual Process

Chapter 5 is where Airbus' direct involvement with the project ends and thus a wrapping up of research and accomplishments is required. A full mapping of the TO process is completed with inputs, outputs and process steps defined and explained. The objective was to reduce variability in the TO process and to aid its use by non-expert members of the design team. The MMP is tested in both a manual form and also a semi-automated form using the pre-process automation phases from Chapter 4. The results in terms of process robustness and speed are dramatic, showing over 90% reduction in engineer time in the automated phases and 70% reductions in variability between operators. (Objectives 3, 5 and 9)

1.9.5 Chapter 6 – Automation of Post Processing

Chapter 6 is concerned primarily with the development of methods intended to dramatically speed, if not completely automate the process of design extraction and revalidation. Investigating several possible methods for design extraction, the research focusses primarily upon methods deemed to be compatible with the Airbus framework for design and analysis in order to speed its integration. (Objective 4)

1.9.6 Chapter 7 – General Results, Discussion, Conclusions and Future work

Within this section are found the overall results, comparing the effectiveness of the automated phases to their baseline as established in chapter 3. In addition, the cost effectiveness of their employment upon the candidate parts is compared. (Research Aim and Objectives 9 and 10)

1.9.7 Chapter 8 – Discussion, Conclusions, Future Works and Concluding Remarks

The section details the accomplishments and limitations of the research along with suggestions for future research.

2 Literature Review

It is intended that this literature review will serve as an introduction to optimization driven design and additive manufacturing, their benefits and drawbacks, as applied within the heavily regulated environs of commercial aerospace design and manufacturing.

2.1 Civil Aerospace Design and Manufacturing

Commercial aviation designers and engineers have striven to meet wishes and requirements of businessmen, politicians and the general public; farther, faster, cheaper are but some of the demands which exemplify the intense century of development through which commercial aviation has passed. Whilst the notable achievements (AIAA, 2015) which define this period are indeed laudable, there is another, less well noted requirement which is, perhaps, even more important in its subsequent achievement; safety (ICAO, 2014). It is this last, initially unwritten requirement which has, for the past 70 years controlled (to a large extent) the development of methods, materials, tools and techniques which today define the aerospace industry as one of *the*, safest means of travelling.

2.1.1 Fundamental Aspects of Commercial Aerospace Design

The request/requirement for the design of a component for civil aircraft may occur at almost any point in an aircraft programmes life cycle and can be dependent upon any number of possible circumstances (Öchsner and Altenbach, 2015). Derivative aircraft models, new designs, in-service failure, performance improvement are some (but by no means all) of the reasons for which a component design may be requested. Dependent upon the circumstance of its request, an engineer will be required to collect the performance requirements and begin the design process in accordance with the strictures of the programme for which it is being designed.

During this phase, a designer will be required to consult and conform to the (aircraft) programme rules for the design of components. Rules for aerospace component design are utilised to ensure that a level of conformity appears in all components of similar class and application, regardless of the engineer tasked with designing them. In general, the rules cover items such as kinematics, attachments, flange thickness, rates of change, etc. Through their application, these rules can dramatically alter the eventual design, mass, cost and performance of any component when compared to one produced in isolation. The rules covering these sections of design are empirically and/or historically derived, usually from extensive test data and experience on both parts and material test samples. The numbers specified within these guidelines are usually safety driven and are, amongst many attributes, related to the interaction of structural components with their effects on stress and fatigue endurance (Uhlmann et al., 2015). These design requirements form some of the primary inputs of a design process.

2.1.1.1 The Effects of Safety Criticality and Design Rules upon Overall Component Design

When considering the design requirements of any component for commercial aerospace, a determination of its safety criticality must first be made. Commonly, a part is classified by the effect of its failure on the operation of the aircraft whole. The most critical parts are those whose loss would directly lead to the endangerment or loss of the aircraft and are identified and categorized as Class 1, with increasing numbers (2,3 etc) reflecting a decrease in part criticality as shown in Figure 1. Safety criticality is determined through a combination of Regulations (DoD, 2004) and internal safety specifications (Airbus, 2014) which, though possessing some commonality between programmes, does have specific requirements in each domain.

Whilst obviously designed to fulfil a particular function or requirement, each categorized component is designed in accordance with a set of carefully determined design rules and material allowables. These design rules are often specific to the components application, material and safety category, but also draw on some, more generalised standards (ASTM, 2013). These standards allow for the tailoring of design standards to specific loading types, manufacturing methods, conditions, etc. It is these categories and subsequent rules which, determines significant aspects of final component design (GrabCAD, 2013).

When the requirement for the design of any new component is raised, many aspects related to the proposed component are considered in respect of the aircraft program for which it is intended. Having spoken with a plethora of designers from many business units within Airbus and its supply chain, the foremost consideration of many designer's is often the required functional performance and its application on the aircraft. However, dependent upon from where the request is raised, an engineer's preference for functional design is already substantially constrained before a single curve has been drawn.

Design constraints can take many forms, but it is those which have been previously (globally) defined by the programme (ASTM, 2011) that will have the most substantial effect on design. Global design factors are determined and defined early in an aircraft program's development phase, and are implemented generically across the entire aircraft program. They are emplaced in order to control growth effects within product developments which, can cause significant problems not only to aircraft mass, but also costs and rates of component supply, if left unchecked. Using mass growth as a prime example - previous to global directives, aspects of design such as component reserve factors were decided on a team/function level. Problematically, in components which connect multiple technical domains or have aspects determined by multiple parties, cumulative, unrecorded safety margins can and do occur. Individually, each effect is small, but its inclusion betrays a very human aversion to risk (Lane and

Cherek, 2000), ultimately inducing a systemic fault, a cumulative effect which can lead to overwhelming and detrimental growth in an aircraft's dry mass. To counteract this aspect of human psychology, component loads are now (globally) inflated in order to create additional service demands, teams were then challenged to design components with a reserve factor (RF) of only 1 and made to justify any reason for exceeding that RF. This global strategy allowed for a more accurate prediction of final aircraft weight and has been largely successful for the prediction of performance in recent programs (Haria, 2014).

Manufacturing efficiency and reduction of material waste during manufacturing are other factors which can be significantly affected by the imposition of global rules during component design. Whilst in almost any circumstance, an airframer would prefer a lighter component to a heavier one, the overall cost to manufacture the lighter component must also be considered. Each aircraft program has a series of efficiency goals (Strüber, 2014) linked to mass and performance which are used to entice customers into purchasing new aircraft at a particular price point. As such, a careful balance of cost and performance must be achieved in order to both attract customers and maintain profitability. At programme start and during the early entry into service, performance, more than cost, may dictate design allowables for component. Later as the model is confirmed to deliver on performance targets and sales develop, profitability and decreasing component cost may replace the initial drivers. Regardless of whether they do, limitations on component cost and complexity will be established in the early phases in order to ensure targets for both performance and cost are broadly met. During manufacturing, these compromises manifest as limitations on the components buy-2-fly (B2F) ratio in respect of its safety criticality. B2F is one measure of manufacturing efficiency in which the relationship between the amount (in kg) of raw material purchased to produce a single component and the remaining amount of that material which is eventually in flight on the aircraft is contrasted. Limitations/targets on B2F are common and are usually constrained below 15, but can be as high as 30 in some extreme cases such as landing gear components (Cotton et al., 2008). B2F can be constrained through use of different manufacturing methods or by the emplacement of design limitation on the number of allowable machining operations for a component. Whilst many other factors will ultimately have influence on the final design, it is the global rules surrounding methods, processes, material and cost which, through their direct connection to manufacturing, feature heavily in the pre-concept selection phase which drives the initial design process for any component. When coupled with safety, this pentagram (methods, process, material, cost and safety) of precursors forms the initial inputs to the material selection phase.

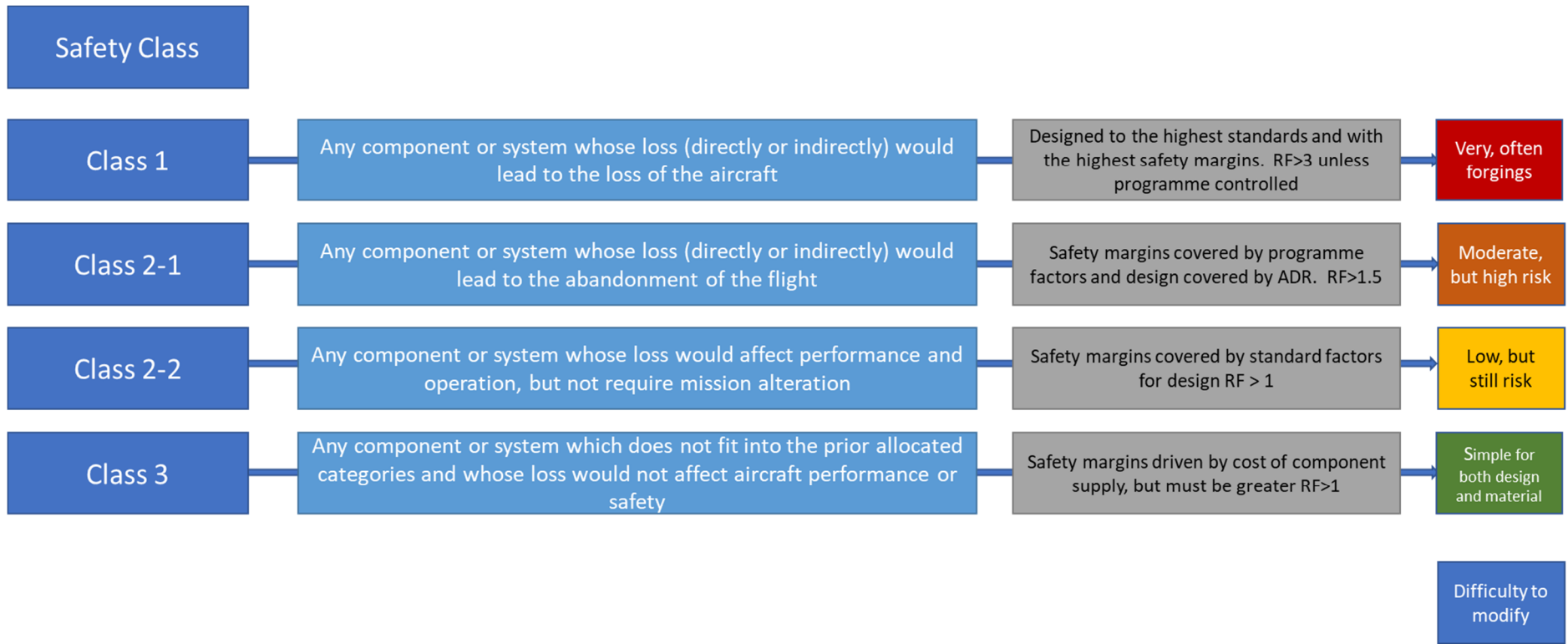


Figure 1 - Safety criticality table for Airbus Structure

2.1.1.2 Material and Process Standards for Commercial Aerospace

Manufacturing for commercial aerospace is a hugely diverse field covering myriad composite, polymer and metallic materials and the methods via which it is acceptable to manufacture and fabricate components (FAA, 2013). Commonly referred to as materials and processes (M&P) The field and technical speciality covers, without exception, all of the techniques used by airframers and their suppliers for the manufacture of aerospace componentry. Within this field, researchers and engineers work in concert with regulatory bodies (Blacklay, 2016) to define standards for materials testing and manufacturing. These combined standards allow Airbus and its suppliers measured assurance of a particular material and/or processing technique before its use in serial aircraft production. These generated standards are used by all within the industry in order to guarantee safety and comparability (Waiker and Nichols, 1997). In addition to generic standards for materials and production techniques, Airbus generates its own specific standards and often in advance of industry specifications. Airbus Material Standards (AiMS) and complimentary Airbus Process Standards (AiPS) are developed specifically to relate certified material performance to its associated production/processing technique (ASTM, 2011) thereby creating design allowables for chosen materials and production methods. These standards are painstakingly generated from vast research (Appendix A – Background Material - TRL Standards, gates from ecoHVP) and development activities designed to ensure that material performance is exhaustively characterised and correlated for each production pairing. Together these documents form additional inputs into the preliminary design phase, further constraining the geometric dependencies of any resulting part. Problematically, whilst all production techniques have this metadata which defies their use and material performance as a factor of that use, the categorization, digitization and inclusion of that vast database lies outside the scope of this research. In order to provide a proof, only a single material, one whose increasing use in aerospace is currently limited by factors including its difficulty to manufacture and work (Ezugwu and Wang, 1997) were selected for furtherment. The use of Titanium64, particularly Grade 5 Ti6Al4V (Ti64) in commercial aircraft has grown exponentially over the last 30 years (Ezugwu, 2005) with manufacturers attracted by its high stiffness to weight relationship and excellent thermos-mechanical attributes. Problematically, its further application now limited by its own unique properties and the associated costs of overcoming them (Boyer, 2010). Such problems have helped to drive the search for additional means of manufacturing components from Titanium, thereby providing an ideal candidate material upon which to focus and further this research (Boyer, 1996).

2.1.2 Conventional Methods of Civil Aerospace Component Manufacturing

With functionality, safety criticality, and program specific rules addressed, a choice of manufacturing processes deemed suitable for the material type must now be made.

Conventionally, titanium component manufacture is performed primarily using one of three methods: The first and most common is for the direct extraction (machining) of the component from Ti64 billet (plate material); The second, and the least common is achieved through metal casting (in various forms); with the final process being that of metal forgings. Both of these remaining two processes ordinarily require some machining after manufacture of the part blank (Nabhani, 2001). Whilst all of the above techniques can and are tailored specifically to the production of Ti64, the resultant material properties of a component or sample made using each technique will vary significantly (Tong et al., 2017), thus adding further complexity to the material and process selection phase.

2.1.2.1 The Effects of Manufacturing Process Selection on Cost and Mechanical Properties

Of the three methods detailed, Forgings yield by far the best material properties, far exceeding those of either plate or castings, with both yield (YS) and ultimate tensile strength (UTS) significantly in excess of other techniques (Suh and Lee, 1998). Contrastingly where forging achieves the highest properties, direct metal casting achieves by far the lowest (Boyer, 1996). This performance drop is particularly noticeable in respect to its functional characteristics under dynamic loading. The shortfall in performance is at least partially due to the components as-built surface quality, and partially due to the parts entrapped porosity. The last technique involves the use of high speed machining to extract a component directly from rolled metal plate. Due to the rolling process used to create the plate from which the components are to be extracted, machining from plate offers notably higher material properties than those from castings. Whilst wrought plate does give excellent mechanical properties they are still not comparable to forgings due to the nature of their crystal microstructure (Antonysamy, 2012). Numerically the general mechanical properties for Ti64 castings are approximately $\frac{1}{4}$ of those for Forgings (300MPa vs. 1200MPa for UTS) and as little as a third of those found in components machined from plate (Boyer, 2010).

As they are for mechanical properties, the forgings and castings occupy respectively the upper and lower echelons with respect to their costs per Kg of material produced. Forgings are usually supplied in either of two forms: near-net or block forgings. Due to their requirements for expensive tooling dies, Near-net Shape Forgings are by a substantial margin, the most expensive method by which titanium aerospace components are produced (da Silva et al., 2013) and are

usually reserved for applications with extreme safety criticality (Guiassa et al., 2014). Block forgings are forged blocks of titanium from which a component is extracted using CNC machining. They provide for high material properties without the requirement for custom forging tooling and are thus available for a lower cost per Kg. Whilst block forgings are cheaper to purchase, due to production from a series of uniform dies, the resulting material waste (incurred during machining) is often substantially higher. Furthermore, due to the hardness of the forged material, tool wear is higher and thus the process costlier than machining from plate (Allen, 2006).

Metal castings occupy the opposite end of the cost spectrum and are usually one of the cheapest means of producing high volumes of metal components, deemed to be either too numerous, too large or too complex for forming processes (Merrula, 2017). Castings are commonly used only for high volume production whereby the non-recurring cost (NRC) invested into the die tooling can be spread over a substantial number of predicted components. Regardless of material process and type, both forgings (NN and Block) and castings require post machining of key interfaces and complex features using CNC machining adding to the total component cost and further limiting design freedom.

Table 1 - Comparison of costs/Kg and predicted B2F ratios for typical titanium components

Process	Cost/Kg (supplied)	Buy2fly	NRC Cost	Use Rate
Near-net Forging	220	3:1	High	Low
Block Forging	120	8:1	Low	Low
Casting	38	1.5:1	High	Moderate
Machining	50	>10:1	Low	High

As the process with the least material variability, whilst simultaneously offering some of the greatest capability for geometric complexity, direct machining is the most common method of titanium component manufacture. With a level of design freedom offered largely due to the flexibility offered by modern CNC Machines (Suh and Lee, 1998), it has become the go-to method for production of complex titanium parts. Problematically, titanium is a difficult material to machine (Pramanik, 2014) with high tool wear due to work hardening even under the ideal conditions of both low cutting speeds and high coolant flow (da Silva et al., 2013). Additionally, whilst CNC machines are directly capable of the extraction of incredibly complex shapes from billet material, increasing complexity correlates directly with increasing cost. Such are the costs

for complex machining which require multiple operations, tools and axes of motion, that significant prohibitions are often placed on the design of complex machinings in order to control programme costs. These emplaced prohibitions can be overturned when the performance benefits are believed justified by cost increases. The restrictions imposed by manufacturing are often not singularly derived, but stem from a number of combinatory factors in addition to cost - production rate, geometric suitability, load and attachment are all rule governed during the design process and must be initially accounted for during selection and concept generation.

2.1.2.2 The Imposition of Manufacturing Related Design Constraints

Regardless of capability or flexibility, all forms of manufacturing impose pre-requisite restrictions upon design as there are no constraintless manufacturing technologies. Of all techniques used for titanium component manufacture, forging has the largest and most restrictive list of prohibitions, all of which must be adhered to in order to ensure manufacturing success. First and foremost, consideration must be given to the severe limitations imposed by the creation of a forging. Forgings, require application of physical force (pressure) directly to the semi-molten component/material, this pressure must be applied uniformly and often repeatedly in order to ensure complete grain refinement in the entirety of the component (Flower, 2012). Problematically pressure can be applied only through direct physical contact with a harder, shaped block and thus access to all areas of the forging must be allowed for during design. This requirement for almost linear access places significant limitations on the allowed shapes for any forging; this is particularly true for near-net shape forgings such as in Figure 2. Due to these severe limitations, even carefully designed near-net forgings can suffer substantial penalties when measuring B2F ratios (Martina, 2015), leading to substantial wastage and higher part cost through required machining.

Castings have substantially fewer constraints than do forgings and are perhaps the conventional manufacturing technology with the greatest level of geometric design freedom when considered only in respect of recurring part cost (Merrula, 2017) (Figure 3). However, like forgings, significant consideration and engineering design must be incorporated into both the part to be cast and the mould design from which the part will be extracted, vastly increasing total cost due to tooling development. The reasons for this dramatic cost increase stem from the symbiotic nature of casting design. The part to be manufactured and the mould in which it is created, must work together to achieve the correct distribution of material along with a suitable thermal environment to control shrinkage, stress and microstructural formation (Merrula, 2017).



Figure 2 - Near-net shape forging (top) and the machined part extracted from the forging (bottom)

Indeed, vast research and development has been poured into casting design factors in an attempt to enable pre, and in-process methods to enable the produced casting to meet geometric and material criteria upon exit from the mould tools. In complex design, simulation must be used, thus increasing NRC for design.

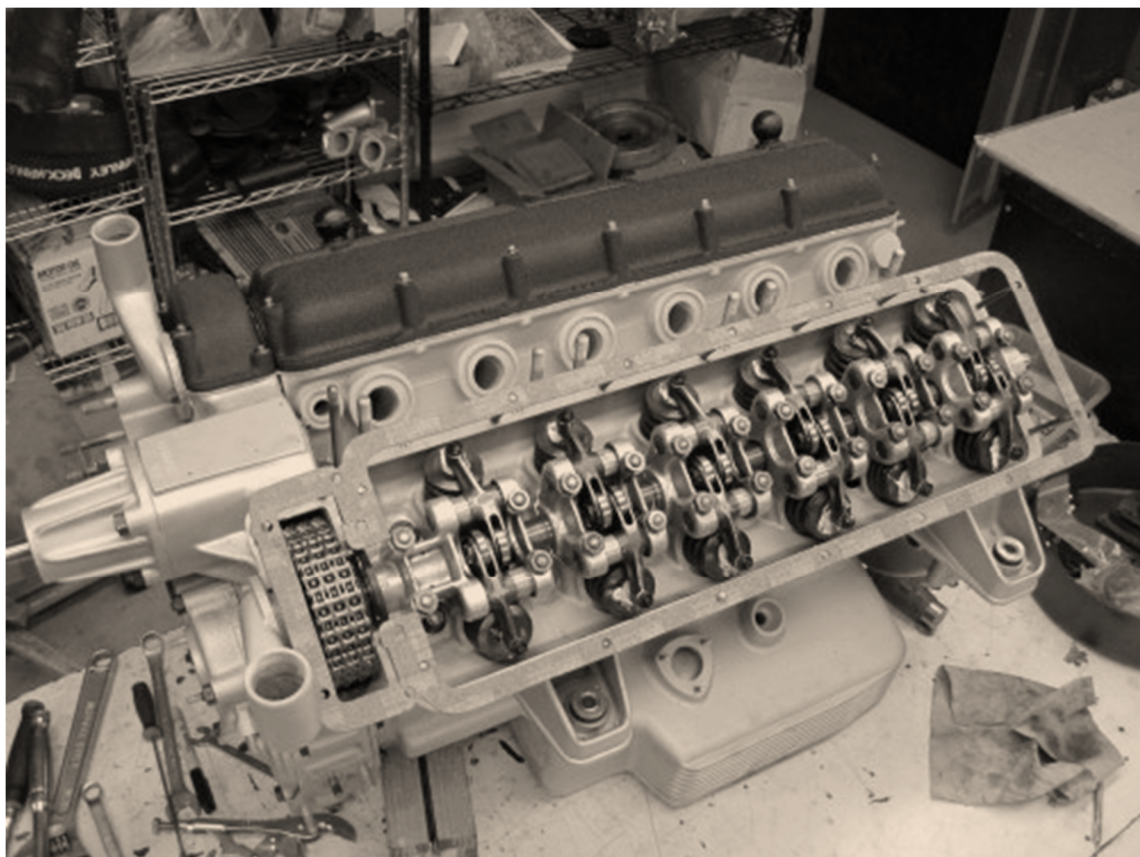


Figure 3 – Showing incredible design complexity of a Ferrari Engine block casting after machining and assembly

Due to cost and resulting complexity, substantial design compromises leading to higher than predicted/wanted B2F ratios are often employed to ensure manufacturing feasibility and repeatability. Regardless of whether castings or forgings are used for manufacture of the part blank (the basic shape of the part) there will always be a subsequent manufacturing phase in which the part is placed into a finishing process. During this phase, key interfaces will likely be machined from an established datum (stated on the part drawing) along with highly tolerated features such as requirements for surface finish quality, bolt holes and system integration points. As such, this additional manufacturing phase must also be considered during the preliminary design phase, lest a design which is suitable for service, but which cannot be efficiently manufactured/machined, be chosen. In effect, this means that regardless of the method selected for titanium component manufacturing, provision for machining of some features will be almost always required in order to meet the engineering specifications for the part.

Machining, as previously mentioned, is perhaps the most flexible/adaptable of all of the conventional methods for titanium component manufacture. Multiple axes of motion along with myriad available tools and complex control language (Guiassa et al., 2014) for machining allow for incredibly complex shapes to be extracted from billet, casting blanks or forgings (Figure 4) However, and as with most things, complexity has a very close correlation with cost, increasing and decreasing (exponentially in most cases) in accordance with one another. This relationship leads inevitably to a requirement to compromise between the two objectives. Three-axis machining platforms are both numerous in supply and precise in capability. By limiting the majority of designs around the limited capabilities of these platforms, a vast and capable supply chain is available for manufacture leading to increased competition and lower part costs. Further design limitations, such as those placed on the number of allowed operations, tool changes and fixture changes, can offer substantial additional cost savings, but will have an inverse effect on both component mass and buy to fly ratio.

2.1.2.3 The Effect of Manufacturing Constraints and Restrictions on Buy to Fly Ratios

B2F is the name commonly given to the relationship between the amount of material required to manufacture a component, contrasted to the actual mass of the flown component; It is often used as a measure of manufacturing efficiency and material waste. As a measure, the B2F forms one of the acceptance criteria for design reviews. As such, limitations are placed on allowables for B2F with any infringement requiring approval prior to procession with manufacture. Even so, when using conventional manufacturing methods such as casting, forging and particularly machining, buy to fly ratios can still be high, often alarmingly so when considering the cost of raw material. For later aircraft programmes (A380 and later) in which a greater emphasis was placed

on reducing airframe mass, these nominal allowables are in the region of 15:1. Whilst a lower figure is, in most cases preferable, there is flexibility to allow for variation based upon comparisons to other manufacturing methods.

By imposing restrictions on design complexity through the use of actual or imposed manufacturing constraints, the resultant mass of any component will almost always be higher than it might have been were a more relaxed approach allowed for. Contrastingly, under such an approach, the B2F will in fact be lower, mostly due to a larger flight component mass. This outcome may prove to be acceptable when cost rather than weight is driving design decisions. When considering B2F, particularly as a measure of waste, and more so, as a means of directly comparing component cost and efficiency of manufacturing with one another, one must also consider the scale of waste. If component 1 is a 17kg component machined from a 50kg block, thus having a B2F of 3:1, component 2 is a 1kg component and is machined from a 13kg block, thus having a B2F of 13:1.

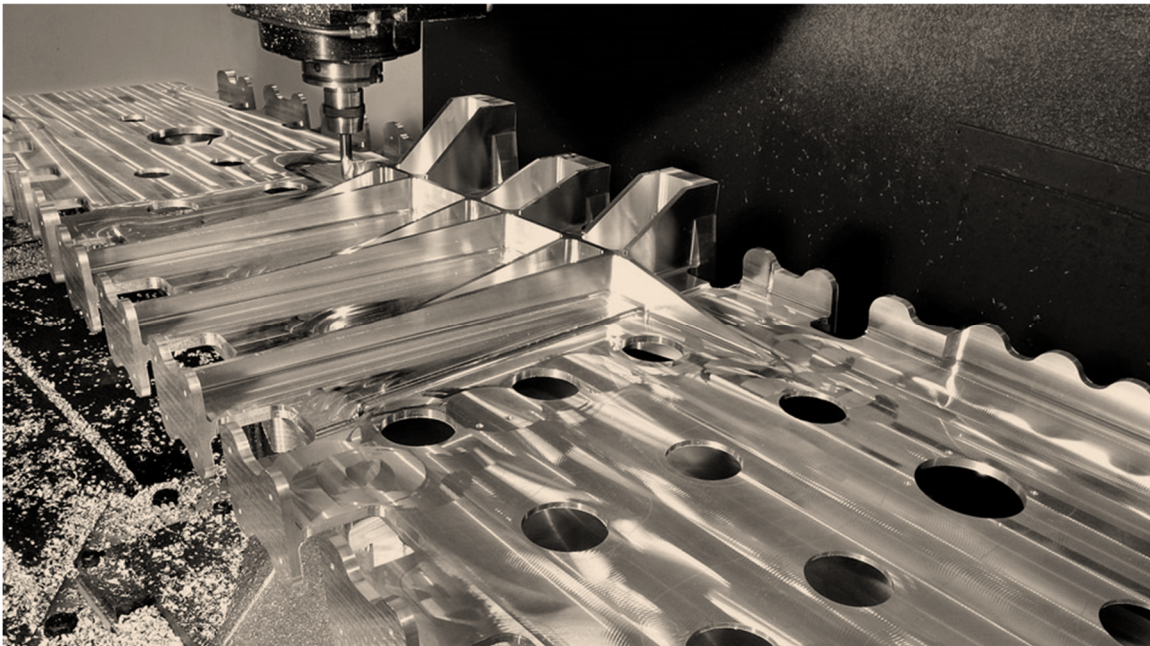


Figure 4 - Complex machining of A380 Rib from billet material at GKN

As a direct comparison based purely upon B2F, component 2 is less efficient, but this belies the fact that whilst 11kg of material is wasted in the manufacture of component 2, component 1 has almost triple this waste at 33kg. In terms of cost, this represents an almost 3-fold waste in material and an almost 4 fold cost in required machining (Allen, 2006).

2.1.3 Advanced Manufacturing Techniques

In order to improve the in-flight efficiency of an aircraft, one must target some (or preferably all) of the three major factors which govern its performance: aerodynamics; engines; and airframe

weight (Schultz and Zagalsky, 1972). In any new build aircraft program, aerodynamics can and do play a substantial part in determining the overall efficiency of an aircraft, but when attempting to introduce a new product which competes with existing aircraft (i.e. A350 vs A330) the effects of aerodynamic modification whilst maintaining a conventional layout (Torenbeek, 2007) and design considerations (Bishop and Hansman, 2012, Saffarzadeh and Masoumi, 2004) are generally small when compared to other areas. In derivative aircraft, such as A320neo, and without re-winging the aircraft, those aerodynamic improvements shrink into very small percentiles with much more emphasis being placed on engine performance (Joosung and Jeonghoon, 2011). Arguably, the largest performance gains in modern aircraft stem from recent advances in turbofan engines; new, large, high bypass ratio engines with multiple spool shafts, internal gearboxes (Tobi and Ismail, 2016) or specialist blades designed to allow higher pressures without noise (Dajani, 2016). Problematically, these new engines, whilst being more efficient to the tune of 10-14% (dependent upon engine and application), are also considerably larger and heavier (600-900kg per engine dependent upon variant) thereby significantly complicating the path to the final performance target – mass reduction.

Aircraft mass minimization has long been at the core of commercial aircraft development programs, and is often used as a measure of success upon completion of a design program, on-time, on-budget, on-target (weight). Problematically, mass targets are not an area where recent development programs have excelled, with both Boeing and Airbus struggling to delivery aircraft on-target to launch customers (Zhang, 2016). In each of these cases, manufacturers have been forced into substantial reactive weight reduction measures. Generally, mass reduction can be accomplished in one of three ways: direct material substitution; design alteration or assembly reduction. In an ideal case, all three would be used in series to realise the greatest practicable saving, but late in the design phase, or worse, when in serial production was far from an ideal standpoint from which to redesign as time was not in abundance.

Designing for a new material takes time to assess, design, validate and test, time which a aircraft programme in the early stages of customer deliveries can ill afford. A material change and rapid validation however can be expediently implemented and, if required, iteratively improved. Through such methods, the aerospace industries use of titanium in place of cast steel for many secondary structural components has become almost common (Greenhalgh and Hiley, 2003). Problematically, cast titanium does not have comparable material properties to steel (section 2.1.2.1) only machined titanium can mimic the properties of cast steel and thus allow for a direct swap. Whilst direct machining of Ti64 from billet does yield the equivalent material properties, it does not do so at comparable cost. Titanium is difficult to machine (Pramanik, 2014)

with a propensity to work harden at high cutting speeds and to oxidise at higher temperatures. Fabrication (welding) from cut plate is also problematic as even with high precision welders and robotics and with welding performed in highly controlled environments, the quality and thus integrity of the weld cannot be reliably guaranteed (John et al., 2003) These problems combine to mean that oddly shaped components often require abhorrent amounts of reductive machining in order to yield the final shape component. Whilst in previous aircraft programs (and during the early phases of the latter programs) the B2F for high value material such as titanium and Inconel was kept in-check, mass targets and delivery schedules has led to some truly extraordinary B2F values in modern aircraft, sometime in excess of 30:1. At this ratio, the cost for a 1kg flying part would be over €2500 in material alone and require in excess of €4400 of machining (Muir, 2012c).

Airframers are all too aware of this trend and have (with global design rules (GDR)) taken steps to address it. Problematically, many components, even those developed under GDRs still have notably high B2F (most are greater than 10) and as such have a high level of material waste; a new approach to reduce this waste is required.

2.1.4 Additive Manufacturing and its use in Commercial Aerospace

Additive Manufacturing has been widely hailed as one of the game changing technologies for commercial aerospace in the next decade and beyond (Wohlers and Caffrey, 2015) The statement, widely echoed by many in the industry, has been substantially and expensively supported by investment in research and technology in projects such as Cleansky (European Commission, 2017) and AMAZE (European Commission, 2013) across a plethora of AM techniques (ASTM, 2013). AM, as the name implies, is a largely additive method of manufacturing, in which material is incrementally added in order to produce a final, pre-determined shape. AM is antipodal to conventional (reductive) techniques which rely on the incremental removal of material in order to achieve the final shape of the component, the latter is often extremely wasteful, the former is not. Whilst vast in complexity and varying enormously in their attributes and methods of material application, all AM techniques have a number of general commonalities which are applicable to all, with each able to trace its origins back to one of a number of technology developments (i.e laser development, the advent of computers, welding of titanium, etc) . As such, generalised AM can be largely split into four primary areas, each of which form the basis for categorised identities as defined by the American Society for Testing and Materials (ASTM) (ASTM, 2013). These identifiers are: Vat Polymerization, Material Extrusion, Powder Bed Fusion (PBF) and Directed Energy Deposition (DED)

Regardless of their category and as previously mentioned, all AM Techniques have some commonalities; all require three primary constituents in order to effectively produce a part: a digital computer aided design (CAD) model; a directed energy source; and a feedstock of suitable material/media. Additionally, all current AM techniques use a layer-wise build-up of material in which a layer of feedstock/media is deposited and, in accordance with a computationally directed 2D pattern, fused to the previously deposited and melted material. A subsequent layer is then deposited on top of the previous one, repeating using unique layer profiles until the structure is complete (Figure 5). The 2D pattern for each layer is developed by slicing (Section 2.1.4.1) of the 3D part into 2D profiles along a pre-determined axis along which the part will be built - usually referred to as the Z-Axis.



Figure 5 - A coarse representation of a 3D CAD part sliced into 2D planar profiles.

The thickness of each slice profile will be driven by the manufacturing process which will be used to realise the part from the CAD. Once a CAD file is sliced and parameterized for specific production platform, the deposition and melting of media in accordance with computer control must be undertaken. It is in this phase that the vast majority of differences between AM techniques are to be found. In order to progress, it seems wise to first detail a list of common terminology used by the various AM techniques to describe their methods of processing and part production.

2.1.4.1 Generic Additive Manufacturing Terminology

Additive manufacturing has a great deal of often confusing and bespoke nomenclature – to reduce confusion and give some context, Table 2 has been created to encompass some of the most often used terms.

Table 2 - Table of General Additive Manufacturing Terminology

Breakout	The removal of a part and the build-plate from the AM machine after completion of the build
Build Chamber	The vessel in which feedstock material is deposited and melted to form parts. Usually air tight and capable of operating under a vacuum or inerting gas
Build Plate	A removable substrate plate onto which the initial material is deposited. Nominally made from the same material as is to be deposited, but not always. Completed parts are usually welded to the substrate and removed later using a variety of methods
Build Tank	The vessel into which a build plate holding the manufactured parts and unused deposited powder will be lowered as the build progresses.
Build-up Direction	Also referred to as the Z axis, it is the direction in which, after initial positioning, parts are sliced and then iteratively deposited within the build chamber.
Deposition	The carefully controlled combination of raw feedstock material and directed energy in order to create new material/shapes/parts
Directed Energy	The energy source (laser, electron beam etc) used to melt material

Dosing	A variable which defines the amount of powder pushed across the plate during recoating
Feedstock Material	The raw metallic alloy from which a part will eventually be created, can be wire, powder, resin etc.
Layer-wise	To form a homologous part from incrementally deposited layers.
Nesting	The positioning of multiple parts into a single build in the most optimal manner.
Residual Stress	The stress formed due to the rapid cooling of molten metal.
Substrate	Similar to a build plate in some AM processes, it is used in wire-fed processes both as a means to deposit the part and often, as an actual part of the final component.
Support Structures	Temporary structures used to introduce, anchor, stabilise elements of a component during layer-wise deposition.
XY Direction	Refers to the plane of each layer and is usually parallel to the build plate
Z Direction	Refers to the normal projection from the build plate

2.1.4.2 Additive Manufacturing Techniques

Since its inception in the late 1970s AM has developed into myriad techniques and applications – this section details the most relevant of those techniques to this investigation, covering strengths, weaknesses and their use/context in commercial aerospace.

2.1.4.2.1 Powder Bed Fusion Techniques

Whilst the most publicly common AM techniques are polymer based wire-fed techniques, the most common industrial research, development and production methods are based upon Powder Bed Fusion techniques (Bhavar et al., 2014). In all AM methods, CAD is orientated and sliced, then parsed and deposited by the platform in accordance with the type of energy source

and the media being used. Unlike other techniques, PBF relies upon the complete deposition of a layer of media, covering the entire build plate, but which is only melted in locations specified by the computer control similar to the manner described in the original SLS patent (Deckard, 1988). By using this method, powder is always available where it is required and thus allows for extremely fine control of the directed energy source and of the melting of material (Frazier, 2014). Furthermore, by controlling the thickness of layer deposition in each slice, fine feature control can be realised in all axes. Due to these factors, PBF is currently the only AM method by which a B2F ratio approaching 1:1 can be realistically achieved without significant post machining.

Like DED techniques, there are numerous methods of directing energy in order to melt the deposited media, but by far the most common method is for delivery by laser ingestion (Wohlers and Caffrey, 2015). Of all the PBF platforms in operation around the world, over 95% are laser based (Selective Laser Melting (SLM), Direct Metal Laser Sintering (DMLS)) with power ranging from as little as 200w up to and in excess of 1kw (Buchbinder et al., 2011). Of the remaining 5% of systems, the most common and arguably most effective of all PBF techniques are based upon melting through Electron Beam Melting (EBM) (Löber et al., 2011). Whilst outwardly similar in appearance and application, EBM and laser are significantly different in operation.

2.1.4.2.1.1 Electron Beam Melting

Unlike the vast majority of AM PBF techniques, EBM does not process under an inerting gas, but under a full and carefully maintained hard vacuum. The requirements for the presence of the vacuum are multi-fold (airborne particles, oxygenation, etc.) but in doing so, the vacuum confers a number of additional benefits. First amongst these are to material properties – by processing under a vacuum, any moisture present in the powder is vaporised and removed from the chamber, thus reducing the propensity of the entrapped water to separate into H and O², and be absorbed into the material make-up of the part, thus increasing elongation and decreasing strength. The second is related to porosity in the part. Common in all PBF techniques, porosity (whilst only very small - AM PBF parts are >99.5% material dense) is a cause for concern as it can exacerbate failure during fatigue loading. Largely an artifact of recoating and energy ingestion, these microscopic pores (Song et al., 2015) can be closed using a post process known as HIPing (Hot Isostatic Pressing) which is highly effective for all PBF techniques. Problematically for most current laser based techniques however, is the fact that the presence of porosity means a simultaneous entrapment of processing atmosphere under which the part was built. Whilst the porosity would still be closed by HIP, the entrapped gas does not disappear, but simply

compresses. If such a part were subjected to high enough temperatures in the future, the entrapped gas would expand and, in conjunction with a malleable material, can agglomerate causing rapid failure of the part. This is a significant problem for any part known to experience high temperatures during service (e.g. Engine bleed air systems) or upon which the safety of the aircraft is predicated during an engine fire (e.g. Pylon parts). As EBM is processed under a vacuum, there is no risk of this occurrence, thus adding to its advantages for commercial aerospace.

Another aspect of EBM which is (for the most part) highly advantageous is its elevated temperature processing environment. In most circumstances, laser PBF methods operate at thermal levels which approach room temperature. As such, each point and profile pass at which the laser is ingested into the powder bed, essentially acts like a zone of micro-flash-casting (Song et al., 2015) imparting substantial cooling related stress (shrinkage and compression) into the part. These stresses are known as residual stresses (RS) and will be discussed later.

Due to its complex physics environment, which requires control of the electron stream from an emitter to the powder-bed, a series of electromagnetic fields are generated to both focus/defocus the electron stream and also to direct the beam to its appropriate location on the build layer. Problematically, the combination of an operating vacuum, interconnecting EM fields and the initial interaction of the electron beam with the powder bed means that, if left unattended/constrained, energization of the powder particles with the freestream electron and the EM fields can lead to airborne particles swarms. These particle swarms can and do destabilise and deflect the electron stream, leading inevitably to a build failure. In order to prevent this from occurring, the deposited layer is subjected to a preheating process during which a fully defocussed electron stream is directed to partially sinter the deposited layer. This partial sintering has the added effect of increasing the overall bed temperature of the machine to $\sim 700^{\circ}\text{C}$. By doing so, every deposited layer in the build is, in effect, subject to continuous, low temperature, stress relieving heat treatment. This means that all completed builds are predominantly free of residual stresses and stress imposed distortion (Prabhakar et al., 2015).

Whilst the elevated temperature is an advantage in the vast majority of conditions, it can also add complications when considering thermal management due to layer-wise energy density (Smith et al., 2017). Currently, very few AM processes have in-built, adaptive, feedback loops based upon either sensing, or pre-computation of layer-wise variation in builds. As such, preheating is applied uniformly to each layer without consideration of the remaining residual heat in the previous layer or visa-versa. This lack of interaction can allow too much energy to be imparted into areas of high deposition, thus leading to thermal distortion through metallic swelling of the component. In some circumstances, the magnitude of this distortion can be

significant enough to again cause build failure, though even without direct failure, over-melting of the material will alter the chemical composition of the deposition leading to compromised mechanical performance and ultimately a necessity to either concession (the customer agrees to a downgraded delivery specification in return for a reduction in part cost) or scrap the part. In extreme cases, the complete build may be scrapped due to over-melting and metallization (Mahale et al., 2007).

A further artifact of the layer-wise pre-sintering process, is that unlike laser based PBF for metallic components, in which the powder is loose and free-flowing at the conclusion of the build, the powder from the EBM process is highly agglomerated (similar in consistency to an OXO stock cube) and must be interactively and laboriously removed from the surrounds of the parts. Whilst in this context the semi-sintered powder is a definite detractor, and often precludes the possibility of producing components with narrow, internal channels (as powder removal would be impossible), in other areas, it can prove advantageous (Smith et al., 2017). Support structures (Section 2.1.4.3.3.2) in EBM are used largely for the introduction of structural elements (Figure 6) and for the control thermal properties during deposition.

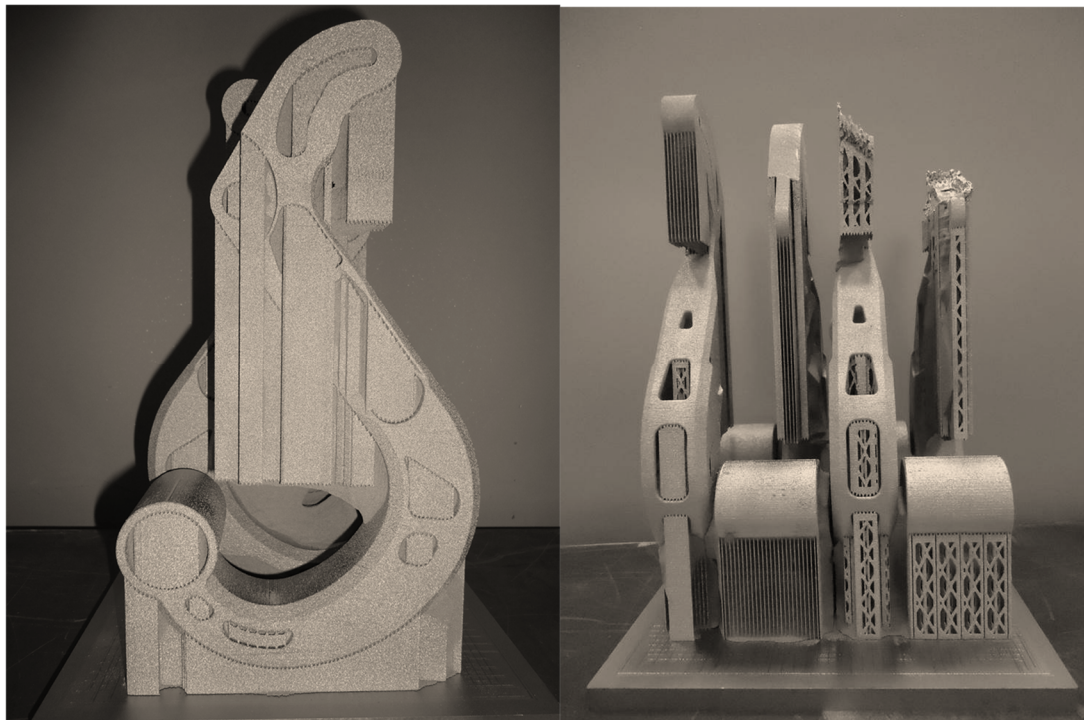


Figure 6 - EBM deposited AM parts showing introductory support structures (left and right) and build errors (top right)

As the supports are not required to carry stress (through anchoring the part to the bed - e.g. DMLS) and due to the semi-solid nature of the powder within the build chamber due to pre-heating, floating supports can be used to increase nesting density in the Z direction thus

decreasing the cost of individual parts through economies of scale. Additionally, the absence of requirement to connect geometry which requires support to the base plate removes further constraints from the application of AM.

2.1.4.2.1.2 Laser Powder Bed Fusion - Direct Metal Laser Sintering

Direct Metal Laser Sintering (DMLS, also known as Selective Laser Melting (SLM) and LaserCUSING (LC) is one of the oldest tradenames of current metallic laser based PBF Techniques. Owned by Electro Optical Systems (EOS) GmbH it is one of a number of (largely German) manufacturers offering Laser based PBF platforms for the production of metallic components. Metallic AM platforms are derivatives and developments from existing polymer based platforms which are also offered by the manufacturers of metallic systems (i.e. EOS Polymer700 and Metallic400). Using similar machine architecture, but with more powerful, highly focussed lasers and operating under more stringent atmospheric (due to risk of explosion), material, processing and handling methods, the systems, developed as research equipment and for limited production, are now being tasked with series production of AM components for many industries (Wohlers et al., 2016). Laser based PBF is, by a substantial margin, the most common means of producing metallic components by AM. Laser PBF machines are common in AM due in part to their long history, relative simplicity, and generative design evolution of the machine hardware, but also due to ease and flexibility of platform use. In addition, machine longevity has allowed for the significant proliferation of laser PBF platforms across myriad industries and has in turn allowed for vast parallel research and development in multiple fields of application. Unlike EBM with its complex operating environment and its ability to process only a small number of difficult to manufacture materials, laser PBF machines, operating under an inerting atmosphere such as either argon (for reactive materials) or nitrogen (for non-reactive materials) are relatively easy to use and operate, and can utilise a vast array of materials (Zhang, 2017). Whilst they are capable of processing multiple material types, some are much easier to process than others and the relationship between ease and material is not as straightforward as might first be imagined.

In order to fuse material, one must first reach the material's melting point without vaporising the alloying elements of a material's compositional make-up (Dinwiddie et al., 2013). In casting, (and to a lesser extent, welding) this is a known and understood quantity, as the rates of energy ingestion and material deposition are linear and thus controlled (Manvatkar et al., 2015). This is not the case for AM. In AM, the melting laser must be controlled and computed, the precise amount of energy needed to melt material in relation to its position in the layer contour and its relation to those layers below must be carefully identified to ensure true isotropic material properties. Whilst the melting point for a material is very well known and thus the

amount of energy required from the laser to melt a proportion of the material should be easy to compute, this assumes perfect absorption of the directed energy into the material deposited with no loss or dispersion. Problematically, the material into which the laser energy is being absorbed has a number of attributes which together conspire to reduce the effectiveness of the laser to melt the material. In order to efficiently melt, the laser beam must be absorbed by the metallic powder in as effective a means as possible. To do so, the powder must have a number of attributes: the first relates to its morphology - a spherical powder particle absorbs energy with far greater efficiency than a faceted particle, which tends to refract laser energy rather than absorb it (Yadroitsev et al., 2013). Related to this is the materials reflectivity, a highly reflective material such as aluminium requires (despite its low melting point) substantially more laser energy to efficiently melt than does a darker, less reflective material such as steel (Williams et al., 2015) as significant energy is simply reflected away, thus making aluminium harder to deposit than steel. Titanium (the focus of this investigation) whilst being a darker powder (similar to steel) and thus more accepting of laser energy than aluminium, is perhaps one of the most difficult materials to deposit. This processing difficulty stems from titanium's thermal nature which has only a 1/3 the thermal conductivity of most steels and only 10% that of most aluminium alloys (Denlinger et al., 2015), making it particularly prone to the build-up and rapid release (through fracture) of gradually accumulated RS during build. The speed and size of this release can, and often does result in catastrophic build failure.

Like EBM, LASER PBF requires the use of metallic support structures in order to introduce areas of previously unsupported geometry into the part being constructed. Like EBM, these structures also perform additional functions beyond their use for feature introduction. Unlike EBM and their use in thermal control, in LASER PBF, they are used as anchors which secure the deposited parts to the build plate in order to help arrest the common distortion (and potential fracture) caused by increasing residual stresses within the part being constructed (Järvinen et al., 2014) (Figure 7). As such, the supports required by LASER PBF must be strong, in some cases so much so that they are almost indistinguishable from the structure of the part itself. Whilst this combination of supports and their method of application is, in a large number of cases, effective at resisting distortion through RS, the stress is not removed, but actually increased, contained within the deposited structure and supports. Should the build complete successfully, the presence of RS will identify itself, at least initially, though elastic deformation of the build-plate until the parts are released from the plate. Upon release, either through band-saw or wire electro-discharge machining and unless expeditiously heat-treated after build completion, the stresses causing distortion in the build plate will cause even greater distortion in the as-deposited

part (Figure 7). Heat treating on the build plate prior to removal helps to reduce this distortion (Aggarangsi and L Beuth, 2006) as the stiffness present in the build plate at elevated temperature is usually greater than the stiffness in the deposited part, thus allowing the heat treatment of the pairing to leave a largely distortion free part (Figure 8). Due to this complex set of pre and post processing requirements in LASER PBF and the variability of the results during build processes, this provides for significant limitations and constraints upon the AM processes.

The major advantages of LASER PBF over its peers stem from its simplicity, ease of powder handling and ease of powder removal, post-build. Due to this, excess, un-melted powder can be immediately and simply removed as the powder condition is identical to the prebuild state, it flows easily and thus can be tipped/brushed/sucked away from the deposited part. In stark contrast, powder used during the EBM process is in a semi-sintered, partially bonded condition upon completion of any build, making its removal substantially more difficult with direct access to the areas required. In addition to powder feedstock, the working environment for most laser based system systems relies only upon a moderately controlled atmosphere environment and optical control of the beam. This simplicity, leads to a high degree of repeatability and system reliability when compared to other processes.

2.1.4.2.2 Directed Energy Deposition Methods

In abstraction, the techniques which fall under the DED heading are those which have the largest commonalities with existing welding methodologies. Largely the techniques fall into one of two primary categories – Wire Fed and Blown Powder.

2.1.4.2.2.1 Wire Fed Techniques

The first, oldest and most common method of achieving direct deposition are through extrusion based techniques such as fused deposition modelling (FDM) and freeform fabrication (FFF) (ASTM, 2011). Extrusion based techniques are predicated on the extrusion, melting and fusing together of material into predefined, computer controlled shapes, using a layer-wise assembly technique. Developed initially using polymers such as ABS and Nylon (Crump, 1992) this technique is by far the most common and cheapest method of performing AM (Wohlers et al., 2016), with desktop AM machines available for less than €500. Whilst any platform bought at this price is obviously incapable of performing metallic deposition, the principles and application (deposition and feedstock control) are largely the same requiring only a means of delivering feedstock, melting that feedstock and repeating at the corrected displaced location.

When considering metallics and the complex physics surrounding the deposition environment, wire-fed techniques can, more than most other techniques, draw on significant

parallels with extensively developed welding technologies (Stavinoha, 2012) allowing for rapid iteration of directed energy input. Systems capable of performing this action with materials such as titanium, Inconel and steel are now in the commercial marketplace (Wohlers et al., 2016) with Boeing and its supplier Spirit being heavily committed to the Norsk (Norsk Titanium, 2018) process for future titanium components. Problematically, many if not most of the commercial and research techniques available at this time are subject to many of the common problems associated with AM such as residual stress formation (Figure 7) and poor surface finish (Figure 8).

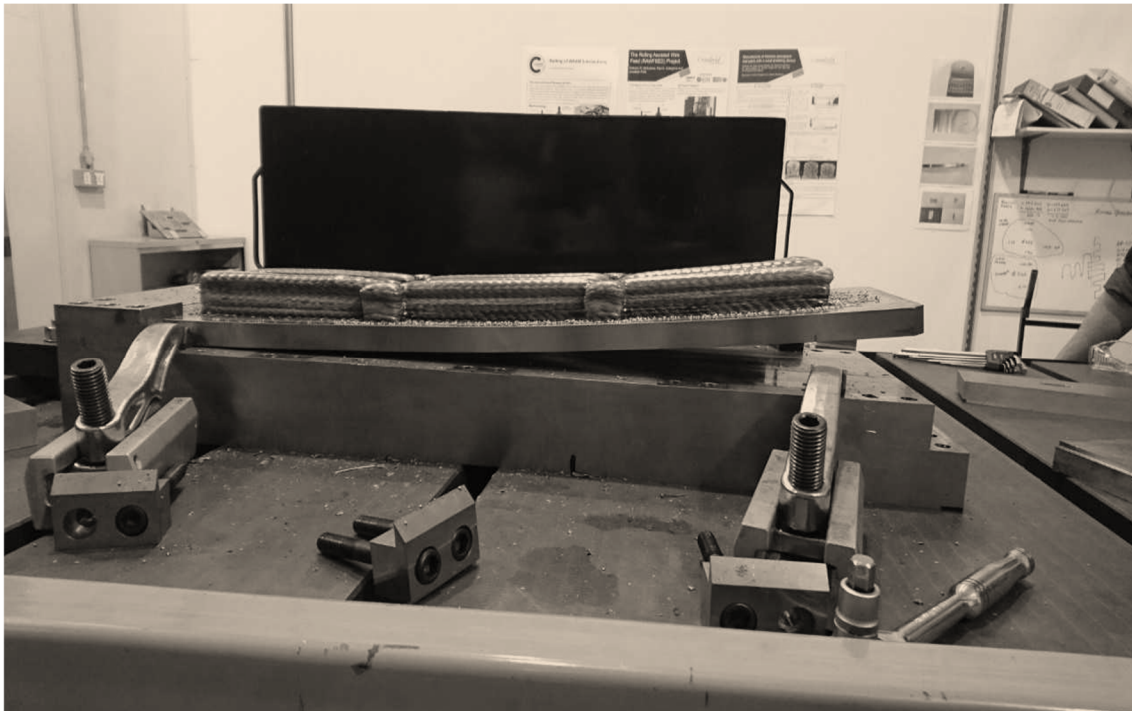


Figure 7 - Distortion of a component due to residual stress

2.1.4.2.2.2 Blown Powder Methods

Occupying middle ground between Wire Fed and PBF techniques, Blown Powder (BP) methods are another form of DED which offer both the best and worst of their respective contributors (PBF and Welding). By allowing for an open, robot controlled deposition system, similar to that used in WF, scale limits applicable to PBF techniques are largely removed, whilst also allowing for extremely fine media control and deposition (Candel-Ruiz et al., 2015). Problematically, whilst indeed offering this benefit, it does so whilst drawing in significant negative factors associated with the use of powder as media. Due to the problems associated with its production, the use of powder as media leads to significant increases in media cost when compared to WF and wire cost. However, whilst the media is more expensive, the accuracy of deposition can be significantly improved thus, reducing the eventual B2F ratio for any manufactured component. Furthermore, the use of a powder delivery nozzle system allows for the delivery of differing

powder media at different stages of manufacture thus allowing for the potential of functional grading – the gradual transition from one material type to another through on-the-fly blending of feedstock (Guo and Leu, 2013) of materials during construction of future parts.



Figure 8 - Similar component stress, relieved on its own build plate and tooling - now almost completely flat

2.1.4.2.3 Vat Polymerization Methods

Developed and patented in the 1980s as a means of achieving and commercializing industrial rapid prototyping (RP), photo-polymerizing techniques such as stereo lithography (SLA) are the pioneers of AM (Hull, 1986). During their 30-year span, the technologies have developed not only a commercially active RP market, but have also developed interest and technologies in 3D-Printing and its advancement into materials more suited to production than prototyping, thus paving the way for AM as a fully-fledged manufacturing technique.

Photo-polymerizing Resin (PPR) differs from all other AM techniques through use of a liquid bath of photo-polymerizing liquid resin as a media source. In a method similar to PBF, a build table is lowered a layer at a time as each new layer is cured and the next one made ready. Unlike PBF, layers are not melted, but cured by their interaction with a pair of low intensity ultraviolet (UV) lasers. PPR can, under the correct circumstances, be a very fast process from which to manufacture parts. This rapidity is partially due to laser speed (little time required to cure material rather than melt it) and partially due to material deposition and recoating

(Tumbleston et al., 2015). Additionally, the process provides for a simple method for removal of any support structures deposited as required during build. PPRs major detractor stems from the root of its greatest strength, the resin used in manufacture. Whilst fast to process material, cheap to procure and possessing of excellent surface roughness qualities, the mechanical properties of the useable resin materials are poor (Szykiedans and Credo, 2016), thus limiting their application to prototyping and model making activities rather than production parts of use in final assembly of an aircraft. Due to this significant detractor, PPRs use in commercial aircraft manufacturing is almost non-existent. However, their commercial use for rapid prototyping has evolved to the point where they are some of the largest commercially available 3D printing platforms (Vanderploeg et al., 2017).

2.1.4.3 Disadvantages of Additive Manufacturing

As mentioned, AM has been the subject of exponentially increasing industrial and public interest over the last decade of its development. Inevitably, and with people/companies entering the AM world at different times and each with different backgrounds and requirements, confusion regarding the capabilities of AM abound (Gao et al., 2015). With so many AM technologies available, each with specific capabilities, advantages and potentials, human nature leads to AM successes being reported and repeated whilst limitations and failures are swallowed by a deafening silence. Problematically, these positive messages get reported, repeated, exaggerated and, most significantly, combined. Typically, this inclines toward a shallow understanding of AM techniques which suggests that there are almost limitless possibilities (Wright, 2015) offered through use of technology. The belief stems from the idea of AM being a constraintless design and manufacturing technology (Hague et al., 2003); nothing could be further from the truth (Vayre et al., 2012). Laser Sintering and its equivalents are the least constraint bound of all the AM techniques due to its thermally stable deposition process and self-supporting powder bed; even so, there are still active constraints upon design and manufacture related to scale (Frazier, 2014), material, geometry and time (Hague et al., 2004) (Gu et al., 2012). Furthermore, these constraints multiply exponentially when the complexities involved with the use of AM for the deposition of metallic components (Frazier, 2014) are included.

2.1.4.3.1 Geometric Limitations of AM

One of the most notable limitations in the production of metallic AM is its capacity for the production of larger parts (Martina, 2015), the vast majority of available platforms for the production of components are in the PBF category (Wohlers and Caffrey, 2015) and of those, a significant proportion are in the 250x250x250mm size category and thus significantly limited in scale. Whilst larger AM platforms do exist (e.g. Concept Laser X-Line, EOS M400, SLM500, etc)

depositing larger parts in AM is not simply a matter of scaling the platform, the complex physics involved in deposition means that negative attributes of AM scale correlatively with the increase in platform size (Ding et al., 2011)

Whilst large parts present a particular problem for AM in terms of machine capacity, small parts and particularly small features in parts also present a problem for machine capability; in most AM platforms, the maximum laser focus limit is to a laser spot size of $\sim 250\mu$, located directly below the emitter (i.e. EOS M280, Concept M2) as the beam is reflected toward the extremities of the platform, some defocussing can occur (Bi et al., 2013), distorting this profile and its interaction with the powder bed. This combination of features limits the minimum producible feature to $\sim 300\mu$ (on standard, non-high-resolution platforms) when built up in the build direction and $\sim 200\mu$ in other orientations. Additionally, there is also significant material sensitivity to laser ingestion which further alters the minimum producible features in accordance with the material, laser type and processing parameters (Mertens et al., 2017).

In addition to minimum feature size and maximum part size, there are other geometric limitations to the producible features in AM. Foremost amongst these are its inability to produce enclosed voids or sealed structures. While the AM process can certainly produce the feature, the powder contained within the void/pocket would be entirely contained and thus irremovable without some form of post processing. Should such a void be required, it is advisable to place a pair of diametrically opposite holes of no less than 2mm (Laser) and 4mm (EBM) to allow for powder removal.

Larger non-PBF AM systems such as Norsk's Plasma Transfer Arc are capable of producing significantly larger components ($>1m$), but suffer from many of the same problems associated with the scaling of PBF, namely residual stress formation and part distortion (Muir, 2016) as shown in Figure 9. Whilst these inherent AM problems exist, the likelihood of production of large parts via AM remains small.

2.1.4.3.2 Feedstock Material

Uniformly, one of the greatest disadvantages of AM is its high feedstock cost in relation to Airbus Standard plate material (wrought titanium plate). Table 3 shows a comparison of six material supply conditions along with their €/Kg and availability. The reason for this high cost stems from the manner in which the feedstock is currently manufactured. Regardless of the eventual AM feedstock product (though there are additional complexities with powder), the manufacturing of that feedstock starts

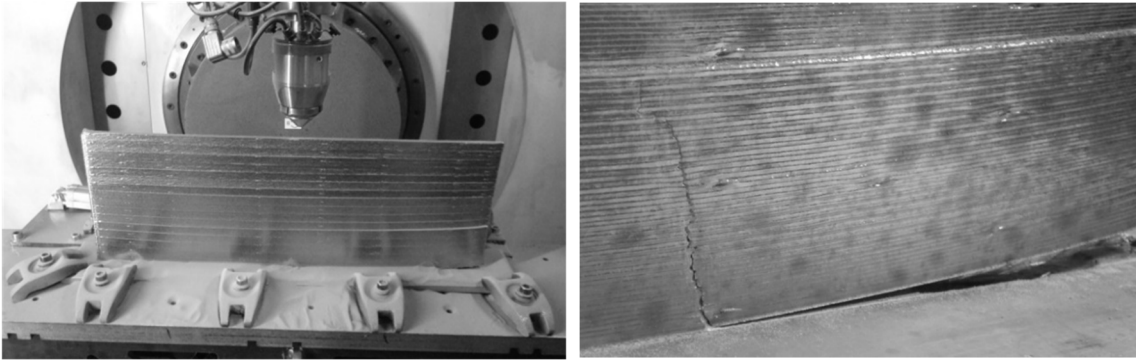


Figure 9 - Irepa Laser test wall from AMAZE showing residual stress fracture due to part length

with the plate material, material which would ordinarily be used to conventionally machine a component directly from that plate. Thus an additional (more commonly, several additional) manufacturing phase is added to the process required to create material from which one would normally manufacture.

Table 3 - Comparison of material cost and availability (assuming stock availability)

Material Type	Cost (€)/Kg	Availability
Bulk ti	18	4 weeks
AS Ti64 Ingot	31	6 weeks
Rolled Ti64 Plate	55	12 weeks
Ti Block Forging	120	40 weeks
Ti64 Wire	120	2 weeks
Ti64 Powder	150	2 weeks

In the case of wire manufacturing, the process is less arduous and expensive than it is for powder as the manufacture of welding wire, performed for over a century and as such is well established and understood. Thus the costs, whilst still high (especially for titanium), are lower than for other methods of AM feedstock creation (Cunningham et al., 2017). AM powder can be created through a number of different methods (Ahsan et al., 2011) using a variety of feedstock materials to initiate the process (Dietrich et al., 2016). Whilst each has specific advantages and disadvantages, they are all expensive, consuming substantial amounts of energy and requiring substantial post processing to be suited for AM (Zhong et al., 2016). The major limitation of powder creation is in the distribution of particle sizes (the yield), produced during each atomization cycle (Wohlers and Caffrey, 2015). The almost Gaussian distribution of particle sizes range from the minimum producible (10 μ) up to approximately 145 μ with the vast proportion occupying the 65-95 μ range (Slotwinski et al., 2014). Problematically, the vast majority of AM

platforms use powder in the 25-55 μ range for production (smaller powder does not flow correctly and larger powder doesn't layer or melt correctly) (Mindt et al., 2016), thus leaving almost 70% of the atomised material unrequired. As this unrequired powder has a limited market, it must be either utilised where possible (Powder HIP or Metal Injection Molding) or recycled at a substantial loss. Thus, the full cost of the material and its atomization is borne by the 40% which is sold to AM, thus increasing its base cost.

2.1.4.3.3 Pre-Processing

The following section details the pre-manufacturing phases required to prepare a metallic component for manufacture via AM.

2.1.4.3.3.1 *Orientation Selection*

Like most forms of manufacturing, the production of a component via AM requires some pre-processing of the part in order to maximise the likelihood of a successfully completed build. Foremost amongst these is the selection/determination of orientation of the production part with respect to the build-up direction. Historically orientation has been performed by highly experienced AM technicians and machine operators, due largely to the vast complexities of part production via LASER PBF (Section 2.1.4.2.1.2). Part orientation must be performed initially on a part level and then, on a build level (all parts of a build) in order to account for aspects such as powder recoating, energy density and laser scanning. More recently, software tools have begun to emerge which promise to deskill/automate the process of orientating a part (not yet a full build) within a certain degree of accuracy (Das et al., 2015). Currently, the means by which orientation is optimised are based largely on the minimization of down-facing surfaces (Muir et al., 2014) in order to reduce the amount of required support material. Problematically, whilst a reduction in supports through the minimization of downfacing surfaces is beneficial to the AM process, it does not address the major cause of AM build failure, RS, meaning any automatic orientation selector may still select a bad orientation.

2.1.4.3.3.2 *Generation and use of Support Structures*

After design and orientation of a part ready for AM, any features which would be introduced as islands prior to consolidation, or which feature a surface normal at an angle of less than 45° from the build plate, require a means of introducing them to a particular layer of the build without distortion or risk of recoating damage. Required by all AM metallic techniques for a variety of different reasons, support structures (SS) are concurrently and coarsely deposited, sacrificial metallic structures which allow these non-ideal CAD entities to be introduced with a degree of control to the layer-wise deposition process. Controlling both distortion and surface

introduction (Strano et al., 2013), SS are additionally used to provide stability to structures susceptible to damage during recoating or which are possessing of high aspect ratios/surface to volume ratios (Everton et al., 2016). Until recently, support structures have been either manually design by skilled AM engineers, or, uniformly applied based purely upon parameterized, projected sketch profiles, defined by the surface normal orientations of the input STL file (Kuo et al., 2017). The former method of application is extremely costly both in general application time and the requirement for highly skilled personnel. Additionally, its success is reliant upon skilled application of AM experience in order to ensure build success; It is highly variable, and thus still fallible. Unfortunately, the second, uniformly applied method leads to excessive material waste (Ford and Despeisse, 2016) due to extreme densities of sacrificial support structures, longer build times and, by not directly addressing the formation of stress within the build-up part, may still fracture leading to build failure. This is the current state of the industry (Wright, 2015).

Recently however, research into the modelling and simulation of the AM build environment has allowed for the possible mathematical prediction of stress and thus the mathematically determined placement and sizing of required supports (Neugebauer et al., 2014). Regardless of their future, the requirement for supports and for the pre-assessment of the part will, perhaps always, lead to a considerable requirement for pre-processing and analysis in order to ensure a successful first time deposition. The nature of this requirement may not be a particular economic factor for serial part production in which a single analysis and support construction phase can be shared across multiple builds. However, for some applications, e.g. a rapid spares shop or lineside production model (Khajavi et al., 2014) in which each part and combined build requires a new analysis the costs could prove prohibitive (Holmström et al., 2010).

2.1.4.3.3.3 Simulation and Modelling of Additive Manufacturing

Due to its unique layer-wise method of material creation and part manufacture, the intricacies of AM must be simulated at a level which can capture the localised time sensitivities of material deposition in order to determine the formation of RS and distortion at each time stamp of the build process. Problematically, this requires a very complex analytical process in which a non-linear, kinematic analysis which includes thermal modelling with creep to a stress based cooling model using eigenstrain modelling at each defined sampling (number of layers) level. The simulation is both costly (in terms of hardware and software costs) and time consuming (CPU Time), thus making it more suited to an environment where other methods (such as repeated builds) cannot be cost effectively employed. In a rapid prototyping environment, right-first-time manufacturing is crucial to achieving a certain price point. In this situation where myriad different

component geometries will be seen on any working week and where a single failed component may delay a whole build with hundreds of parts, simulation may be advantageous if run times can be reduced.

2.1.4.3.4 Rate of Material Deposition

One of the significant limitations of AM (particularly in PBF) is its rate of material deposition (the rate at which a part can be constructed). The rate of deposition varies from process to process, but is usually highest in WF techniques (i.e. Norsk (Almeida, 2015)) and lowest in PBF methods (i.e. Renishaw (Pinkerton, 2016)) with BP occupying the middle ground (i.e. Trumpf (Candel-Ruiz et al., 2015)). When considering AM for serial production, a careful assessment of the part to be built, must be undertaken. Size, shape, nestability and required production rate must all be accounted for during this initial analysis phase, in order to determine if AM can be practically applied. The rate of material deposition has a particular effect on the rate of available production. This rate cannot easily be offset in either WF or BP methods through careful build nesting and must be accomplished by either multiple parallel processes or investment in multiple build platforms. Furthermore, whilst rate of deposition is easily compared between processes, the accuracy of that deposition must be cross compared to the deposited shape vs the design shape.

Currently, when comparing parts which could be effectively built using either EBM, WF or BP, their effective buy-to fly ratios for the as deposited parts are 1.125:1, 3:1 and 2.25:1 respectively (Figure 10). Obviously, this ratio will alter depending on the part being deposited. The component in Figure 10 has a high surface to volume ratio and thus lends itself to a process with near-net deposition capabilities; conversely, a component with a high volume to surface ratio would almost certainly favour DED techniques due to rate of deposition. Regardless in such circumstances as the component class in Figure 10 and despite the higher cost of material for both the PBF and BP approaches, the total amount of material required for deposition is substantially lower when using PBF, thus making parts built using these processes cheaper to produce.

2.1.4.3.5 Post Processing

Upon successful completion of an AM build, a series of post-processing activities must be undertaken in order to facilitate the final delivery of the part these consist of: Stress relieving heat treatment, Hot isostatic pressing and support removal.

2.1.4.3.5.1 *Stress Relieving and Heat Treatment*

Upon completion of almost any AM build (the exception being of those performed at significantly elevated nominal temperatures e.g. ARCAM EBM), significant residual stresses will have been accumulated within the deposited structure and build plate (Sillars et al., 2018). It is imperative that stress relieving (prior to removal of parts from the build plate) is performed with alacrity after build completion due to the high likelihood that the part will fracture from its supports or the build plate if left for any length of time (Figure 11). Whilst stress relieving must be completed quickly after build, heat treatment can be performed at any point after build and even after removal from the plate.

Numerous heat treatment methods are available for each material type deposited and each can result in demonstrably different material properties dependent upon the atmosphere, heat and cycle time utilised (Venkatesh et al., 2009).



Figure 10 - Airbus Demonstrator component made by Norsk Titanium

2.1.4.3.5.2 *Breakout and Support Structure Removal*

Upon completion of an AM build, recovery of the unused feedstock, removal of the build from the machine, removal of the support structures and finally, removal of the part from the build/substrate plate must be performed in series. The most time consuming of these actions is the removal of the SS and the clean-up of the attached surfaces. Careful consideration of the part orientation along with

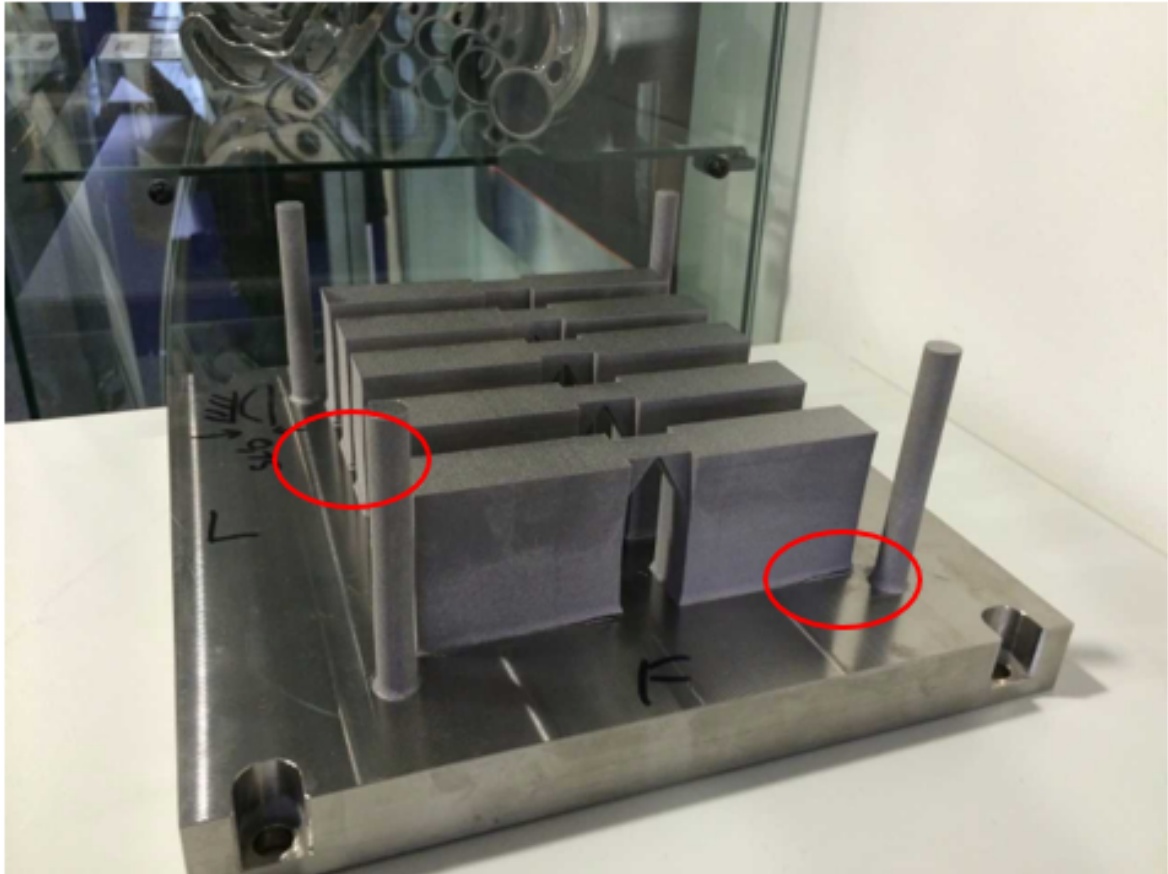


Figure 11 - Cracks in as deposited samples (InSiGen Project) which occurred after build completion.

the simultaneous design of both the part itself and the supports which introduce it is critical, and can substantially minimise this post-processing phase and thus, the cost of part production (Muir et al., 2014, Campbell et al., 2012).

2.1.4.3.5.3 Hot Isostatic Pressing (HIP)

HIPing is a process in which a (usually metallic, but can be ceramic) component is subjected to a slightly alternating isostatic pressure whilst simultaneously being subject to an extremely high temperature, just below the materials primary transition temperature (Antony, 2012). For titanium, the nominal parameters for this are 820°C and 1.02bar of pressure. The primary purpose of HIP for AM is to close any entrapped porosity present in the deposited part thus ensuring both full material density (not the 99.5-99.7% common in as-deposited AM parts (Tammas-Williams et al., 2016) and that fatigue endurance is dramatically increased. HIP is a now commonly applied and cheap post process for AM and whilst it does lower material properties (Mower and Long, 2016), the benefits of applying the technique vastly outweigh the drawbacks.

2.1.4.4 Certification and Standardization of Additive Manufacturing

AM, like any manufacturing process, must be deemed safe for use in the manufacture of components for civil aircraft. To achieve this, a manufacturing process qualification must be undertaken under the guidance of standards created by/in partnership with standards bodies. To certify a process for the production of flight parts, each aspect of that process must be performed according to the standards defined by the governing regulatory bodies such as the European Aviation Safety Agency (EASA), Federal Aviation Administration and the Civil Aviation Authority. For a conventional manufacturing process such as casting or machining, process certification requires considerable effort for the first application of the technology, but subsequent, derivative processes can be qualified using delta-quals (partial qualifications) which prove compliance to the already established process. In these archetypal process, there are few steps which require monitoring as their effects on the bulk material properties are negligible. Problematically, AM, as the name implies, is an additive means of component creation and as such, does not extract a component from an already materially complete billet. Instead, during the process of component creation, AM simultaneously creates a new material from the feedstock provided by the deposition process. This means of producing components creates a number of additional complexities which must be quantified and controlled, and done so in a manner which conforms to measurable standards. Without this, assurance of construction robustness and conformance from build to build and part to part is difficult to establish.

2.1.4.4.1 Material Performance and Qualification

In order to design and certify components for flight, the mechanical properties for the material from which the component is to be made, must first be determined and design allowables established. As previously shown, mechanical properties for even a single material, such as Ti64, can vary dramatically dependent upon the method of manufacture and heat treatments applied. As a layer-wise production method, AM can make use of multiple manufacturing methods, on myriad different production platforms, thus presenting additional complexities which must be exhaustively evaluated before design allowables can be released. Considering for the moment only a single manufacturing process - EBM, and a single production platform for that process - an ARCAM A2; the platform has a working volume of 210x210x320mm (XYZ) meaning that titanium material can, at various points of the build, be created anywhere within that volume. A component built within this chamber may occupy a substantial part of its volume and thus, one must ensure material conformance everywhere within it. This means that any mechanical testing method must for example, ensure that material deposited at the start of the build, in the lower left hand corner, has identical (or at least statistically similar) properties to material deposited at

the end of the build in the upper right hand corner. Furthermore, one must ensure that not only do the mechanical properties correlate, but that the chemical composition and any propensity for defects is similarly matched. Additionally, one must consider the effects of component orientation within the chamber and its potential to affect the results of mechanical testing. Consider, a tensile specimen orientated with its longest length parallel to the y-axis and thus parallel to the re-coater's traverse path. In such an orientation, and assuming a slice thickness of 50 μ a 13mm diameter tensile sample would be comprised of over 260 manufacturing layers. Should the sample be re-orientated such that its longest length is in the Z direction (build-up direction) the specimen length of 98mm would require the deposition of almost 2000 layers. In the first orientation, the part would have fewer layers, but each would have a greater scan area leading to greater energy density per layer (Tapia and Elwany, 2014); (Everton et al., 2016), in the latter sample there is less energy per layer, but almost 10 times as many required layers. The first sample would be more likely to suffer degradation in chemical composition and distortion due to residual stress, whilst the latter sample is more likely to encounter a defect due to recoating such as a lack of fusion defect (Wycisk et al., 2014). In order to ensure that material properties are exhaustively proven and statistically stable, a stable baseline must be first established, in this, the default material melt and processing theme for a AM platform intended for certification are frozen. A material testing matrix is then used to determine the effects of orientation and location within the build volume of a particular platform. Samples are then produced (in multiple builds), tested and compared to an established material database for other AM results. Should the results of this testing meet or exceed the established Airbus Material Specification (AiMS) with statistical significance, the platform can be qualified for the production of certain classes of parts dependent upon the mechanical testing samples produced and tested.

2.1.4.4.2 Process Standardization and Qualification

Like any system tasked with the delivery of an output product, the quality of those outputs are dependent on the quality of the inputs to the system (Garbage in Garbage out GIGO). Unlike many manufacturing processes which have few inputs and process variables, AM has substantial quantities of both, each of them linked and each a potential source of non-conformance during the manufacturing phase (Figure 12). Through extensive testing and development, Airbus has determined that high degrees of standardization, operating alongside tightly confined tolerances for input and process variables for each phase of AM are required in order to achieve stable mechanical properties from multiple AM platforms. For each phase defined in Figure 12, a process instruction exists and must be followed in order to prevent the degradation of either produced material or geometric conformance of the as-deposited parts. Whilst these required

processes would appear to indicate fragility, the necessity for rigid controls stems from both the strict requirements of the process itself, along with the highly serialised nature of its inputs; it is not from inherent unreliability in the system. The nature of this serialised, repetitive process means that the effect of minute, cumulative errors can, due to the huge number of iterations in the process, quickly lead to critical errors, hence the need for control and monitoring. In a conventional manufacturing process, such as CNC machining, a large billet of titanium is delivered to the machinist, the delivered material comes complete with a certificate of conformance stipulating its adherence to a defined material specification. The creation of parts from that delivered material is performed in accordance with an AIPS which allows for the extraction of that part at certain cutting speeds, under certain coolant flow conditions, so long as certain geometric criteria are applicable to the part being created. Upon completion, the Certificate of Conformance, plus adherence to the AIPS (Airbus Process Spec), coupled with simple geometric checks (against engineering drawings) on the final component, would be sufficient to guarantee conformance against both AIMS (Airbus Material Spec) and AIPS, thus allowing for Airbus acceptance of the part for use and eventual flight.

The conformance documentation from each stage along with evidence of process controls and their effectiveness would also be sufficient to allow for regulatory certification of both the manufacturing process and the parts made using it. In most circumstances, a large billet of delivered material would not be consumed by the manufacture of a single component (except in the case of ribs, spares and major landing gear components), but would be apportioned based on nominal external dimensions for a series of parts and then reduced to reveal the final part. In this manner and so long as the unworked, remaining material is free from visual defects and is not subject to volatile chemicals and heating, the entire billet can be apportioned and utilised until nothing more can be extracted; no further material conformance is required. Material removed from that billet during machining (swarf) will be sold for scrap due to the potential risk of particulate inclusion or the contamination of the previously conformal material and can thus be discounted as a source of potential contamination. Though waste in this process is extremely high, the process and conformance methods required for certification are simple to establish, easily followed and most importantly easy and cheap to operate effectively. When coupled with a relatively low material purchase cost per/kg, some of the reasons for the ubiquitous use of CNC machining for titanium parts becomes apparent.

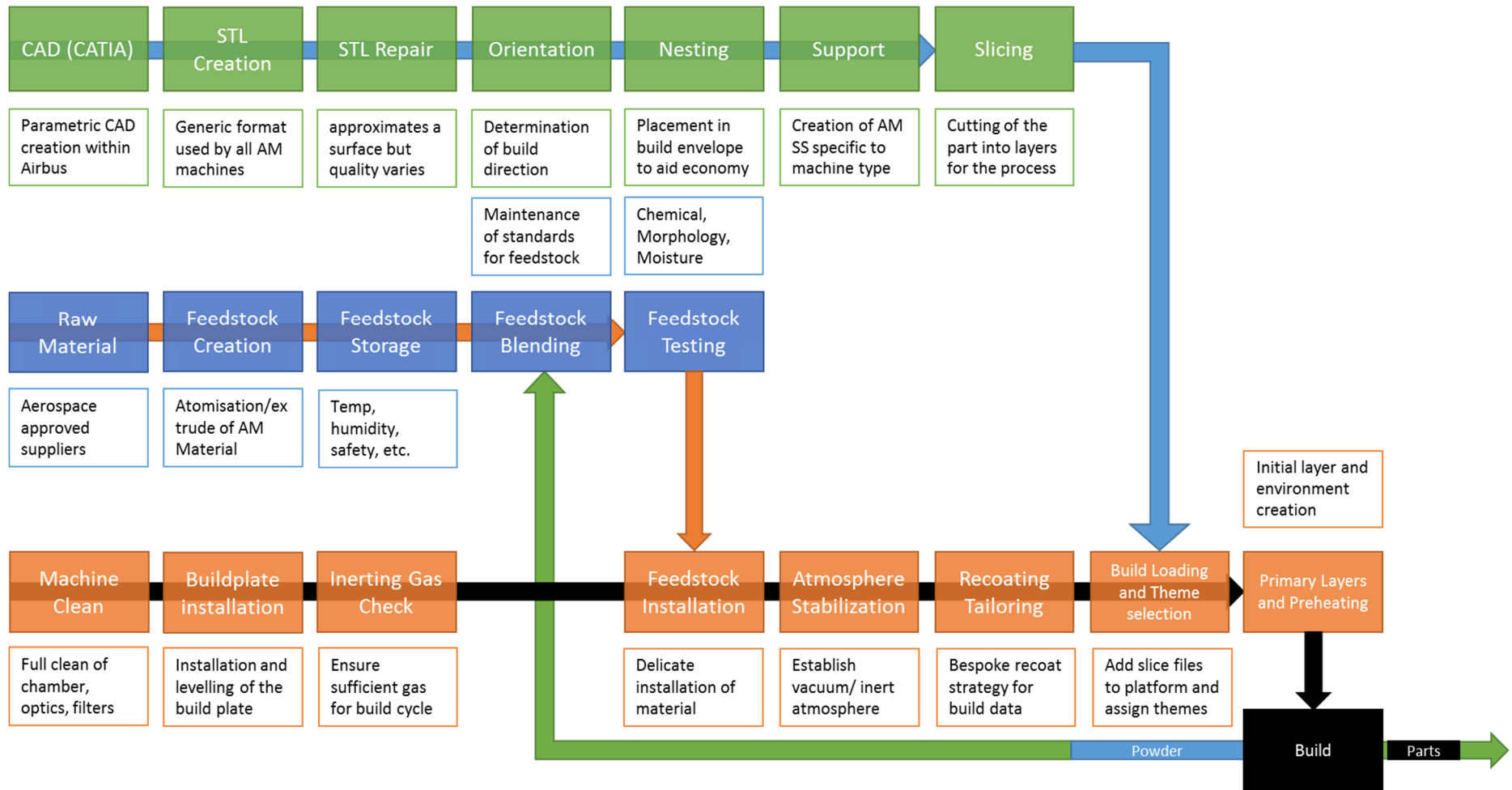


Figure 12 - AM Manufacturing flow process showing the digital (top) material (middle) and platform (bottom) process stages

The addition of extra process controls for AM are in order to ensure continued conformance of the feedstock material and platform during each of the extended processing phases associated with AM. Due to its enormous surface to volume ratio, and the extent to which AM powder can be affected by inappropriate storage conditions, methods of maintaining a powder's moisture content must be developed and taken into account (Spierings et al., 2016). Furthermore, and unlike conventional techniques in which the material removed during construction is both in a different form from that supplied, and, potentially contaminated after use, PBF AM attempts to reclaim ALL unused powder for recycling and blending prior to reuse. Unfortunately, AM powder can become slightly oxygenated during build (Yan et al., 2014) and thus would, during multiple uses eventually move out of specification and thus be scrap, by blending this material with highly controlled, unused material, conformance with specification may again be achieved. Unfortunately, by choosing to re-use and thus having to blend powder in order to ensure good build economics and high environmental efficiency, additional sources of variation are introduced, thus requiring more rigorous process control. Therefore, in order to qualify an AM process for the production of aerospace componentry, the standards/processes required to ensure rigorous control must be first developed, then tested and proven effective to the satisfaction of regulators and standards agencies.

Problematically, unlike CNC machining, which has largely homogeneous manufacturing methods regardless of machine vendor, the intricacies of AM can be applied in a multitude of ways during production (Wohlers et al., 2016) all of which can dramatically affect the resulting output from the platform. This level of platform variability means that process knowledge derived for a particular platform cannot be (on the top level) transferred to another platform vendor's architecture. However, despite the myriad AM platforms, many of the standards and processes developed for powder handling, recycling, storage, testing, blending, etc can be applied to multiple materials and feedstock types, thus simplifying the process of certification. Additionally, whilst the top level data for validation of a platform's manufacturing capabilities cannot usually be transferred, the lower level data, the methods and means of testing can be transferred and quickly adapted from another, certified platform in order to measure the metrics of the new one.

Currently Airbus has qualified four different AM platforms for the production of Class 1 and 2 components from Titanium Grade 5 alloy. Each of these qualified processes follow the develop AIPS specific to the process that has been qualified, along with the generic pre and post process API (Airbus Process Instruction) methods which are used to control feedstock, digital data, and atmospherics for AM. Together these process documents will contribute to the AIMS

which details safe material allowables for the design of components built using additive manufacturing. Some of this data will be important for the development of any method intended to use design optimization as a means of designing parts to be built using AM.

2.1.4.5 Additive Manufacturing and its Effects on Design

As previously noted, AM has been identified as a tool for change in commercial aerospace, not only in manufacturing, but foremost in design and the potential advantages offered through design flexibility and freedom. Whilst the above statement is certainly true, the earlier sections detailing the disadvantages of AM also hold true. Indeed, AM's major strength lies not just in the removal of *physical* constraints but also in its relaxation of the economic constraints upon design and manufacturing (Muir, 2017). Section 2.1.2.1 referred to the limitations placed on component design through the use of global design rules for individual aircraft programs, and how the decisions regarding the restrictions within those rules were based upon a careful balance of performance and cost. Many if not most of these restrictions are employed in order to limit the number of required machining operations (stop, position, start) and the number of specialist machines (4+ axis) required to complete the final part geometry, thus minimising machining cost. Uniquely, AM can (if designed correctly) provide for a level complexity beyond that available through the use of even the most advanced multi-axis systems in the marketplace and can do so at little to no cost increase (and sometime a cost decrease) over a simply designed, less optimal component with more redundant structural mass. However, whilst limitations on certain economic constraints of manufacture can be relaxed or even (dependent upon the conditions) removed entirely, constraints upon design, inspections and conformance, can and must exist. Ultimately, the critical features of any designed part must still be capable of being captured on a technical drawing in order to allow for inspection/measurement and thus determination of manufactured compliance. Beyond economic constraints, AM allows for substantial relaxation (but not complete removal) of the need for conventional machining access (the machine head/cutting face) to conventionally pocketed areas of the part. What the use of AM does not remove for components intended for commercial aerospace is the requirement a high degree of tolerance on areas where the part interfaces with other components or systems. In these regions, a requirement for post-build machining exists and access to these areas must be accounted for when designing the part.

Example - in almost any manufactured component there will be certain regions of that component (usually where there is an interface between another component/system) that require a high degree of tolerance, and certain quality of surface finish; As-built AM cannot provide for this (Brajlih et al., 2011). Commonly the feature tolerance of AM for the majority of

PBF platforms is +/-250 μ (i.e EOS M280, Concept Laser M2, etc.) with nominal surface roughness of approximately 30-60 μ dependent upon process and orientation (Kaji and Barari, 2015). Whilst most AM features are much more accurate than the 250 μ figure would tend to imply (this is usually a global measure of total part conformance), the surface roughness alone is enough to guarantee a requirement of post process machining of any identified key interfaces in order to ensure conformity of manufacture to design intent. As such, CNC machine access to certain areas of the part must still be considered, thus adding constraints to both design and manufacturing.

As alluded to earlier, design complexity is the key area in which AM can offer benefits beyond those of conventional manufacturing and can do this in a number of ways: The first is in terms of absolute capability; due to its ability to manufacture at a minute level and (in areas which do not require post machining) to do so with little to no limitations on shape, geometry which would have been previously discounted as too complex, is now realistically feasible. The second is in terms of economics; in some cases, complex designs may still be capable of being manufactured (perhaps not to the same extent as with AM, but close enough to compare), but the cost to do so becomes economically prohibitive due to spiralling part cost as a result of additional operations, tools, etc. (Muir, 2017). Only for critical applications in which performance *and* mass reduction are highly sought would such a design normally be created. Applications such as Satellites and launchers in which the mass penalty incurs a higher cost to the launch than the manufacture of the complex part are a prime example of this trade (Booth et al., 2016). Conversely, complexity in AM is consistently stated to come largely for free (Vaneker, 2017, Wong and Hernandez, 2012) as there are few/no moving parts or machine operations required to enact the complexity of manufacture. There are some additional costs for processing such as beam-time related to surface melting (Rosen, 2014) and surface area to volume ratio, but these are small in comparison to conventional manufacturing (Baumers et al., 2016).

2.1.4.6 Novel Design Enablement Through use of Additive Manufacturing

AM is capable of manufacturing features previously considered to be impossible through use of conventional methods. The types and complexity of structures now considered feasible through AM, particularly using PBF methods, are myriad and whilst an exhaustive description falls outside the scope of this report, some examples should be showcased in order to highlight the benefits and potential constraints for later in the project. One specific area of interest and growth has been in the field of microstructures/cellular lattice type structures. Lattice type structures have been used predominantly on spacecraft and high performance vehicles where stiffness to weight/thermal/energy/performance overrides any economic restrictions imposed by the extreme cost of assembly and inspection. Now, with the advent of layer-wise processing on a

macroscopic level offered by AM, the true potential for the development of microstructures can be realised (Yan et al., 2012). The idea of lattice structures is not new (Dong et al., 2017) and whilst it has shown some theoretical benefits for mass reduction (Pettersson, 1996) and redundancy (Kocvara and Stingl, 2008) compared to a conventional structural layout, replicating the lattice in the real world has been difficult unless constructed on a large scale thus reducing the benefits (Chen, 2016). Now however, lattice type structures produced via AM are starting to be used for true replication of the ideas surrounding the Variable Thickness Sheet methods with partial density represented through modification of the lattice unit cell (Haslinger et al., 2010). Figure 13 shows the result's uniform microstructural definition, manufactured by AM.

Like microstructures, AM is capable of creating complex internal pathways within a structure. These pathways can be as small as 100μ in diameter (dependent upon the material) and can be manufactured at multiple angles and rates of curvature, thus enabling for complex internal fluid channels for conformal cooling and flow measurement in highly tailored aero-structural applications such as heat exchangers and manifolds. In addition to the above, and in carefully applied methods, AM can be used to adapt structures and preforms made with existing techniques with the added complexity features offered through AM. This hybrid approach to manufacturing may represent one of the most cost-effective means of applying AM advantages to parts which would prove economically unfeasible in most circumstances. Hyperpins are small, titanium (though they can be other materials) arrowhead pins between 1mm and 4mm in length. Their purpose is to create a bondless mechanical interlock between a metallic bracket and a CFRP panel. They are produced via AM, pressed at temperature and resonance into uncured CFRP and then co-cured to create a hybrid joint with phenomenal mechanical and electromagnetic properties (Parkes et al., 2013) (Figure 14). Whilst it is of course possible to produce the entire bracket with its associated pins using AM, in some cases, the larger bracket design is so simple, that it can be made from thin plate and cheaply stamped and bent into the correct shape. Obviously, this cannot be done for the pins themselves, but through the creation of bracket specific tooling, the pressed/stamped brackets can be emplaced within an AM build chamber and have the pins deposited onto the required surfaces.

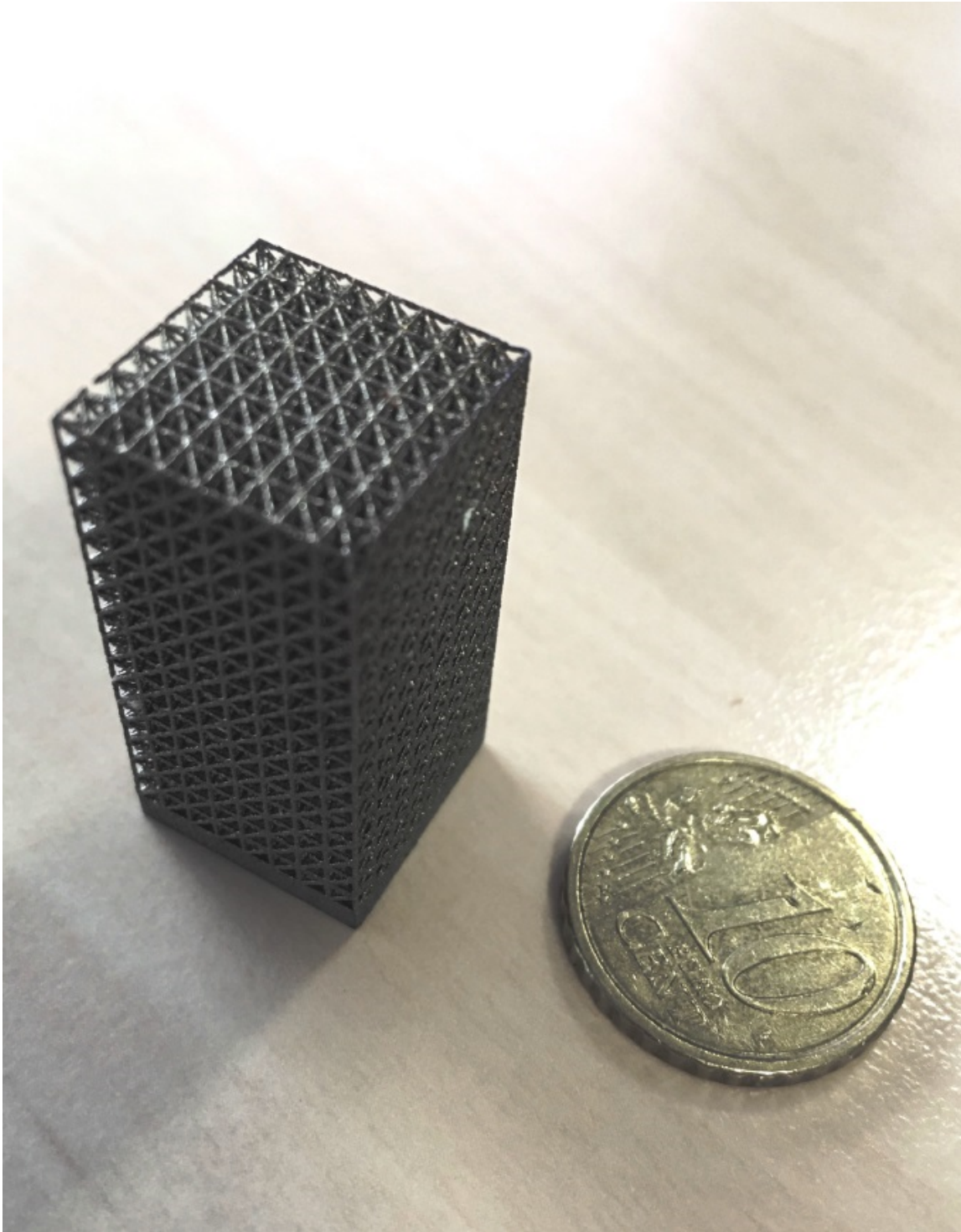


Figure 13 - Uniform micro-lattice by PBF AM

This minimises the requirement for expensive AM material to only the features which truly require it, thus maximising the benefits of AM whilst minimising the part cost.



Figure 14 - HYPER pins embedded into CFRP leading edge wing skins

The above examples represent some, but by no means all of the potential for novel design development enabled by use of AM.

2.1.5 Design for Additive Manufacturing

As showcased in the previous sections, novel design enablement is a key benefit of AM, but whilst the relaxation in design constraints can allow for novel developments, use of AM must be carefully applied especially when the limits of process capabilities are being explored.

2.1.5.1 Layer-wise Construction and the Effects of Build Orientation

When considering the conceptual design of a part intended for construction using AM, prior determination of an approximated build orientation is a crucial input into the design process. Build orientation is an attribute which is (largely) unique to AM and one which has multiple factors which are influenced by its alteration. Surface roughness, nesting, support requirement, and build time are several factors directly affected through any change in build orientation (Muir, 2015). Additional to these are some small material property and microstructure changes in as-built AM components/samples. Whilst most of these factors are affected by a change in orientation, few if any of them are critical to the successful completion of a build should they be shifted toward their extremes (Hernández-Nava et al., 2016). Conversely the one factor of

orientation which can have a significant effect on build success, relates to the rate of change of area in proximate layers, and the connectivity changes between areas in each layer (Figure 15). In terms of physical effects, the results of unconsidered area changes can lead to significant increases in residual stress/over-melting, resulting in either complete build failure or a lack of geometric conformance. Knowledge of, and subsequent tailoring of the orientation allows for either mitigation of the factors which would cause build failure, or, where not possible, the bespoke redesign of the part allowing for the controlled introduction of potentially build threatening features during the layer-wise deposition process. Figure 16 shows how a poor combination of design and orientation can lead to significant build problems in both laser and EBM PBF processes, with the former depicting failure due to residual stress and the latter showing swelling/over-melting of the part due to poor thermal dissipation. Contrastingly the same part can be built correctly with either the application of more support, a slower recoating speed or a gentler melting theme.

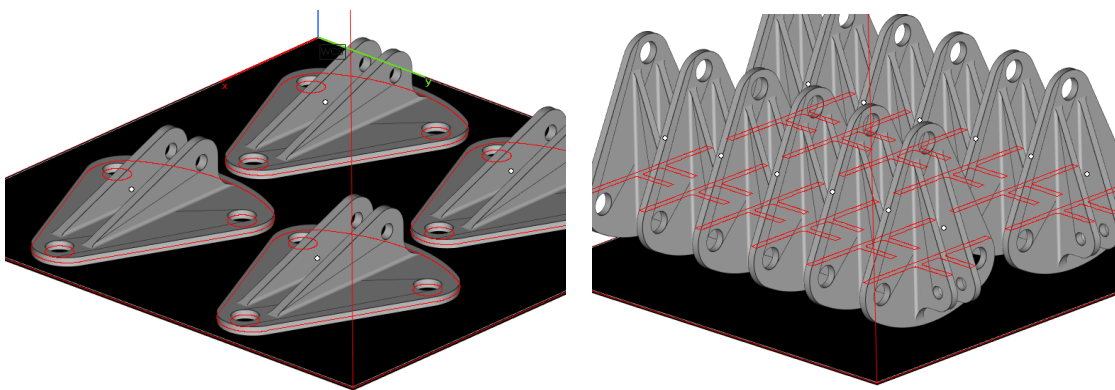


Figure 15 - Showing the effects of altering orientation on both build economics (numbers on the plate) and scan area (red lines).

Bridging, or the confluence of several previously distinct melting areas into a single profile during deposition (i.e. depositing the 3 legs of a tripod – eventually, they will meet as one profile) can lead to significant increase in potential for residual stress (Internal Airbus COBRA tool), and also to the presence of undesirable witness lines in manufactured parts. Bridging is also common in pipes or arches which are parallel to the build plate and exhibit themselves as a collapse or ovalization of the hole under deposition.



Figure 16 - Overheating of the deposit caused by a combination of inadequate thermal dissipation and fast scan and recoating strategies

The effects of these features can be controlled through either the addition of supports intended to aid feature introduction or to resist residual stress; a more considered approach to the feature introduction problem is through careful redesign of the troublesome feature in order to best suit manufacture by AM. There has been significant research and development within Airbus concerning the formation and effects of residual stress in AM, but none is published due to the sensitivity of data and the difficulty in protecting it for public disclosure. The Airbus AM design principles and the in-development COBRA tool are the prime carriers of the summary of these investigations.

Whilst an ill-considered build orientation in AM can lead to significant problems, careful consideration of build orientation can be used to harness additional capabilities from the unique layer-wise build-up process. When designing for layer-wise manufacturing, consideration of the manufacturing resolution of each layer (specific to the manufacturing platform) should be given weight. If harnessed correctly, the minimum feature capable of being deposited at angles close to parallel with the build plate can be as little as 75μ . This metric is significantly less than the minimum wall thickness allowed by machining (Polishetty et al., 2014) and almost 2/3 less than the minimum manufacturable wall constructed using AM when perpendicular to the build plate, thus extremely delicate structures could be deposited in this orientation when previously impossible in a more conventional manner (a wall is usually built up, not across).

2.1.5.2 Feature Changes for Additive Manufacturing

Redesign of a structure for a new manufacturing process is often not as simple as a CAD re-design of the part. This is particularly true in commercial aerospace where consideration of the downstream effects to functionality must be evaluated and proven acceptable to regulatory bodies. When altering any component to suit a new manufacturing process, continuous consideration of its post-build application and post-process requirements (Figure 17) are paid particular attention, often taking priority over manufacturing necessities. Due to its build-up method of construction, AM performs best when features are introduced gradually allowing each new feature to be spawned from and thus remain connected to the main part mass. This almost organic means of construction allows for careful control of emergent features in a way that can enable self-support. Self-supporting features, can if designed correctly, significantly reduce the amount of required SS required during build for a modest increase in part mass (Muir, 2015). Doing so, whilst technically decreasing part optimality from a performance standpoint can yield tremendous benefits from an economic one, decreasing time required in post processing and material waste. Parts designed using this philosophy will often most closely resemble a tree with the large trunk (the main body of the part) leading to the branches, each of which supports further aspects of the final part. Most structures have the greatest detail on the periphery, however systems components do not always benefit from this approach. During the build phase, it is important that, in as much as is possible, no latter scan layer be of greater volume than the minimum interface to the connecting layer or the sum heatsink capacity of the already deposited structure. This rule ensures that there is sufficient thermal flow capacity to allow the structure to sufficiently and uniformly cool during each deposition cycle. When considering the redesign of fluid carrying channels (a known problem for AM when required to be produced at angles which approach parallel to the plate), it should be noted that careful trade-offs must be applied. Small changes to circular pathways in order to aid manufacturing can lead to substantial increases in both stress and loss within the channels (Muir, 2017). Often, the best solution to the problems of CAD feature introduction in AM builds is through slight modification to the build orientation (Muir et al., 2014), thus altering the bridging/closure of pipe features across many layers, thereby mitigating significant risk of residual stress formation and the generation of witness lines within the part. With build orientation decided, and critical features identified and, in some cases adapted for the AM process, other aspects of the structure/component can now be addressed in order to increase their suitability for the AM Process.

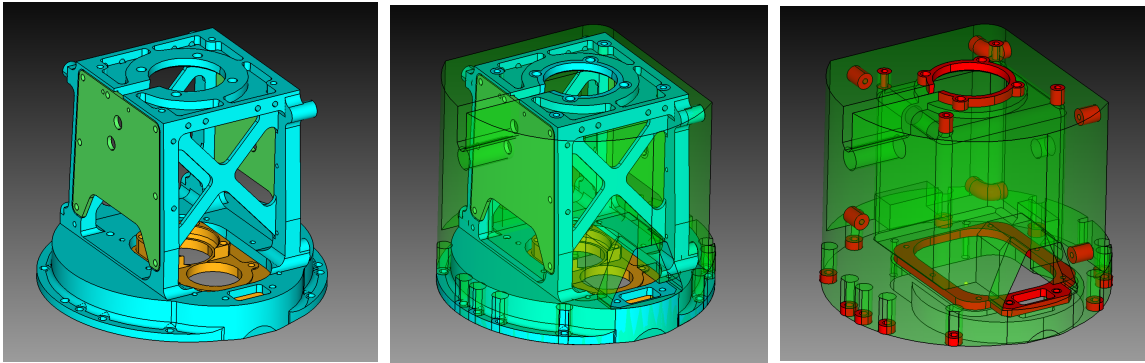


Figure 17 - Analysis of existing part (left) expansion of design space with consideration of manufacturing and assembly (centre) and allocation of non-design areas (right)

In reductive manufacturing, the removal of material incurs an economic penalty, a penalty which increases exponentially as more complicated, lightweighted structural designs require realization through manufacturing. The 80:20 rule whereby 80% of the design performance should be unlocked from 20% of the total potential design effort, (Nisonger, 2008) is commonly applied to structural design and manufacturing and thus extremely optimal parts are rarely realised through machining, especially where cost is of greater/equal importance to performance. Conversely, in AM unrequired material which contributes little to the performance of the part, but is simply there due to manufacturing or economic considerations imposed via manufacturing is an unwanted expense. Having to first purchase (at high cost), then deposit (build and energy cost) and support (larger structures tend to incur higher residual stress) material which serves no performance purpose in a part design can incur substantial costs, cost which are unrequired and can be removed if a determination of where unrequired material can be identified and incorporated into design.

2.1.5.3 Determination of Optimal Material Layout

Lightweight structures have long been a crucial component of many industries, but none more so than aerospace and aviation. In these fields, where performance, in many cases more than cost, is sought at the expense of almost any factor except safety, aerospace engineers have paved the way to novel designs and methods of analysis. In the earliest attempts at lightweight metallic designs (Supermarine 1931), a repeated, mathematically determined placement pattern for truss members was utilized to provide, for stiff, lightweight aircraft ribs intended for use in the fighter aircraft of the second world war the pattern and the profile of each rib and each truss within those ribs was standardised to allow for cheap manufacturing of the members, but higher expensive (in terms of work hours) assembly operations in order to provide the completed ribs. Design ideas and solutions were validated sign beam calculations and superposition (Patel, 1978) to determine approximate performance in each rim and the overall wing. Later, in the 1950s and

with the advent of the jet age and commercial jet transports subject to high loading, requirements and for many years of service, the design of aircraft ribs changed from a truss based design, with a potential to buckling to a web/flange arrangement with mathematically determined lightening holes strategically placed throughout the web stiffness of the rib (Krog et al., 2004).

Again, beam theory, coupled with mechanical testing allow for both design and validation of the resulting designs and thus the methods of lightweighting. More recently and with the advent of cheap, high performance computing, stiff, lightweight designs have taken a further step forward. Using a combination of high definition CAD validated with FEA and realised using high speed CNC machining, incredibly stiff, lightweight, repeat pattern designs have begun appearing on products such as Airbus' A350 in the outboard wing segments (Figure 18).

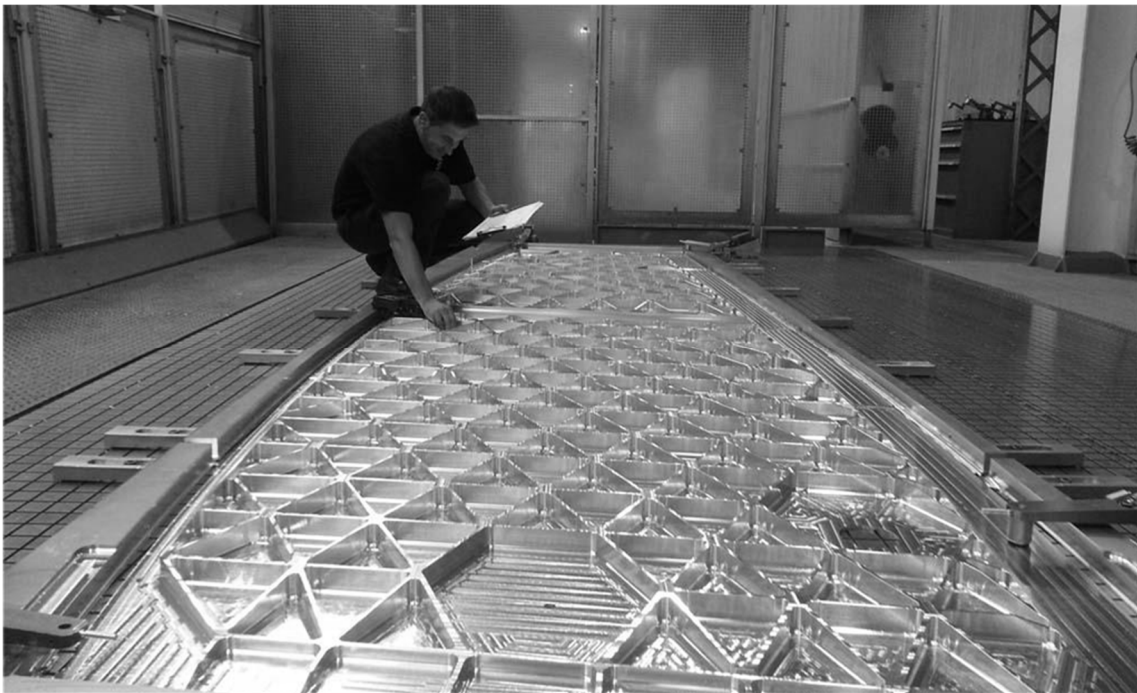


Figure 18-A350 Outboard wing rib complex design

In each of the cases detailed above, conceptual designs were painstakingly developed by skilled engineers, draftsmen and machinists over a substantive length of time. Before starting the design process, a detailed understanding of the flight loads, safety factors and material allowables must be gleaned. Flight loads must then be enveloped in order to reduce their number to a manageable level, able to be solved (or at least validated in the case of A350) using hand calculations and superposition. Problematically, using such an approach, significant safety factors must be included during analysis in order to account for the limitations of the approximation techniques required to design the structural elements. Thus, as structures and their requirements/loading

environments become more complex, the ability of simplified techniques to evaluate their performance and thus design a solution becomes difficult, requiring greater safety factors to account for greater numbers of unknowns (Noor et al., 2000). For aviation, this becomes a problem as increased complexity and thus safety factors equal greater structural mass and a drop in performance. Historically, the industry has circumvented this problem by having structures designed from elements of known performance and linked by designers and engineers of extreme skill and experience in specialist roles (wingbox/pylon/centre wing box, leading edge, etc). Challengingly, as aerospace drives toward more efficient, more cost-effective designs, this segregated approach is a hindrance to progress and so must be challenged through use of newer tools such as Finite Element Analysis (FEA) and Structural Optimization (SO) to provide guidance and validation to designers and engineers. Once designed, the FEA will reveal areas within the design which have the lowest stress, indicating areas which could be targeted for further design improvement and mass reduction. Whilst this method of design is effective, its highly iterative and time-consuming nature tend to preclude its use for small parts. The reason for this is that the effective mass reduction per part (whilst high in percentage terms) is low in terms of total aircraft mass; a quicker means of determining targets for mass reduction and thus an optimal material distribution is required in order to make the best use of AM for small, metallic parts (Muir, 2012a).

2.2 Optimization and its use in Commercial Aerospace and Component Design

Optimization is, whilst not a common tool in aerospace design, a respected method for achieving lightweight designs and solutions to design problems when encountered. The following sections detail the origins, principals approaches and applications with commercial aerospace, where relevant to the scope of this research.

2.2.1 History, Principles and Design Optimization

Originating from the Latin word "*Optimus*" optimization in the modern vernacular is the search for the best possible solution to the conundrum of a particular problem, or, set of related problems.

Historically, the broad field of optimization can be easily and primarily divided in to those methods which address pure design optimization and thus encompassing the ground-breaking 17th-19th century works of Euler, Bernoulli, etc., and those which support numerical design optimization, popularized by the advent of affordable digital computing in the 1960s and 1970s.

Most commonly an optimization problem is formed by the definition of several parameters including but not limited to: the design domain, design variables (4), constraints (2

and 3) and the objective function (1). Together these functions and values combine to create the definition of an optimization problem.

$$\begin{array}{llll}
 \text{Min:} & \min_x f_0(x) & & \mathbf{1} \\
 \text{Subject to:} & g_i(x) \leq 0, & i = 1, \dots, m & \mathbf{2} \\
 & h_i(x) = 0, & i = 1, \dots, p & \mathbf{3} \\
 \text{Where:} & x = [x_1, x_2, \dots, x_n] & & \mathbf{4}
 \end{array}$$

2.2.1.1 Optimization definition – The design domain

Also known as the design space or operating environment, this is the bounding definition for all possible design variables (DV) as defined by the DV range limits prior to the application of constraints.

2.2.1.2 Optimization definition – design variables

A design variable (DV) in the context of optimization is a numerical input which is allowed to vary throughout the design optimization process. In equation 4 the direction vector "x" is allowed to vary in the range specified with an optimum vectoral path x^* defined by the minimum resultant value of all possible values. Commonly DVs are either continuous or discrete, but can also be Boolean, dependent on the situation under study. Invariably, numerical optimization problems with discrete DVs are substantially simpler to solve than those with continuous numerical DVs as the number of potential candidates for the optimal solution is considerably smaller. However, adaptations to discrete problems can be utilized in order to simplify the optimization problem, one such solution is the conformal rounding of DVs associated with closely spaced values (Haftka et al., 1992) Another approach is to deal directly with the discrete data using suitable optimization algorithms and then penalize results which do not conform to bounds of the optimization problem, thereby limiting the number of variables with which the solver has to assess in each iteration (Ramakrishnan and Francavilla, 1974). All of the approaches described thus far, rely on previously defined and somewhat invariant data inputs in order to derive suitable DVs for the optimizer. However, in many modern design cases a complete series of potential outcomes (DVs) are not known, in fact only the limits of the problems are known. This is a problem for the vast majority of optimization algorithms as they cannot perform a blind/randomized search based on random variables (Spall, 2005) due to the inherent uncertainty of such a process. In order to effectively deal with uncertainty in design and optimization it is necessary to move the design

variables from expressions of exact values, into functions extrapolated from the probability density functions defined by their likelihood of constraint infringement. An optimization problem may then be formulated (from either continuous or discrete data inputs) with the express purpose of minimize the probability of design failure. Methods capable of controlling uncertainty within design variables are commonly known as Stochastic Optimization Methods (SOM) and by association Stochastic Programming Methods (SPM) with the latter being referred to as robust optimization based on best and worst case scenarios (Beyer and Sendhoff, 2007).

2.2.1.3 Optimization Definition – Constraints

The majority of design problems are subject to a series of requirements in order for the design to be seen as fit for purpose. These requirements are not the principal design driver, as that role is satisfied by the objective function, however, the additional requirements can have a substantial effect on the finalized design (Sobieszcanski-Sobieski and Haftka, 1997). The effects of constraints upon design can be clearly seen in section 2.2.3. In numerical optimization additional requirements are manifested as a series of constraints (boundaries) which act on the design domain by defining restrictions, areas into which the optimizer (whilst attempting to satisfy the objective function) cannot stray (Bendsoe and Sigmund, 2003). Optimization problems can thereby be classified as constrained or unconstrained dependent on presence/absence of constraints in the problem definition.

Additional to the application of constraints is both the type of constraint used and the manner in which they are incorporated into the optimization definition. Constraints can be applied as either equality constraints or inequality constraints (equation 2). Further to this, the use of equality constraints does not preclude the inclusion of inequality constraints into the same optimization problem. However, prior choice of an optimization algorithm may have a direct effect on which type of constraints are permissible as part of the optimization problem. This problem can be mitigated by the inclusion of slack variables (Boyd and Vandenberghe, 2004) thereby allowing inequalities to be expressed as equalities and vice-versa.

In many cases it is also good practice to normalize constraints in reference to the objective function prior to beginning the optimization process as this can reduce the computational load on the optimizer (Bendsøe and Sigmund, 1999)

2.2.1.4 Optimization definition - the objective function

In its simplest form, the goal of any mathematical optimization is to minimize or maximize a real function through systematic analysis of a set of specified real values (DVs), analyzed as a part of the function, as in equation 1. It is this analyzed function which forms the objective function for any optimization problem. While historically it has been common practice to have a single

objective function bounded by constraints within a specified design domain, the increase in computational power offered to the modern designer has led to more complex design problems being tackled by optimization.

Multi-objective optimization such as maximizing stiffness while minimizing aerodynamic drag and reducing structural mass would be a common multi-disciplinary optimization (MDO) problem facing an aeronautical engineer in the modern age. To contend with multiple objectives, a number of approaches exist; the oldest and simplest is to identify the single most important objective function and to reframe the secondary objectives as constraint variables (Bendsoe and Sigmund, 2003) Another approach is to apply weightings to the objective functions in accord with their importance and to subsequently combine them into a single function as shown in equation 5.

$$f(\mathbf{x}) = \sum_{i=1}^n W_i f_i(\mathbf{x}) \quad 5$$

Finally, and if neither objective function can be transposed into constraints nor separated by importance, the creation of a Pareto-optimal set based on the vector directions for both objective functions can be formulated to address the problem function. These Pareto sets conventionally form a frontier upon which the various combinations of minima for each objective function, in respect of its partner function can be found. The Pareto front shows the complete relationship (not simply a single combined minimum point) between the two objective functions allowing for analysis of multiple design points. All are optimal dependent upon the weighting applied to each function.

2.2.2 Approaches to Design Optimization

Currently there is no single optimization technique which is demonstrably superior to others in every situation, despite claims by some manufacturers (i.e. ENGINSOFT). Commonly the best approach is usually problem specific, requiring analysis and/or experience with both the problem and the design space sampling techniques used with it. Whilst there is no truly universally effective optimization technique, certain techniques are known to be favorable to particular problems and design cases (Onwubiko, 2000). The field of numerical optimization can be split in a number of ways depending upon the attributes chosen for classification of individual techniques. Section 2.2.1 defines the principal steps required to formulate an optimization problem and begin to define requirements for the application of individual techniques based on

the inputs to and outcomes from the optimizer. In essence, by knowing and understanding the objective function(s), the design constraints and the initial data type, one can begin to understand the types of optimization applicable to the problem to be investigated by process of elimination. The optimization tree (Figure 19) was developed to provide for a visual breakdown and classification method.

However, to truly classify most if not all optimization types, categorization must start with the largest field into which the majority of approaches can be allocated. Three of the largest fields into which design optimization is categorized are: Mathematical Programming (MP), Metaheuristics and Optimality Criteria (OC).

Any analysis, no matter how shallow, attempting to assess, describe and fully classify these techniques would generate a body of work which is far beyond the purview of this investigation. As such a number of the major techniques considered conducive to, and prevalent in germane research will be addressed and compared in context with the study to be undertaken.

2.2.2.1 Mathematical Programming Methods

Arguably the largest defined area of optimization is that belonging to methods of mathematical programming (Wolsey, 2000). One of the oldest and simplest forms of optimization still in regular use, MP methods are what most people would first think of when they mention optimization.

In its most basic form Mathematical Programming Methods are a method for maximizing or minimizing a function (6) based on a vector for a given set of design variables (7) such that each iteration is an improvement in the design.

$$\begin{array}{ll} \text{Min:} & \min_x f(x) & 6 \\ \text{Such that} & f(x_i) \leq f(x) & 7 \end{array}$$

There are several subclasses of methods which sit under the banner head of MP, through the primary distinction within the group surrounds the differences between multi-modal and multi-objective optimization. In the case of the latter, the competing objective functions, when solved simultaneously, create a region of solution in which a series of design points which are not dominated by any neighbouring design point are plotted and solved. In this manner a Pareto front can be depicted showcasing the optimal solutions when solving for combinations of the objective functions. In the case of multimodal optimization, the solution of the problem is found by multiple analyses, starting from different points of the design space, with solution for further sampling found using a combination of local and global search methodologies. In such a search,

heuristic methods are often used to prevent the solution from converging toward local minima of the design space as opposed to some true global minima (Storn and Price, 1997).

2.2.3 Applications of Design Optimization in Airbus

Design optimization has been used in myriad circumstances at Airbus in both the structural and systems domains. Shown below are a number of design optimization examples enabled through AM.

2.2.3.1 Optimization for Cost and Manufacturing - A400M Bulkhead Seals

The A400M Bulkhead seals (BHS) were a particular problem faced by Airbus in the summer of 2015, the parts in question are pairs of hemi cylinder currently machined from a solid billet of titanium which yields an almost ridiculous B2F ratio of 14:1 due to the unusual shape of the part (Figure 20). Asked by Procurement to find a more cost effective solution and constrained by use and criticality, Airbus Defence and Space (DS) approached Airbus Central Research and Technology (CRT) to provide an AM solution. Whilst initially appearing an ideal part for AM (small, lightweight, high cost, low volume) their shape and feature presented a unique problem and one which could not (at the time) be readily solved by structural optimisation. During deposition and as previously highlighted, laser based processes are subject to shrinkage which in turn causes a build-up of RS. In the BHS this tendency exhibited itself as a tendency for the open cylinder of the part to want to flatten during build, thus resulting in significant distortion. The presence of the large flange also presented a problem for both nesting and deposition without excessive waste. Ultimately, using a series of smaller optimization studies, the design was iterated by minimizing each problem in turn.

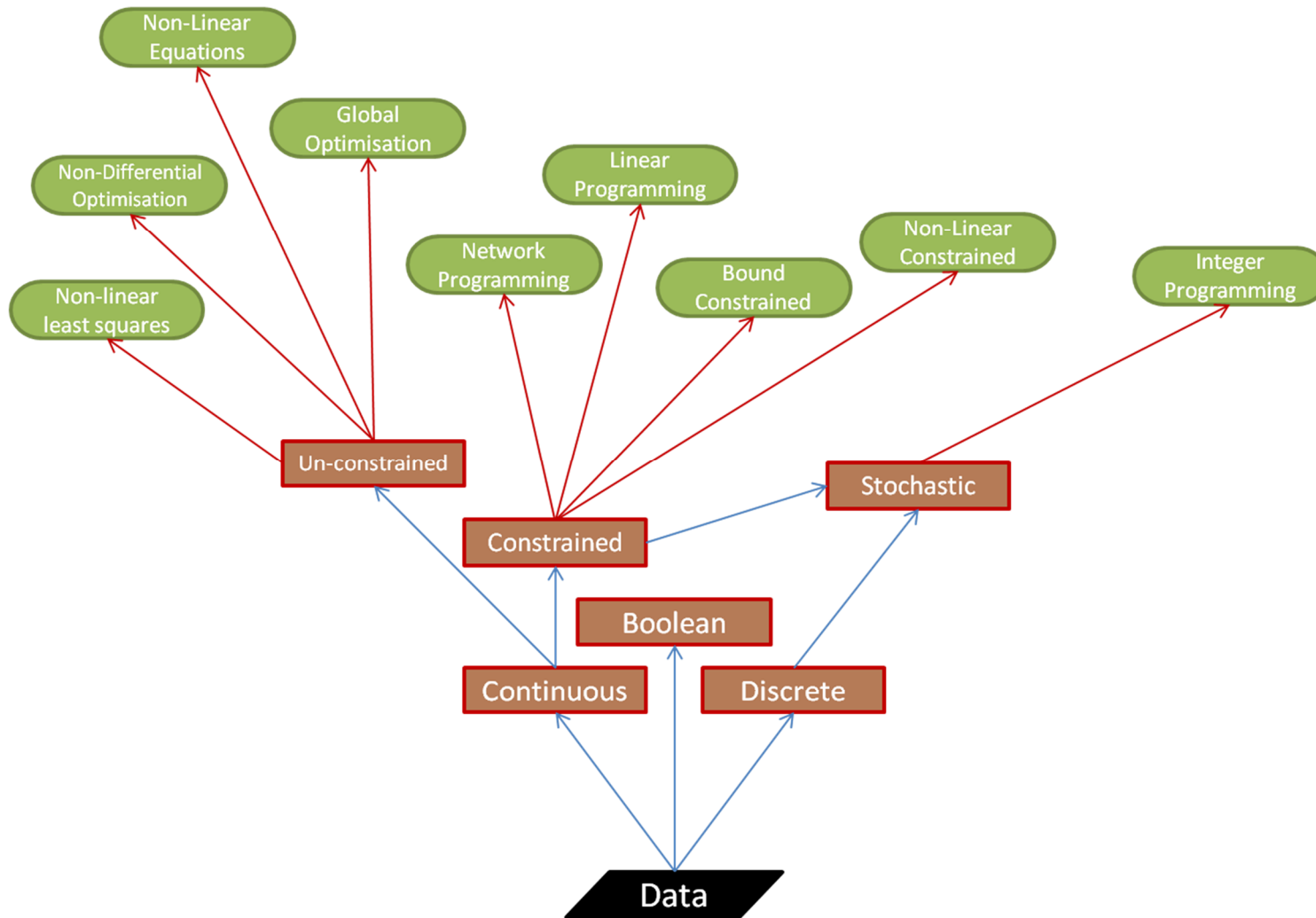


Figure 19 - Showing the different branches of optimization and the pathways to their application

First orientation was established and the design adapted for that which could not be controlled by orientation. Secondly the design was tailored for not only its use, but also its installation. Finally, the design was adapted in order to minimise or at least maintain its current structural mass and thus the final cost of the part. In seeking a cost reduction, significant NRC was expended in order to effect an optimal design suited for the AM process. The path of the design change can be seen in Figure 20. The new design is 42% cheaper than the original one, is of similar mass and performance characteristics, whilst being available in less than 2 weeks as opposed to 4 months.



Figure 20 - A400M Bulkhead Seals - Original (right) and design for AM (left)

2.2.3.2 Unconstrained Optimization for Cost Through AM – Spoiler Safety Collar

In 2013, CRT were approached by Airbus MRO (maintenance and repair operations) to produce some small pieces of aluminium tooling used during assembly of A320s wings. In this case, the cost of the tooling was expensive and time consuming due to the infrequency of order from

Airbus MRO. They sought a cost and lead time reduction. Machined from billet aluminium plate (T6061-T6) the parts were some €400 per item when ordering batches of 80. Most of this cost was driven by the infrequency of the order and the expediency with which airbus required the items. AM was believed to be a suitable solution due to the belief that it is a means of rapid production. Problematically, Aluminium powder for AM is very expensive (12* the cost of plate) and is difficult to process (shiny material requires MORE power to melt due to refraction and is possessing of poor mechanical properties (Brandl et al., 2012). As such, whilst an AM solution was available, the reduction in cost was only 10%. In this context, material was largely irrelevant so long as it was capable of supporting the loads required during operation, as such a rough design optimization was applied in which the approximate mass of the part given the loads safety factors required was undertaken. In this study, the minimum processing features of AM for each material were parameterized and a sizing optimization helped to demonstrate the approximate mass of each component. In this context mass is largely a non-issue, but in AM, Mass is cost and so coupled with the ease of processing materials such as Ti and 316 stainless steel a determination was made that a titanium solution could prove more cost effective IF mass (and thus lasertime) was minimised. After a brief structural optimization and design extraction, the resulting part (designed specifically to take advantage of AM produced a part with a total cost of only €137. A 60% saving despite using a more exotic and expensive material. The series of design optimization can be seen in Figure 21.

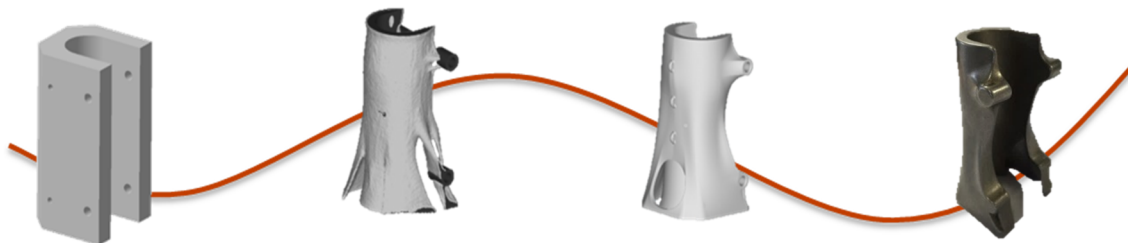


Figure 21 - Safety Collar for MRO - Design optimization for cost and AM – red arrow indicates flow of design from left to right

2.2.4 Design Optimization vs. Structural Optimization

Design Optimization (DO) is not fundamentally different from the more bespoke structural optimization (SO), in fact they can, if parameterized correctly, serve the same purpose; the principal difference between the two is in the manner in which they are applied and the method in which results are presented. SO (particularly using Size or Topology) gives a designer a new structural layout which requires little or no prescribed design variables (DVs) (other than domain size) in order to effect a new result. DO in the classical sense, creates a response surface using

combinations of design points from suitable design variables. The intention is to highlight the global minima commensurate with the problem under assessment. Its output is usually a series of numerical values intended to guide an engineer/designer to a more optimal solution created elsewhere and then re-evaluated. In many cases, the techniques are applied together either sequentially (iteratively) or in parallel in order to yield a suitable solution (Krog et al., 2002). An example of this can be seen in Figure 22.

2.3 Structural Optimization

Structural Engineering as a field or profession has its origins in the hands of masons and builders of ancient cultures as early as 3000bc. However it was not until the great pyramids of Egypt were constructed that the idea of calculated and scaled building techniques were used effectively (Holtzapfel and Reece, 2000). Up until the early 1800s, structural design had been a relatively iterative process, highly dependent upon existing structures and designs (with a few notable exceptions) for guidance and inspiration. Advancement in the field of metallurgy allowed design freedom with Bridges, battleships and buildings becoming statements of power and prestige in addition to purposeful structures; this change in design ethos fostered novel ideas and techniques.

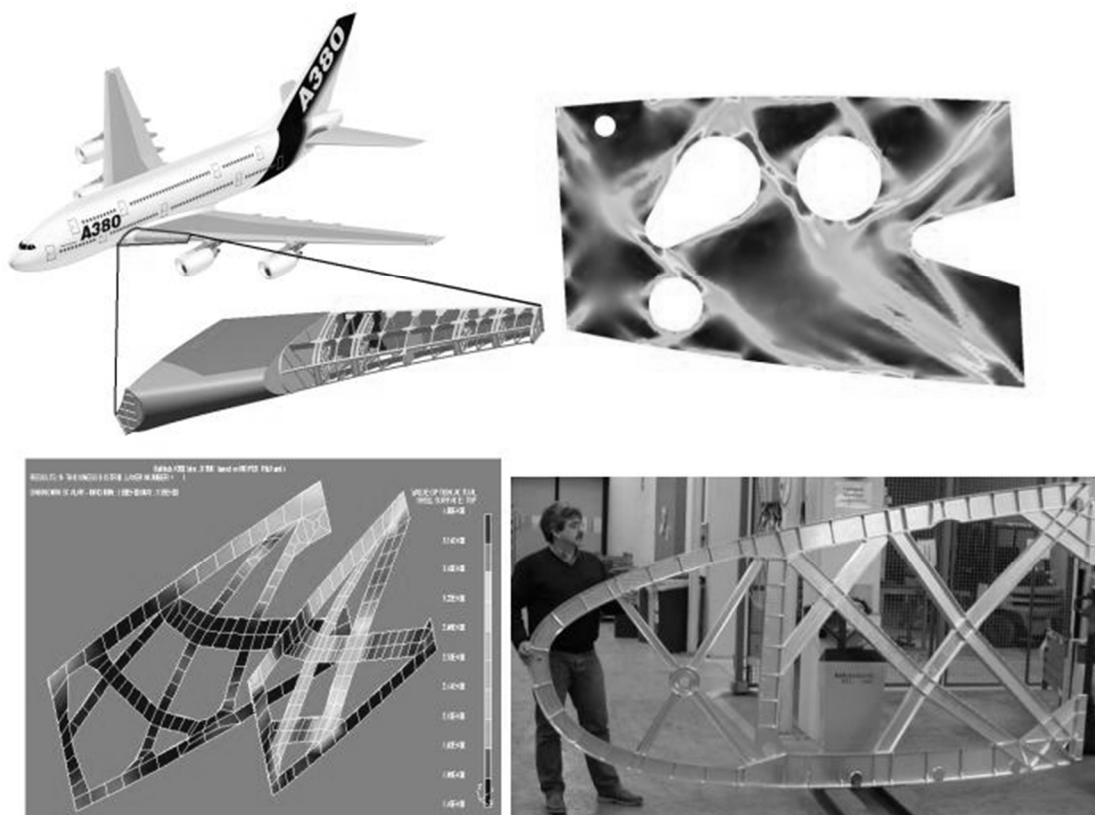


Figure 22 - A380 DN ribs : design and manufacture (Krog et al, 2002)

However, a number of very public failures (Burdekin, 2006) and subsequent enquiries led to the eventual creation of establishments for empirical testing of material samples prior to their use in structures, modern metallurgy was born (Burdekin, 2006) The development of this aspect of materials science allowed for engineers of the day, to create bespoke mathematically assured structures. These structures were designed not just for an engineering purpose, but with flair of design previously unseen in industrial architecture. The effect of this change in design process can be clearly seen in the iron structures of the 19th century



Figure 23- Brunel's suspension bridge in Clifton, Bristol

2.3.1 Fundamentals of Structural Optimization

The use of mathematics in structural design increased considerably throughout the 19th and 20th and early 21st century with ever more complex structures being analytically assessed (Figure 23). It was however, the advent of powered flight which introduced a new dynamic into the field of structural analysis; lightweighting (Cautley and Mazet, 1932). Soon, the complex internal structures of modern aircraft were beginning to test the limits of what could be accurately analyzed using simplified structural assessment methods and a new process for analysis was required.

The early 1940s saw dramatic technological progress with many fields receiving substantial funding for research during times of war. It was during this period that two unrelated and largely ignored pieces of work were published; the first defined a means by which a structure could be discretized (Hrennikoff, 1941) while the second related to a method of analyzing torsional problems using multiple connected domains (Courant, 1943). Combined, the two approaches define the basis by which a structure can be discretized, and subsequently analyzed numerically whilst solving (at least approximately) the partial differential equations associated

with their connectivity. These works and subsequent papers (Argyris, 1954); (Turner et al., 1956) define the seminal method for discretizing and subsequently analyzing external effects on interconnected and interdependent domains. Despite the research throughout 1960s the “finite element method” did not reach its full potential until the early 1970s when it was finally twinned with digital computing and the development of the NASTRAN code fundamentally changing both the method and the types of structure which could be analyzed.

Figure 24 show the effects on component design allowed through the advancement in analytical techniques and the development of manufacturing technologies which allow realization of more complex designs. The images together show that despite dramatic leaps in aircraft performance over the past 70 years, state of the art developments in design tools and methods of structural assessment largely kept pace allowing for high reliability and ease of certification (De Florio, 2011).



Figure 24 – Aircraft rib development in-line with loading and performance requirements and the development of better analytical techniques

2.3.2 The Finite Element Method and its use in Structural Optimization

Foremost amongst these developments in analytical and design techniques was the creation, industrialization and dissemination of the FEM. Developed from a series of publications by different, unconnected authors from the 1940s onwards, it was NASA (in the 1960s) who first created software specifically for the analysis of a structure using finite elements. NASTRAN (NASA, Structural Analysis) was developed specifically a means of quickly analyzing complex, lightweight structures which defy analysis using conventional methods such as beam theory and superposition. The use of the FEM has expanded dramatically in use over recent years, being used not only for structural analysis, but for fluids as well. This increase in use has largely followed in decrease in price and increase in availability of high powered computational resource, thus providing for easy and cheap simulation capability

The principal idea behind the FEM is the discretization of a volume into multiple, connected interdependent domains, which together represent the total volume of the system under investigation. In essence, the discretization process transforms an infinite number of degrees of freedom within the continuum into a finite number of linear approximations defined by the elements (and their connectivity) that make up the whole.

The type of domain (fluid/solid) under study by an FE method is largely irrelevant, it matters only that the discretized elements fully represent the volume. The volumetric discretization process is known as “meshing” and it is this mesh that will be subsequently analyzed by the solver. Generation of the mesh usually propagates from the outside of the system progressing inward until the total volume is filled. In a solid structure, the outer surfaces of the model will represent the boundary upon which nodes (initial point co-ordinates) will be seeded. From these node seeds a 2D surface mesh will be generated based on the requested element configuration (See section 2.3.2.1) It is from this surface mesh that a 3D volume mesh will be created to fill the entire capacity of the system.

One of the key principles of the FEM is that the nodal co-ordinates for each element must not connect/overlap with any other element except at the point at which the co-ordinates coincide. (Figure 25) This condition ensures that elements are linked only and directly through the nodes which define the boundaries of the elements.

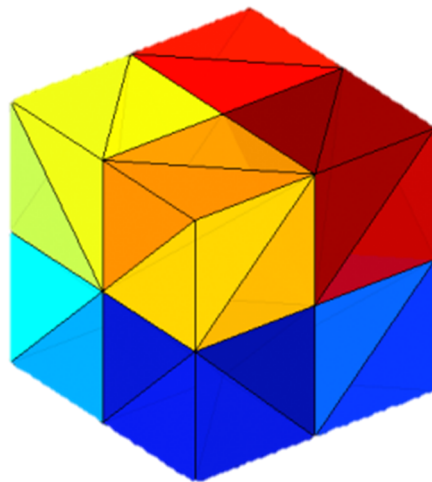


Figure 25 - A 2x2x2 cube showing a tetrahedral volume mesh with an element size of 1

2.3.2.1 FEM – Elements and Nodes

In the FEM, functions are used to define the relationship between the boundary equation and elemental map (Ridgway and Shangyou, 1990). The accuracy of the meshing process in respect of the domain is highly dependent on the type of function used (basis/shape/trial etc.) and/or the defined density of the mesh and the effects of this can be seen clearly in Figure 26

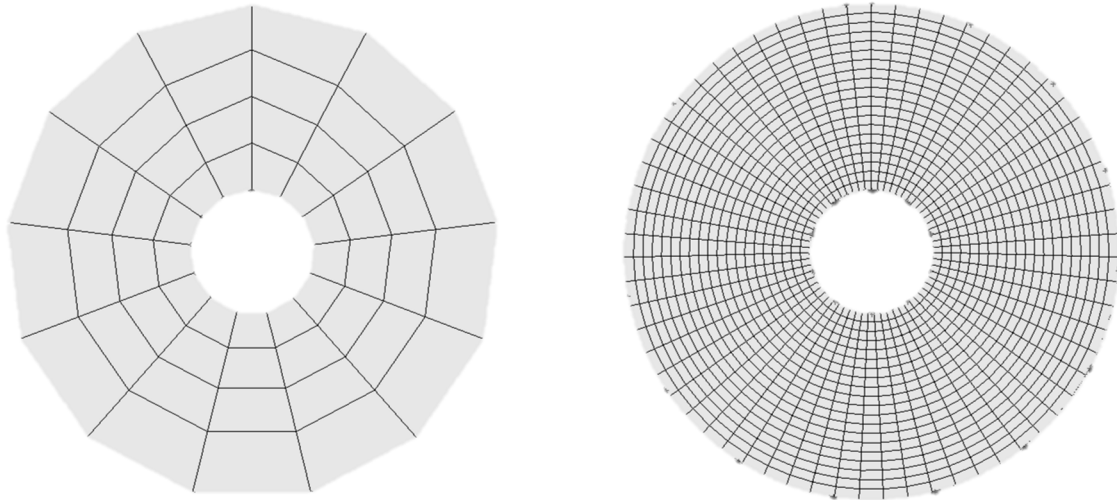


Figure 26 - Showing the effect of variable mesh density and higher order functions to represent geometry

Higher order elements can also be used to more accurately map a geometric domain. These elements can be fewer in number due to their increase in nodes at intermediate positions along the element boundaries. These elements can be successful in reducing computational requirements (in the case of high order Hex elements), but can be problematic to employ on complex geometry. For this reason, many solvers rely on Tet4 (1st order) and Tet10 (2nd order) elements for meshing as they are easier to map to complex geometry and more forgiving of bad CAD (Brenner and Scott, 2007).

2.3.2.2 Governing Principles of the FEM

The finite element method relies on a number of overarching mathematical principles in order to be effective. The first and foremost of these is the Lax-Milgram theorem for Weak Formulation (Brenner and Scott, 2007). The driving criteria behind weak-formulation is that the requirement to hold a specific value absolutely is relaxed, effectively allowing results to be returned as a series of approximations forming a distribution to the problem. The application of weak formulation allows conceptions of linear algebra to be applied to other domains such as (in this case) partial differential equations, by allowing approximate answers to be held as real values for unknowns.

Considering finite elements as applied to Laplace's equations, the formulation of Poisson's equation in Euclidian space (8) is transformed into its weak formulation (9) and condensed

$$\nabla^2(x) = f(x) \quad \text{For all } x \in \Omega \quad 8$$

$$\int_{\Omega} \nabla u \cdot \nabla v \, dx = \int_{\Omega} f v \, dx \quad 9$$

valid for all functions of v .

Galerkin methods then make use of weak formulation in order to transmute a continuous domain into one comprised of discrete values or elements once operational domain constraints are applied to the design space. The major version of the Galerkin method utilized for FEA is the method of Mean Weighted Residuals (MWR). Under this theorem it is assumed that the governing equations are well approximated by functions which have a finite number of degrees of freedom (DoF) to which weighted residuals can be applied. The purpose is to find the path of least resistance to some minimized version of the residual function and what values that the DoFs must take in order to achieve this (Brenner and Scott, 2007).

2.3.3 The Finite Element Method and its use in Structural Optimization

Whilst not completely reliant on the FEM, the vast majority of structural analysis and optimization is performed computationally, using aspects or the majors of the FEM to perform the calculations which approximate structural behaviour. However, though the majority of techniques use FEA in order to assess structures and their behaviours, they do not all do so in exactly the same way. Some of these differences are discussed below.

2.3.3.1 Structural Sizing and Shape Optimization

A principal method of structural optimization and one which has, until very recently, seen the most engineering use, is that of size optimization. Sizing optimization is the eldest of the primary triumvirate of structural optimization methodologies, having been used (in one form or another) from as early as 2000BC (Anderson et al., 1927); Sizing optimization is a method by which the population of a structural domain as defined by the beam members which form that population, are individually adapted in response to an objective function, applied load and design constraints. An archetypal problem for size optimization might be the variation of beam cross sections for truss type structural designs such as a bridge or crane jib. Typically performed through direct analysis of predefined structural layouts using the FEM, the optimizer is then used to alter the cross sectional area of each truss section in response to its level of structural loading in order to minimize or maximum a particular objective function for the problem. Key to the use of the approach is a requirement for a heavily seeded design space in which most possible connections are mapped (Haftka et al., 1992). A heavy population density is required as connectivity and member numbers remains unaltered throughout the optimization, with none added and none removed. As such, variation in cross section will showcase which beams carry the highest load and approximately what their ideal cross section should be. In this way the mass of the structure may vary in response to the imposed cross sectional area, but without post analysis, the overall

layout and nodal connections of the output will remain identical the input (Bendsoe and Sigmund, 2003).

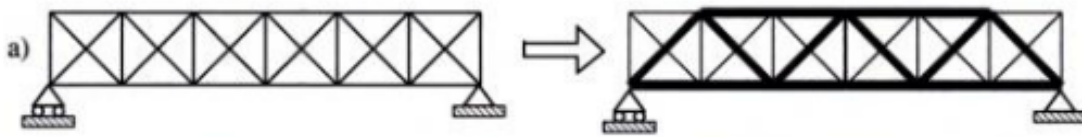


Figure 27 - An example of sizing optimization (Bendsoe and Sigmund, 2003)

Shape optimization offers a direct contrast to the size optimization approach previously defined and does so by varying the very thing which must remain fixed in elder approach; the Domain. Utilizing the boundary nodal co-ordinates defined in the generation of the FEM as variables, the optimizer, in response to some objective function, attempts to alter the outer boundary of the structure by translation of the nodes which make up the surface elements (Rao, 1996). The translation allows, in conjunction with repeat FEA, the minimization/maximization of an objective function (stress/deflection/mass) by tailored modification of the design domain in response to structural loadings and/or constraints (Haftka et al., 1992). Despite its ability to modify the design domain, shape optimization does not permit complete and free form modification of the continuum solid, beyond that allowed by a pre-determined set of criteria (Bendsoe and Sigmund, 2003).

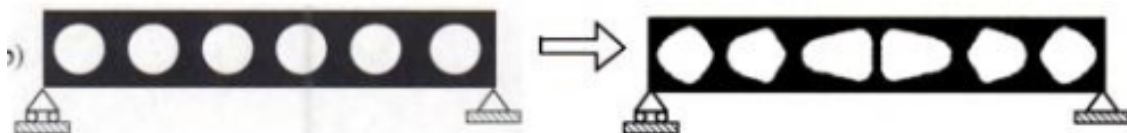


Figure 28 - An example of shape optimization (Bendsoe and Sigmund, 2003)

As with the number of structural members and their associated nodal connections in sizing optimization, the number of nodes in shape optimization also remains constant throughout. As such, shape optimization cannot create or remove holes from a domain, it can only modify the shape of any already present holes by translation of their boundary co-ordinates. In this way, shape optimization can both add and remove material and can actually expand the boundary of the original domain (unlike topology optimization) where permitted by the optimizer. Whilst shape optimization can vary the domain boundary, its ability to determine a global optimal solution is based upon the accuracy of the initial hole seeding and thus is susceptible to convergence upon a local minima, rather than a global one. Due to its modification of boundary nodes, shape optimization is commonly associated with the optimization of shell element based

models, but is also commonly used as a post processing optimization for topology based results (Rao, 1996).

2.4 Topology Optimization – An Introduction

Topological Optimization (TO) is by far the newest (Bendsøe, 1989) and currently most researched area (Adeli, 2003) in the field of structural optimization. Enabled though further use of the FEM, TO differs from earlier techniques by allowing almost complete modification of a defined design domain in response to objectives, input variables and constraint functions. Whilst TO cannot be categorized as completely freeform (due to fixed external domain boundaries), the technique does allow for total modification of the material distribution within the continuum (Bendsoe and Sigmund, 2003) A pioneering technique, it introduced the (now) logical addition of material microstructure into existing structural optimization, utilizing the FEM. The study spawned a wave of follow-on research into structural optimization which continued in some form for almost a decade. The technique allowed for the introduction of voids (porosity) into the design domain through a variation in the input parameters (density and elastic modulus) of individual elements in the FE grid. In doing so, the apparent material density of a particular element, or series of elements can be varied through modification of its stiffness tensor. The effect of this material variation thereby alters the inherent characteristic response of the structure in answer to loading conditions and a driving objective function.

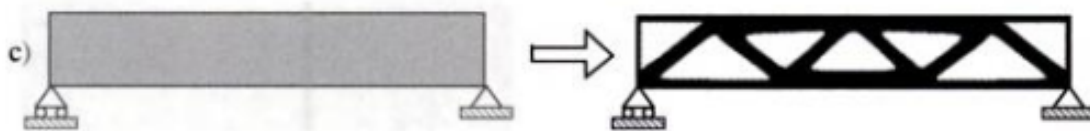


Figure 29 - An example of topology optimization (Bendsoe and Sigmund, 2003)

The variation of the domain elements happens iteratively with elemental selection driven by a domain sampling techniques (Berke and Khot, 1987). During each iteration, after modification of the sampled elements, the entire domain is analyzed, with strain in each element computed and compared to their results in the previous analysis phase. Should modified elements and/or their neighbours experience dramatic changes in strain rate, as measured by distance between nodal neighbours, the variable material properties are either retained or partially/wholly restored to the elements. Further seeding and modification is then performed with the sequence repeating until (if successful) convergence to a global minimum is achieved. In some of the more prevalent commercial software packages the search techniques are heuristic, thus slowing the optimization sequence (i.e. Abaqus), but almost removing the possibility that the solver will converge to a local minimum. The values for density and modulus can vary discretely within the cells and can be

implemented cumulatively across the domain to further convergence of the problem. Problematically, and without further computation, the optimization problem will achieve its objective with many domain cells at discrete values between the MinMax values for both modulus and density whilst mathematically acceptable, the replication of such a structure as this in the real world is problematic at best. An improved technique is required.

2.4.1 Topology Optimization – Methods and Comparisons

2.4.1.1 Solid Isotropic Material with Penalization

Whilst several variations on the specifics for TO exist, by far the most widely used are those which utilize forms of penalized proportional stiffness model in order to eliminate material of intermediate density in the search for optimal material distributions. Of these techniques, one of the most efficient (Rozvany, 2001) and popular approaches is known as the Solid Isotropic Material with Penalization (SIMP) method. SIMP utilizes the initial material properties and assumes isotropic material formation throughout the design domain. It then evaluates the density (calculated via volume) as a design function through interpolation between initial material input values and zero (Bendsoe and Sigmund, 2003) The use of interpolating functions allows the SIMP approach to, in effect, function in a similar manner to a typical sizing problem, but with a vastly increased number of design variables (DV). The increase in problem scale means that the effectiveness and efficiency of the optimizer is crucial to its success; As such, a compromise between DVs and constraints can be realized, thereby maximizing the efficiency of the optimizer in returning a satisfactory result in an expedient manner.

MinMax topology studies, with simple objective functions and minimal constraints are one such example of this trade-off; with compliance based optimization providing the toolset most commonly used for structural optimization under simplistic loadings (Bendsøe et al., 1994).

Whilst SIMP is undeniably an effective technique, the requirement to introduce proportional stiffness through variations in material properties, can lead to computational difficulties. In order to ensure that an optimal material distribution is attained, heavy domain sampling must be utilized (Wu, 1994) along with (in many cases) complex search functions which (at least in the early stages (Bulman et al., 2001)) use heuristic methods (Tabu, Simulated Annealing, but most commonly genetic based techniques) to ensure full capture of the domain space shape. This process leads inevitably to a quite heavy computational dependency, particularly on complex problems. Furthermore, by introducing such a wide sampling methodology and with each DV (element) being allowed to (in most cases) vary continuously, there is significant potential for both elements to become disconnected from the domain major and for even neighbouring,

connected elements to have vastly different density maps (Zhou et al., 2001). In order to address both of these concerns, the penalty functions within the optimizer apply increasing levels of penalization to the problem, targeting elements on the domain boundaries in order to force their density maps toward values of 1 (present) or 0 (removed) in the final iterations of the solve (Stolpe and Svanberg, 2001). Again, this is computationally inefficient and means that the result of problem is not truly resolved until the final iterations (Rozvany, 2009).

2.4.1.2 Level Set Methods

Whilst the SIMP approach is the one most widely utilized by commercial software, it is not without its detractors; computationally heavy and, when employed in many applications, not capable of delivering a satisfactory optimization result until completion the final iteration of the problem, many have sought alternative techniques (Bruns, 2005, Delgado, 2014, Wang et al., 2007b) Of these, the most researched and developed is the field of Level-Set Methods (Wang et al., 2003, van Dijk et al., 2013) In a similar manner to that which AM uses to slice a build file, using distributed planes at equal, discrete intervals, level sets function in the same way, applying planes to equal, discrete intervals of a function. In the level set method, these planes are applied to each iteration of the solution problem. Where they intersect the mesh, a smoothed contour profile is created around each structural element within the slice (Sivapuram and Kim, 2016). This approach using Cartesian curves in Euclidian space allows for the gradual change of the contour planes in response to the objective function and a smoothing parameter both between points and planar profiles. The approach whilst effective in reducing both problems associated with SIMP (Dunning and Kim, 2013), introduces many of its own (Cai et al., 2014, Zhu et al., 2015) and although present in a number of commercial codes, is not the prime method of deployment, due to notable downstream problems and significant solution sensitivity in respect of initial sampling placement (Allaire et al., 2004, Dunning and Kim, 2015).

2.4.1.3 Variable Thickness Sheets

Whilst TO, particularly in the form of SIMP is based upon the 1989 works of Bendsoe and Kikuchi (Bendsøe, 1989), it is actually an improvement upon an earlier technique (Rossow and Taylor, 1973) which concerned itself with the study of sheets of varying thickness (Ramakrishnan and Francavilla, 1974). In these studies and like those that came later, voids/bubbles are introduced into the domain through a variation in elemental density. Unlike those methods which come later, no penalization functions are applied to the domain, thus, elements of partial density are not only allowed, but encouraged. Checkerboarding is largely permitted and results are interpreted as can be seen in Figure 30 (Guess et al., 2015) These results are vastly different from those achieved under SIMP when using the same conditions, but as they are essentially a porous

structure, they are extremely difficult/impossible to create in the real world without extensive cost at least until recently. AM, particularly when linked to microstructures and lattices can be made to emulate the porous nature of the VTS (variable thickness sheet) model, and thus can begin to approximate the VTS and release its benefits. Problematically, the VTS method doesn't scale well into 3D, though it is possible (Guess et al., 2015) . To do so, certain compromises are required (Hawreliak et al., 2016) and the resulting structure does not always yield any particular benefit (in pure mass saved terms) over that of SIMP when solved using a large FE grid. What the VTS method does yield, is a substantial saving in solution time. During the solve each cell, in each iteration, does not require penalization, thus, not only is computational time is reduced, but valid solution gates are achievable at the close of every iteration of the solve.

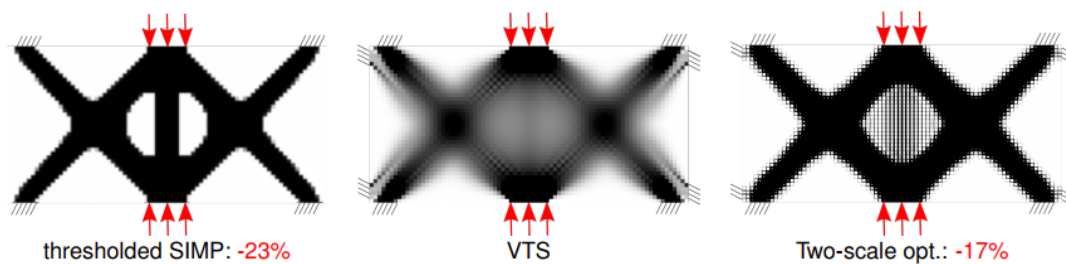


Figure 30 - VTS when compared to SIMP and two scale lattice

2.4.1.4 Evolutionary Methods for Stiffness Optimization

Like other SO methods, evolutionary structural optimization (ESO) utilizes the FEM performing assessments of the grid to determine elements contributing little to the stiffness/carrying capacity of the structure under investigation (Xie and Steven, 1993). The solver then gradually reduces those unused elements until only distribution of load/stiffness contributing material remains (Xie and Steven, 1997). The choice of algorithm for the solution is critical to its overall efficiency (Lagaros et al., 2002), but with even a poor choice, the process of optimization is substantially faster than a SIMP based solution on a similar sized grid (Shojaee and Mohammadian, 2012). Whilst much has made of the lack of mathematical theoretical basis for ESO, recent studies have proven that the remarkable resemblance of output topologies to those of the classic Mitchell truss are not coincidental (Tanskanen, 2002). The programming and solutions methods for ESO are substantially simpler than for SIMP, converging quickly and commonly into predictable patterns. However, the designs presented by ESO are, more-so than SIMP and significantly more so than for LS methods, heavily dependent upon the input grid definition and the response of that structure within the grid. One of the more impressive features of ESO comes in a later iteration of the software called BESO (Querin et al., 1998) with the B standing for bi-directional. This means the algorithm can both remove and add material, giving

it a unique capability when compared to ANY other STO software methods. The effects of BESO mean that a structure can actually grow in response to its loading rather than being purely reduction and computationally heavy in the initial iterations, the software performs like AM, adding material only where required and thus reducing (computational) cost. Regrettably, few commercial code can use ESO, let alone BESO and thus if it were to be used for this investigation, unique software would have to be created, trialed and approved by Airbus. This level of work on a parallel project is far beyond the scope of this investigation, but would be worth maintaining awareness of any developments within commercial code.

2.4.2 Implementation of Topology Optimization

Conventionally the application of STO to an existing design case is in an attempt to address some functional issue with the original design, or to offer some form of iterative improvement. By discretizing the original design domain using the FEM and analyzing each element in turn for its structural applicability/suitability the resulting structural depiction is constructed from those elements deemed important to the design case. As a result, the elementally defined structural output is defined by the nodal boundaries of the elements wherever they happen to terminate. As such, the final design output (even with the highest quality and density of mesh) is generally quite rough (Figure 31) requiring some form of post analysis modification in order to render a usable shape ready for production. Shape optimization (boundary modification) is often used to fulfil this requirement. Shape optimization in this form can be applied in a number of methods, though by far the most common is through the definition of offset surfaces, surfaces to which the outer boundary nodes of the topology optimization result are allowed to displace and that, in response to a further optimization definition.

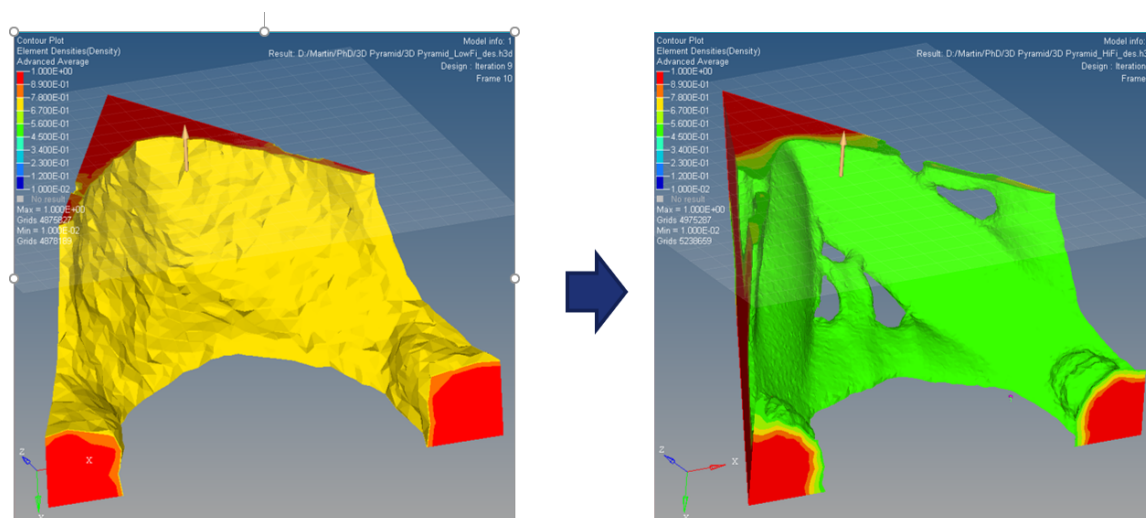


Figure 31 - The effects of mesh refinement and STO on the quality of the resulting design output with a low density mesh shown on the left and a high density mesh on the right.

Though simplistic to describe and even to visualize, the definition of sufficiently accurate offset surfaces around either a direct topology output, or those of an extracted design can be incredibly time consuming (if possible at all) and difficult to automate due to its highly bespoke nature.

2.4.3 Use and Applications of Topology Optimization in Aerospace

The use of structural topology optimization (STO) is increasing in a variety of engineering fields as designers and manufacturers strive to reduce costs and increase operational efficiencies; indeed within several domains, the use of STO has become almost common practice for the design of new components and the iteration of old designs into new models. The rapid adoption of this novel design methodology is increasingly common within low risk fields such as the automotive community (Cavazzuti et al., 2011) Conversely, and despite an ever pressing requirement to reduce both cost and maximize performance, the distinctly conservative field of commercial aviation has been a much slower adopter of the technology, particularly for safety critical structural designs. However, even with this domain reticence, there are an increasing number of examples of its use. This is particularly true where an existing design has been deemed to be historically problematic (Muir, 2013) or where a significant mass saving is believed to be achievable through use of the technique (Muir et al., 2013).

Topology optimization of already lightweight, large structural components (fuselage ribs/spars) is problematic at best, with mass savings often in single digit percentages which barely justify the effort required for its redesign. However, the highly competitive marketplace for commercial aircraft is driving designers to extreme lengths in order to make their products, at least as good if not superior to competitor products. As such, uneconomic or previously infeasible practices have been deemed acceptable at many levels if a justifiable performance increase can be attained. Airbus, based on the strength of past optimization work (Krog et al., 2004) have now begun to accept STO as a means for design as opposed to a tool for the correction/mitigation of mass gain in aircraft projects (Altair, 2006) Furthermore, Airbus have gone a step beyond the majority of their industrial peers through the use of STO for the analysis and design of large structural sub-assemblies such as the A350 aft fuselage subassembly (AFS) shown in Figure 32. Through a complete analysis of the A330 AFS Airbus has determined that a mass saving of approximately 10% can be achieved with only limited impact to manufacturing time and cost.

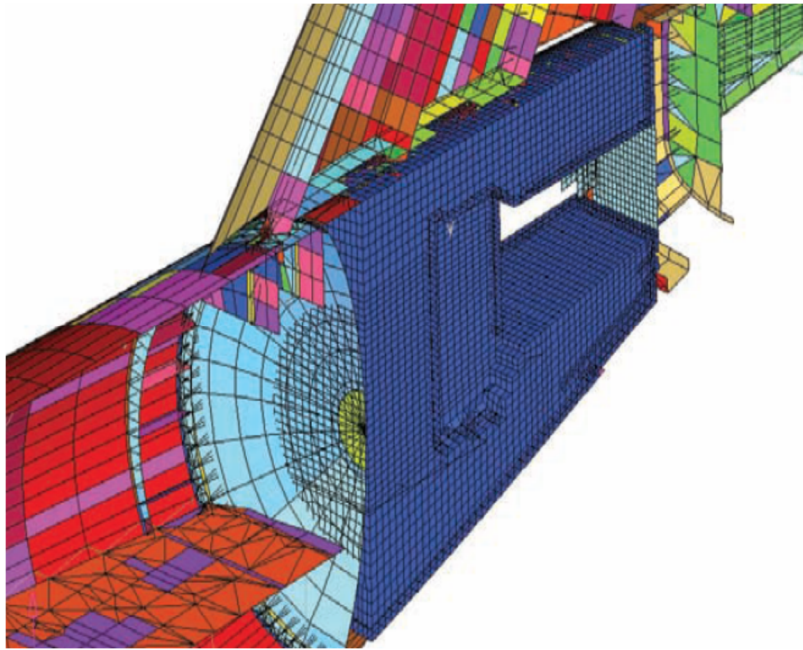


Figure 32 - Parameterized design space for Airbus A350 rear fuselage

This approach represents a radical departure from previously employed methods of isolated STO for individual components (Tomlin and Meyer, 2011) (Figure 33), instead embracing the technology and using a holistic approach in order to affect both increased mass savings and reduced computational analysis time.

Finally, and of unique interest is the use of STO as a tool for initial design or even redesign, by its inclusion in the preliminary design phase. STO can then be used to dramatically reduce the required design time through the principal analysis of the structural domain and subsequent assignment of required structure (Muir, 2012b)

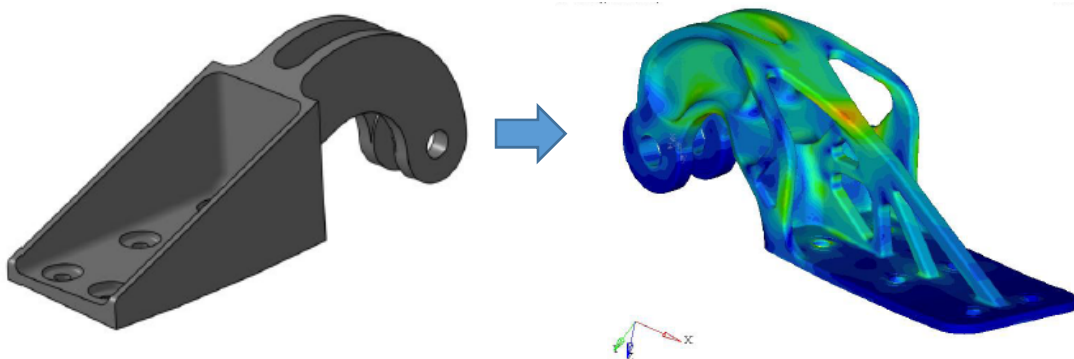


Figure 33 - EADS A320 hinge - Optimised using compliance based STO

2.4.4 Limitations of Topology Optimization for Design and Development

Whilst the versatility of STO cannot be denied, the most widely used of the approaches (SIMP) does have certain limitations which must be considered and accounted for when undertaking any form of structural optimization problem. Principal amongst the limitations of the SIMP approach to structural problems is its inability to assess buckling loads in thin walled structures, especially when modelled using shell elements. A further idiosyncrasy of STO using almost any applied technique, is the tendency of structure to evolve towards a mathematically feasible, but practically unrealistic design when optimizing for a single load case (Muir, 2012a). Careful application of the technique is required.

2.4.5 Manufacturability of Topology Optimised Structural Designs

One of the most common criticisms of TO and its resulting designs are that they are either impossible to manufacture or, whilst possible, too expensive to contemplate for serial applications involving large quantities of parts. As such TO has historically found limited use in the design of small parts for either the automotive (very high volume) or aerospace (high volume, high safety) industries. Recently however many people have been using the capabilities of additive manufacturing to remove or reduce the restrictions upon TO for high value parts.

2.4.6 Additive Manufacturing and Topology Optimization

The research detailed above demonstrates the effectiveness of topology optimization at affecting mass reduction on even lightweight structures, and also showcases the required manufacturing constraints which must be applied to the optimization in order to realize an effective design at the end of the process. Similarly, the advancement of AM as a means of economic and expedient production for complex aerospace components has also been aptly showcased. So, if topology optimization has a tendency to reveal complex designs from mundane examples, and AM has the ability, and indeed thrives upon the production of lightweight, complex designs, can the two be paired to create greater savings (in mass and cost) than could each individually?

2.4.7 Combinatory Benefits of Technology Pairing

Whilst the potential for design freedom has been exploited and demonstrated effectively for multiple types of AM over the course of decades, the potential for totally unconstrained design is somewhat unrealistic, particularly when it requires realization into a physical product (Figure 34). In design, shape is largely a product of requirements and cost, as defined by material and manufacturing time and holds true for most forms of manufacturing.

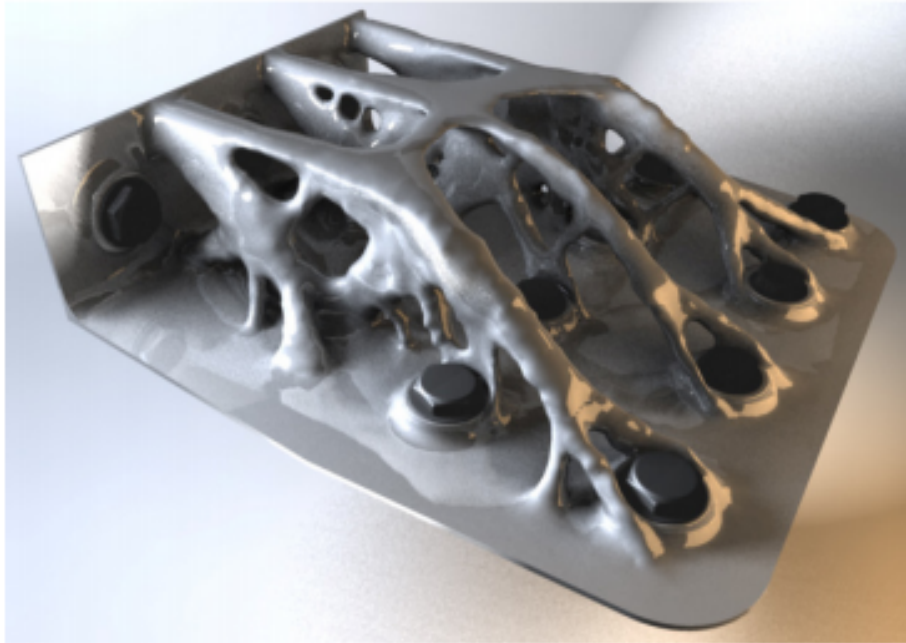


Figure 34 - Unconstrained TO applied to an aerospace bracket - note the poor seating of the bolts - image courtesy of Nottingham university at the Farnborough Airshow in 2012

The limitations imposed by conventional machining exacerbate this problem, leading to designs which are functionally compromised in order to adhere to manufacture and costing requirements. In AM, many of the constraints imposed by conventional manufacturing techniques are removed, leading to far greater design freedom. Problematically, most designers are trained to analyze a requirement and create a part suitable for a particular manufacturing approach, usually machining or casting. Designers, whilst certainly competent engineers are not structural engineers and are thus (generally) poorly versed in the methods required to exhaustively determine the layout of a part, based purely on its functionality. For this, a structural engineer would provide better insight into how the optimal layout for a part might appear, at least for simple load cases. To simplify design, a means of revealing this feature without requirement for highly skilled and experienced operators is required to truly unlock the capabilities of AM. TO, when parameterized correctly, has the ability to act as a guide for designers, a concept generator, showcasing what a largely unconstrained, functionally driven design approach using AM for manufacture might look like. As a first-pass-approximation of a new design layout, the potential for TO as a structural design tool intended and to utilize AM as a means of removing manufacturing constraints for complex design, has significant benefits. Whilst the realities of metal manufacturing using AM is significantly more complex, TO has nevertheless been utilized on several prototype aerospace products to produce descendant designs with great success (Muir, 2013, Muir et al., 2013, Muir, 2017, Muir, 2015, Tomlin and Meyer, 2011).

2.4.8 Optimization Driven Design for Enhanced Concept Generation

In many of the established examples, an existing design has been iterated to success using either structural optimization to reduce mass (Cuillière et al., 2014), an assembly reduction, to reduce complexity (and also mass) (Muir, 2017) or design freedom in order to allow for better component performance (Muir, 2013). For many of these new designs, *an* optimal point has been reached, but has been attained within the design space of the existing ancestor component. Therefore, and as topology optimization is an almost entirely reductive process (Tomlin and Meyer, 2011), any descendent design can only be as good as the design freedom allowed for in the ancestor design space. In order to allow for truly optimal design, a first stage must be the removal of constraining design aspects (or to reduce as many of them as is possible) thus allowing for almost full design freedom and the potential for a truly optimal design. The first phase in constraint removal is to target the design space in which the optimizer operates, thus removing the constraints of the ancestor design and the decisions for their inclusion which preceded them. Secondly, the space considered, should, where kinematics and attachments allow, be expanded in order to provide the maximum possible space to the design explorer. Once the expanded domain is established application of service loads and attachment constraints provide the basis for simple TO problem. The resolution of the problem provides an indication as to the potential structural layout, thus providing a rough design concept. This optimization driven concept design generation provides new, relatively unbiased concept solutions, solutions driven by the performance requirements and not by its cost and manufacturing limitations considerations (Cuillière et al., 2014, Susskind and Susskind, 2015). This means of delivering enhanced concept generation has been aided by the development of new tools (i.e. inspire, 3DE, Fusion), tools which bypass the known difficulties in converting TO structural layouts into usable CAD data (Muir, 2012a, Taylor, 2016).

2.4.8.1 A New Design Process for Additive Manufacturing

With these tools, the traditional approach of moving between software packages in order to perform specific tasks is reduced or even eliminated. Whilst there is still no direct link between the output FE and the new CAD, the use of T-spline derived modelling techniques (Schillinger et al., 2012) vastly reduces the required skill for extraction and progression...at least for simplistic designs (Riesenfeld et al., 2015). T-splines are in essence a form of NURBS, but unlike NURBS functions, the control points are not required to be affixed (either directly or indirectly) to the surface they create and thus can be terminated upon the surface (rather than at the ends). The advantage of this method is that it initially reduces the number of control points, thus enabling connectivity between surfaces, but when later subdividing (for the addition of detail), can

dramatically increase both the number of points and the difficulties of maintain the connected network. This T-spline derived methods of concept design generation has recently been introduced at Airbus, specifically to deal with the rise of AM as a production method. Their intent is to offer design solutions which might best provide an answer as to whether AM might provide for a lighter and or cheaper part than a conventional design and manufacture process. The new toolsets, whilst effective in many cases, are not intended as a replacement for ANY tools within the Airbus design methods, they are intended as an addition with a pure focus on AM and its capabilities. The development and employment of these tools within a large commercial airframer such as Airbus helps to demonstrate the perceived benefits of the technology pairing of AM and TO.

The toolsets and use cases demonstrated above highlight the effectiveness of the combined techniques at producing lightweight concept designs for aerospace structures. However, the capabilities of the software are still limited and require access to, and parameterization of, substantially more information in order to produce a suitable concept design. Historically, concept designs were created by skilled and experienced draftsmen/engineers in accordance with rules and guidance on how a part should be designed for a particular use case. Using the new software, it is not yet possible to include these rules and regulations within the software, thus limiting the validity of the final concept design, or requiring substantial pre-processing prior to optimization. Additionally, whilst many of these tools are based upon more powerful solvers, their capabilities to perform design optimization are limited to mass and stiffness based optimality criteria and have limited capability to apply constraints. Furthermore, whilst the software (under a Design Engineers guidance) is capable of rapidly generating a new design, substantial additional work is required downstream in order for it to be transformed into CAD suitable for manufacture and use on an aircraft, design which cannot be completed solely within the new software packages. Finally and more importantly is the fact that during the reconstruction phase, the link between TO and CAD is again broken, despite being within the same environment, meaning that any iteration, still requires substantial manual effort.

2.4.8.2 Maintenance and Repair Considerations of Topology Optimized Components

By definition, an optimized design has less reserve within its structural make up than a non-optimized structure. Whilst the amount of reserve will differ between parts, significant redundancy exists within many existing designs. The effect of this additional reserve under most circumstances is a negative one as mass which is not required for service loads is being carried and flown within the aircraft; TO aims to reduce or eliminate this structural reserve, thus saving fuel and, in AM, cost. Problematically, whilst under normal circumstances this additional mass is

not required, should the part become damaged in any way, this additional structural reserve may allow the component to endure damage and still function. Later inspection will confirm if the component may continue as-is, or if it requires repair or replacement. Conversely, should a topology optimized structure incur damage, so little redundancy remains, that the damage will be likely enough to render the structure unserviceable. Should such damage go unnoticed, and in a structure which approximates a full stressed design (Razani, 1965), it is highly likely that the structure will fail catastrophically whilst in service (Ostrom and Wilhelmson, 2008). In order to guard against the likelihood of catastrophic failure, failure mode analysis allows for the determination of the structural performance of the part when the most highly loaded members are removed in sequence (Shao and Murotsu, 1999). This analysis method allows for a prediction of structural resilience and can be parameterized within the main TO problem to allow for greater structural redundancies. A more difficult parameterization considers the effects of less terminal damage to the load carrying members and facilitates their ability to be repaired. Should a conventional part be struck and notched, a smoothing/ramping activity (Boeing, 1997) will be undertaken which reduces the severity of the damage in a localized zone to a slight thinning of the area over a larger area. In a TO design, the notched area may already be of minimal thickness and thus cannot be subject a smoothing operation whilst still carrying the required load. In such a case, the part would require the addition of material in order to remove the notch. Problematically, whilst there are techniques which might allow the repair of steel parts, titanium (for reasons mentioned earlier) cannot be easily repaired in the same way. There are concurrent research activities which aim to address titanium (Kumar and Krishnadas Nair, 2017) repair and these could easily be used for the repair of TO components.

With the current design, manufacture and repair processes available to the industry, the best practice for the optimization of structural components whilst considering in service repair and redundancy, would be that during parameterization of the optimization, that some redundancy be retained within the major load carrying members of the resultant design. In this way, a component would be capable of fail-safe operation (Howard, 2016) and should service damage occur, that a certain scheme of damage may be tolerable and repairable. Problematically, failsafe design requires substantially more analysis than does a conventional analysis driven design approach and additionally requires more skill/experience in order to parameterize correctly. These factors can add substantial non-recurring costs (NRCs) to the design process.

2.4.8.3 Non-recurring Cost Increases for the Design of Highly Complex Components

The most substantial NRCs in the current design process are incurred during the early design and validation phases, where engineering judgement and analytical skills are put into practice to determine an appropriate design direction. In designs which are based around three, four or five axis machining, these designs are ordered and logical, based largely upon the Boolean removal of simple shapes from larger simple shapes. This design methodology keeps the total number of surfaces within a model to a nominal level making it easy to manipulate and to alter if later changes are required. When a component is designed/redesigned using a functional driven design approach, especially one which incorporates few constraints upon the design output, the resulting solver output can be extremely complex. Using traditional CAD software to facilitate the transfer of the structural output into a form which can be used for engineering drawings for manufacture, the resulting surfacing designs are both complex and requiring of significant skill in order to generate successfully. The NRC cost for this type of design extraction and detailed design is thus far costlier, and often serves to shift the cost from an RC to an NRC.

2.4.8.4 Multi-Disciplinary Optimization and Design for AM.

When considering optimization, and particularly within the purview of this research, the focus has been limited purely to structural optimization in which a single study (or multiple parallel studies) with a detailed objective and constraints is sought. This has allowed for proof of the research aim without delving into the complexities of multi-objective optimization for AM (Haslinger et al., 2010). However, it would be remiss not to mention research and applications of multidisciplinary optimization (MDO) and AM within the researched literature for this project. MDO and AM has been used on several projects, most over the past 5 years (Tomlin and Meyer, 2011, Muir, 2012a, Muir, 2015, Muir, 2017), in most cases, a linked fluidic, structural, manufacturing and kinematic analysis has been undertaken, again either in parallel or, more conventionally, in a serial manner. The most recent examples of this type of application have shown that by using MDO as opposed to simply TO, that significant additional savings can be made not only in mass, but also in cost and performance.

2.4.9 Material Problems Arising from the Combination of Topology Optimization and Additive Manufacturing

As a layer-wise build-up process, the orientation of a part within the build chamber of an AM process, can have a significant effect on a number of aspects, each which can directly affect its resultant mechanical properties. By altering orientation, the number of layers can be dramatically increased/decreased which has a direct effect not only on cost, but also, potentially, on the likelihood of defect formation/platform error due to the significant increase in the number

of required operations to complete the structure (more layers = statistically higher chance of error). Similarly, a change in orientation can alter a consistent, repeating layer area to one which alters position and area dependent upon location in the build. In doing so, the thermal conductivity of the structure will be altered which in turn will affect the resulting microstructure of the metallic part once completed. Effects of orientation on total build height (and thus the number of layers and in turn, number of repeat operations to complete the sample), area deposition/position and nesting can be found in (Muir et al., 2014). The changes in microstructure caused by the thermal conditions in the build (Machry et al., 2016), coupled with the increased melt and recoating area (Körner, 2016) are probable causes for the changes in material properties often seen when conducting testing of AM (Tong et al., 2017). The evidence which suggests material variability subject to build orientation is a significant, and potentially terminal problem for the use of TO and AM. The methods used for TO generally (in commercial tools) rely on the use of SIMP, which, as the name implies, requires an isotropic material in order to accurately predict the structural requirements. If such material variability exists, only three options are available: 1, quantification of the variability and determination of the lowest material allowable for use in TO; 2, determine if the variability in the process is (as literature suggests (Antonysamy et al., 2013) a direct result of orientation, or if other factors in the process chain lead to variability which is only shown in samples of increasing build height (Wang et al., 2016); 3. finally, and most complex, would be the use and/or development of an anisotropic material methods for use in TO. Of the three and considering the downstream effects of the choices, the most likely to be accepted by both Airbus and the regulatory bodies is option 1 with the precedent set by Titanium castings (Oates et al., 2011). However, use of such knockdown factors is known to significantly limit the use of the technology as parts designed for such methods incur huge mass penalties as a result of the material knockdown. As such and given the scope of the work and the opportunities afforded, options 1 and 2 will be investigated as part of this research. Option 1 will be a fall-back option intended to allow for the use of TO and AM whilst Option 2 will be investigated with the aim of industrialising AM and reducing any potential knockdowns through robust process operation.

2.5 Reducing the Cost of Complex Design

Regardless of complexity, detailed design of components for almost any application where serial manufacturing is being considered, is expensive and time consuming. Requirements must be captured, kinematics considered, lifecycle estimated, interactions planned and manufacturing elements included. Complex design, one which moves away from traditional solid modelling and machining approaches, adds a further level of difficulty to almost every aspect of this design

process and can have significant effects on the cost of any component designed in this way (Bhavar et al., 2014). Complex design traditionally requires the use of surfacing methods for modelling and can have an exponential effect on required design time and cost (Masood et al., 2015). The use of complex design is often discouraged for structural applications for this very reason and as such, is rarely used within Airbus unless significant constraints upon the shape of the structure are required (i.e wing shapes).

2.5.1 Conceptual Design vs. Detail Design

As previously mentioned (2.4.8.1), In the design process for any aerospace component, there is a significant difference between the concept design phase and its more detailed sibling. During the concept phase, almost any form of design method can be used, from solid modelling to surfacing and beyond, though this is rarely the case for most design engineers. During the concept phase, the primary requirement is the creation of one or more concepts which broadly fit the requirements for service loading, whilst paying small considerations toward assembly and manufacture. The part will be simplistically validated for performance and then reviewed during the Airbus Preliminary Design Review (PDR). The new toolsets developed for Airbus by Dassault and others are intended to serve this requirement whilst allowing designers to simplistically take advantage of design freedom offered through the use of AM. Whilst the new tools offer some link between the simulation driven design environment and the detailed design world, significant additional work is still required to create a detailed design. In the detailed design phase one must now, first and foremost consider the transfer of any nascent design from the virtual world to the real world. To do so, a designer must place manufacturing and kinematic considerations to the fore, and even with AM, this will add significant constraints to the design. In essence, every real-world requirement of the part which does not form part of its service loads must now be listed onto an engineering drawing. If a critical feature cannot be dimensioned/tolleranced and subsequently inspected and measured, it cannot be included in its present state and revisions must be made. This is often why even concept design generation is completed with fully controlled and parametric tools such as the PD and GSD workbenches of CATIA (Dassault Systems, 2012a). Within these workbenches and crucially, missing from the newer tools, is the ability to fully constrain and detail any feature of the model and its interactions with other features. Radii, tangency, connectivity can all be controlled, measured and thus recorded on an engineering drawing for use during manufacture and later, inspection. The problems surrounding the new modelling methodologies are not unknown to Airbus and indeed are acknowledged in the placement of these new tools within the design cycle as pure concept generators. A subsequent phase of adaptation/redesign must then be completed as per normal detailed design methods.

2.5.2 Difficulties in Extracting Complex Designs from Topology Optimised Results

TO uses an FE grid to determine material placement in response to structural loading – commonly, many of the smooth outer boundaries of the design domain are eroded (Figure 35) as the solver eliminates elements with little usefulness from the structural whole. In doing so, a rough, tessellated surface is exposed as individual elements are removed or retained (Figure 35). It is this tessellated surface which forms the primary basis for the extraction of the TO result. Exported directly or through a series of smoothing algorithms dependent upon software and settings, the resultant output is exported as an STL file which defines a series of triangles through 3 points and their associated surface normal orientation. These files comprise thousands, sometimes millions of individual triangles with no connectivity to neighbouring elements save for their points of contact. Surfaces which appear tangential are not, appearing so only due to relative similarities of their surface normal (Figure 36). This output surface file is ordinarily a mess (Brackett et al., 2011, Kumar and Krishnadas Nair, 2017) with inverted normal vectors, overlapping triangles, intersecting elements, multiple shell elements within the model. Substantial clean-up of the surfaces is required in order to create a single shell model from the boundaries of the optimised result, and, from the various elements of non-design space within the model. Even when complete the model is essentially useless to most forms of CAD program with manipulation impossible due to its fragmented surface bodies and lack of real connectivity between elements. Highly detailed STL files can seriously hamper the ability of CAD software on even powerful PCs to manipulate and visualise results. Repairs to this STL can be performed using specific software for STL repair such as those associated with 3D printing methods. Materialise Magics and Autodesk Netfab are possibly the two most common commercial software packages and are used by Airbus in this role. Even so, and after such repair the resulting STL is still barely useable as a design guide and is totally unusable as a means of design progression (Fadel and Kirschman, 1996). As such, it is common with both conventional techniques and with the new design tools to use the TO result as a guide and to remodel over the top (essentially 3D tracing), thus mimicking the result of the structural output, but without direct use of it. Problematically, this represents a complete break in the digital chain between simulation driven design and final CAD and means that should any reanalysis/design be undertaken, that there exists a high probability that previous designs may be invalid/unmodifiable without significant re-work. Ignoring for the moment the break in the digital chain, now that an STL has been extracted and prepared for modelling, the design process may begin.

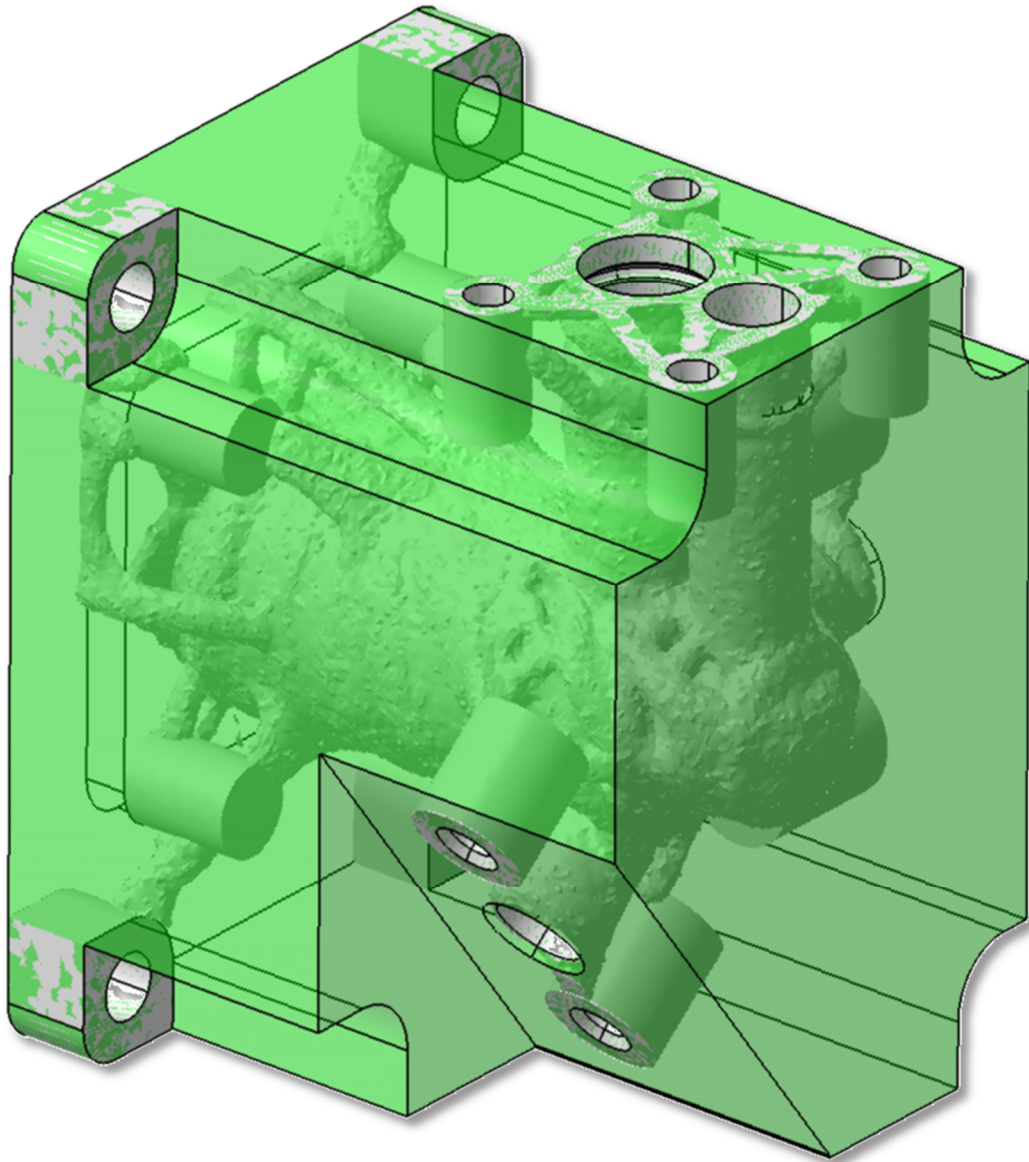


Figure 35 - showing the resulting optimised design (white) from an original design space (green) and the erosion of the original surface topology

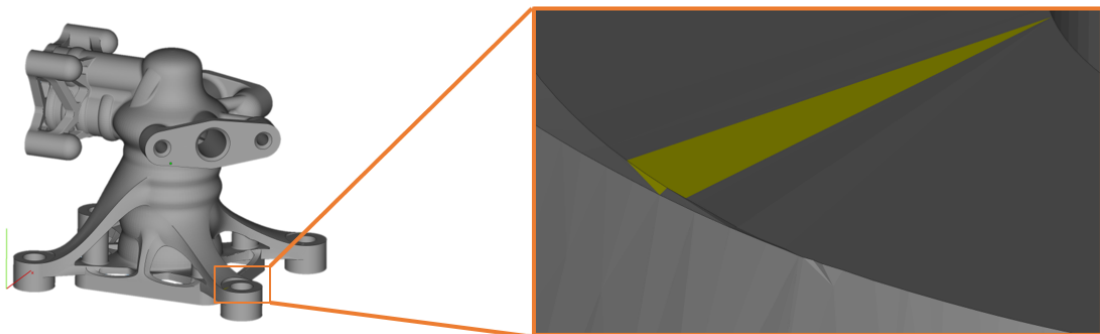


Figure 36 - Extracted design showing misalignment of triangle surface normals in close proximity to one another

TO whether constrained or not has a tendency toward truss based solutions to stiffness driven problems (which most mass focussed problems are typical) and as such has a propensity toward the replacement of single, large, simple structures with complex ones represented by many connected structural members. Consider the optimization in Figure 37 of the pyramid in initially the structure is represented by 5 points, 5 curves and 5 surfaces. In the recreation of the TO result from a coarse grid, the structural result has not only an outer contour, but also an inner one and several complex curves.

The total number of geometric entities required for the new design is an order of magnitude greater than its predecessor and required a similar increase in required design effort in order to recreate. Part of this effort stems from the inability of the engineer to reference the TO output directly such as through recognition of a design point/vertex amount of design. Such points and axes must be painstakingly, but approximately created in 3D space in order to form the basis of any design extraction. On a design with few vertices or structural interactions, this is a manageable task, but on more complex outputs, the task is both costly and tedious. Compounding this problem is the extraction of relatively unconstrained topological outputs which can be intricate and highly complex, with myriad interconnecting features and complex surfaces; In such outputs, the level of complexity within the TO output can be directly influenced by the density of the TO grid used to create it (Muir, 2015). High density grids have a propensity to reveal details within a structure which might not be intuitive to a designer, but which can significantly increase performance whilst reducing mass. In a direct comparison between two optimization results as shown in Figure 37.

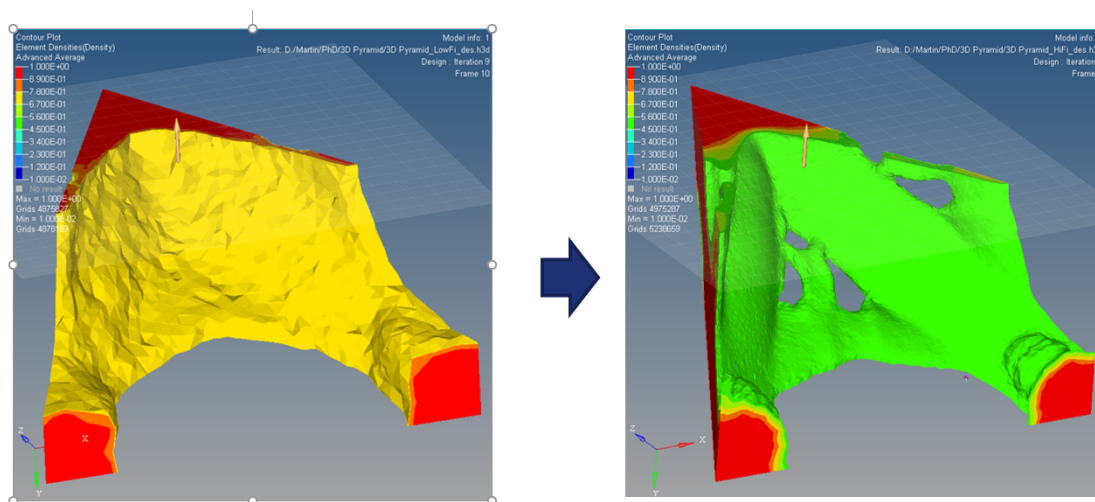


Figure 37 - Showing substantially greater detail revealed through use of a high definition FE mesh

substantially greater detail has been revealed in the TO result which used the refined grid definition on an otherwise identical parameterization. In addition, mass reduction has been

improved by a further 18% and performance by 9% over the baseline result. Whilst performance savings can be seen in the use of reined grids for TO, the complexity of the output structure is exponentially more detailed and requires a commensurate level of effort in order to extract the detailed design. Whilst the direct approaches will be discussed and compared in detail later, the complexity associated with an intricate structural map is extremely difficult to accurately extract when using a solid modelling approach. This stems largely from the difficulty in representing nodal connections and transitions within the design without inadvertently creating notches and discontinuities. As such, and in order to control these factors, a surface based approach is required. Unfortunately, whilst solids are generally created using a series of planer sketches along with simple solid commands such as revolute and pad, a surface model requires not only a dramatic increase in the number of required operations, but also a significant increase in required skill and CAD knowledge in order to maintain order and parametry. Without this, post verification sizing modifications become problematic if the surfaces which require alteration are at an early point in the design tree.

2.5.3 Available Methods for Design Extraction

Many methods for the extraction of topologically optimized designs exist and whilst all can be applied to the extraction of designs from a TO solver, the selection of an appropriate method can save vast time and cost. The selection of the correct method is dependent on several items: the availability of software; the skill of the user and perhaps most critically, the details of the component under investigation. Only when the latter is understood and the former are in balance can a correct means of extraction can be selected and applied.

2.5.3.1 Direct Extraction

The most simplistic and obvious method of extraction is through direct export, repair and manufacture of the results of the TO process. Under such circumstances, the parameterization of the TO formulation must be perfect in order that the output be suitable for its intended purpose. Loads, material data, non-design space must all be extensively understood and contextually mapped to the design domain. Even so, the resulting design will be extremely sensitive to the density of the domain grid and thus subsequently to the effects of the density slider (a visual representation of density penalization as present within SIMP) present in most TO programs (Muir, 2013). The effects of poor grid definition and subsequent use of the density slider can be dramatic, whilst the results of a well-defined grid and the minimal effects of the density slider can be seen in (Muir, 2013) and (Tomlin and Meyer, 2011). A dense grid removes some ambiguity in structural decisions, but unless paired with conservatively applied material

properties or artificially applied loads will reduce a structure to an Reserve Factor (RF) approaching 1 thereby removing almost any structural redundancy.

Once complete and an appropriate extraction density has been achieved, the resulting STL can be either exported directly, or first validated against loads using FE and then extracted to STL. Regardless, once exported, the STL can be imported directly into an AM build environment simulator, repaired and prepared for manufacture. Using such an approach, resulting features cannot be tolerated, nor accurately manipulated, nor can definition of the STL be guaranteed. By this phase, several mesh smoothing operations will have been completed and the resulting mesh will be statistically different to the original geometry which was used during the optimization phase. Again, this lack of achievable definition must be accounted for in the creation of the original model and the parameters required during solution of the problem. Several documented examples of this approach have been demonstrated (Brackett et al., 2011, GrabCAD, 2013) (Figure 34) and all exhibit significant problems when considering industrialization, making the approach suitable only for rapid prototyping activities and realization of concept models. Regardless of assumptions based upon established results, this approach will be evaluated during the course of this research.

2.5.3.2 Mesh Morphing Methods

In order to overcome the tessellated nature of the TO output, perhaps the most common method of attaining a workable solution is through direct manipulation of the output STL. The output STL is effectively a series of simplistic triangular surfaces which combine to create highly complex, connected surface in the STL. As the features of the STL are based entirely upon the nodes and vector normal(s) which comprise the boundary surface, manipulation of the nodal positions will alter the surface normal direction, the opposite is also true. The first phase of a mesh morphing approach is usually one of mesh smoothing (which also occurs automatically in some forms of extraction from the TO software) and involves the average displacement of some node positions in relation to those of neighbouring vertices and in response to the employment of a smoothing algorithm such as Laplacian smoothing (Kai-Ming et al., 2017). Once smoothing has been completed, techniques are employed to facilitate the large-scale displacement of mesh patches whilst maintaining connectivity to adjacent elements. In doing so, the shape of the STL can be modified by the designer to achieve a broadly suitable output shape. Several examples of mesh morphing (Alexa, 2002, Staten et al., 2012) have showcased the capabilities of the technique with several examples having been directly manufactured using AM. Of the examples found, none have been shown to have made it beyond the prototype phase for safety critical applications. In the absence of fully investigating the software systems and methods for using this approach, the

reasons for this can only be speculated at, but most resultant designs still appear to have artefacts of the TO process present in their final design. Also, while mesh morphing and smoothing do allow for modification of the STL, feature creation and constraint will be as problematic with a morphed mesh as it will with a direct output, creating problems for detailed design and later manufacture as shown in the earlier sections.

2.5.3.3 Solid Modelling Methods

Solid modelling methods (SMM) are a generic term which describes the fundamental design process upon which the majority of modern CAD methods, techniques and software was initially based. The method purports that the digital representation of any physical object should be capable of answering any questions which could feasibly be asked of the physical part. The technique does not rely upon any particular approach to the CAD representation but upon computation of features, thus making it provider independent. Like their physical counterparts SMM rely on well-defined and well behaved boundaries in order to provide part representation. Boundaries can be represented using a number of techniques, but by far the most common and well used is that of point continuum topology (Baum, 1964). No matter which technique is used, boundaries for solid modelling must be in the form of closed loops (multiples are permissible) as the majority of techniques used for solid modelling utilise a 2D plan in 3D space which is translated into a 3D shape using additional features within the domain.

There are many methods of implementation for SMMs and whilst all are reliant upon the fundamentals defined above, their employment can alter the means by which a CAD system performs operations and generates designs. The most common methods used for commercial CAD software are those based upon Constructive Solid Geometry (CSG) and Feature Based Modelling. CSG allows for the creation of seeming extremely complex shapes, using a series of combinatory additions or removals known as Booleans. The Boolean approach used allows each remove to be modelled in such a way as to mimic a machining operation, thus also including design for manufacture within the initial approach. The combination of relatively simple modelling methods and a propensity for commercial aerospace to use machining for the manufacture of small components has led to CSG and Feature Based Modelling being the default modelling methods for Airbus CAD. Additionally, a simplified modelling approach is easy to standardise through training and simplistic to enforce (at the 2D level) through admin and Product Lifecycle Monitoring (PLM) tools.

2.5.3.4 Advanced Surfacing Design

Like solid modelling techniques, Advanced Surfacing Design (ASD) is an umbrella term used to define a series of methods intended to allow for the generation of complex, interconnected surfaces which eventually combine to create the boundaries of a solid part. Within ASD are myriad techniques for the creation of 1D, 2D and 3D shapes in 3D space. They allow for the creation of surfaces with complex curvature and for the sympathetic attachment of those surfaces to adjacent surfaces so as to allow seamless lines between sections. The primary base constructs of the ASD method are axes, planes, points, lines and splines (compared to CSGs use of Axes, and planar sketches). Of the latter, a combination of B-splines and NURBS are used to generate complex curvature splines in 3D space which can be subsequently used to create complex curvature, fully controlled and parametric surfaces. Ultimately enough connected/trimmed surfaces are created to represent a full body or structure. The technique is used extensively in the automotive industry as Class-A-Surfacing (Fernholz, 2013) and ensures that generated surfaces are created with extreme sympathy to their light reflection qualities, thus generating bodywork with no flaws. Whilst this approach is, in appearance, purely cosmetic, it also reduces the likelihood for stress concentration factors caused by geometric artefacts. Additionally, Class-A-Surfacing is also used for complex aerodynamic shapes in fields such as formula one and commercial aerospace as it provides for the maintenance of flow attachment through the management of complex curvature.

The use of ASD requires the generation of almost all features required to create a single surface (references, points, curves and connections), as a result, the number of required operations is significantly higher than for a solid modelling approach. When creating surfaces from construction curves, there are often with several methods of implementing similar, but discernibly different features, and an unwise selection may lead to later problems with the model. As such, the techniques used in ASD are highly complex and requiring of significant operator skill and experience in order to maximise their potential (Thompson, 2015). Whilst experience can significantly help to reduce design time, the requirements for substantial operations (when compared to solid modelling) cannot be mitigated against and will always contribute to NRC, particularly for complex design. Furthermore, more so than with any other means of modelling, design tree management and ordered CAD creation is crucial to successful modelling as buried errors will create infinite loops which cannot be parametrically corrected.

The combined effect of these factors has led to a significant reluctance from Airbus and its supply chain to embrace ASD as a means for enablement of AM. Instead, the focus has historically been on the application of constraints to design (previously based upon

manufacturing restrictions) in order to limit resultant design possibilities (particularly for high volume parts) to those that can be manufactured simply by machining operations or casting. Some design latitude is available for low volume or prototype designs, but skills in these areas are limited due to lack of experience and exposure. For complex topological designs, a simpler approach is usually required.

2.5.3.5 Freeform Surface Modelling

Freeform Surface Modelling (FSM) is a relatively new approach to surfacing design, having been developed in the mid-2000s (Sederberg et al., 2004) to fulfil a need for a computational equivalent of the clay modelling approach used by Automotive primes. Developed initially by a consortium of companies, the resulting T-splines software was eventually spun out to form T-Splines Inc (Sederberg, 2007) and purchased by Autodesk. The T-splines software (and its siblings) function like a superset of NURBS, allowing manipulation of the control points for the NURBS surface(s) with respect to the connectivity properties of the attached and surrounding surfaces. Freeform surface modelling maintains a closed volume with full connectivity tangency connectivity between all surfaces at all times. The developed surface set initially uses the existing control points of the NURBS and applies a local axis to each node allowing for local manipulation of that node. The node position can be translated in any axis or compound vector, stretching or compressing the surface in the direction of the translation. No additional nodes are created. In addition to simple translation, the node may also be rotated around any of its new local axes. Doing so, the connectivity of the surface must be maintained, but can easily create twisted surfaces. T-Splines also have the ability to seed additional control points onto a nubs surface through interpolation and segmentation of the surfaces of the existing model (Sederberg et al., 2003). The advantages of segmentation are their ability to intricately control the movement of the surface through the additional placement of control nodes. The T-spline software allows for similar translation/rotation of surfaces in a similar way to that allowed for individual nodes and does so through the uniform manipulation of that surface's control nodes. The technique and the use of T-splines allows for the rapid development of complex surface models which maintain relatively smooth connectivity between elements of the domain. The literature suggests that the software can dramatically reduce the required time to extract complex designs from topology optimised models, thus reducing the total required design effort and the NRC of the design process. Currently, T-spline software exists from a number of vendors such as Autodesk, Rhino, Dassault an Altair to name but a few. The effectiveness of FSM will be fully evaluated as part of this investigation

2.5.4 Difficulties of Safety and Certification for Complex Designs

Foremost amongst concerns and costs for Airframers when considering the employment of novel technology and new designs, are those aspects which pertain to the safety and certification of parts and/or aircraft. When considering the combined use of AM and TO, the combined cost and complexity of the qualification process for either technology on their own, might well be the highest cost and longest development cycles for any research programme – together they represent a substantial obstacle to entry into service. The reasons for this stem largely from the novelty of the developing techniques and the fact that standards usually lag behind the development of new methods and tools for product improvement. This is certainly the case for AM, and currently Airbus is in the unusual position of knowing substantially more about AM than either the supply chain or the regulatory bodies. In order for Airbus to progress the technologies and in the absence of developed standards for aerospace, Airbus utilise parallel standards developed for other industries and applications and use/adapt those standards with the fundamental methods for material and process testing for Aerospace. This facilitates the development of internal standards for the use of AM. Latterly, jointly developed (between Airbus and regulators) standards for the certification of AM TO structures can be attempted, often with regulators adapting and improving upon Airbus developed standards in order to progress rapidly and economically. This process allows Airbus the assurance required to progress with technological development whilst influencing the development of safety certification standards. This process has worked well for the introduction of AM for low-risk, existing designs which are simply manufactured using the newly developed AM techniques and standards. However, whilst the newly developed standards may well have similarities to the Airbus internal standards, the risk in progressing without developed industry standards are significant, both in terms of delay and cost. Any changes or discrepancies in the internal standards will require addressing through either adherence or arbitration with the regulatory bodies.

One of the principal difficulties in the certification of AM stems from the complexity and manner in which the material which comprises the structure is created. As AM materials are produced in layers and are generally created using a combination of two melt profiles in each layer (boundary and core), the material properties of each are slightly different due to the resulting microstructure of the utilized melt theme. On large, thick walled structures, this is not a problem as the wall may only represent 5% of the total structural mass and is thus inconsequential for properties (Antony et al., 2013, Lin et al., 2013) for thinner structures, the effects of boundary to core ratio become more acute and in extreme cases, boundary may comprise the majority of the deposited structure. In such circumstances, the change in material properties can

be extreme and thus must be guarded against (Airbus Internal research). Consequentially, when not subject to post machining, Airbus has imposed design rules which limit the minimum thickness of deposited structures in AM in order to allow for the assumption of Isotropic material properties within the deposit. This limits the effectiveness of mass reduction activities, especially on parts which are already thin walled. These are internal standards and are generally not mirrored by regulation.

An additional complexity for TO (and in addition to the phased introduction of AM) is that novel designs produced via TO, tend to have limited redundancy within their structure, especially for simply loaded designs (see section 2.4.8.2). Structural damage caused by debris or maintenance mishandling can lead to dramatic reductions in their performance capabilities. Consider a design such as the one shown in Figure 39, should any of its load carrying structures sustain damage with an effective depth of $>1\text{mm}$, structural effectiveness will depend greatly upon the location of that damage as this is an almost fully stressed design (Hinton and Sienz, 1995). In the case of impact damage as shown in Figure 38, the notch reduces the effective thickness by a $1/3$, thus reducing its load carrying capacity by 25%. The remaining structural members cannot support the difference in loading for the structural whole and thus the structure fails. In contrast to a conventionally designed part where the same damage is applied, the structure supports loading without problem under static conditions, but would need still repair for dynamic loading in order to remove the sharp notch. In such a repair situation, the TO part due to its already minimal structure cannot endure the repair techniques intended to reduce the notch as they would further reduce the thickness, thus further decreasing its performance. The result of this lack of structural reserve and a structural inability to endure damage without catastrophic failure, has led to significant constraints being applied to the allowable minimal features of TO designs in addition to those permitted within the Airbus design guidelines.

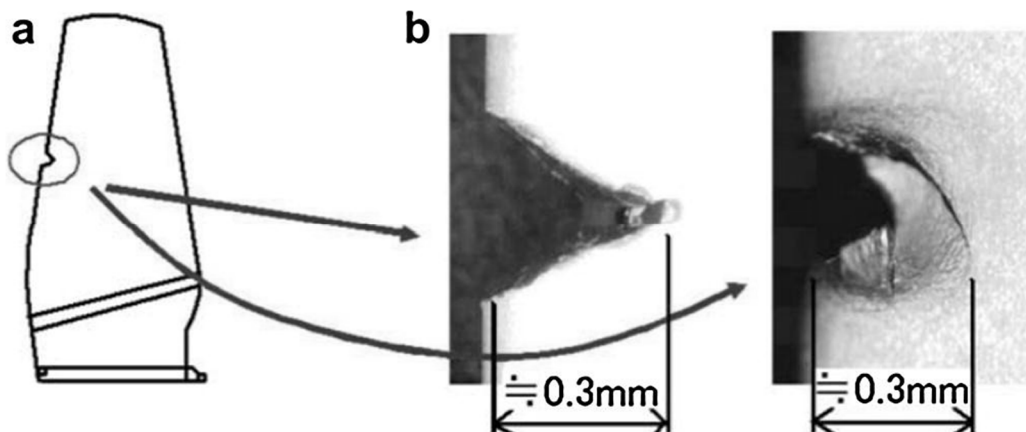


Figure 38 - Typical notch impact damage and the subsequent creation of a fatigue initiator

The only means of mitigating the effects of these global design rules, are through a complex analytical process known as failure mode effects analysis.

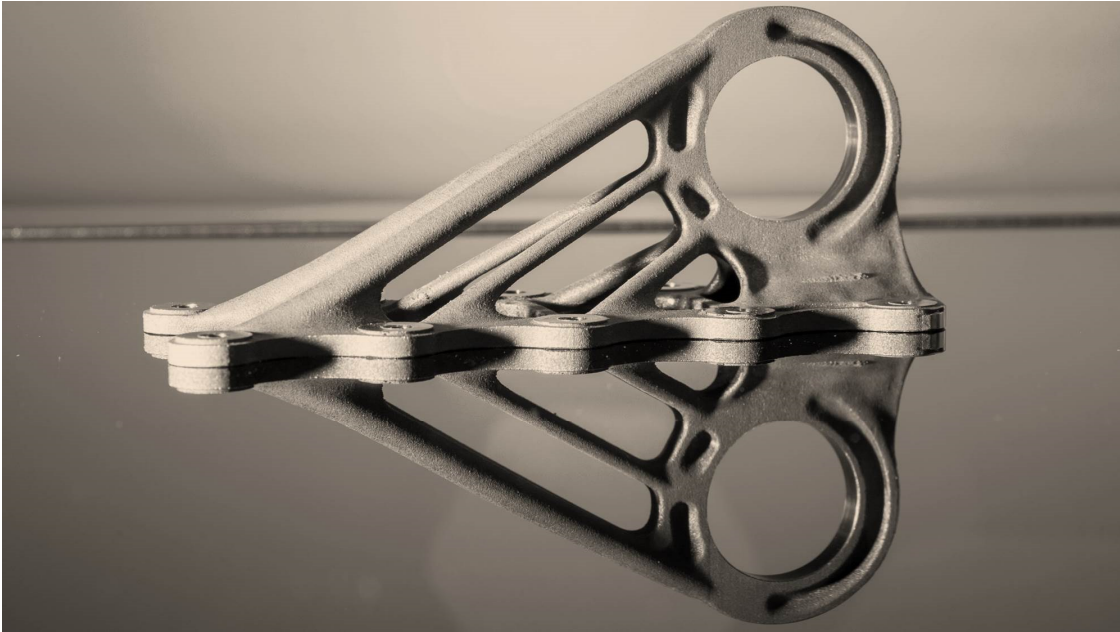


Figure 39 - Fully Stressed Design through optimization and AM

If used, mass can be safely reduced without compromising structural redundancy, but the costs of design and analysis is extremely high as it cannot be performed adequately using design tools, but requires full stress analysis, thus increasing NRC for part design.

2.5.5 The Total Design Cycle and its Non-Recurring Cost

Regardless of the method used for analysis, extraction and manufacture of topology optimized designs, the complexity of the combined cycle for design and manufacture is substantial when compared to those of a traditional process map. Figure 40 shows the major process steps needed to accomplish design, analysis, manufacture and verification of a conventional design using solid modelling, simplistic verification and manufacturing via and CNC machining. The process is simple and robust with very few steps, each requiring only limited time to complete and check. In contrast, Figure 41 shows the extreme complexity of an optimization driven design approach with realization through AM. Due to the significant increase in required design time and analytical processing, along with the dramatic increase in manufacturing complexity expressed in substantial pre- and post-processing activities, the time and thus cost of the complex approach is orders of magnitude higher than for the conventional approach to design. Even ignoring for the moment, the substantial NRC costs for manufacturing in AM, the magnitude of the NRC for design is such that an approach as described above could only be justified for components on which high mass savings could be guaranteed and application so similar but smaller parts could

not be justified. In order to allow for the expansion of this process to familial parts which fall outside of those part with high mass saving potential, a reduction in design NRC is required

2.6 Processes Automation as a Means of Cost Reduction

Automation, was a term coined by the Ford Motor Company in the late 1940s when establishing a department aimed at implementing automatic controls within sections of their manufacturing and assembly plants (London Business School, 2003). Since that time, Automation, both the word and the method, has been employed in numerous applications across myriad industries each with the intention to reduce recurring costs through elimination of labour intensive, repetitive operations. Historically and commonly associated with robotic methods of manufacturing and assembly, automation of assembly lines in most developed nations is now common place, providing significant economic benefits to the owners of those companies and the *potential* for reduced costs for consumers. Automation is generally thought of by the general public as a means of reducing costs for the manufacturer whilst simultaneously increasing profits by reducing staff. Within economic circles however, automation is usually employed only when labour rates increase to unsustainable levels. At this point the cost of automation becomes worthwhile for the manufacturer when amortised over 3-5 years. During this amortization period, the consumer would expect a price decrease based upon a perceived reduction in labour, but due to the cost of automation, it is rarely seen. What is seen by the customer is that the price over time does not increase despite over the same 5-year period inflation being over 15%. It is for this reason that automation would be sought for the redesign of components for AM. Monitoring and automation of process systems is dependent upon the infrastructure present within the facility or process to be automated and whether the metrics of the process can be recorded, compared and discrepancies attributed cause and thus corrected. The most minimal level of automation usually employed is that of a Process Automation Systems (PAS) which utilises a series of sensors, controllers and actuators to allow for active control and correction of process drift. PAS methods are usually employed individually on independent systems and operations throughout a production system – they are not usually interlinked for data or control, thus requiring oversight by skilled operators to ensure their output falls within approved levels for the process whole. Higher levels of control and automation are available using superior, interconnected methods and systems for control. Supervisory Control and Data Acquisition systems (SCADA) differ substantially to PAS methods in that they allow for the use of automation on a global scale, linking each system to an overarching controller for all sub-systems in the process.

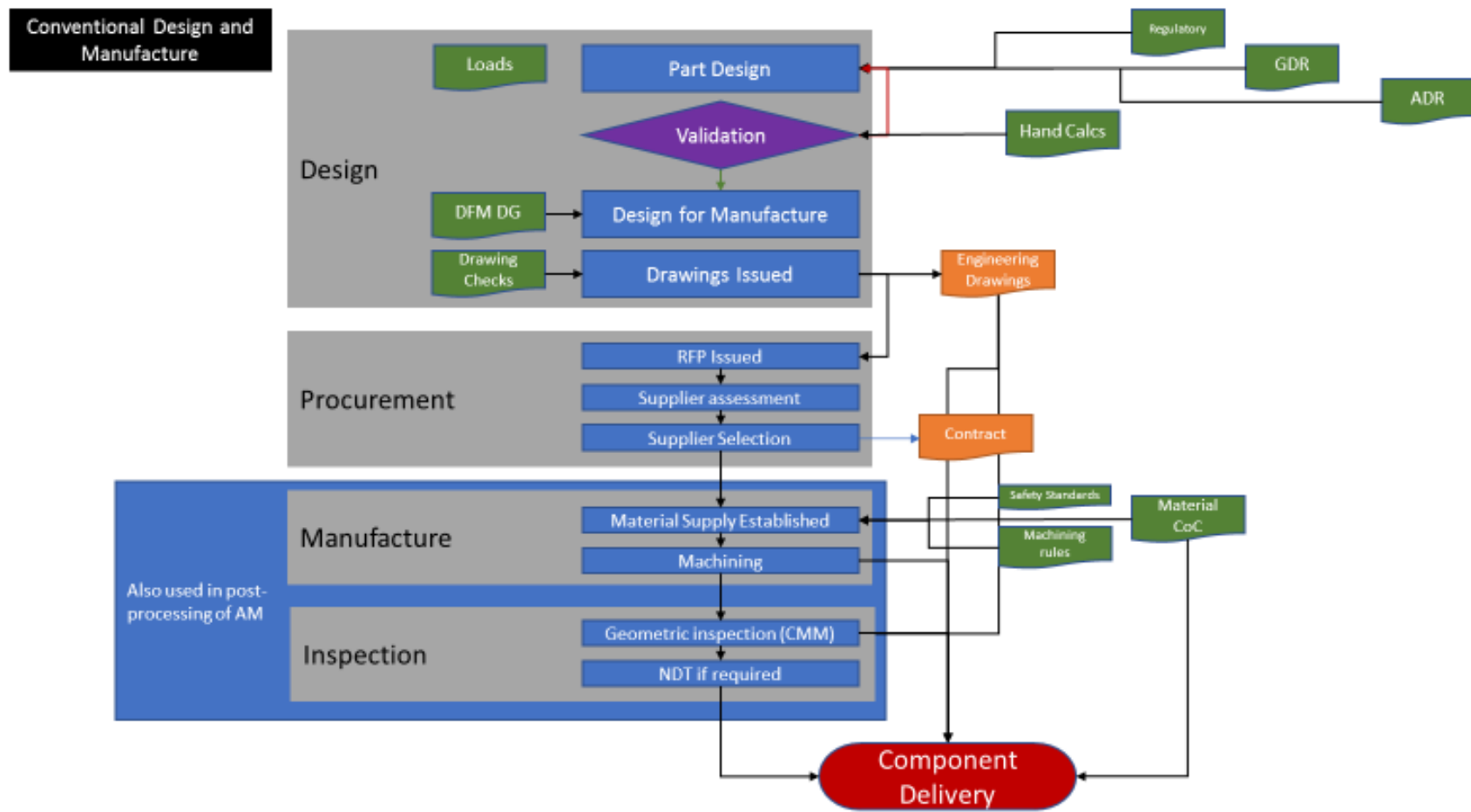


Figure 40 - Typical process for the design and manufacture of an Airbus designed, supplier manufactured part

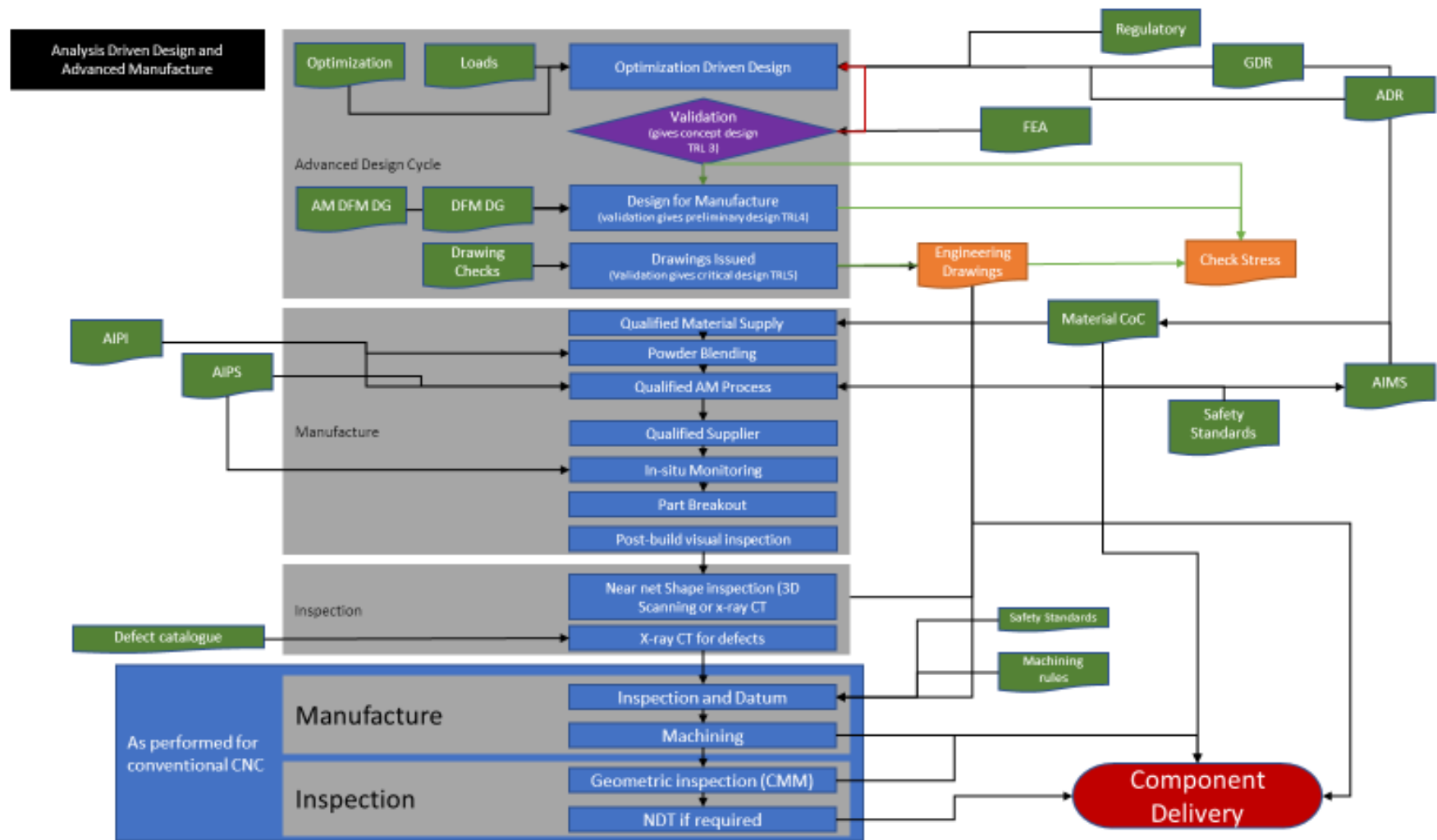


Figure 41 - Analysis driven design cycle without complex supplier engagement shown in Figure 40

Thus, a network in which data and instructions for operation are shared and transferred to allow for optimal use of the entire process in response to a governing objective. Use of SCADA systems are now common for many complex systems in which software and hardware are required to work in harmony with one another and are interdependent upon one another for continuous operation. Similar digital control systems could be of substantial use in automating aspect of the software process for this project.

Investment in automation is often most effective when the number of total units to be produced is very high and thus the investment in hardware and software infrastructure can be spread thinly over the vast number of units (Ruffo et al., 2006). However, whilst the reduction in cost associated with assembly operations is easily quantifiable and is often the most commonly used method for the justification of automation, there are other notable benefits which can be used to justify the use of such techniques. Beyond the obvious economic benefits, perhaps the other most notable effect of automation is the potential for error reduction/process stabilization. Through automation, each step of a required process can be mapped, digitised and coded into a system. The system cannot miss any steps, nor can it vary the order or specifics of each step, they are completed indifferently and identically to all other sets unless a problem with the system occurs. ABB instrumental, one of the worlds leading suppliers of robotics for automation has shown that through use of a carefully and sympathetically automated process, process error and re-work can be reduced (Hui et al., 2006). Whilst the most obvious examples of process automation are in manufacturing, automation of digital processes can also yield substantial savings, especially where the time of skilled professionals are required for its manual operation. It is this level of automation that is required in order to reduce the NRC of complex, optimization driven design.

2.6.1 Fundamentals of Process Automation

The automation of any process must begin with a full understanding of the process to be automated (Mustafa and Cheng, 2017). A detailed mapping must be completed in which specifics of both stages and the sequencing of each stage along with any required dependencies and resources for its completion must be captured. Once fully understood a suitable level of process control may then be considered and implemented. In addition to a complete mapping, an understanding of the process error bounds must also be attained (Gaul and Ritter, 2012). This information allows for the automation of any linked process based upon sub-system performance providing that error bounds can be programmed into the automation, thereby allowing for a

certain tolerance and recovery from error in the systems whole (Loborg, 1993). In any complex system or process, a series of sub-systems will perform functions which together link to create the process flow. In a fully automated process similar to a SCADA system, the ability for each process to be part of the whole is related to its ability to communicate with the process controller. Even in the absence of a full SCADA system, an automated process relies upon the ability of each sub-process to pass on its outputs to the next step in the process. As such, the outputs of each sub-process must be either through careful design of the input/output systems, or through manipulation of the data, compatible with the next/other stages of the process. Whilst all of the earlier literature is related to physical systems and automation the robotic, the principles of automation are common whether applied to physical manufacturing or digital design systems and so can be used as the basis for automation of TO. When considering the linking of production systems and particularly software packages, consideration of file types for transfer between system nodes must be assessed. Commonly open source file types and codes are the preferred methods of data harmonization between sub-processes, as they allow for the use of many different systems at that automation node, thereby allowing for redundancy and no direct dependency on a single supplier. This is of particular concern if certain sub-processes require the use of proprietary software for their implementation. The use of open source code and formats allows for flexibility in both file transfer and the black box solvers required for the operation of the optimization, this method will be the primary method investigated as a means for implementation of automation.

2.6.2 Historical Use of Automation in Design Optimization

Since the earliest days of Computer Aided Engineering (CAE) and Computer Aided Design (CAD) during the late 50s and early 60s, the complexities of the techniques has driven many to seek automation as a means of reducing the required time and associated cost of the design cycle. ASTROS (Automated Structural Optimization System) was one of the first (and so far, one of only a few) such systems. Whilst defined as a structural optimizer, the software does not make use of topological optimization methods, but instead uses sizing and placement methods for the determination of the optimal layout for aircraft designs. It is frequently referred to as an MDO tool due to its consideration of the effects of layout upon the basic range equations used during preliminary sizing for aircraft, but it's a structural optimiser in practice (Neill et al., 1990). This is the primary objective of the ASTROS software – preliminary sizing and layout. Many other similarly derived techniques have been developed from the fundamentals of the NASTRAN solver and the developments of NASA for CAD, but without exception, these techniques are isolated to conceptual design and are not intended for use in an end-to-end process. Sadly, due to the age

of the software and its limitation in handling solid elements, the potential for use as part of this investigation is limited

2.6.3 Automated Structural Optimization – Methods and Limitations

When considering the automation of SO, specifically TO, there are several levels at which automation can be applied to the process. These are most easily broken down into the three primary stages of any optimization cycle: pre-processing; solving and post-processing, each of which is usually completed within a unique software environment. It is through application of automation to one or many of these stages that most approaches to the partial automation of SO have been attempted. The reasons for partial application stem from the difficulties in moving from CAD to FEA, through SO and then back to CAD thus, and because most forms of optimization rely heavily on the FEM, most commonly, it is the analysis and optimization aspect of the solve to which automation is commonly applied (Adarsh et al., 2017, Thigale and Shah, 2016). Historically, once into the FEA environment and after creation of the FE grid, the CAD use to create it becomes irrelevant, thus, any subsequent modifications to either the CAD or the grid, create difficulties in subsequent phases, making any linked, automatic, optimization very difficult to implement. By remaining in the FEA program after initial parameterization and the gathering results from primary analysis and optimiser, the decisions of the optimiser can be applied directly in so far as they affect the layout of the structure, and can be applied directly to the FE grid through use of a mesh morpher. The altered structure can then be re-analysed and, if required, the optimiser can run a second iteration or subsequent analysis (Hernandez, 2017)(Airbus 3DX). This level of automation can save vast amounts of time as it usually eliminates the requirement to re-mesh and thus re-enter the pre-processing phase after geometry modification. Whilst this method can reduce the RC incurred during an optimization phase, it does not directly address the requirement to parameterize, nor does it address the necessity to recreate the CAD once the optimization is complete (Muir, 2012a). The latter of the two problems is perhaps the most critical as, dependent upon design complexity, it can be one of the most time consuming tasks and one that cannot be simplified without heavy constraint upon the optimization definition (Babic et al., 2008, Daroczy and Jarmai, 2011, Muir, 2012b). To mitigate against this, a means of linking input CAD directly to the output FEA and the optimizer is required.

In A CAD based approach, the CAD which represents the structure under analysis is heavily parameterized during the pre-processing phase (Chang and Tang, 2001, Egerland et al., 2007, Hardee et al., 1999). The mesh is then automatically and coarsely generated with respect to the geometry and the optimization is subsequently created. The optimiser then works through allowable modification of the CAD at the parameterized control points upon its surfaces. Once

the CAD has been altered, the mesh is adapted through either movement, recreation or morphing (dependent upon the technique) of the grid to match. These techniques allow for rapid, almost instantaneous extraction of an optimized structural design, but at the penalty of higher pre-process time and extreme limitations on structural output commensurate with a highly constrained domain (Holmberg et al., 2013). The success of many of these CAD based techniques rely upon their interaction with the FEA domain, and the types and placement of elements within the grid (Hardee et al., 1999) and can create coarse boundaries and irregular CAD when compared to traditional manual methods.

2.6.4 Automation of Structural Topology Optimization and Design Extraction

There exists a certain paucity of research which considers the automation of TO, particularly when concerning the automation of the entire process from CAD>CAD. This is perhaps because, in abstraction, the optimization process itself is already largely automated or, perhaps it is because the process is often used on an individual basis, and then, largely in a corrective manner and so the pre and post process time requirements are acceptable; regardless, little material which covers the end to end automation of a process for SO or TO exists. The earliest piece of research which claims to address fully automated SO (but not specifically TO) shows, through use of a divergent computational techniques to FEA, that a automated structural optimiser which parameterizes and solves can yield substantive time benefits to the operator in the generation of new structural designs for which limited historical design data is available (Pier Davide et al., 2012, Terwilliger and Berendzen, 1999). Regrettably, the research does not cover the entirety of the process as it omits the design extraction phase, one of the most time critical aspects for complex design (Muir et al., 2014). Later work again shows the effects of heavy pre-parameterization and looped optimization based upon mesh morphing via shape optimization (Ali et al., 2013), but in reality does little to reduce the time required to perform closed loop optimization. In such examples, the NRC of engineer time is merely shifted from sequential manipulation to, heavy front loaded and bespoke parameterization; whilst automation is indeed included, its effects on cost of design are minimal, drawing only from reduction of computational requirement and potential performance saving from the generated design. Again, these likely stem from the methods in which SO and TO are usually applied and thus the need for automation of the process does not exist. Conversely, Airbus would like to use TO for optimization driven design and so automation of the process is required if many parts are to be assessed expediently and cost effectively. Up until 2013, few methods existed which would allow for any simplistic means of linking the pre, solve and post processing activities in an automatic fashion, but developments in CAD (T-splines) had not gone unnoticed. Introduction for T-splines into CAD

packages had begun as early as (2009) but at this time, CAD and FEA were rarely to be found in a single package and even those that were (i.e. CATIA) had limited capabilities. Slowly however, the largest industrial players for modelling and simulation began, through development or acquisition, to offer suites of products (CAD, FEA, AM) intended to allow the user to perform all required functions of design within one package. Each provider proposed the use of T-splines as a means of rapid extraction in contrast to conventional techniques in an effort to reduce time and smooth the output of TO. Problematically, even with the use of T-splines and their derivatives, the process of TO is still difficult to automate as there are still several design and parameterization stages which require significant initial input to allow progression to the next stage of analysis. Additionally, whilst the new CAD developments aimed to reduce design time appear effective, internal research suggests that this effectiveness is strongly related to user competence and experience and that these organic designs are exceeding difficult to robustly design. If this is in fact true, it would be difficult, without further development, for Airbus to allow for its introduction as a final design tool as output would vary from engineer to engineer.

Regardless of their detractions, these techniques and the underlying research which defines their fundamentals represent the state of the art when considering optimised structures and design, if not automation and as such research on their capabilities, which show great promise for the reduction in required design time will be investigated. If found to be useful, the extraction techniques described above will be incorporated into the research being undertaken as part of an intended automated approach.

2.7 Summary of the State of the Art

The use of AM within Airbus, aerospace and the wider engineering community is increasing with alacrity, indeed Airbus' budgets and projects in this regard have quadrupled over the past 2 years, thus demonstrating the potential that Airbus sees in this technology. Similarly, the advancement of analytical design tools for the exploitation of those developmental AM methods is also increasing. However, in the development of both technologies there exists a number of gaps which limit the application of the technology due to either cost or safety reasons. The most recent tool developments from both Autodesk and Altair (utilising T-spline software) have significant advantages over previous techniques by both companies for the rapid extraction of designs and modification of design space in preparation for optimization. For AM, the development of reliable understanding of powder conformance and recoating problems have led to a more stable and well understood process which is now capable of producing repeatable and reliable parts and material in multiple different platforms and materials. However, when looking at an end-end chain in which an existing design is analysed, optimised, extracted and

manufactured, several notable holes in both literature and software still exist. Of these perhaps the most notable are mechanical property data for compound build angles in AM (critical if unconstrained TO parts are to be produced), direct links between FEA and CAD extraction and finally, methods of easy parameterization based upon existing load catalogues. Each of these must be solved to allow for fully automated topology optimization to exist. The completion of this comprehensive literature review covering all stages from regulation and design rules to AM, FEA and STO directly addresses Objective 1 of the key research objectives.

3 The Automation of Structural Topology Optimization and its Recreation into Parametric Design Data

In this chapter, the focus is on the establishment of baselines, both software and process, from which the research can be launched and ultimately measured against once complete. To that end, the baseline processes for both the current and future AM design cycles are mapped along with the tools currently used to perform each major stage. A detailed work breakdown structure is then captured from the conventional process in order to determine in detail the potential targets for automation. In order to accurately and without bias determine the effectiveness of current tools, a series of candidate parts were selected which together can be said to represent a sample of the population of total target parts. Using current airbus toolsets and processes, the expert community of Airbus was then tasked with the optimization of the candidate parts (using standardized tools) and subsequently surveyed to determine potential targets for automation. Whilst this research was ongoing, the state-of-the-art in optimization and design tools were evaluated to see if benefits beyond current airbus tools could be derived.

3.1 Research Motivation and Context – Why is the Research Project Required

In order to understand the need for higher automation requirements, some context must be provided. Airbus has vast quantities of small, high mass, conservatively designed, structural parts on myriad aircraft platforms (section 0), many of which would benefit from a material change and manufacture using AM. Problematically, the cost of analysis and optimization driven redesign, whilst individually quite low, is cumulatively prohibitive to any business case. Currently, the catalogue of small, metallic, structural components on Airbus aircraft numbers into the 10s of thousands. Of the components identified, there are a mix of material types with older aircraft types (and their derivatives) having higher quantities of heavier, less optimised parts made from cheaper materials. Later aircraft, particularly the A350 have higher quantities of titanium components which are optimised for weight and machining. The result is that whilst there are significant cumulative mass savings to be made, the highest are often found on the older aircraft and are achieved through a combination of optimisation (Tomlin and Meyer, 2011), AM and a material change to titanium. With each component taking up to 100 hours to optimise and redesign (this does not consider any requirement to test and recertify) the predicted cumulative required design time is economically prohibitive and it is cost not weight which is currently driving innovation at Airbus. With a heavy backlog of aircraft orders, orders which have been sold on performance figures which have already been achieved. Additional mass savings and performance are of limited concern. Of paramount importance to Airbus at the present time is

the reduction of manufacturing cost and maximization of profit from orders taken, but not yet delivered.

The Cost of AM production is difficult to quantify as design, machine and material are all factors of AM build economics. However, cost savings in AM can usually be realised on either high B2F ratio or high material cost components where optimization and redesign are permissible (ie Ti or Inconel) (Muir, 2017). In either case, the potential savings are only realised through combined optimization/material change and manufacture using AM, as individually, the technologies do not often provide for a cost saving. Cumulatively, these potential mass and cost savings are large, but are quickly offset by the required NRC for design especially when performance/weight is removed from the cost equation. Thus, in order for Airbus to apply the combined use of optimization and AM and for an equitable business case to be made, the NRC for design must be reduced through simplification and automation. Automation of the analysis and design process would seem to be an effective solution to the problem, but is seemingly an area of research interest which is specific to a very limited pool of businesses. As such, little research and development has been focussed on the automation or simplification of a complete CAD>CAD (whereby an existing design in CAD is analysed, optimized and redesigned, returning a new design in the same CAD format as the input) approach to design optimization of large numbers of existing components. This research intends to address the dearth of material in this field.

3.2 Baseline Establishment – What is the Current Process for the use of Structural Optimization in Airbus

In order to provide an improved method of applying structural optimization for Airbus, an in depth understanding of methods by which it is currently employed were required. The following sections aim to capture the tools and methods used along with a detailed work breakdown and flow-process for data when using TO for the redesign of components or systems.

3.2.1 Current TO Process Applications within Airbus

As previously identified in sections 0 and 2.4.8, there are two primary uses for TO within Airbus commercial aircraft – one concerned with analysis and improvement of existing components and the other with the development of new designs based upon guidance provided by TO. As such, there is a markedly different approach to each design cycle and the inputs and outputs therein. During the former, the import of existing data and the capture and parameterization of requirements are critical steps in the design cycle as without them, the structural output may be fundamentally flawed. Also, as this approach is usually concerned with the improvement/correction of existing parts, aspects of detailed design will be critical to eventual

layout and thus must be addressed. In the latter process, the TO output will be utilised as the basis for a concept and eventual detailed design and thus is less constrained due to its position in the design cycle, with detail and requirements subsequently added in later, more detailed phases of design and validation.

3.2.2 Primary Work Breakdown Structure for Airbus TO Processes

Each of the identified processes has been investigated and a detailed map of discrete work phases and their position in the design cycle, identified and populated thus showing the work breakdown structure (WBS) for each phase. The twin process maps can be seen in Figure 42 and Figure 43

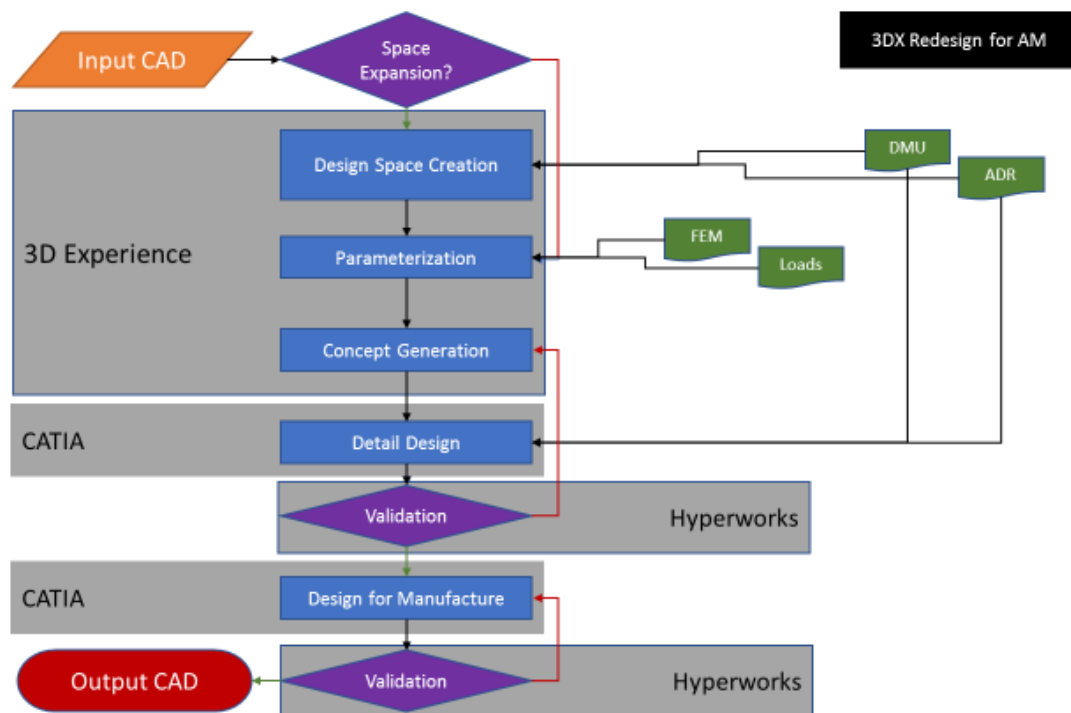


Figure 42 - Coarse work breakdown structure for concept design using Dassault 3D-Experience Software in Airbus

Having investigated and used both of the above processes on and for a variety of components, it was determined that the secondary and newer process of concept generation for AM (Figure 42) provided for a less automatable and less beneficial resulting output than for the initial application. The reasons for this judgement stem from the limited use of novel software to that of layout guidance, with little or no intention on the side of Airbus to using the tool in a more robust design environment due to its lack of appreciable constraint systems. As such, this investigation will thus focus on the potential advantages offered through the use of automation on the primary process and its sub-stages.

Within the flow process for the primary method of optimization detailed in Figure 43, the major substantive portions of the topology optimization process are identified, but to accurately target the potential for automation, a more detailed work breakdown structure must be attempted. After further analysis of the process, noting each step within the chain, its attachment to adjacent processes, along with any required inputs and outputs, the following detailed work breakdown structure (WBS) was created (Figure 44).

This WBS represents the digital nervous system of any TO process for SO and allows for the determination (through subsequent analysis) of where delay in the transmission of data from one node to the next can occur.

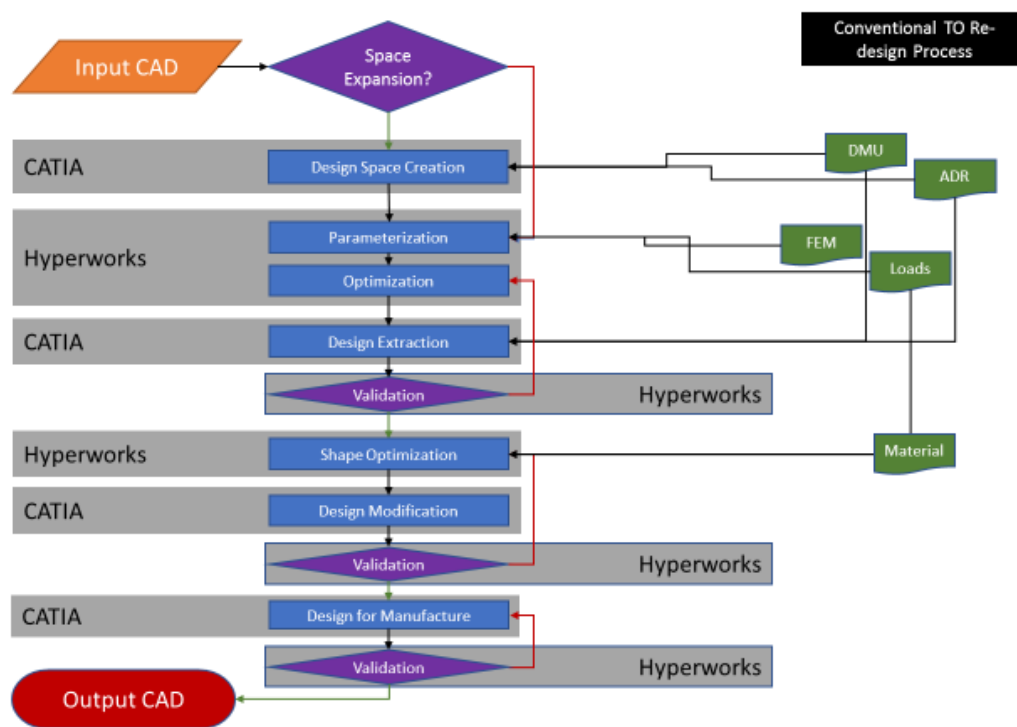


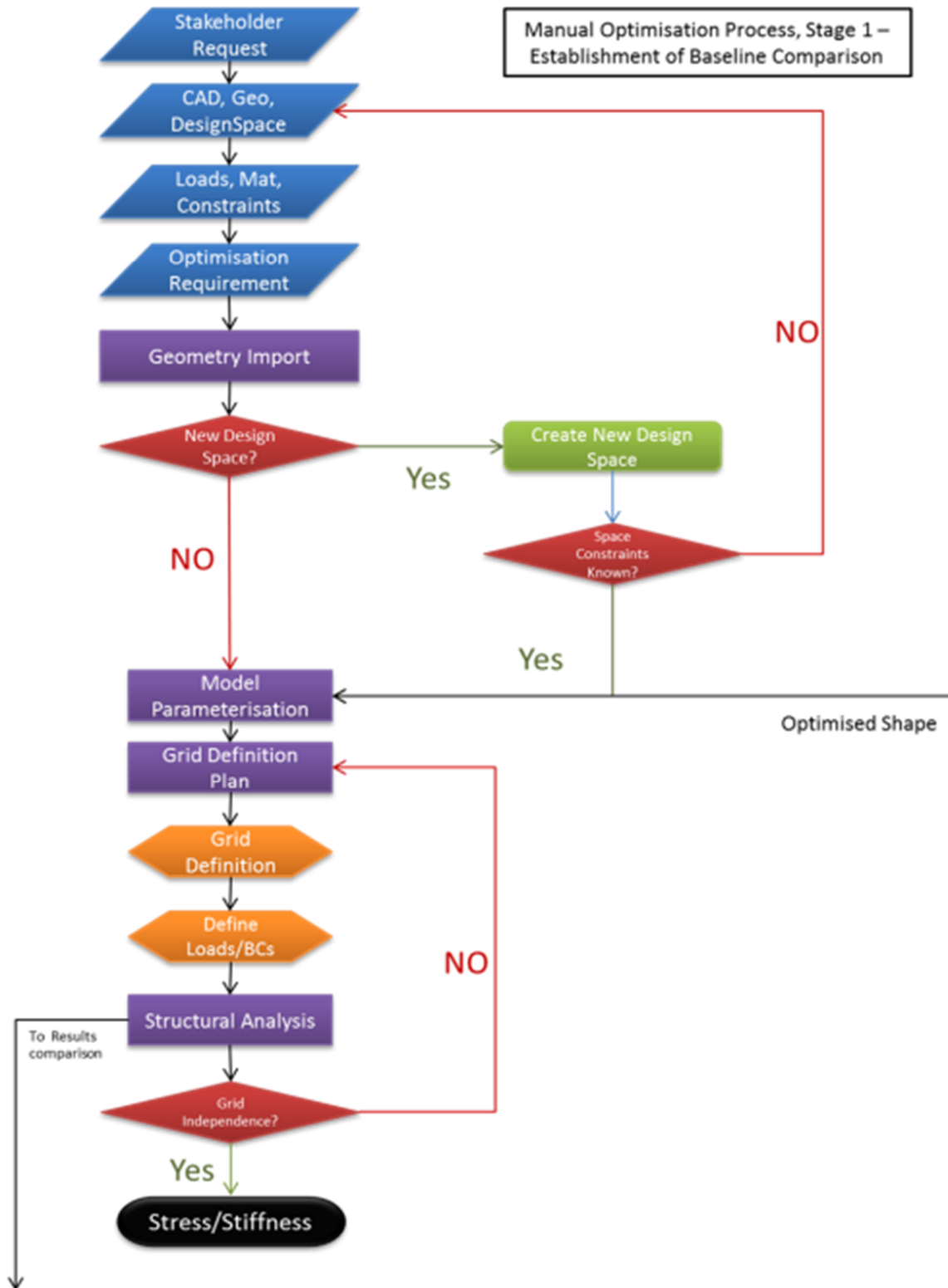
Figure 43 - Conventional approach to the redesign of components using an analysis inspired design approach

3.2.3 Evaluation of Baseline Topology Optimization Process

3.2.3.1 The Effect of Geometry and Application on Time Required for Optimization and the Selection of Candidate Parts

Within each segment of the design process, a certain amount of required manual effort must be applied before progression to the next process segment can be attained. Literature (Machunze, 2013, Muir, 2016) and experience suggests that the total time required to fully optimise and redesign a component using TO, is heavily dependent on the geometry and loading of the

component under investigation. As such, and in order to determine, independent of the geometric dependencies, where the largest time consumers in the process lie, a series of five small titanium parts were identified for TO trials in order to establish an average baseline time for the TO process as it stands today.



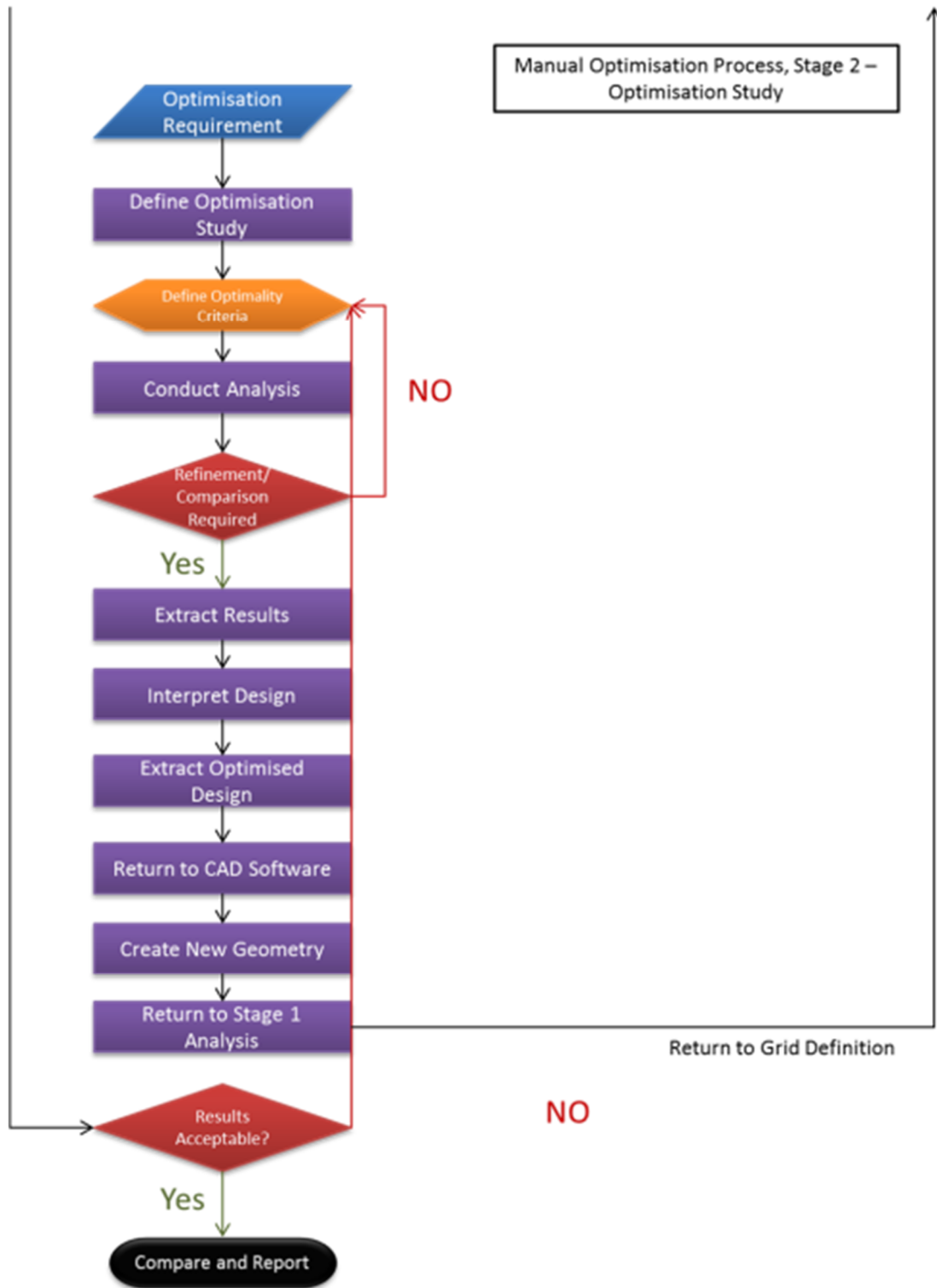
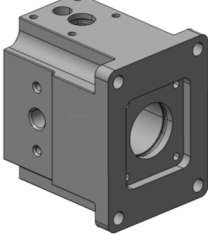


Figure 44 - Full WBS for the manual TO Process within Airbus Group

The selected parts are shown in Table 4 along with their application, primary loading types, approximate size and objective for optimization. All parts are either titanium or are to be subject to a material change to allow for titanium manufacturing in AM thus giving all parts

identical manufacturing tolerances in AM. Initially this list contained purely structural components (brackets) as Airbus manufactures mostly the primary structure of the aircraft, but with Airbus considering moving back into the systems domain, it seemed appropriate to include a systems level component within the part list. STR5 is an hydraulic manifold part and thus has design requirements both internally and externally, thus providing more of a challenge to design extraction techniques as T-splines cannot be easily applied.

Table 4 - showing the down-selected list of candidate parts for use during the investigations

Component Name	Designation	Component Image	Component Size (mm) LWH	Material	Buy to Fly Ratio	Principal Loading Type	Current Mass (Kg)
Under Wing Panel Bracket	STR1		130x90x60	Ti64	9:1	Static	0.26
MED hinge (gooseneck)	STR2		170x90x225	Ph15-5 (material change allowed)	13:1	Fatigue	1.6
Nacelle Hinge	STR3		170x60x85	Ph1 (material change allowed)	8:1	Fatigue	0.993
Engine Bracket	STR4		210x90x95	Ti64	3:1	Static (torsion)	2.1
Manifold	STR5		80x70x90	Ti64	2.5:1	Low cycle fatigue (FESL)	1.56

3.2.3.2 Software Utilised for each Phase of the Design Process

An investigation of available software packages for the implementation of the end-to-end process for TO for commercial aerospace was undertaken at the outset of the project. Whilst already familiar with certain design and optimization tools, several alternative solutions were commercially available and in use by partners and competitors and were deemed worth of investigation within the scope of the project. For each of the primary phases of pre-processing, solution and post processing, alternative software packages capable of compatibility with the derived flow-process and existing Airbus design tools were identified Table 5.

Using two of the identified candidate components (STR2 and STR5) each of the software packages was procured and integrated (as best as was possible) into the existing design process for TO and subsequently evaluated and cross compared. As functionality and ease of use is significantly skewed by the experience of the user, the software evaluation was performed only by the researcher and only superficially for each software set. The comparison considered several factors including ease of use, functionality and cost along with many other items. Weighting factors were applied to several categories in order to either penalise or promote their effects on the results score and in relevance to their importance. In the pre-processing phase and despite significant penalization for familiarity and cost, Dassault CATIA (Dassault Systems, 2012a) proved to be a strong contender with surpassing capability and interconnectivity (Table 6).

Table 5 - List of toolsets for primary phases of optimization process

Process Phase	Software Identifier
Pre-processing	CATIA (Current) Autodesk SolidThinking/Inspire Rhino Solidworks Patran
FEM/Solver	Optistruct (Current) Nastran Sol600 Abaqus ATOM Genesis Siemens NX
Post-Processing	Hyperview/Evolve CATIA (Current) Rhino Solidworks

Only its poor performance with T-spline software in the Imagine and Shape (Dassault Systems, 2012b) workbench detracted from the user experience. Autodesk Fusion (Autodesk, 2012) and

Rhino (Rhinoceros, 2012) were the other strong finishers with both possessing significantly better application of more novel CAD developments allowing for the easy creation of design space models. In the Solution phase and despite the familiarity with the Altair Optistruct software (Altair Engineering, 2017) and its presence in Airbus, the Siemens NX software (Siemens, 2012) proved to be equally capable whilst being significantly easier to use and cheaper to procure. In the final phase, looking at minimal manipulation and design extraction, it was necessary to separate the two tasks as the process of design extraction would likely be performed in the CAD tool utilised for pre-processing and so had been partially pre-selected. Focussing instead on manipulation, validation and possible alteration of the TO problem for re-analysis, Altair's HyperView (Altair engineering, 2012) coupled with OSsmooth proved to be by far the most capable pairing with simple and effective interrogative software and simplistic means of design extraction to either STL or FEM for re-validation. Direct manufacture of the exported STL could not be accomplished with any of the software packages trialled (though Autodesk was close), due to the quality of the output surface with multiple inverted normal, ghost shells and damaged/intersecting/overlapping triangles. The results of the software trials can be seen in Table 6.

Table 6 - Excerpt from the results of the software selection trials for pre, solve and post-processing. Blue shows highest capability, green shows the selected software.

		Scores out of 10 (10 being the best)					
		Autodesk	Solidthinking	Optistruct	CATIA	Solidworks	3DX
CAD Manipulation/ Preparation	Ease of Use	8	6	2	4	7	7
	Cost	7	10	2	2	5	5
	Knowledge	6	5	2	5	6	8
	Capability	4	5	4	10	7	7
	Totals	25	26	10	21	25	27
		Fusion	Inspire	Hypermesh	CATIA	Abaqus	3DX (Solidworks)
Pre-Processing	Ease of Use	6	8	4	8	8	8
	Knowledge	6	8	2	6	5	5
	Capability	4	3	10	2	6	4
	Totals	16	19	16	16	19	17
		Fusion	Optistruct (light)	Optistruct	NA	Abaqus (light)	3DX (Atom light)
Solution	Ease of Use	6	6	2		5	7
	Knowledge	6	6	2		4	4
	Capability	5	4	10		3	3
	Totals	17	16	14	0	12	14
		Fusion	Evolve	NA	CATIA	Solidworks	3DX
Extraction	Ease of Use	6	7		5	6	7
	Knowledge	5	5		5	5	5
	Capability	5	4		10	6	4
	Totals	16	16	0	20	17	16

Ultimately and after consultation with Airbus, it was determined that whilst other software toolsets fared better within the trials and could (potentially) be used, a significant improvement in performance would have to be demonstrated before Airbus would consider the purchase of even a single license for further evaluation and possible integration. Given the marginal and

subjective benefits in performance, a decision was made to utilise (with some differences) the toolsets either currently in use by Airbus or which would be accessible at some future date within the organization. Resultantly, the following software selections were made for each phase of the process tree. Figure 45.

3.2.3.2.1 Input Parameters and Design Variables

In order to reduce the likelihood of any process errors during the import, analysis and optimization phases, a number of initial parameters were stabilised and locked into a uniform template file prior to the start of the trials. Standardised parameters included:

- 1) Material properties (Elastic modulus, Poisson's ratio, density)
- 2) Feature recognition and de-feature parameters (fillet radii, holes etc)
- 3) Optimization objective (compliance)
- 4) Constraints (stress, displacement, volume, etc.)
- 5) Optimization controls (minimum feature, checkerboarding, draw directions, convergence, etc)
- 6) CAD format

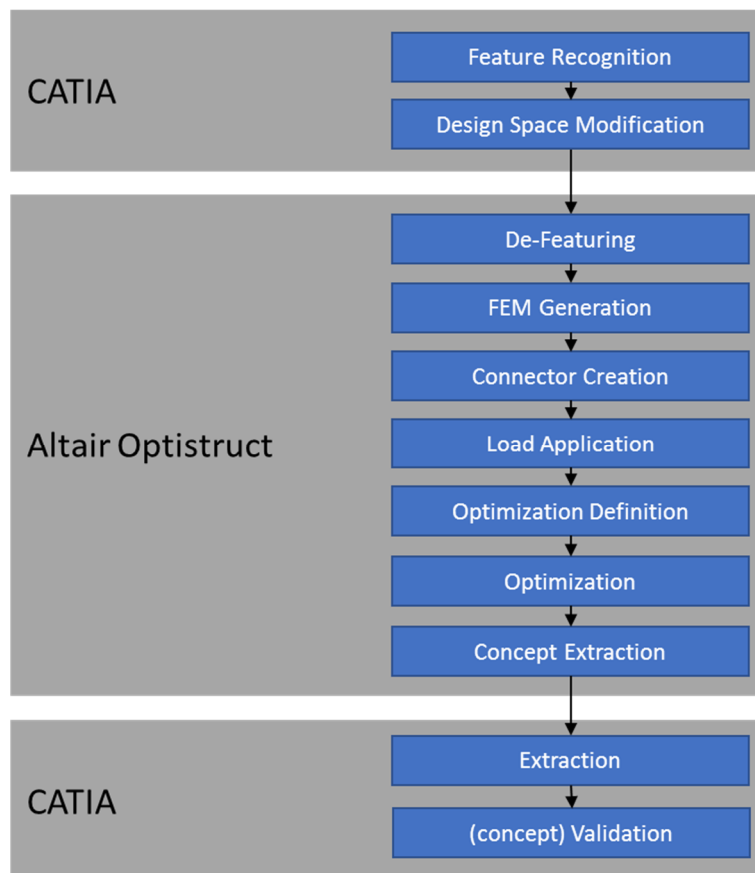


Figure 45 - Software selections for future progression within the project

On the last point (6), CATIA had already been decided upon as the initial CAD generator, but possessed multiple means of exporting CAD data, most notably, STP, IGS and CatPrt. Analysis of the import/export quality of the various formats was performed with the results shown in Table 7. It can be seen that in the majority of cases, import problems were encountered when using open source file formats such as STP and IGS and that only when utilizing import of CATPrt's into Hyperworks was geometry readily usable without need to correct/repair. CATPrt's will, wherever possible be used for the transfer of data from CAD to FEM.

Table 7 - Results of CAD export>Import trials between CATIA and Hyperworks

Geometry Number	File Format	Full Solid Part	Surfaces Undamaged	All Surfaces Present
STR2	IGES	N	Y	Y
	STEP	Y	Y	Y
	CATIA	Y	Y	Y
STR1	IGES	N	N	N
	STEP	Y	N	N
	CATIA	Y	Y	Y
STR5	IGES	N	N	Y
	STEP	N	Y	Y
	CATIA	Y	Y	Y

3.2.4 Standardization of Tools and Processes

In order to normalise the responses of the participants in the survey and to ensure that specific tools were not being used to either increase productivity or decrease manual effort, a standardised set of tools and a series of input templates were created. Table 8 shows the standardised software and version numbers for the assessment phase.

Table 8 - Version control for all software used during the PhD

Design/Analysis Phase	Software Name	Version Number
CAD Generation/Preparation	Dassault CATIA	V5 R21 – 06-30-11.20
Preprocessing	Altair Hypermesh	V11.1.1.2.1
Solution	Altair Optistruct	V11.1.2
Post-Processing	Altair Hyperview	V11.1.2
STL Correction	Materialise Magics	16.0
Design Extraction	Dassault CATIA	V5 R21 – 06-30-11.20 SL3
Coding	Python	2.6

Whilst some operators were still using HW10 and versions of CATIA ranging down to V5R18, it was believed that a common toolset, with each part pre-tested on the selections would be more beneficial and the results more comparable if the software were to be harmonised. It would be remiss to fail to highlight that the slight interfaces change notable between software versions, will hamper the effectiveness of those engineers using obsolete versions of software over those using current software variants.

During the initial software testing and benchmarking, and in preparation for the survey, the time required during each design phase was tracked and recorded for each of the shortlisted candidate parts. The reason for this approach was twofold, the first was that it would provide a baseline of software operation from a skilled and familiar user, thus providing a norm against which outliers from the survey could begin to be identified. The second reason was to ensure that all software and templating files were functional and available on the Airbus network prior to roll out of the survey.

3.3 Targets for Automation – Application and Survey of Optimization as Applied to the Candidate Parts

With common toolsets now established, an investigative study was undertaken in which time required for the task was cross compared to the generated performance improvement, the aim being to determine suitable candidate process steps for targeted automation. The study utilises the expertise of experienced TO engineers within the Airbus group, each using a standardised set of software and modelling data in order to perform the analysis (Table 8 and Table 6 respectively). The results of the study were delivered in two parts; the primary output utilised the candidate parts and a common toolset to determine the effectiveness (and variability in capability) of TO users within Airbus Group. The secondary output was to use the categorical outputs of the segmented optimization flow process as topical headings for a time mapping exercise. The exercise was intended to find the greatest time consumers and perceived satisfaction in a standardised optimization problem, thus providing potential targets for automation. In order to directly quantify perceived satisfaction, three methods of approaching the assessment were considered, these included:

- 1) Ease of automation – which tasks would be the easiest to automation and integrate and visa-versa.
- 2) Computational time – which tasks required the largest CPU resource
- 3) Engineering input – those tasks which required the greatest engineering value add

Ultimately, and since this software was intended not to replace optimization engineers, but to aid them in doing more by having to do less, task satisfaction, experience and skills building tasks

and enjoyable/rewarding tasks were used as the secondary means of selecting optimization targets.

3.3.1 Experimental Methodology for the Survey of Topology User in Airbus

In order to both identify targets and establish a baseline performance for current tools, thirty-five operators from Airbus Operations UK were approached and agreed to participate in the survey aimed at assessing time required per task and perceived usefulness of that task. A pre-requisite for inclusion within this group was familiarity with both Optistruct and Catia. In order to remove language bias, the survey was undertaken only using members from Airbus UK. Whilst the common language in Airbus is English, research has shown that both non-native language processing and organizational culture can play a part workplace productivity and comfort. Ethically, it is difficult to select TO users based upon nationality or native language. Even were this method of selection ethically acceptable, information related to primary language and place of birth is not captured/visible to Airbus HR. However, by limiting the survey to those member employed by the Airbus UK NATCO, some measure of control can be established over both culture and language. These limitations were applied to the candidates approached for the survey.

As a subjective matter, feelings of satisfaction in relation to a task undertaken and completed can be surveyed in myriad ways. This sampling methodology used is often dependent on the quality of data required and means by which it is to be sampled (Suresh et al., 2011). The sample size for the gathering of this data is relatively small (<35 operators) and thus, the quality of the data to be gathered must be both high quality and, as unbiased as possible within the constraints of experience and the limitations of imposed software selection and component geometry. Due to the constraints on the sample size (Optimization engineers in Airbus, particularly those familiar with Hyperworks and CATIA are limited in number) there are few methods for the surveying of participants and the gathering of data (Banerjee and Chaudhury, 2010). Of those available, by far the most widely used for this type and size of population is a basic, non-bias evaluation and this has been used to design the survey found in Appendix A – Background Material. The principal goal of the survey was to locate, from a business case point of view, where non-value-add time was being consumed and how it could be reduced. From the engineer's perspective, the point of the survey was to find those tasks which the engineers found either boring, prone to error or of extreme irritation. Evidence suggested that these areas are common to one another and are often the source of systematic errors in the programming chain, due to the application of muscle memory (Johnson et al., 2017) or through attention drift (Matthews and Wells, 2016). It is acknowledged that this survey approach cannot completely

fulfil the requirements of a non-bias survey as the order of tasks within TO is largely fixed. As such, the chance that if a participant finds a precursor task boring/mundane, that their feelings and response will affect the grade of subsequent tasks cannot be avoided.

The survey was set out in as simplistic and unbiased a manner as was possible, with no leading questions or attempts at obfuscation through multiple blind responses. Engineers were asked to record, during each phase of the process chain, their feelings (both numerically and in direct, but constrained language) related to the tasks to be undertaken and upon each piece of geometry. The tabulated survey template is shown in Table 9.

Table 9 - Survey template for optimization responses

Task	Feelings of Satisfaction/Usefulness 0=dissatisfied/useless, 10=satisfied/useful	How was your experience of performing the task? Poor, moderate, ambivalent, good, excellent
CAD Import		
Feature Recognition		
Parameterization		
Export		
De-featuring		
FEM Guideline		
Optimization Definition		
Optimization Iteration		
Assessment and Interrogation		
Extraction and Re-creation		
Re-validation		

Each participant was asked to record the time (in hours) required for each distinct optimization task and also to give each task a pair of responses related to usefulness and ease of use. To calculate time per task independent of operator or geometry, the data was given as a percentage of the whole task for each participant then summated with the other participant responses and finally averaged. For satisfaction/ease of use, the data for ease of use was transposed into values of 0-10 in increments of 2 for each response from poor>excellent. These values were then multiplied by variable for satisfaction and again summated and averaged. Finally, the data from the satisfaction/ease of use was cross multiplied with the decimalised time percentage in order to again give a results as a percentage of the total time required. For all data a 6-sigma variation method was used to detect and eliminate outliers in the experimental data.

Once both time and satisfaction are each summated and averaged, they are given a ranking of 1-10 with 10 being the worst result in both cases. The results for each phase are then summated with the highest values depicting the best targets for automation.

3.4 Results of Baseline Optimization Trials

3.4.1 Results - Performance vs. Cost of Design

The results highlight the effects of geometry on both resulting mass fraction and on time required for extraction with two clear groups emerging – those for which additional time yields extra mass reduction and those which do not. When sifted and sorted into part categories, it can be seen that STR5 (Table 4) requires substantially more time to both parameterize and extract than other designs, but has a much tighter grouping of topology results, thus reducing the variability in the mass savings. This is because the nature of the loading (internal pressure) means that only grid definition truly changes the topology result once convergence is achieved. In STR1, the outlying result was achieved through creation of an extended design space, and thus required extra time to parameterise, but also yielded a better result. STR4 is mostly converged with a single outlier. In this case, the user enveloped the load cases and iteratively refined the grid to provide a very smoother, more converged output, but required significant additional time.

Design with complex geometry such as those in STR2, 3 and 5 (Appendix B) revealed the skills of the operators at manipulation of the software, with experienced operators achieving remarkable results in relatively short timescales regardless of the part geometry, whilst those with less developed skills were slowed significantly. This was particularly notable in the early stages of model preparation. This helps to validate the decision to use multiple part geometries during testing and analysis in order to mitigate the effects of design upon time required.

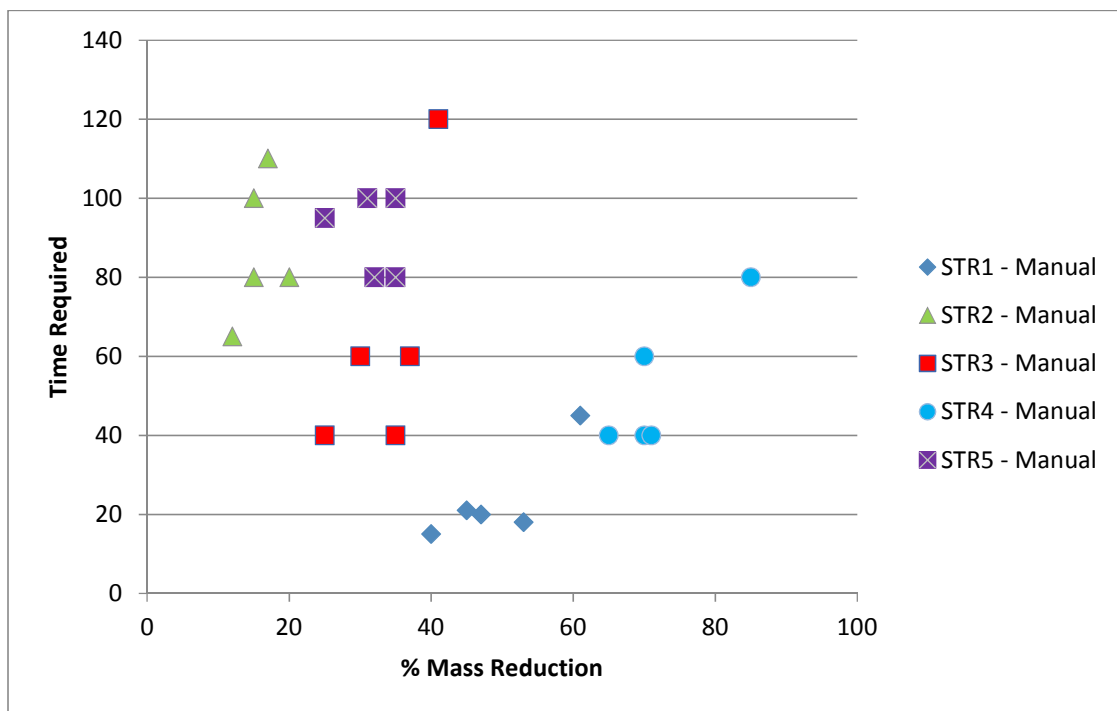


Figure 46 - Percentage mass reduction vs time required (hours) for each of the user on the five candidate parts.

The results in Figure 46 also whilst significant percentage mass savings are achievable, the small mass of the original parts (Table 4) yields a quite low total mass saving. When compared to the time taken, this becomes a very high £/Kg saved due to the high non-recurring cost of design.

3.4.2 Results - Time Required for Process Phases

The collected and collated time data from the engineer's optimization analyses can be seen in Figure 47. The data relates to the active/consumed time within the process, but does not consider any required solution time for either FEM generation or solving of the optimization.

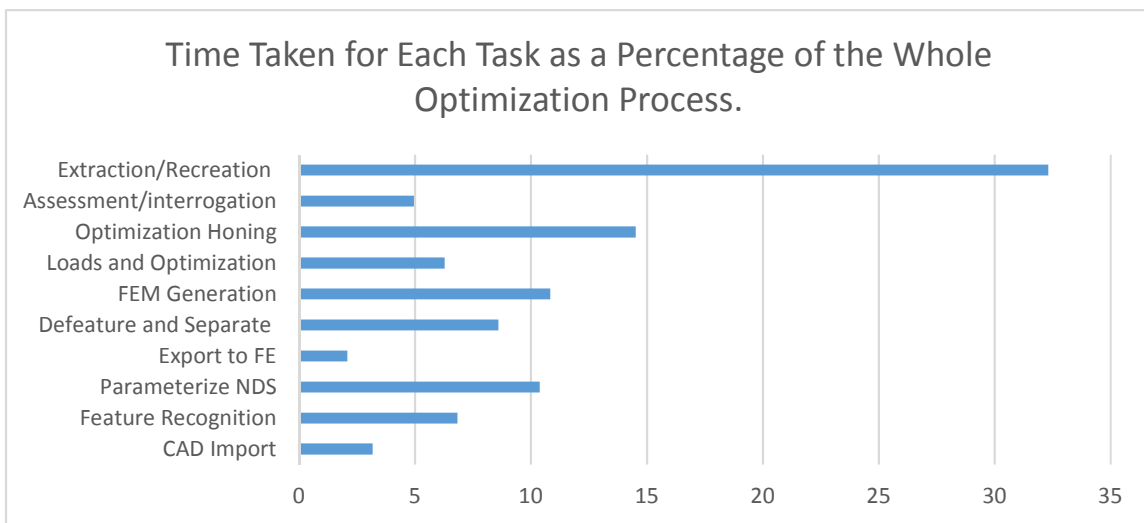


Figure 47 - Chart showing the time required for each task within the optimization cycle as a percentage of the whole task

The results clearly show that two largest time consumers within the optimization process are those pertaining to Optimization honing and to extraction/recreation of the final optimised design layout from the topology solution. After these two, the results are quite close between FEM generation, Parameterization of the NDS and Defeathering.

3.4.3 Engineer Satisfaction/Value Add of Each Optimization Task

Only 4 results from the data set were deemed to be outside of the data range of the mean-std variation totalling less than 2% of the total responses. The collated and formulated data is displayed in Figure 48 with larger segments indicating a higher level of perceived satisfaction.

The results of the survey demonstrate that the greatest perceived satisfaction stems from the FEM generation, Optimization Honing, Assessment and Interrogation. In contrast, it can be seen that little satisfaction is derived from the Extraction/Recreation, and CAD parameterization phases (Parameterize NDS, Defeature and Separate, CAD Import).

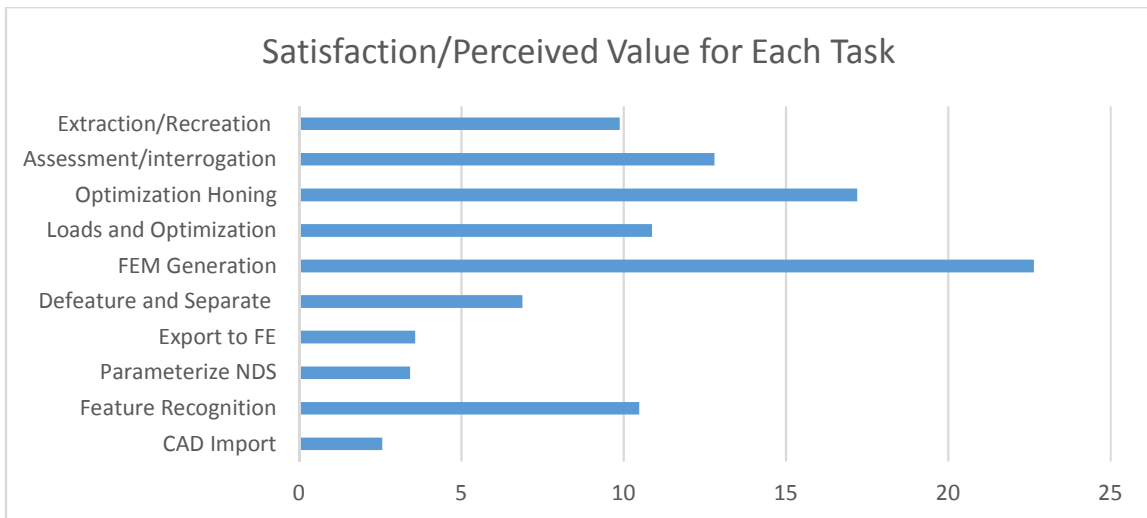


Figure 48 - Perceived satisfaction/value add time as a percentage of the whole task undertaken

The combined numbers refer to the worst time consumers (highest ranking) and the least satisfying (highest ranking) and when combined form the results column (Table 10). From these results, two clear targets can be seen from the resulting data – Extraction/Recreation and Parameterization. After this there are a host of mid table results which have similar (+/-10%) values. Of the mid-level values, optimization honing is by far the worst time consumer, whilst de-featuring is (at least to the Stressmen) the least satisfying.

Table 10 - cross compared rankings for time required vs. task satisfaction (value add) - Higher is worst in both columns

Number	Task	Time (ranking)	Satisfaction (ranking)	Result
1	CAD Import	2	10	12
2	Feature Recognition	5	5	10
3	Parameterize NDS	7	9	16
4	Export to FE	1	8	9
5	De-featuring and Separation	6	7	13
6	FEM Generation	8	1	9
7	Loads and Optimization	4	4	8
8	Optimization Honing	9	2	11
9	Assessment and Interrogation	3	3	6
10	Extraction and Re-creation	10	6	16

3.5 Discussion of Survey Results

Looking at the “positive” vs “negative” attributes of the identified processes, one can generalise that the processes which are deemed to have little satisfaction and learning are those which involve manipulation of the CAD using either CATIA or directly within Hyperworks, thereby causing a requirement to re-mesh. Conversely, those tasks (with the curious exception of optimization variation) which focussed heavily on the requirement for the use of FEA were rated to be of the highest value to the operators. Initially this was an unexpected result, as it was thought that tasks which were either repetitive or mundane (FEM Generation) possibly coupled with those which were frustrating (extraction) would be those given the lowest satisfaction scores and for those reasons. Subsequent analysis of the survey participants and more specifically their skills and backgrounds led to an unforeseen problem in the survey section and methods. As an employee of AGI, the researcher (me) has in depth knowledge of all software in use for topology optimization and uses them with enough regularity, that none is more appealing than the other; they all have pluses and minuses when in use. In Airbus however, use of specialist software (such as Hyperworks and CATIA) is performed predominantly by skilled and experienced users. In this rigid organizational structure, there is a notable division between design staff and analysis staff and that whilst some TO staff have familiarity with and use of CATIA, there are very few CATIA operators with familiarity with Hyperworks. As such, the staff surveyed for data in this investigation are all members of the Engineering Structures Analysis or Optimization specialities, meaning their primary experience and function is the use of FEA, not CAD. Thus, staff familiar with and whose job depends upon their skill with FEA, are likely to find aspects of the TO process which focus on FEA to be of more use/satisfaction.

Whilst this discovery is, at first impression, a problem for the identification of targets for automation due to the bias of those surveyed, the eventual developments of the automation process will be intended for use by this specialist group and thus must be of value to them. By this, the targets for automation, however biased should be acknowledged and included in the assessment of targets for automation. However, it would also be advantageous if the developments in automation intended for use by Airbus, could help to expand that pool of specialist operators by de-skilling some aspects of the process, thus enabling expansion, possibly to the design working groups in alignment with airbus concept generation proposals. And so, by cross referencing the results of the two surveys and at once trying to mitigate the effects of the survey bias, whilst simultaneously taking into account the unacknowledged preferences of the stress-based staff couple to the need to expand the software use to a wider pool of engineers,

3.6 Identification of Primary Targets for Automation of the Design Process

Two of the primary targets for optimization are easily identified from the results of the survey; the first, perhaps predictably, is Extraction and Recreation, being both the highest time consumer and the least well liked (by the Stressmen). It is perhaps one of the most difficult tasks to automate due to the nature of output from optimization and the difficulty of design reconstruction from an unstructured grid definition. The second target is that of Parameterization – the formulation of design space, vs non-design space, the definition of the loads, constraints, materials, additional forces etc. Rated as the second-least satisfying task, its automation, whilst initially appearing complex, should be able to be further broken down into small, serial automation tasks. If one were to stop at these two tasks and be able to automate them, it was believed that the total reduction in required manual effort would be in the region of 60-95% dependent upon the efficacy of the automation method. If this were extrapolated into the total optimization cycle, and if one were to assume the highest level of automation effectiveness (~95%), the total time saved would be in the order of 45-50% of any optimization cycle. However, if the effectiveness of the automation implementation were only 60%, this would equate to only a 30% improvement in overall time consumption during the partially automated process. This level of automation, whilst undeniably effective at reducing required effort, may not be sufficient to justify the development and industrialization of yet another software package along with the training and maintenance required to operate it.

As such and again reviewing the tasks in terms of time consumed, the largest time consumers from the sections which aren't provisionally targeted for automation, would be those belonging to FEM generation and to assessment and interrogation. Of the two, assessment and interrogation is deemed to be the more satisfying task, and based upon personal experience, is one of two sections of the optimization process in which the experience of the engineer can have significant benefits upon the quality of the design output. This is not to say that FEM generation is valueless, but rather that its value as part of an optimization process (as opposed to that of a dedicated structural assessment) is somewhat diluted due to the changing nature (not numerically, but iteratively) of the FEM during each iteration stage. Nominally, and in order to receive a smooth output graph from the optimiser, the highest possible, uniform mesh density would be the one required during the final run of the optimization. Whilst inefficient from a computational point of view, with no clear knowledge of the eventual structural layout prior to the running of the optimization, a uniform FEM provides for the most independent topology solution from the solver. As such, and if a third target for automation is required, it will be the

FEM generation process which will be included into the method, possibly with user selection and guidance, but through a largely automated approach to the task.

By selecting the above three targets for automation, it is believed that a 50% reduction in design NRC can be realistically achieved and with minimal effects upon the quality of the output and the satisfaction of the engineers undertaking the task.

3.7 Summary of Automation Targets

Within this section, a detailed outline of the research premise and its industrial requirement are detailed along with an establishment of a current state of the art baseline against which the newly developed research can be compared. During the baseline establishment, standardization of tools (Objectives 5-8), versions, file formats and methods were established culminating with a sample survey of Airbus optimization staff detailing their thoughts on optimization, specifically, why they believed their time was wasted and what percentage of that time was taken by each sub-task of the optimization process. Through analysis of the gathered data, a series of optimization targets looking at the Parameterization (design space, load application and BCs, etc) and post-processing (design extraction back to CAD) targets were selected as the primary targets for automation within this research. (Objective 2)

4 The Development and Application of Robust Material Data into the Pre-Process Automation Phases

Section 4 of this research is a quite broad and tackles not only the complexities of applying automation to the parameterization stages of optimization driven design, but also aims to add robustness to the process by standardizing both mechanical performance of AM built titanium and the minimum geometric constraint features present in the manufacturing platforms.

Automation - In the survey undertaken, some effort was made to discretize the initial pre-process parameterization in preparation for design optimization. This discretization led to the identification of parameterization of the NDS and Separation of the NDS being the primary targets for automation. The detailed work breakdown structure (Figure 44) can then be used to determine the precise information flow through the design optimization tasks, thus defining the ideal inputs and outputs for each process phase. From this, the following small-scale automation sections were identified:

- 1) The automation of feature recognition
- 2) The automation of minimal feature based defeaturing based on thickness
- 3) The automation of design space separation
- 4) The automation of grid development
- 5) The automation of loading perturbation for single load case structures

Robustness – Mechanical properties for AM are known to vary dependent upon build orientation, thermal conductivity, etc. This has led to concern that topology optimised parts may be subject to failure if optimised on generic data and then printed in a compromising orientation. In order to alleviate these concerns, a study was devised which would test the effects of orientation on mechanical performance whilst reducing or removing as many uncontrolled variables as was possible from the manufacturing environment.

4.1 Automation of Pre-Process Parameterization Phases

In this section, the application of serial automation to the pre-process phases identified in the introduction will be detailed.

4.1.1 Feature Recognition – Introduction

Feature recognition (FR) is an important pre-pre-process phase at the beginning of any design optimization task. When applied correctly, the FR can be used to identify and remove features which provide little or not benefit to the analysis phase, serving only to consume CPU time in proximity meshing and analysis. Additionally, FR can, if applied and subsequently adapted, be

used to create identifying features to be used later in the creation of no-design space elements. As such, the automation of FR in this research targets those features which form the critical interfaces to adjacent structure/components and as such are governed by Airbus Design Rules (ADR). Initial targets are thus bolt holes, attachment flanges and specific radii for the each candidate part.

4.1.2 Feature Recognition – State of the Art.

CAD based feature recognition (CAD FR) is one such aspect which has enjoyed some attempts at automation. In addition to its use during the initial parameterization phases of either CNC programming and FEA parameterization as a means of reducing extraneous detail from CAD data (Muir, 2012a) it can also be used to adapt dumb (non-parametric) CAD files into active CAD which can be adapted correctly rather than boded to suit a required design change.

In the former applications, the use of CAD FR can significantly reduce the requirements on subsequent CNC coding or FE meshing through removal of fillet radii (applied automatically by the cutter size or present to remove handling difficulties such as sharp edges) and holes/pockets of little relevance to the analysis/manufacturing. It is most commonly used in preparation for machine coding in processes such as CNC machining, but as previously mentioned, can be used in conjunction with de-featuring in preparation for analysis. It is this application of FR that is of most interest in this investigation. Figure 49 shows the features which would be recognized for CNC machining and tool selection whilst Figure 53 shows the effects of extraneous CAD detail on mesh generation.

CAD FR is a reasonably well-developed area within many advanced CAD tools such as CATIA, and Autodesk. FR works by scanning the input geometry and recognizing the basic design elements from which features a 3D CAD model is ultimately created. The software then creates sub-elements which populate the CAD design tree which the user can then access and manipulate as required.

It is commonly limited to the recognition of isolated features (Suh and Lee, 1998) without compound or derivative items applied in series (such as fillets on top of fillets or pockets) which can oft-times confuse the analyser during recognition (Cunningham et al., 2017). Commonly in CAD, FR is applied coarsely resulting in damaged or bad CAD in-turn can lead to significant shortfalls in quality which requires significant remedial action (Chang and Tang, 2001). Additionally and problematically, some features share basic design elements (holes and circular pockets use the same mathematical attributes) and so can be incorrectly identified and categorised. Improper recognition (even semi-automatic) is not a particular problem so long as it has review and oversight along with an easy means of rectification.

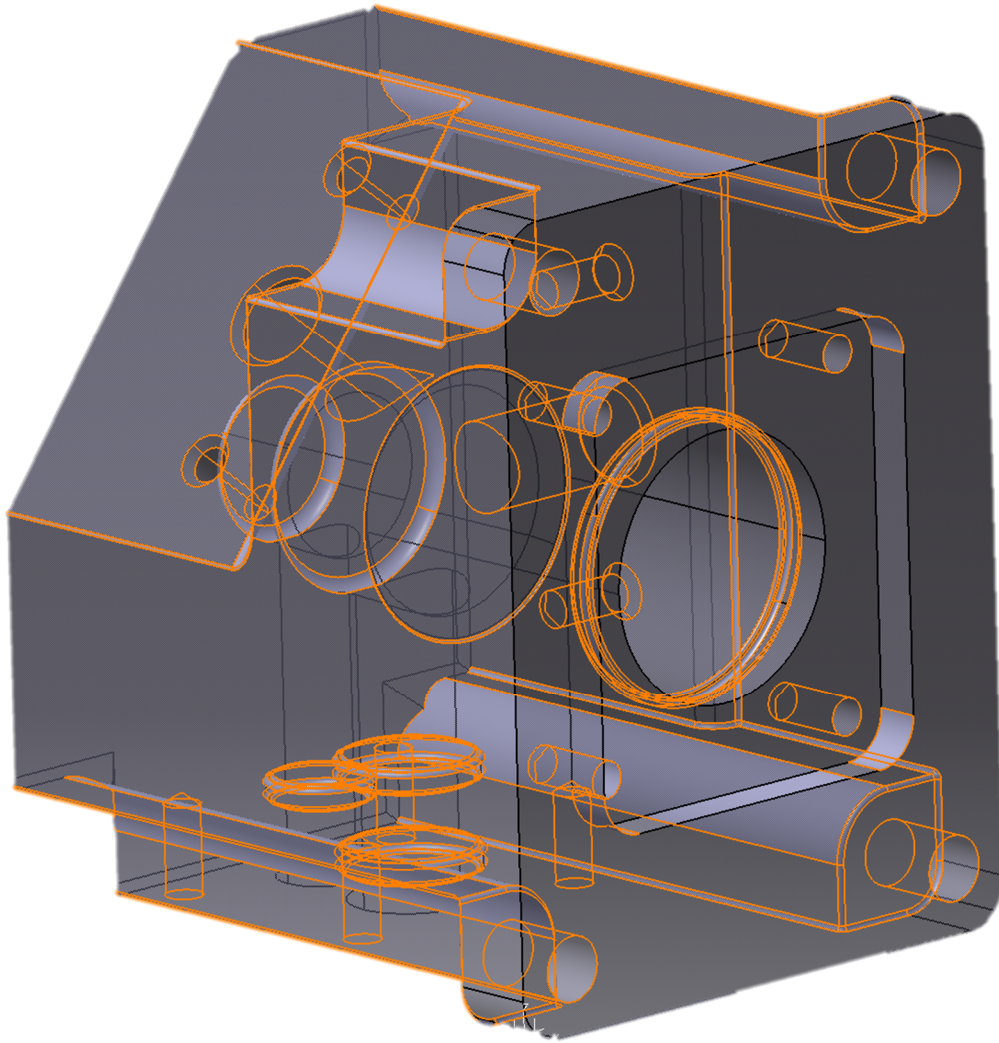


Figure 49 - features recognized by commercial codes in preparation for CNC machining

Figure 50 shows this effect when using FR within CATIA for the detection of bolt holes within STR5. As can be seen, several hydraulic pathways within the model have also been incorrectly recognised as bolt holes, not fluid pathways. CATIA would normally defeature those holes for analysis or preparation for first stage CNC machining with subsequent stages being added for the bolt holes and ports. For analysis however, the bolt holes must be recognised in preparation for the application of ADR and the creation of NDS, but no such application is required for the fluid pathways. A custom approach is required.

4.1.3 Methodology for Automation of CAD Feature-Recognition

Automation of FR in CAD, whilst not standard practice can be accomplished with relative ease. Using CATIA and simple VB Script, a simple macro (shown in Appendix C – Coding and Scripting), has been written which calls the feature recognition aspects of the software and tasks them with the recognition of certain features (such as holes and fillets) and asks that they be appended to

the CAD file being analysed by the software. The developed macro is unique in that it also filters the recognised holes based upon the depth of those holes when considering ADR. As such, holes deeper than twice their diameter are filtered out and those not categorised.

4.1.4 Results of Automated Feature Recognition

The effects of the automatic FR can be seen in Figure 49. When compared to the image in Figure 50, the effects of the hole filtering are noticeable with the large pressure channels no longer recognised.

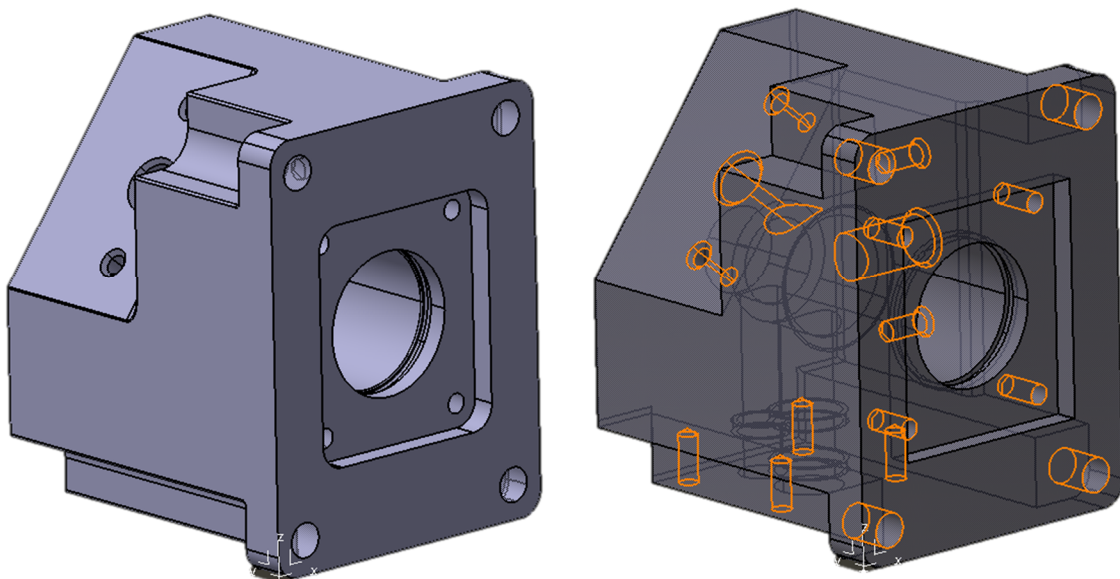


Figure 50 – The results of adapted CATIA FR for bolts and radii – note the removed fillets and highlighted bolts in without the centre pressure channels being selected (right).

4.1.5 De-featuring - Introduction,

De-featuring of the CAD previously recognised in FR is commonly performed in CAD environment and is often performed in preparation for machining by removing features of the design cad which will happen purely as a factor of CNC machining, e.g. fillets caused by ball cutters. De-featuring can also be applied to reduce complex features which would otherwise require a complex grid assignment in order to replicate. As such, removing them prior to meshing can save considerable time during both mesh generation and analysis, thus making them an ideal target for automation.

4.1.6 De-Featuring – State of the Art

De-featuring can occur in both the CAD and FE environment and works well in the CAD if the CAD is native to the CAD software, but conversely can cause significant errors when not. Repair of broken CAD from this result often takes considerable skill and knowledge to be able to apply

correctly. When evaluated using CATIA with STP, IGES and CATprt input, it was found that CATIA performed well with its native file format, but quickly created errors on compound features (fillets into fillets, or Booleans into holes), creating large holes in the surface model or un-recoverable topological errors in the solid

The effects of successful CAD defeaturing within the CAD environment can be seen in Figure 49 in which the fillet radii have been recognised (Figure 48) and suppressed in the right hand image of Figure 49.

FR and de-featuring is also a function of some FE packages such as Hyperworks and Abaqus. FR and de-featuring can be applied in a number of different ways dependent upon the software and item under investigation. The most common method of application is the identification of features and their subsequent removal from the CAD through deletion of the surface features and repair of the neighbouring features. This approach, when evaluated with Autodesk Abaqus and Hyperworks enjoyed moderate success with uncomplex CAD and bespoke input files, but can prove problematic. An example of a fillet radius being removed using Hyperworks from the test manifold can be seen in

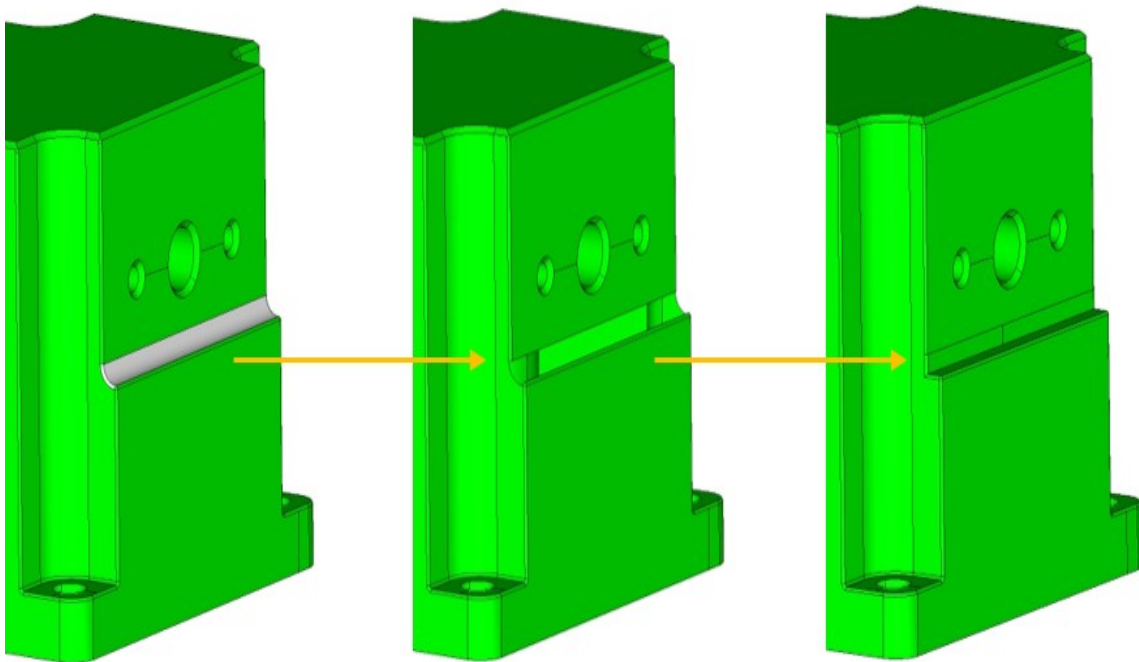


Figure 51 - an example of fillet removal from within Hyperworks

The more recent method of FR and de-featuring employed within Hyperworks does not function through direct alteration/interaction with the CAD, but through manipulation of the transfer of data between the CAD and the FEM generator. The recognition works in a similar (and equally

flawed manner) to other CAD packages with the ability to recognise fillets, holes, surface defects etc. In addition, the software is also capable of finding and removing

duplicate surfaces (2 adjacent bodies should have a shared surface, not 2 surfaces in the same space, but this is not how CAD exports geometry) and performing minor repairs. The difference between the previous de-featuring and this newer method is what happens next. In the new software the CAD is scanned and the features recognized as normal, but the de-feature works by suppressing some of the edge details of features identified. Whilst the outer boundary of the CAD remains unaltered, suppressing some edges removes the need for the FE mesher to seed and thus adhere to the CAD boundary on that edge. Figure 52 shows the visual representation of edge suppression on the same Manifold part.

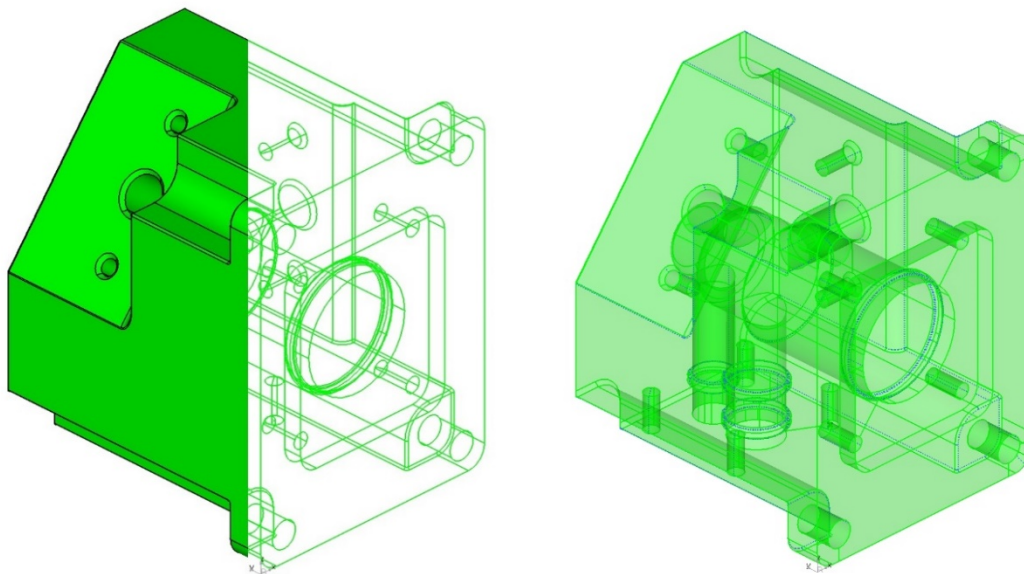


Figure 52 - Figure showing the effects of de-featuring on complex geometry through the removal and adaptation of proximate geometric features and their removal (dashed lines) from the mesh seeding process

4.1.7 Results of Defeathering Trials

In practice, edge suppression of unrequired features can yield substantial savings in mesh density and a higher likelihood of a high-quality mesh generation on even complex parts. Figure 53 shows the effects of mesh generation with and without edge suppression along with the corresponding mesh size.

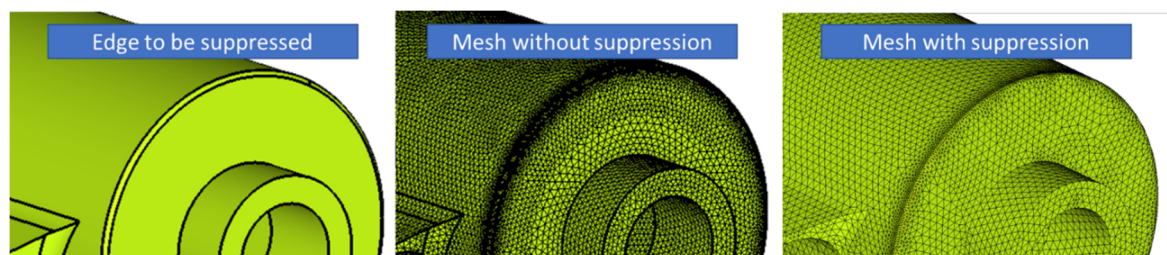


Figure 53 - Effects of line suppression on mesh size: without line suppression (middle) the mesh is ~1m elements, with line suppression, the mesh reduces in size to ~0.3m elements

4.1.8 Automation of De-Featuring in Preparation for Meshing

With the ability to recognise features successfully automated, the application of automation to defeaturing is the next target. As shown, defeaturing within FEA proved to be the most robust course of action, but to implement the capability automatically, more data is required. Within Hyperworks there are a series of tools which can be used to activate suppression of geometric features, identified by element size. As such, feature suppression requires a specific input value bespoke to each component, relative to its thickness and the projected element size. This is problematic as FEM generation is usually performed after de-featuring and not before, but in order to automate, the nominal smallest element size is required. The default rules for 3D meshing indicate that any thickness in the model not be represented by less than three elements and so the best means of determining the minimum element size is through analysis of the minimum wall thickness for the part. Wall thickness can be analysed easily in several CAD packages, but is not normally performed on a whole model at once to determine the global minimum. Most CAD packages only measure wall thickness at a single point interrogation.

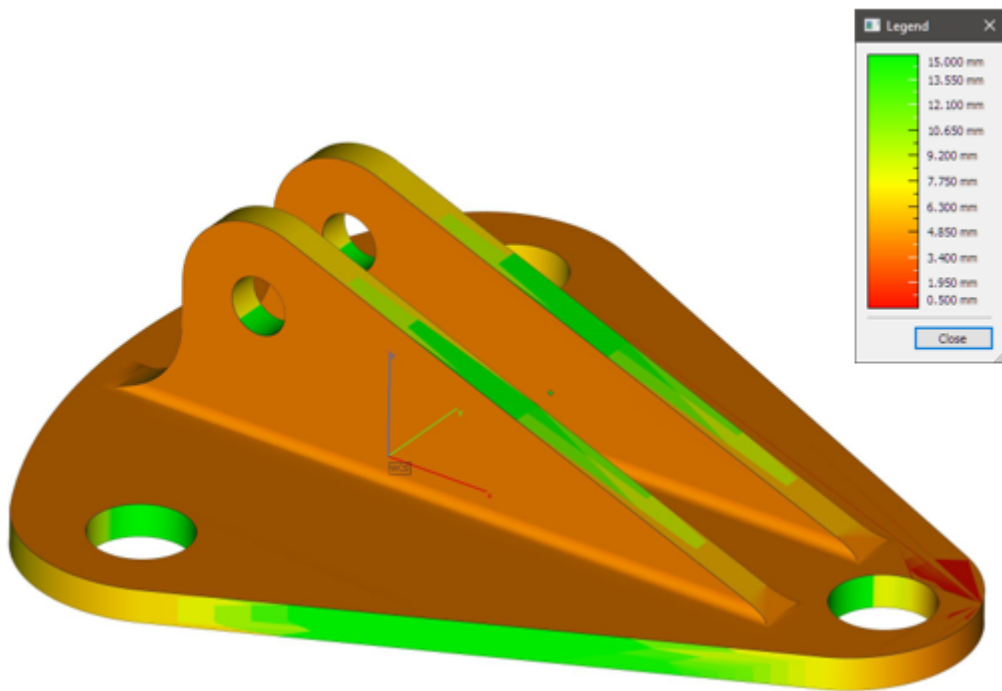


Figure 54 - Wall thickness analysis from Materialise Magics showing some areas of almost negligible thickness (red) due to problems with the triangle mesh normal

Materialise Magics can assess the STL version of CAD and display a global map of wall thickness onto the part, but again this does not determine the minimum, only the distribution.

Additionally, the result is often incorrect as shown in Figure 54. In order to analyse wall thickness globally, and without introducing another software package, a unique code was written which analyses the STL output from CATIA through comparing the normal vectors of surface triangles with their nearest inverted neighbour (found via a vector search from the normal vector of the first wall encountered). After searching, the magnitude of the vector is then tabulated for each of the elements (mesh densities up to 10m elements have been tested), compared and recorded. Whatever the minimum value, this is the minimum wall thickness and thus, through division by 3 is the value needed for the minimum required element size during de-featuring (general best practice). The developed code can be found in Appendix C – Coding and Scripting.

As a process intended to analyse myriad different types of parts/components ranging from brackets to manifolds, a robust process is preferable to a highly efficient one. This distinction must be made as whilst the two are not mutually exclusive, compromises are usually made in the pursuit of one or the other. In this case robustness in meshing complex geometry with a uniform, high quality mesh is given preference over the efficacy of local, non-uniform mesh refinement. This is not to say that localised mesh refinement will not be used, but that the global max element size will be defined through the minimum part thickness as determined through the STL scanner above. In this way, the mesh and the de-featurer can be highly coupled.

For expediency, and given the previous down-selection of software conducted as part of this investigation, it was determined that using the newer, inbuilt de-featurer within Hyperworks (the line suppression method detailed above) would be, if programmed correctly, sufficient to achieve the results of a high quality, largely uniformly dense (important for optimization of unknown geometry), automatically generated mesh. A series of trials were undertaken to determine, based upon industrial standards for mesh seed sizing, what were the best combination of defeaturing settings required in order to provide for robust, automatic meshing within the software. Within the tool-box, the following settings are available, (Figure 55) in each, the feature recognition is targeted with respect to the expected element size boundaries and the size range of the category features which are the target of the de-featuring.

The geometric features within the component can also be recognised and suppressed with respect to a targeted quality index for specific element types. Under testing this feature tended to be less reliable than general de-featuring, often requiring extra work for little or no benefit (only 99-99.75% of elements passed the detailed quality criteria, so needed tidying anyway) in terms of time reduction.

4.1.9 Results of Automated Defeaturing

The sequencing shown in Figure 55 was determined to be the optimal method of applying ordered defeaturing to any imported STEP file into Hyperworks. Using this arrangement limited the number of meshing errors whilst increasing mesh quality and decreasing overall FEM size by up to 60%.



Figure 55 - the selectable and modifiable elements of the feature suppression aspect of Hyperworks.

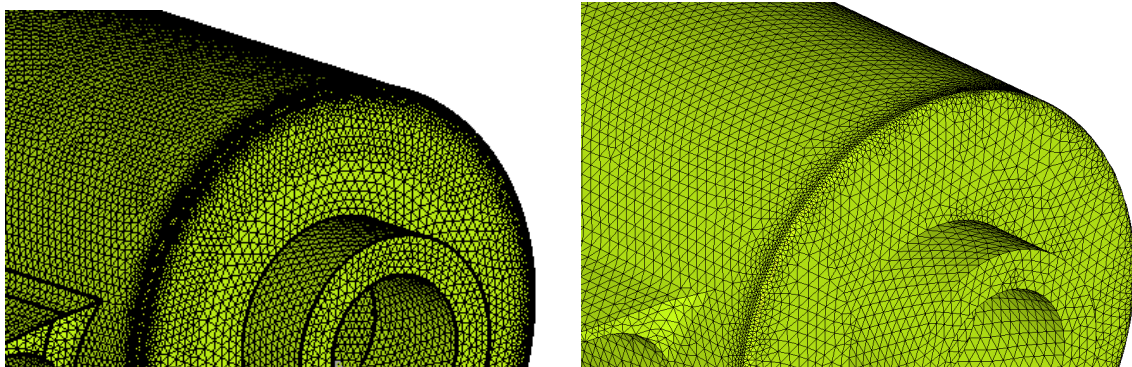


Figure 56 - The effectiveness of the implemented de-featuring on mesh sizing and quality

4.1.10 Conclusions for Pre-Process Automation of Recognition and Defeaturing

Using a controlled sequence of CAD import, geometrically analysed and constrained feature recognition, coupled to serialised de-featuring, automated functions which are now capable of controlling de-featuring in accordance with Airbus design rules (ADR), have demonstrated a significant reduction in process variability.

Table 11 - Time reduction through the use of partial automation in the defeaturing phase

Structure	Feature Recognition Time (Hours)		Defeaturing Time (Hours)		Percentage Reduction
	Manual	Automated	Manual	Automated	
STR1	3.5	0.15	1.1	0.25	~91%
STR3	4.1	0.15	4.4	0.5	~92%

In addition and whilst not the primary accomplishment (which will be delivered during the automated meshing phase) a significant reduction in interrogation and manipulation time have

been accomplished (Table 11) through the implementation of macro controlled defeaturing and geometric feature recognition in preparation for volume separation.

4.2 Domain Separation into Design and Non-Design Space – Introduction

In order to perform structural optimization on a component, a determination of what proportion of the volume of that component should be assigned to the optimiser should be made. Whilst it is possible to assign the entirety of the volume as the available design space, it is considered to be bad practice for boundary conditions (and sometimes loads) to be assigned directly to the design space, this is due to the fact that the design space will alter during optimization. As such, it is common practice to separate the component under investigation into zones into which the optimizer can and cannot go and those it can. Commonly referred to as design space and non-design space, correct identification and allocation of these zones takes time and the interpretation of secondary and tertiary requirements from the ancestor design, beyond those of the primary component function. As an example, Airbus has specific design rules related to the size of flanges which sit around loaded bolt holes and attachments. These rules are predicated upon both the material and the safety criticality of part. If digitised and used in conjunction with the material and classification data, some aspects pertaining to design space separation could be used to parameterize to begin the separation of the component. Ordinarily this separation is performed in either the CAD or in the FE pre-processor environment at the discretion of the user, but always prior to meshing and the application of loads.

4.2.1 Methods for the Separation of the Structural Domain

Design space separation in CAD is problematic when importing into FE due to the manner in which the CAD and FE programs utilise solid bodies. In FE, the requirement is for separate, but connected solids. In this way, the bodies share a contact surface and thus a surface mesh, meaning separated elements, but shared loads. In CAD, there is no way to represent connected but independent solids, the bodies must be separate. When imported into FE, this means that each solid possesses its own surfaces with no connection. This means they are free to generate their own mesh structures, independent of each neighbouring solid. As such, should parametrics be used to parameterize the creation of non-design space (NDS) / (DS) design space, within the CAD environment, a suitable process automation phase for dealing with these duplicate surfaces in the FE environment must also be created. Whilst it is possible to partially automate this process within Hyperworks, the manual process for doing so often requires deletion of the imported CAD solid prior to modification of the surfaces. In doing so, the surface topology may become damaged, leading to difficulty in recreation of the solid after modification.

4.2.2 Methodology for the Separation of the Structural Domain

To fully address both of these concerns, it was determined that modification of the input CAD external to CAD software was the most expedient approach and allowed for the easiest integration with the FE environment. The approach was to modify a STEP file exported from the CAD environment and subsequently adapted using a Python command script (Appendix C – Coding and Scripting). As a STEP file is completely open format and thus interrogable, the script then uses the identifiers for feature recognition and applies offset splines based upon the 1x diameter functions specified in ADR. Subsequently, swept surfaces (concentric and parallel along the normal vector from the bolt plane respectively) are coded normal to the splines and numerated later in the STEP and are used to segment the structural domain.

When imported into FEA, several connected bodies with shared internal surfaces are correctly created allowing for easy preparation for the FE Meshing. After segregation of the design space has been completed, the bodies can be allocated directly to collectors for the design space and non-design space (Figure 57). Previously this process would have taken between 1 and 2 hours on a simple part and substantially longer on a complex one and is now completed automatically with almost no user input beyond organization.

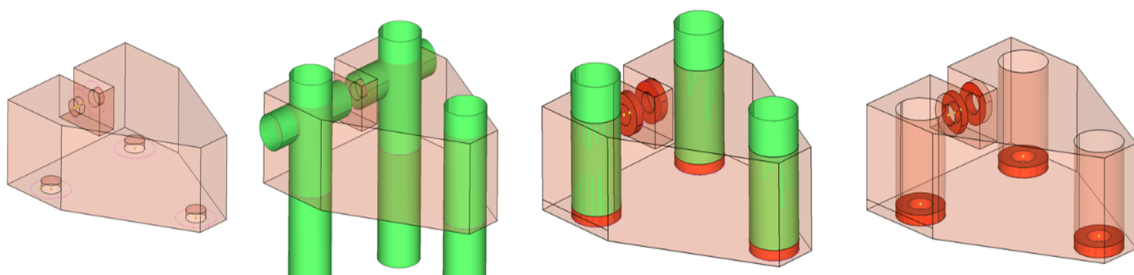


Figure 57 - Showing the automated design space progression after feature recognition

4.3 Automated Loading Perturbation for Simple Load Case Topology Optimization

When considering the application of topology optimization to simply designed and simply loaded components, there is a danger that the optimiser will provide for a mathematical solution rather than an engineering one. In this context, the mathematical result is one in which the structure would theoretically survive the single load case for which it has been designed IF and only if the conditions and material properties are exactly as detailed within the problem formulation, which is unlikely. This potential danger can of course be mitigated by adding either a knockdown factor to the material properties, or an inflation factor to the load case, thus providing redundancy in the structure and this is indeed common policy within Airbus. However, the methods of robust TO indicate that that this is an inefficient approach to structural sizing when considerations of mass reduction are foremost in mind during the application of SO. An analysis of several of the

shortlisted candidate parts which were identified as being designed specifically for unique applications and singular load cases was performed in order to determine the manner in which these parts were loaded, and how improper application of that load could cause early onset failure of the part. In each case, it was determined that the most likely cause of failure was a perturbation of the load due to improper mounting, variance in panel fit or deformations in the attached structure for the parts in question. It was decided that an investigation should be performed to determine the effects of loading perturbation on a number of parts. In each case, it was shown that a 15deg change in load would cause rapid failure at approximately 2/3rd of maximum load. The 15deg load variation was chosen as this represented the most extreme example (+20%) of allowable deformation in any connected structure based on its attachment. This judgement was made based upon the assessment of a small population of the candidate parts and so could be in error, but in this context, it is the method which is being tested, not the value and could be easily modified later if required.

Thus, it was decided that for any structure loaded with a single load case that a series of perturbed load cases based around and off the components of the primary load case would be created. In this cone of forces, the optimiser would be required to provide a weighted optimization solution in which each case was regarded equally during the process. The total number of load cases increased from 1 to 9 with a similar increase in computational load.

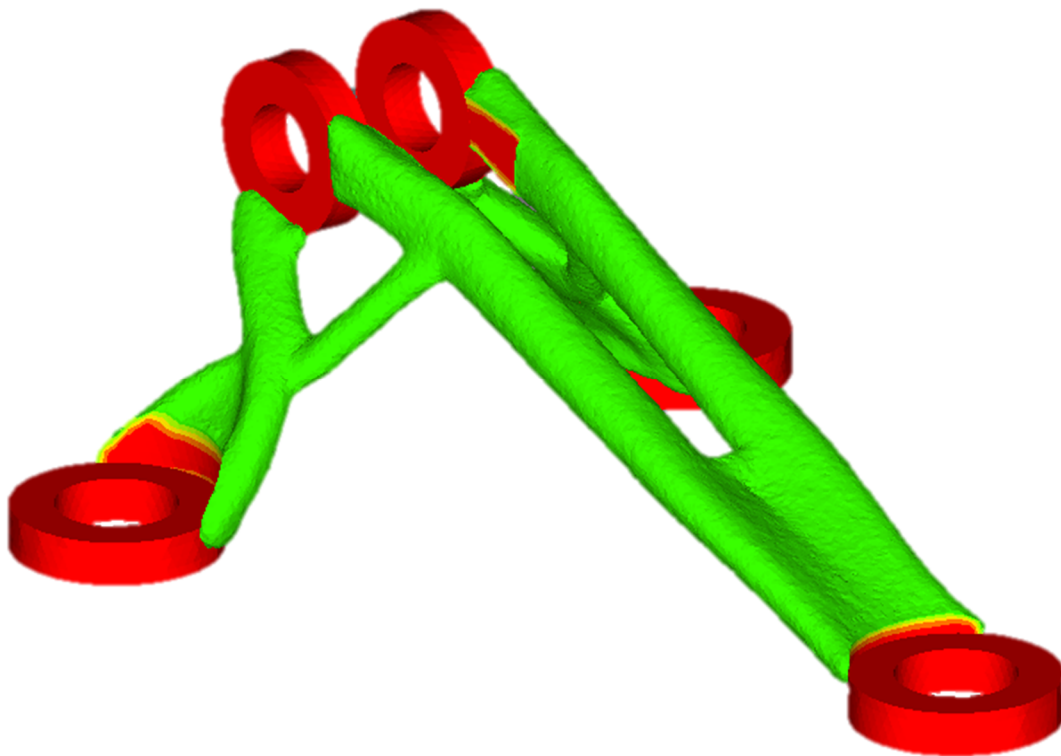


Figure 58 - Single loadcase optimization of STR1 on a high definition mesh using an expanded design space

The application of the perturbation was performed using a script which reads the FEM deck as output from Optistruct and replicates the primary loadstep into nine almost identical cases. The script then replaces the primary compliance optimization response which is referenced by the objective function with a weighted compliance response in which each of the load cases is referenced. By this method, the automatic application of perturbed load cases is performed without user knowledge or intervention with the result being a slightly heavier, but significantly more robust structure. (Figure 58 and Figure 59) The resulting mass gain/reduction in mass saving is, on average, around 7% when compared to the un-perturbed output from TO when used on three of the candidate parts with the resulting change in output shown in Figure 60. In comparison, applying a typical minimal Airbus knockdown factor of 1.5 yields an almost 20% penalty in structure mass thereby showing a significant benefit through use of the perturbation method. The automatic application of the perturbation cases means that no increase in required parameterization time occurs.

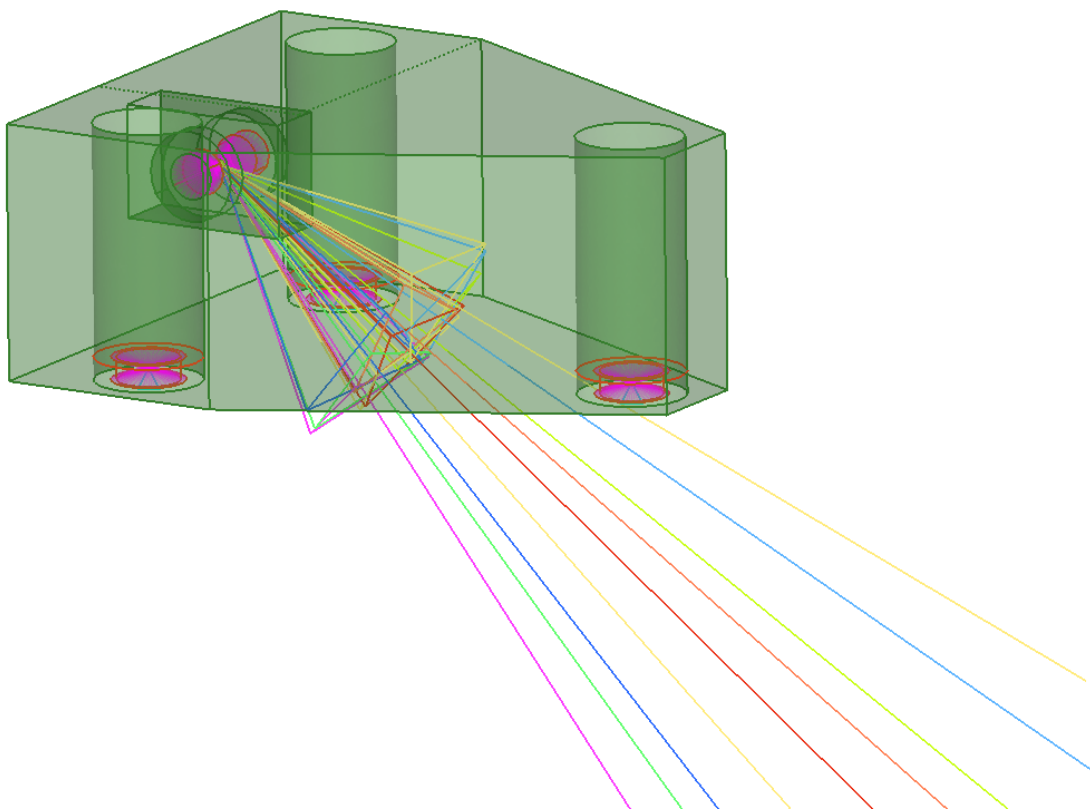


Figure 59 – Depiction of perturbed single loadcase optimization of STR1 using an expanded design space.

4.4 Conclusion of Robust Design Methods

Whilst the approach here is substantially different to the approaches usually considered for robust design and even the emergent research on robust topology optimization (Kim 2016) the complexities of applying robust optimization methods to wildly varying topologies cannot be

easily implemented or automated. As such, the described approach is both robust and practicable.

4.5 The Application of Constant Mesh Density Topology Optimization

One of the major difficulties with topological optimization is the rationalisation of grid size with solution sensitivity. Whilst outwardly similar to the problems of grid sensitivity in FEM, the TO requirements are arguably tougher to meet within computational limits, due to difficulties in establishing stress proximity in shapes of unknown topology. Conventionally, this is not viewed as a particular difficulty as the visual output of most TO solutions are just that, visual, and thus subject to interpretation (however vague) by the design engineer. However, as this process is eventually planning to automatically extract the resulting topology back into CAD, a more refined, less ambiguous result which uses significantly less penalisation in order to achieve convergence would be beneficial.

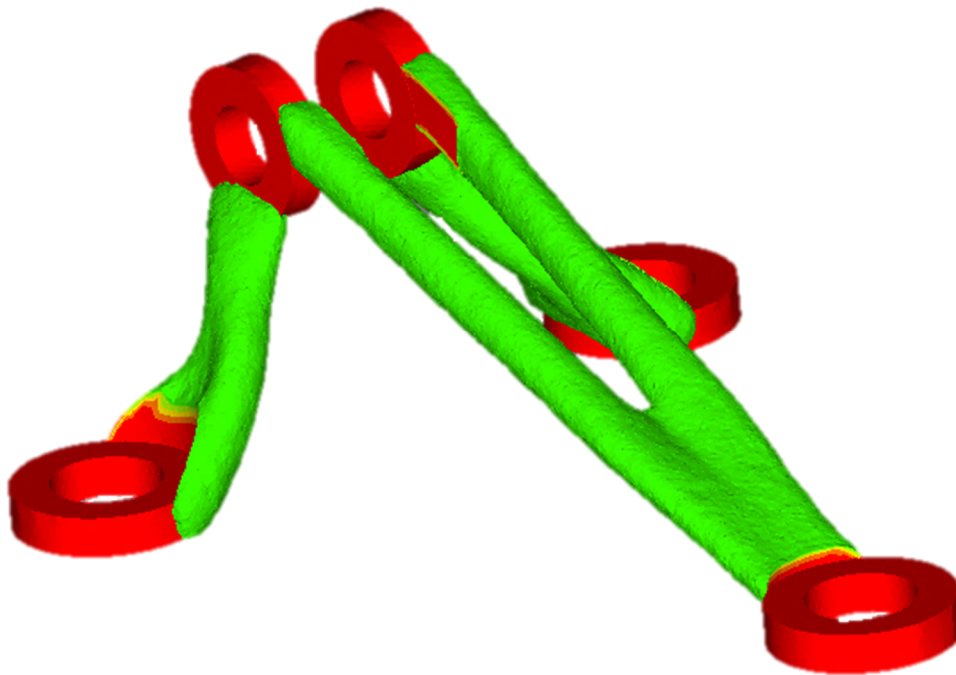


Figure 60 - Topology change when applying perturbed loadcase application to STR1.

However, the most robust and unambiguous TO outputs are usually obtained with the correct definition of the problem when applied to a uniformly and highly refined mesh. Due to computational limits and time requirements, the generic application of this approach is extremely inefficient, often necessitating 10s of millions of elements and thus requiring of substantial time between iterations and final solutions. A new approach was required.

4.5.1 Methodology for the Implementation of Mesh Refinement

When observing the convergence of the optimization during myriad TO cases as part of my daily work, it was observed that rapid convergence (to approximately 80-90%) usually occurred within the first 10 iteration of the optimization with the final iterations only refining the topology obtained within the first 10, thus making only marginal gains and changes. If those elements which are still present in the stiffness matrix, but are not currently relevant to the design could be re-allocated to areas of use, refinement could be achieved with little or no increase in computational power. The proposed solution to this was to cap the convergence limit of the optimization at a lower value of ~90%, well in advance of objective convergence and thus rapidly achieved through the removal of elements certain to contain little-no strain. The grid definition for this was capped for a fixed run-time as determined by solution time on a single node within the HPC at Airbus thus giving each structure ~5m cells. Once complete, the density function was set at 65% (all elements with a density greater than 65% would be retained) and the design extracted back to Optistruct for remeshing and re-optimization. At this juncture, the same 5M cells are applied back to the extracted topology, though this time the design space is smaller and thus a greater mesh density is achieved. The process is repeated several times with the convergence limit increasing only if the solution is achieved before the iteration limit is reached.

4.5.2 Results of Constant Mesh Refinement

The result of this process can be seen in the depiction of the refined result of optimization of STR2 in Figure 61. The output is heavily refined and reveals smooth, unambiguous features similar in topology to those found when using level set methods for topology optimisation, but achieved in a fraction of the time and with a fraction of the time required for a solution convergence to be attained. Additionally, the resulting mass as a result of that optimization process once converged are very positive when compared to a conventional solution on a similar sized grid. Indeed when compared to the same optimization problem solved on increasingly higher density grids, it is not until an almost 4x increase in mesh density does a similar solution present itself and when presented, the solution time difference is extreme.

4.5.3 Conclusions of Mesh Refinement

Whilst constant mesh density TO was highly successful, it required vast amounts of manual intervention during each extraction and remeshing phase due to the state of the extracted mesh based STL. The STL geometry required re-ordering of the surface normal in many locations and the patching of holes in many others. None of this could be easily included without a significant increase in NRC design time in exchange for a small percentage change in mass. Ultimately, the defined method of iterative grid refinement was not one of the primary objectives of the research

and thus could not be afforded the time required to investigate and complete the automation of the process. The method is however an ideal target for future research.

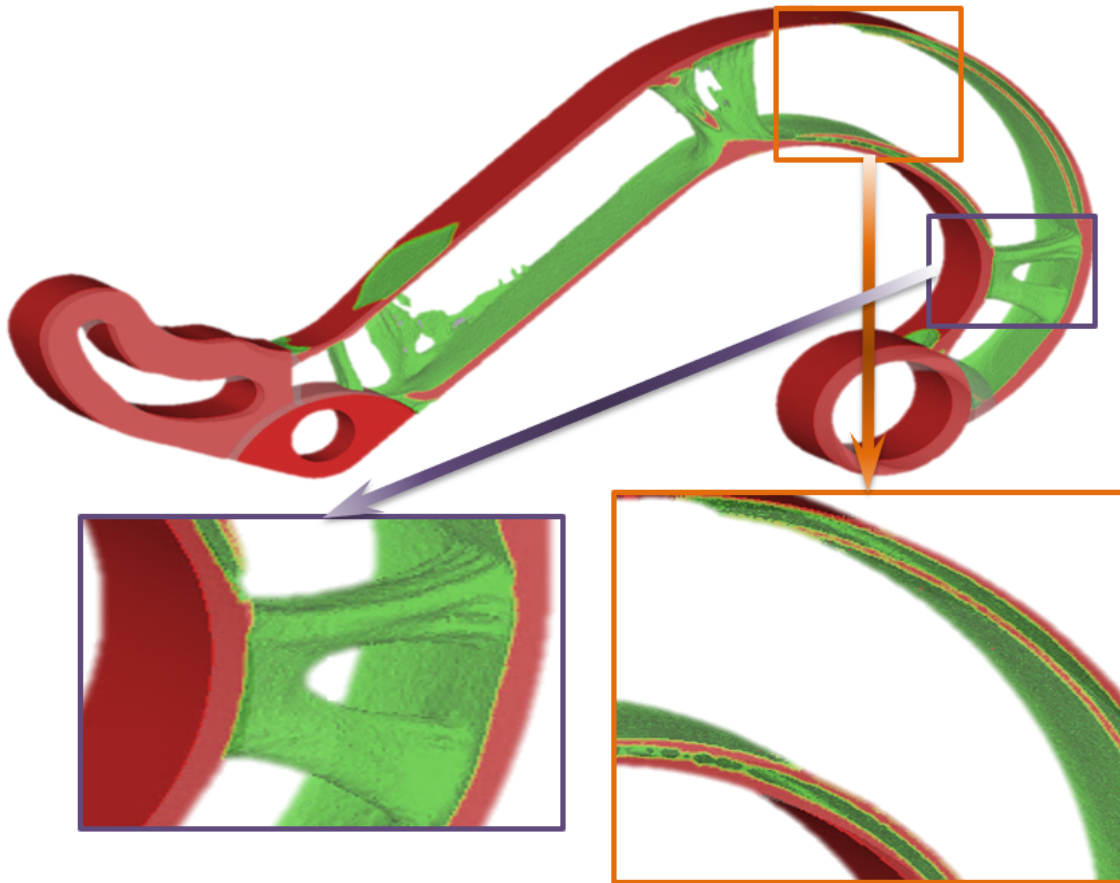


Figure 61 - STR2 optimised using an iterative mesh refinement technique - note the detail revealed in optimisation

4.6 Determination Optimization Constraints in Relation to Mechanical Performance and Geometric Capability Data for Powder Bed Additive Manufacturing

One of the greatest sources of error in both FEA and Optimization is from input error during the initial parameterization phase. During this phase, material properties, loads, boundary conditions and property collectors must be specified and specified accurately in order for the solver to achieve a suitable output. Should even one decimal be misplaced in a material card or a miscalculation between unit conversions be made, the achieved results will be inconsistent with real world performance. In addition, when considering the use of AM, few materials are available and all have different mechanical properties to their wrought brethren. In order to prevent each department within the group either sourcing material data from the internet or requesting access to our (Airbus Group Innovations) preliminary material data, the creation of a set of statistically

proven mechanical and geometric performance data, specific to PBF AM in titanium 64 was deemed appropriate.

4.6.1 Material: Additive Manufacturing and the Effects of Orientation upon Material Properties

There are several unique qualities of AM which can affect the material properties of as-built parts. Orientation is the biggest cause of material difference, but it is the effect of that orientation which must be studied as the underlying case may be related to thermal, recoating or downstream effects (Körner et al., 2014). The following sections detail the means by which these effects are captured and quantified to give usable material data for analysis and optimization.

4.6.2 Determining the Effects of Build Orientation on Material Properties

One of the key differences between AM and other forms of manufacturing is that the material is created through not in a single operation (like casting or wrought material), but through several thousand iterative operations. These, almost repeated layer-wise operations begin at the build plate and end at the top of the parts within the build. Due to this layer-wise construction, altering the orientation of a part can dramatically alter several aspects of its character through alteration of melt area, changes in thermal gradient or total number of layers deposited (Figure 62).

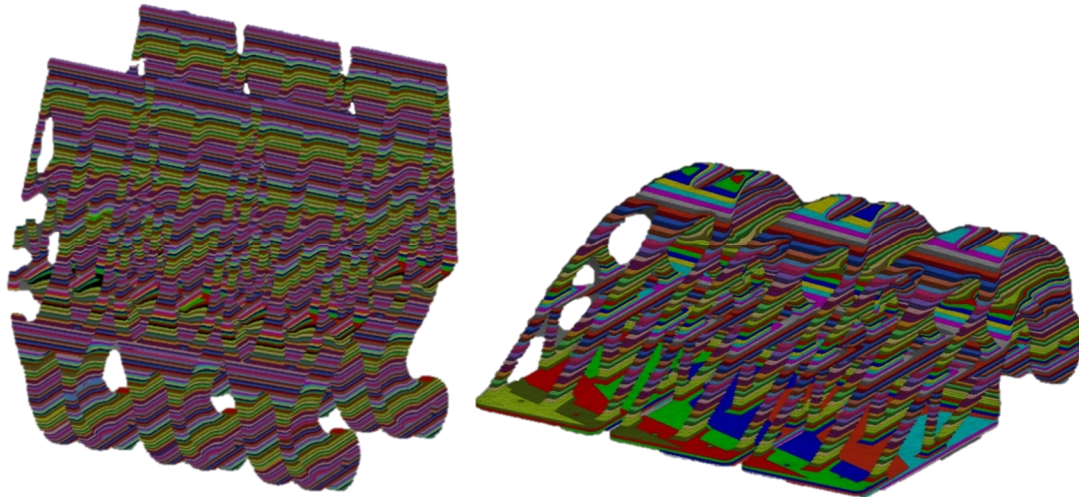


Figure 62 - demonstrates the effects of orientation alteration on multiple optimized versions of STR3. On the left, scan areas are minimised, but build height is increased (400 layers vs. 135). By assuming a vertical orientation more parts can be built at once, thus offsetting build cost against a higher number of parts.

Any anisotropy in the mechanical performance of AM structures at angles away from the vertical and horizontal, must be accounted for in the setup of any topology problem and thus must be understood in order to create a usable template for future AM optimization problems.

Problematically, many if not most research studies undertaken into the effects of orientation on mechanical performance (Baufeld et al., 2010, Machry et al., 2016) focus on only two aspects of the build, the orientation of the samples and the resulting mechanical properties. It thus assumes that only orientation has an effect of material properties, thereby implying that correlation equals causation (Wright, 1921). Additionally, the vast majority of these studies are also performed on a single AM platform using powder feedstock with limited traceability and provenance (Buchbinder et al., 2011, Antonysamy, 2012).

4.6.3 Test Methodology for Determining the Effects of Orientation on Mechanical Performance

As mentioned, there are several potential reasons for poor mechanical performance in AM, but only orientation has a direct bearing on topology optimized parts. As such, a study which controls as many other sources of variation as is possible/practicable, whilst allowing orientation to vary was required. As such a test methodology was defined which considers and attempts to control the effects of recoating, thermal stability, chamber location and material variation. To do this, a pair of test builds were created which were suitable for production in both EBM and SLM (though the support structures differ due to the differing thermal effects in the respective environments) in a variety of AM machines. In each of the two builds, a minimal quadrant approach (identical numbers and series of samples in each of the four corners) was designed. Each of the two builds were then completed on four different AM platforms, with each using the powder from the same specification and batch. This then controlled material variation, thermal, recoating and positional variables within the platforms, thus limiting effects to either the platform or the sample orientation. The builds are comprised of a series of twenty tensile, four fatigue crack growth and 50 axial fatigue specimens in accordance with ASTM standards. The tensile and fatigue crack growth specimens are installed in the above described minimal-quadrant-approach with each quadrant containing five tensile specimens at angles of 0°, 22.5°, 45°, 67.5° and 90° and formed the main test for orientation. In the second build and again using a quadrant approach, but with additional samples at the centre, fifty axial fatigue (twenty-five vertical and twenty-five horizontal) specimens are manufactured, ten per quadrant and ten centre. These samples provide for data in excess of the minimum requirement as stipulated by ASTM and as determined by Airbus testing experience. No intermediate orientation was tested in fatigue due to the number of samples (and thus cost of testing) required to create the SN curve. Each of the samples was manufactured with 1mm of stock material (material added specifically to allow the sample to be machined back to correct dimensions after removal of the as-built AM surface) and was machined to correct dimensions at the testing house. Engineering drawings and pictures of the samples can be found in

Appendix B – Design Work, and the resulting build setups can be seen in Figure 63 and Figure 64.

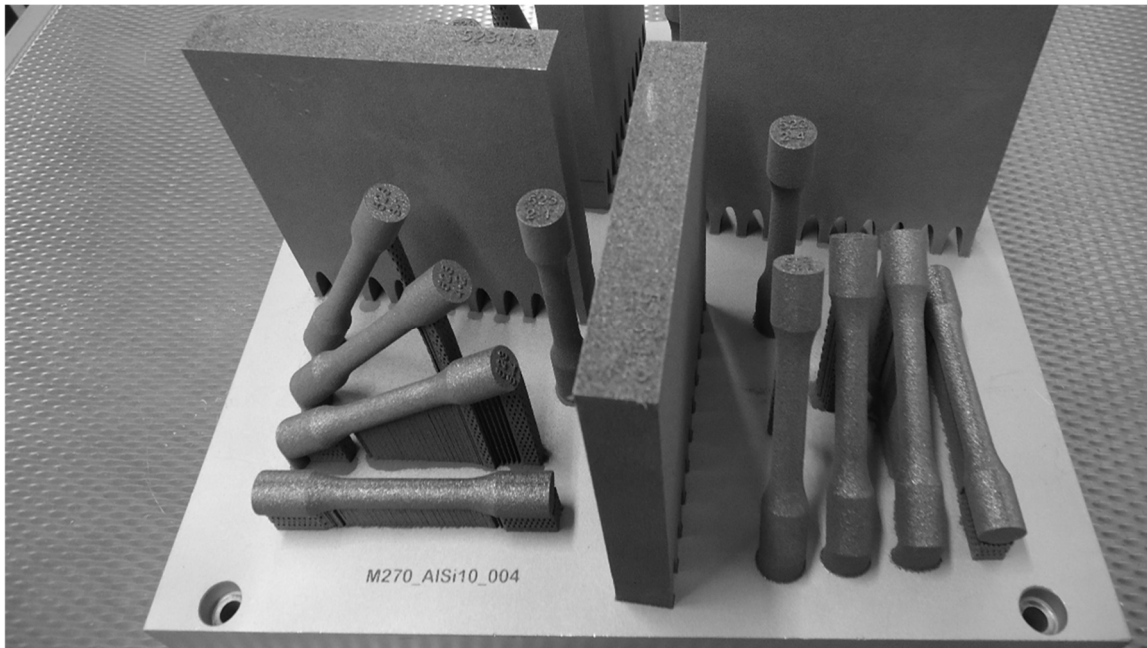


Figure 63 - Build setup #1 showing fatigue crack growth and tensile specimens in multiple orientations and chamber locations

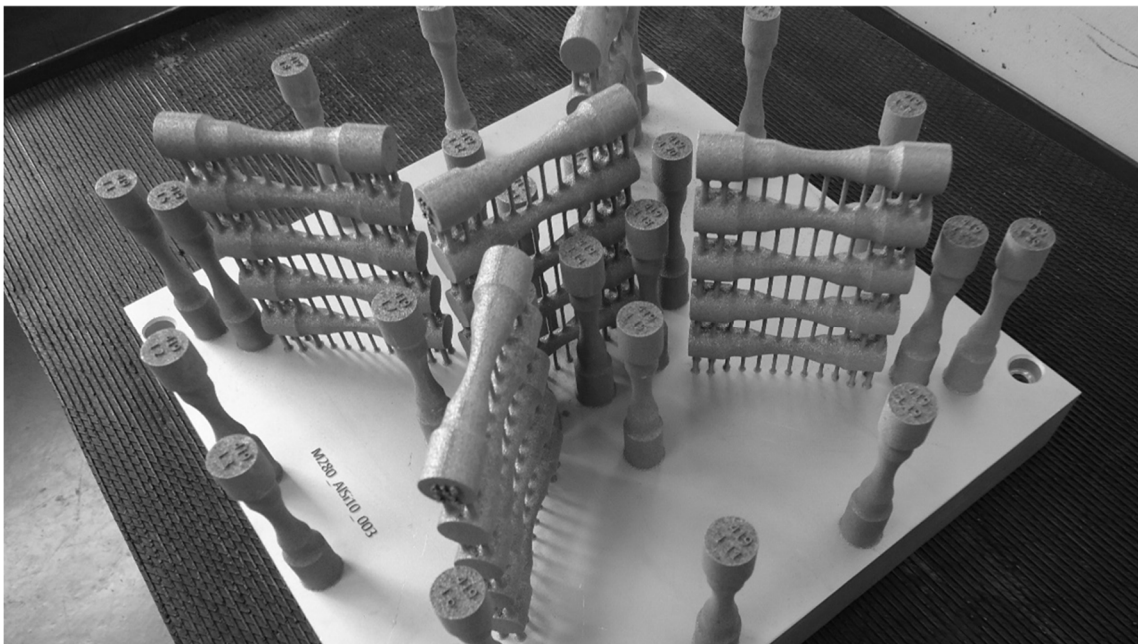


Figure 64 - Build setup #2 showing axial fatigue specimens in multiple locations and orientations

4.6.4 Manufacture and Test of Mechanical Specimens

Whilst the builds on each of the AM platforms are possessing of identical digital geometry, the themes used by each of these platforms when performing both melt and recoating operations differ subtly from one another. It is these effects coupled with gas flow, which are the active

components of any AM build and which this series of trials cannot directly control but should be able to contrast through use of multiple build platforms. The variables assigned to the active components for each platform are listed in Table 12.

Table 12 - Table showing processing capabilities of each platform under investigation

	Concept Laser M2	EOS M280 (SLM)	Renishaw AM250 (SLM)	ARCAM A2 (EBM)
Layer thickness (μ)	30	30	25	50
Theme	Ti64	Ti64 30M	Ti64 ELI 25M	Ti64 50M
Recoat Speed (m/s)	150	200	200	140
Gas	Argon	Argon	Argon	Vacuum

Upon completion of each build, and after stress relieving heat treatment (the specifications of which can be found in Appendix A – Background Material) each build was subject to Hot Isostatic Pressing in order to close any deep porosity within the samples. In addition, the use of HIP on all samples aids in the normalization of the samples between the vacuum processed EBM process and the argon inerted SLM process through near elimination of porosity as specified in the AIMS. After HIP, the samples were removed from their build plates using either direct force or Wire Electro Discharge Machining and sent to Westmoreland Test Houses for machining and test. Whilst testing could be performed in house, and by the researcher, in order to be compared directly to and thus contribute to the body of mechanical data within Airbus, the testing of such samples must be performed on NADCAP (National Aerospace Defence Contractors Accreditation Program) approved and certified equipment. Whilst Airbus UK does possess such equipment, it is reserved for use for aircraft programs and cannot be used for extensive periods as would be required by these almost three-hundred samples. A NADCAP approved test house (Westmoreland) and one of Airbus' approved labs for large scale mechanical testing and reporting and as such were the default choice for the testing of these samples. In total, eight builds were required for manufacture of the samples (two per manufacturer) but twelve builds were completed due to a need to repeat the samples from both Concept Laser and Renishaw. The former required repetition due to visible abnormalities in the samples whilst the latter had a problem during the stress relieving heat treatment causing oxidation of the samples.

4.6.5 Results of Mechanical Testing

Whilst all four platforms completed the builds during the manufacturing phase, it quickly became apparent that there were (again) issues with the samples produced by the Concept Laser M2 Cusing. The first tensile specimens tested showed significant variation in mechanical performance with a standard deviation more than four times greater than the worst seen so far and up to seventeen times greater than the best. It was decided based upon these early results

to discontinue testing of the Concept Laser samples as there was clearly either a malfunction with the platform or the post processing. The remaining samples from other manufacturers were tested successfully with the summarised results shown in Table 13. Upon later inspection of the tested tensile specimens from Concept, it became apparent that high density inclusions were causing the drops in performance. It has been later speculated that this is caused by the manner in which the Concept system introduces its gas and proceeds to melt. The high-speed gas flow coupled with the island scan pattern causes particles to be ejected from the melt pool and later reabsorbed into subsequent melt-pools. This causes the inclusions and subsequent early failure.

From the results obtained, it can be clearly seen that laser-based processes yield generally better specific material properties when compared to those of the ARCAM EBM Process. In angled orientations it can be seen that both the EBM and Laser processes have similar mechanical performance, but differ substantially in 0°/90° configurations in which the EBM process suffers heavily. It is believed that whilst the material properties are similar, that the reason for the early failure of these samples is distinct to each orientation. In the 0° (horizontal) samples, the testing shows a significantly lower elongation to break when compared to almost any other result. Low elongation is usually a factor when alloying content (specifically aluminium content) is altered. As such, it is believed that the 0° samples were overheated (insufficient support) and thus the aluminium became too hot and was vaporized during the melting process, resulting in a performance drop. For the 90° (vertical) samples, it is believed that combination of both microstructure (large grain formation) and surface condition may have led to performance deficit.

The results obtained from material testing show excellent agreement with existing research data (Antony, 2012) and yield an acceptable design limit for both yield and fatigue endurance. From the results obtained and to account for all possible combinations of orientations and TO layouts, the material allowables for Ti64 were determined based upon the lowest values obtained through testing (highlighted in green in table 13). This approach is common for Airbus when introducing new materials and manufacturing methods as it allows for use of the material/method with a reasonable safety factor. Detailed raw material data along with the calculations used to determine outliers from standard deviation can be found in - Appendix D – Calculations. Table 14. Ultimately and based upon the data, allowables for yield stress, ultimate stress, elastic modulus and Poisson's ratio (table 14) are determined then applied to the correct material cards commensurate with the manufacturing method within the optimization template, thus allowing the optimization to be performed with accurate data.

Table 13 – Showing the results of tensile testing with outliers (more than 2 SD from the mean) noted in red and lowest values in green

PhD Mechanical Testing Results					
Machine	Angle	Locaiton	0.2 YS (MPa)	UTS (MPa)	Elongation %
Arcam Tensile Testing	0	LL	719	802.53	6.4
	0	UL	841.97	951.61	14.9
	0	LR	853.19	979.26	12.9
	0	UR	862.654	955.76	13.8
	30	LL	845.16	942.61	19.9
	30	UL	881.65	984.15	18.2
	30	LR	882.26	987.16	16.2
	30	UR	880.08	981.77	16
	45	LL	865.45	959.81	19.4
	45	UL	885.24	991.15	18.4
	45	LR	889.62	984.94	18.5
	45	UR	881.47	989.62	18.6
	60	LL	875.58	976.45	19.1
	60	UL	883.65	989.19	18.2
	60	LR	889.27	986.76	18.1
	60	UR	882.62	987.93	18.3
	90	LL	831.65	937.1	17
	90	UL	828.67	937.26	17.1
90	LR	828.91	943.57	16.9	
90	UR	830.43	944.56	17.4	
Renisha w Tensile Testing	0	LL	920	1016	18.6
	0	UL	921	1018	19.9
	0	LR	927	1024	11.1
	0	UR	943	1042	17.6
	30	LL	897	984	20.9
	30	UL	922	1017	17.9
	30	LR	897	990	20.2
	30	UR	912	1003	22.2
	45	LL	922	1034	17
	45	UL	921	1017	17
	45	LR	927	1032	17.7
	45	UR	927	1036	18.3
	60	LL	878	1008	18.7
	60	UL	895	997	25.3
	60	LR	916	1031	18.5
	60	UR	846	1002	18.1
	90	LL	919	1007	18.9
	90	UL	865	992	17.1
90	LR	781	965	17.9	
90	UR	784	964	17.5	
EOS Tensile Testing	0	LL	920	1030	19.1
	0	UL	916	1022	18.9
	0	LR	915	1028	18.7
	0	UR	922	1031	19.2
	30	LL	915	1055	18.6
	30	UL	910	1046	18.7
	30	LR	922	1051	19
	30	UR	912	1042	19.1
	45	LL	935	1059	20.1
	45	UL	919	1061	19.3
	45	LR	922	1051	19.4
	45	UR	917	1046	18.9
	60	LL	935	1042	19.2
	60	UL	922	1045	18.8
	60	LR	918	1051	19.1
	60	UR	918	1049	19
	90	LL	889	1039	20.1
	90	UL	887	1033	17.1
90	LR	899	1031	20.3	
90	UR	893	1032	19.9	

Table 14 – Summary of material results showing derived design variables for Ti64 produced using Powder Bed

Fusion AM

Variable	Value
Elastic Modulus	119GPa
Yield Strength	828MPa
UTS	937MPa
Fatigue Endurance	187MPa
Poisson's ratio	0.345
Density	4450Kg/M ³
Elongation to break	16%

4.6.6 Conclusion of Mechanical Performance Trials:

Whilst the testing did attempt to control as much variation as was possible, one item which was knowingly excluded was the effects of supports and thus thermal conduction from the depositing area to either the plate or surroundings during the manufacturing of the tensile build. The reason for the non-standardisation was that EBM and SLM use differing support strategies and thus one style of supports is rarely suitable for the other on angular structures. Regardless, the testing demonstrated without question that intermediate angles of deposition are in fact stronger than the 0° or 90° samples when built on any of the AM platforms, thus, by selecting the lowest figures from table 13, there should be no difficulty in applying an isotropic value to Ti64 during the optimization process.

4.7 Definition of the Processing Limits of AM Platforms.

Whilst all AM machines within this study are comparable to one another in terms of broad capabilities, they are by no means identical and it is the small details in processing patterns which separate the final capabilities in build-up. These machine limits are of importance when defining templates for the automation of the TO process aimed toward the production of the new design through AM, as they form a constraint upon the optimization design process. Categorization of these features and application to constraint functions occurs through the definition of a minimum feature allowable which is related to multiplication feature of the minimum element size, as such the limit and those other limits must be linked to the iterative meshing defined later. In order to capture these feature details, a series of sample builds were created to test the minimum processing features of each platform. The designed samples test the individual machines capabilities to process features at the extreme ends of the machines operational scale. Most notably, the tests were designed to determine the minimum possible feature definition capable by each of the platforms.

These factors were important as the minimum depositable feature were used in the definition of the optimization constraints for minimal features and implemented through both the earlier thickness calculation and the empirically derived minimum manufacturable feature from these trials. The resulting test builds can be seen in Figure 65 with further details in Appendix 0. A summary of the findings can be seen in Table 15. All results were obtained through use of X-ray CT metrology using a Rayscan6000 system with a voxel resolution of 2μ at these wall thicknesses in this material.

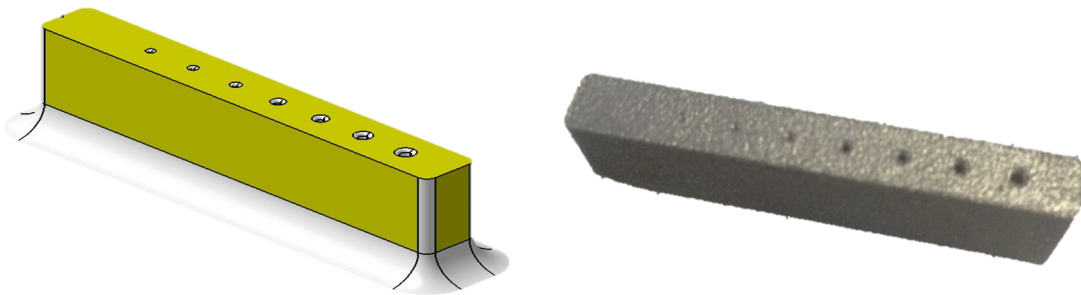


Figure 65 – Example of geometric sample builds designed to test minimal features on a range of different platforms

Table 15 - Tabulated features showing design allowables attained from geometric testing.

Feature Type	SLM Measurement	EBM Measurement
Minimum Single Feature Size (Pin)	0.25mm	0.65mm
Minimum Hole Size (vert)	0.6mm	1.1mm
Min Hole Size (horiz)	0.7mm	1.8mm
Minimum Wall Thickness	0.2 (with porosity)	1.1mm
Maximum Offset Feature	0.15mm	2.25mm (some shrinkage)
Maximum Thickness	32mm	NA
Aspect Ratio (height to thickness) restriction	~7:1 at lower limits and >10:1 above 1mm	NA

4.7.1 Conclusions of Design Constraints

Whilst the resolution of the CT scan is incredibly high, the variation in holes size and wall thickness is also subject to consideration of wall effects and powder agglomeration which can skew the hole size by $\pm 15-30\mu$ in the laser-based process and $\pm 60\mu$ in the EBM process. It should also

be noted that geometric features are dramatically affected by processing parameters, especially when operating at the limits of the machines capabilities and so should be re-evaluated should the machine theme change.

4.7.2 Manufacture and Economics: The Constraints of Layer-wise Production and their Inclusion within the Templates

Whilst AM technology might well be capable of manufacturing **any** geometric output from the TO solver, there are still a significant number of factors which can, if left unconstrained, create layouts which will add time/complexity and ultimately cost to the AM part being produced. Orientation, the requirement for support structures (SS), nesting (parts per build, think Tetris) and the rate of change of area between layers are all factors which can have significant effects upon manufacturing cost and conformance. Problematically many of the aspects detailed above are/can be influenced by build orientation (Figure 66) and in order to include considerations related to build-up orientation into the optimization definition, the orientation must be broadly decided before any optimization has taken place. This presents a paradox in that the optimiser requires knowledge of the approximate build orientation in order to apply constraints, but any priori decision related to build orientation must be based on the original part, and thus could be totally incorrect for the new derivative topology. Reversing the situation means that build orientation is determined based upon the correct topology, but the topology will not be optimal for the manufacturing process, thus requiring substantial additional DFM and SS in order to correctly manufacture in AM.

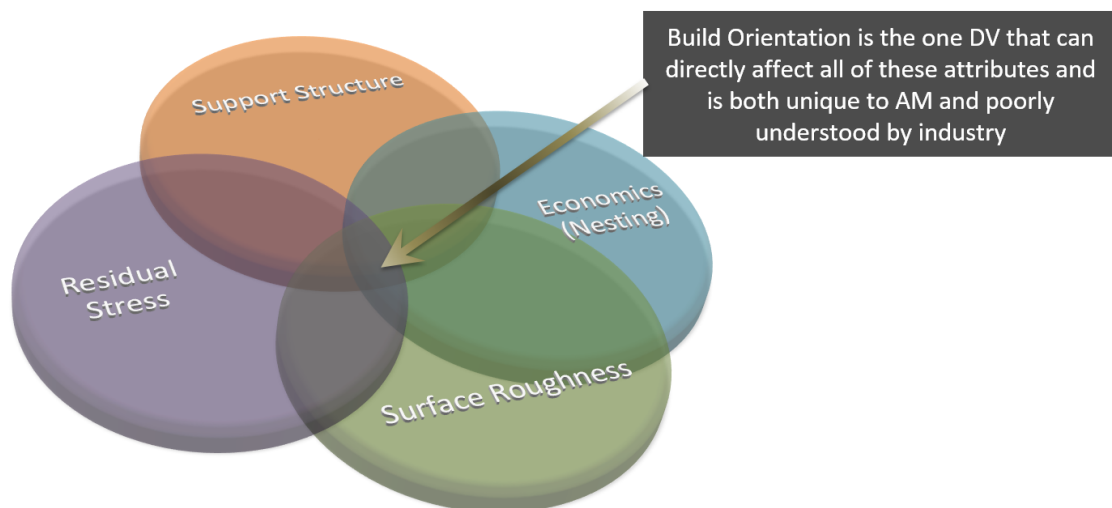


Figure 66 - Aspects of additive manufacturing which are affected by changes in orientation

This is further complicated when considering a structure in an expanded design space (EDS), which thus represents neither the ancestor part nor the new topology, just a block in 3D Space. Ultimately, it was decided that a decision on orientation based upon ancestor design could not be accurately and automatically implemented for all aspects of AM, but could be made with consideration of machine constraints and general rules.

The first of these general rules considers the combined effects of residual stress formation with that of long scan lengths in the EBM and SLM processes. As such, bounding box dimensions of the part are extracted from the CAD (using the STL and Max/Min vertex points in each of the primary axes) with a vector placed upon the longest length of this computation and subsequently applied to the Hypermesh Template. To this vector, the constraints for AM material growth are constrained and long scan lengths mitigated against. AM layerwise growth constraints are difficult to control in SIMP (substantially easier with level-set methods) as boundary control methods are difficult to employ on what is essentially an unstructured grid. Despite this, many SIMP solvers have the ability to apply casting directions to the solver (similar to symmetry planes) and can, in some cases help to prevent the solver from creating a structure with poor thermal connection to the build plate, thus reducing the chance of build failure through distortion. The casting constraint is automatically applied to the template based upon the vector extracted from the longest length as this is the approximately determined orientation for build based upon the ancestor design. The casting constraint factor is present in both Hyperworks and Inspire and can be applied using a vector coded into the input deck or directly within the software template.

Minimum allowable feature definitions within TO are a commonly used feature to constrain design outputs to easily manufacturable elements. The optimiser penalises elements/topology artefacts smaller than the constraint size to either converge on larger common pathways or to be eliminated as inconsequential. These controls for minimum feature size are simple to implement and easy to automate once the required constraint values have been determined. For this application, those values were linked to the minimum feature tolerance of the machine in which the final part will be manufactured. In addition, these values were compared to the real world data provided from the design studies as detailed in Section 0. The feature definition was further constrained by the AM design guidelines created (for Airbus by the researcher) in parallel with the testing and material standards. When applied, the minimum allowable feature is defined as 1mm or 2x the minimum deposited wall thickness, whichever is lower. This figure is then appended to the Opti-control aspect of the Hyperworks template based upon user selection of the final manufacturing process as shown in Figure 67.

<input checked="" type="checkbox"/>	DESMAX=		3	0	<input checked="" type="checkbox"/>	OBJTOL=	0	.	0	0	5
<input checked="" type="checkbox"/>	MINDIM=	3	.	0	0	0	0	.	5	0	0
<input type="checkbox"/>	MATINIT=	0	.	6	0	0	0	.	2	0	0
<input type="checkbox"/>	MINDENS=	0	.	0	1	0	0	.	5	0	0
<input checked="" type="checkbox"/>	DISCRETE=	3	.	0	0	0					
<input checked="" type="checkbox"/>	CHECKER=								1	0	
<input type="checkbox"/>	MMCHECK=						1	.	0	0	0

Figure 67 - Opticontrol modification script and its effects.

4.8 Summary of the Automation of the Pre-processing Phase

Looking at not only design aspects, but also material performance from AM and its inclusion into standardized tools and Hyperworks templates, automation of several of the pre-processing phases for the application of TO have been attempted within this section of the research (Objective 3). Whilst each of these automation steps are isolated, their cumulative effects on the time required for TO parameterization is substantial and simultaneously increases process robustness through their application. Problematically, TO is an already complex process and the application of several additional tasks to the already intricate process chain can lead to substantial potential for process error. In order to control this aspect, some means of controlling the process phases and ensuring their correct serial application was required.

5 Development of the Mapped Manual Process for Airbus and the Effects of Automation on its Implementation

Chapter 5 details the work involved in wrapping up the project as Airbus's direct involvement comes to an end. The main focus of the work is concerned with the deskilling of the optimization driven design approach through the development of a detailed process mapping and description exercise into which the developed stages of automation can be applied. The chapter concludes with an evaluation of the effectiveness of the detailed process map and the automation processes at increasing speed and decreasing process variability.

5.1 Introduction to the Mapped Manual Process

The original aim of the research was to have an automation process capable of vastly expediting the application of topology optimization to small aerospace parts. This was to aid in deriving substantive cumulative gains in mass reduction through optimization and redesign for AM, without incurrance of enormous NRC for analysis and redesign. Of the entire TO process, the most skilled and complex section (though not the most time consuming) is that which relates to the analysis and optimization of a given component. It is this phase for which the fewest number of skilled operators exist within the divisions of the Airbus Group and is thus where the greatest bottleneck in resource occurs. As such, it was believed that by reducing this resource bottleneck through automation of the pre-process phases, that at higher throughput could be achieved without increase in resource, thus reducing (per part) the total cost. By automating the TO phases, the research deskills the optimization phase for simply loaded components, thereby allowing analysis and optimization to be performed by the software, and direct redesign performed subsequently by the Airbus design engineering community. In this manner, the new design process (which includes optimization) can be employed by substantially more users (there are far more trained CAD operators within Airbus than there are Stress and/or Optimization engineers), thus increasing the cumulative gain, whilst partially reducing design time. Regrettably, this approach does not reduce the NRC for design as the design extraction task must still be accomplished entirely manually. However, it does substantially reduce the required time for the generation of the preliminary or concept design, as this is now performed by the semi-automated analysis and optimization process.

As the operators of this new process will by majority be design engineers and not stress engineers, their knowledge of the importance of certain analysis and optimization phases will be limited. In analysis and optimization, the correct application of the correct steps in the correct

order, is critical to achieving the required design objective. Thus, design engineers proceeding without

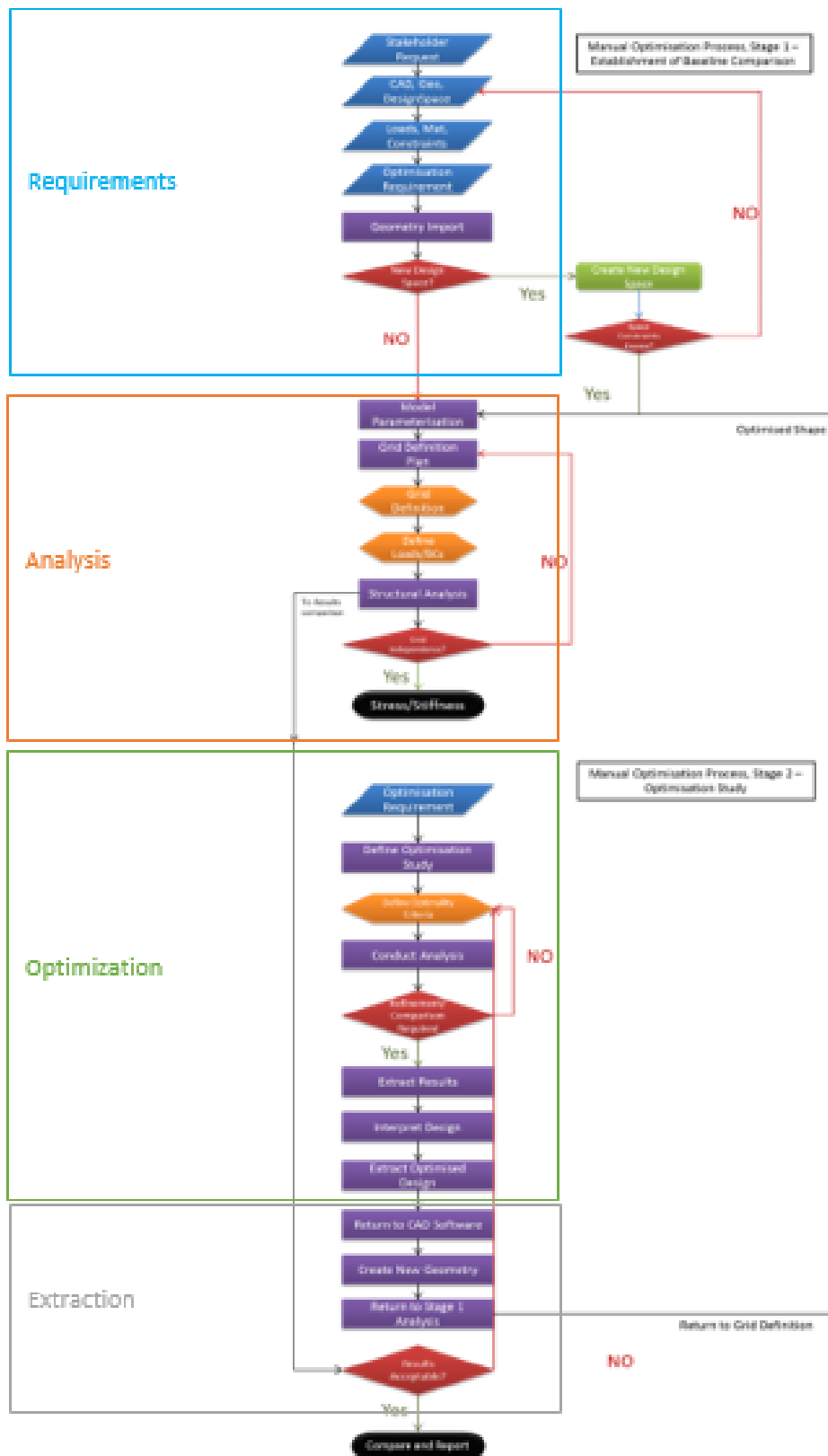


Figure 68 - Flowprocess for design optimization showing major areas and their sub-processes

detailed knowledge of the process and its intricacies, makes for a far greater likelihood of process error and thus concept design error. In order to remove this error potential and increase the robustness of the process, a method of integrating the research completed thus far into a new process instruction and toolset was proposed to Airbus. The proposal was to create a new instruction which would facilitate the use of complex software by a larger pool of engineers through a prescribed method, a checklist which would clearly define the required stages, the necessary tools/methods and the process order needed to deliver accuracy in each use of the technique. The Mapped Manual Process (MMP) was created to perform this function for the optimization and AM departments of Airbus Commercial Aircraft.

5.2 Methodology for the Development of the Mapped Manual Process

The first step in the creation of the Mapped Manual Process (MMP) was to quite literally map the manual process for design optimization in Airbus, noting each phase, its connections, parents and child tasks along with any other dependencies. In order to not generate a myopic view of the process based on the researcher's singular experience, the process mapping was developed and iterated in collusion with colleagues from Airbus Stress and Non-linear dynamics, thus stabilising the inputs and more importantly, the expected outputs.

Once again, the candidate pool of Optimization users in Airbus were asked to participate in an interview process during which they would be asked to detail a flow process for TO, specifically recalling their experience with optimisation of the candidate parts for this study. Each participant was interviewed individually, during which each interviewee was asked to detail the steps involved in optimising a component. This was an interactive session in which the steps, their inputs, outputs, dependencies, etc were mapped on an interactive whiteboard in front of them and manipulated in response to their feedback.

Using the initial work-breakdown structure as a guide from which the interview process began, the broadly defined process has four distinct, but interconnected phases: 1.) Requirements Capture 2.) Analysis Parameterization 3.) Optimization Formulation and 4.) Interrogation and Extraction. Each of these defined blocks has a number of high level sub-processes which are identified in the process map shown in Figure 68. The process map (Figure 68) shows the individual stages required, the order in which the steps interact and the loops activated under certain circumstances or criteria. it does not detail the specifics required during those steps, nor the means in which they should be utilised and information transferred, that was the aim of the interviews

5.3 Results of the Interview Phases in Development of the MMP

5.3.1 Requirements Capture

Analysing each major section in turn; the requirements capture phase is, on the surface, largely self-explanatory and easily understood. However, there are details and subtleties within the capture phase which can have significant implications on the final optimization output if either miscalculated or misapplied to the optimization problem. Foremost amongst these factors are the requirements pertaining to the design space expansion, along with the forces for post processing (machining of key interfaces, thread tapping, vibratory grinding etc) and assembly as required by the final component.

5.3.1.1 Expanded Design Space

New aircraft programmes (A350/A380) are designed with full CAD architecture and have a space allocation model (SAM) which allows for easy determination of allocable space around any component, thus making for easy determination of potential for expanded design space (EDS). Almost all components found on aircraft programmes which pre-date computational architecture design (A320, A330 etc), have no master map of space allocated to individual parts, thus making determination of total available design space for a particular component a problem. For the parts derived from earlier aircraft programmes, by the time a component makes it into final design, most criteria which provided the requirements for its space allocation have been lost/buried, thus severely limiting any potential for an EDS application. In the latter case, a visual inspection and measurement of the area for each component is required to create an EDS and as such, is largely impractical within the scope of this investigation. For the former, the data from the older SAM can be indirectly interpreted into the EDS and subsequently the optimization using the Aircraft Axis System for location. Using the aircraft axis system as the global axis makes for simple assimilation of the SAM into the EDS as this is identical for both the EDS and the SAM and thus provides for easy integration between the CAD entities using Boolean operations prior to other parameterization activities. For ancestor programmes, the EDS will have to be performed manually using a careful examination of the existing part and, if possible, its environment. In later phases of design, the SAM is completely overwritten by the aircraft digital mock-up and thus cannot be easily interrogated, but instead must be gradually created from the extraction of solid structures and systems in a particular operating space.

5.3.1.2 Digitalization of Post Processing Requirements

The post processes machining requirements (in terms of the process steps) are again relatively well understood, but unlike loads pertaining to service conditions (which are well known and thus included in the requirements capture as load conditions) the inclusion and transference of post

processing requirements into constraints/loads is not widely considered during analysis and optimization. Problematically, manufacturing and assembly forces can be substantial and for a lightly loaded component can quite easily become the driving load condition for the optimization. And so, whilst not technically critical, the loads can often represent the highest loads to which a part, particularly a TO part is subject, if included in the initial parameterization. The application of post processing forces (grinding, cutting, boring, etc) into the structure are often (but not always) in regions similar to those of attachment/force induction positions. Conversely, they are commonly in different force vectors to their constraints/attachments, thus making any structure derived without their inclusion, substantially flawed. The inclusion of additional forces can thus cause a dramatic difference to the optimised structural layout, thus highlighting the importance of the inclusion of post processing loads in the definition of the problem.

However, the loads and more importantly their magnitude are generally unknown to design engineers (as they are considered during manufacturing preparation, not concept design). This is largely due to design rules for conventionally manufactured/designed parts which when applied, give substantial structural robustness. To include these forces in the optimization, their approximate value must first be determined. When considering the types of forces encountered during post processing, the most commonly occurring (based on an assessment of the parts catalogue and meetings with GKN Aerospace) are those stemming from grinding, boring, cutting and thread tapping. Of those, only cutting, boring and tapping are commonly used for titanium. A parallel study was undertaken at AGI in order to determine the correct magnitude of these PP forces on the workpiece during finishing operations. As such, a small research study was undertaken to determine the reaction forces of the component to several different types of machining load. The most commonly applied post processing operations are those for 1) hole drilling 2.) Surface Grinding and 3.) Thread Tapping. In order to determine the forces required to perform these actions on as-built AM titanium, the 3 axis CNC machine at Airbus Innovations was instrumented with a pair of 10kN load cells intended to record 1.) and 2.). item 3.) was determined manually using a torque wrench on a thread tapping tool. The forces were ultimately found to be 1.) 1050N, 2.) 990N and 3.) 1200N and are applied as direct force and torsion loads respectively. As a result of this work, post process forces will be given a uniform magnitude load of 1.5kN applied with the correct force description (torque, vector, etc) thus giving substantial reserve, but allowing for process robustness. Many of these loads will have to be manually applied as screw threads are not mapped onto all CAD plans, but are later defined in engineering drawings and are thus incompatible with the FR software created earlier in section 4.1.3. It is worth noting that the forces to be applied to the analysis and optimization are coarsely defined

and by no means exhaustive. The machining project investigated but a few combinations of cut depth and tool types in order to determine suitable allowables and so the forces have been applied with conservatism wherever used. Whilst technically outside of the scope of this research, the project required little funding (beyond time and the load cells) and was critical in providing data required for the optimization process. The work was completed in 12 weeks, most of which was awaiting delivery and calibration of the loads cells. The machining trials took only a few weeks.

5.3.1.3 Definition of Optimization Objective

An optimization objective can take many forms such as cost, weight and performance, but ultimately, and no matter the other considerations, there is usually one particular condition which has driven the demand for a better design. Most commonly, this is objective is for component mass reduction and is as such, is the primary focus of the main research project, but others such as stress, reserve or failure mode are also sought. An easy solution would appear be the inclusion of secondary and tertiary objectives functions within the optimizer, thus providing a solution for all problems, perhaps at a slight mass penalty; problematically for TO within Hyperworks, a primary objective cannot be paired with a secondary objective as the software is incapable of performing multi-objective optimization in an STO context. As such, any additional objectives, were reformulated as constraints upon the domain, and so whilst mass reduction (through a compliance formulation) remains the objective of the optimization, the current structural performance for deflection and stiffness for the component will be captured and subsequently constrained. The initial analysis phase is designed to perform this function and thus capture data to be included as constraints on the solver. The result is that any derivative structure should have almost identical structural performance whilst achieving lower structural mass.

5.3.2 Analysis Pre-process Parameterization Phase

The analysis section of the optimization process is where one of the greatest chances for error is likely to occur. During this phase, geometry is imported, modified for meshing and segmented in preparation for optimization. Meshing is applied and refined along with the addition of material properties (which can define the response of the whole model if incorrect). Finally, loading conditions and boundary conditions along with their transfer structures are created.

5.3.2.1 Material Data for Analysis and Optimization

The material capture phase documents the current material of the component and the reasons pertaining to the selection of that material for this application. For the primary analysis, the material data of the existing component must be either provided with the CAD or, in the event

that it is not available directly, sourced from alternative routes. Though precise values would be preferable, the existing material data is only used to determine current structural performance and transmute those responses into constraints for optimization and thus some degree of variability can be tolerated. The capture phase also details whether an allowed material change to Ti64 is permissible. In such cases, the material data is taken from the testing established earlier in the research and will be populated into the Hyperworks template.

Hyperworks is a unitless software package and so geometric features cannot be truly evaluated until consistent value for elastic modulus and material density are applied to the material property collectors within the software. As such, the correct and constant application of unit properties is crucial in order to preclude the possibility of a systemic error being introduced during analysis. Again, order is important during this phase and so properties are created before CAD is imported and segmentation should be performed prior to both geometric clean-up and FEM generation. Failure to adhere to the order will cause incorrect application of element properties to solid component or will overwrite correct data with incorrect or incomplete data. Additionally, material collectors are applied to property collectors, then to component collectors and so must be created in reverse order to allow each subsequent collector creation to reference the relevant property, thus preventing errors in between elements and geometry. If incorrectly applied, it is relatively common for models to have one property assigned to the geometry and another applied to the mesh intended to represent that geometry. This will cause a software error during reading of the FEM deck by the solver.

5.3.2.2 Model Parameterization and Design Space Separation

The conventional method usually employed when performing structural analysis as a precursor to TO is to mesh, load, analyse and then begin the setup for TO. Using this method, the mesh and loads must be removed and reapplied once the design space separation is complete. The method undertaken as part of this research was to segment and de-feature the geometry (through it is not required and adds complexity to the solution) prior to the analysis phase. Doing this, meshing and load application are performed only once during a cycle. The problem with this method is that a substantially denser grid is applied to the analysis mesh than is required for a stress solution due to the need to establish a grid independent stress and displacement solution. If solved (optimization) on this grid, it will dramatically increase the computational solve time without much benefit to the solution. The derived benefit stems from the engineering time saved at the expense of computational time which is non-interactive and thus marginal when compared to engineering time. During the parameterization phase, washers are placed around mounting

holes at a radial distance equal to the Airbus Design Rules pertaining to the material and fixing size. These washers couple to the vector of the hole to which they are associated and creating a surface which can be used for segmentation for non-design space. To these spaces, a uniform 2D mesh is applied and extruded through the NDS element, thus creating a Hex mesh with excellent unit cells of the introduction of loads and constraints. Once complete, nodes from the 2d mesh are associated to the surface topology and a 3D. Tet 10 mesh of uniform element density is created for the primary design space model. Finally loads are applied to structures using a combination of RB3 and RBE2 connector elements and the analysis is ran. The pictographic representation of these phases can be seen in Figure 69.

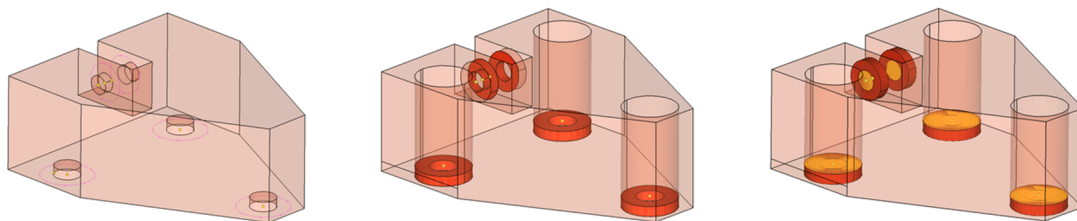


Figure 69 – Automated recognition and separation of NDS (left) followed by uniform meshing of NDS (centre) and application of rigid elements (RBE3) for loading transfer (right).

5.3.3 Optimization Problem Formulation

Through use of the pre-defined Hypermesh template defined in section **Error! Reference source not found.**, the majority of the parameters for the optimization are already defined, but require assignment to the geometry imported earlier and the FEM created from it, coupled to the loads added to that FEM in previous phases. Initially, the previously segregated design space is organized into appropriate collectors for DS and NDS which were provided in the template. Once complete, the optimizer is assigned design variables particular to the DS collector only, thus leaving the NDS untouched during the process, exactly as planned. After allocation of the DVs, application of design and optimization constraints (captured during the analysis phase) to the FEM occurs next, with the final details being related the choice of optimization objective and the constraints therein.

5.3.3.1 Difficulties with Optimization Constraints for Topology Optimization.

When component mass reduction is the objective of an TO problem, the commonly applied industrial method of achieving this mass reduction is not to directly minimize mass, but to minimize total compliance, that is to minimise the total strain energy of the domain subject to a selected volumetric constraint. Problematically, nothing in the analysis phase can help determine just what the potential for mass reduction in any given structure might be, and so, how is the

volumetric target value determined? The usual approach is to start at outlying bounds (say 50% and 90% of the total volume) the lower of which is too conservative and the higher of which is too extreme and thus infeasible. By gradually converging, the lowest bound for the given domain, mesh, constraints and objective can be determined. Regrettably, using this method will require 10s of different computational runs are required wasting considerable time and CPU resource. It was determined that a much a much faster means of attaining this approximately mass target (volume Fraction (VF)) is to first run a minimum mass objective optimization with heavy dimensional and frequency constraints upon the problem. The result obtained determines the approximate structural potential for any component using only a single optimization run, but does not provide a convincing structural layout (it lacks robustness, see Figure 70) and thus should normally be used for guidance only.

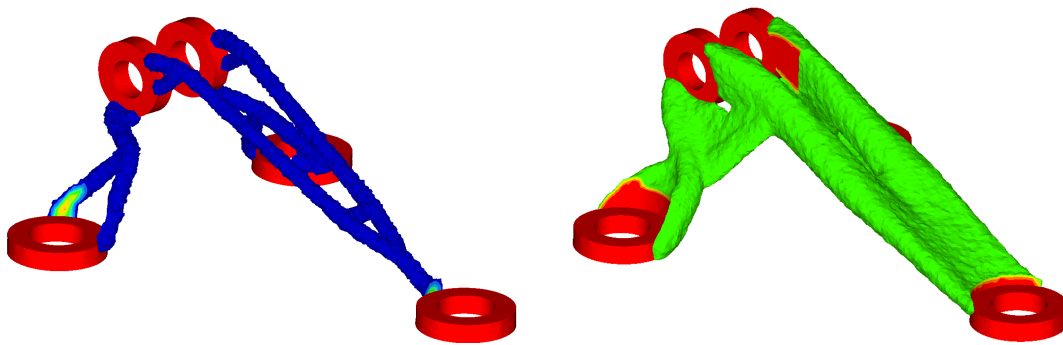


Figure 70 - Typical results from a Mass Objective optimization problem (left) vs Compliance (right).

5.3.3.2 Reduction of Computational and Engineer Time from Implementation of the duo Optimization Approach.

Using the above described approach for optimization, a series of trial studies were undertaken on parts external to this investigation, but similar in application, design and topology objective (Figure 71). The results of the investigations show the effectiveness of the approach in reducing the total number of iterations and the rapidity of solution of those optimizations even without the iterative grid refinement techniques discussed in section 4.5.



Figure 71 - Graph showing the total time required to reach optimal mass fraction using conventional methods and duo approach

5.3.4 Interrogation and Initial Extraction of Concept Design

Assuming the optimization has converged on a solution, a check must be made to ensure that the resulting structural performance is within the acceptable bounds of the customer requirements and/or the ancestor part from which the new topology is derived. To do this, the final optimization result is viewed within Hyperview and the maps related to stress and distortion are visualized and compared to the original part. After a visual inspection of the results to determine suitability of the design output, design extraction can begin. With a new pre-defined method for grid generation and a means by which the optimization constraints and design space separation are harmonized from the mapped manual process, the resulting outputs are unsurprisingly similar now that the variation in input methodology has been reduced, but even with refined grid parameters and optimization controls, a number of elements with partial density still persist. These elements of partial density usually occur on the boundary of the resulting topology, and their effects on that topology are dependent on a combination of grid density and optimization convergence. Regardless, the new TO layout will have some (no matter how small) variation in topology at the boundary dependent on user selection of the partial density visualisation from the available results. As a final step toward robustness and noting the effects of partial density on TO layout (Figure 72) a visualisation showing only elements with density greater than 70% has been selected as the default choice for the layout extraction based largely upon an examination of the candidate parts and their resulting layouts. This value has been selected as the default

value based upon the significant improvement in result clarity/definition through use of the Mapped Manual Process.

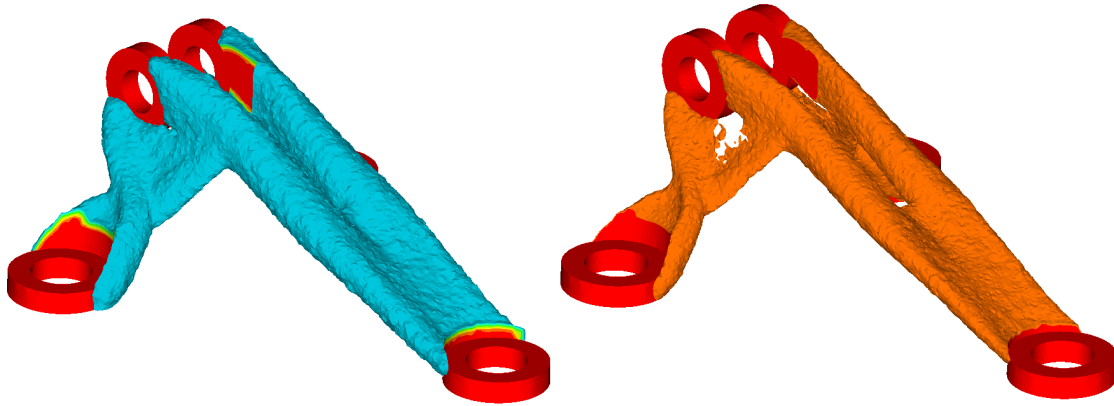


Figure 72 - Variation in topology through modification of density parameters – 40%+ density shown in blue (left) and 70%+ density shown in orange (right).

At 80-90% the resulting visual is heavily tessellated and hard to interpret, whilst the result at 70% is largely similar in refinement to the Hyperworks default of 50%, but with more material. 70% presents a minimal mass, high quality solution to the engineer from which to start his design extraction.

5.3.5 Design Extraction Methodology

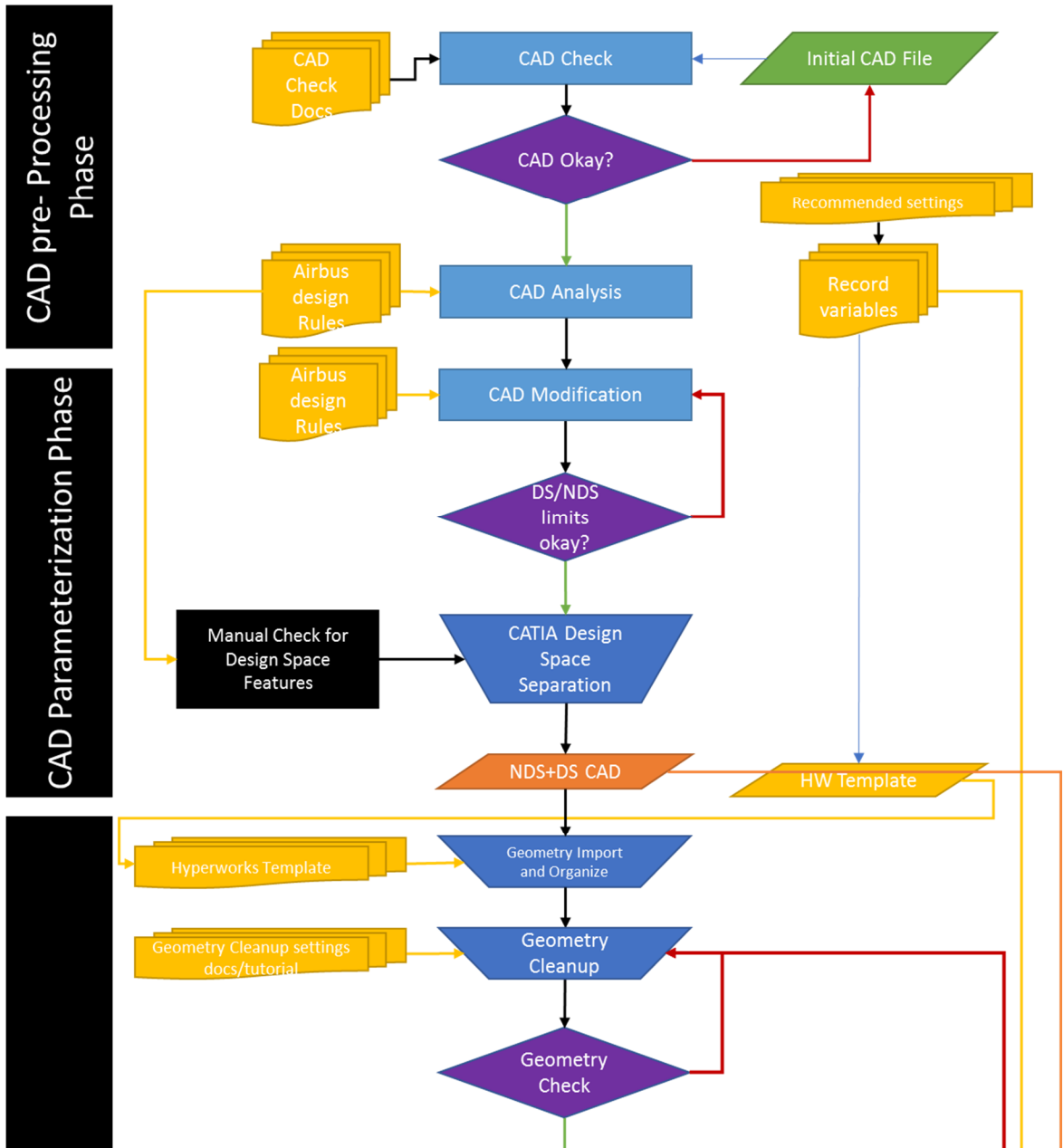
In order to maintain conformance with Airbus standards and systems, it was decided that any new designs achieved through the use of optimization driven design approaches, should be treated as concept designs and recreated using conventional tools such as CATIA. As such Detailed design were accomplished in CATIA V5 R21 (Airbus standard) and thus requires a means of translating/transferring the output from TO (Altair) into the Detailed Design environment (CATIA). STL is the standard method of output from either Hyperview or Hyperworks. Problematically, CATIA is not equipped for the manipulation of STL files and can only view them as dumb components of product assemblies. This means that the STL cannot be manipulated only viewed and thus limits its usefulness to that of a guide to final design extraction. To achieve this guide, a further template file (a CatProduct) has been developed as part of this research which incorporates both the output STL and the Ancestor design part along with a new, blank part in which a series of geometric collectors have been pre-created in order to aid rapid extraction. When the TO output STL has been created, one need only open the template file and append the new file locations for the ancestor part and its TO STL output.

5.4 The Development of Mapped Manual Process for the Application of Topology Optimization

Bringing together the detailed process mapping and the completed series of inputs, outputs and explanatory steps, the developed MMP is shown in Figure 73. It is this exact process which Airbus design staff will follow when attempting topology optimized designs for derivative products.

The developed process shows each step of the optimization process, what the required user inputs are and what the typical outputs should be. Each phase in a blue rectangle demonstrates an initial CAD phase common to airbus CAD operators. Each phase in a blue wedge represents a manual task required to move the process to the next step. For each of these phases, there is supporting documentation (yellow data inputs) which provides commentary as to why certain values and features are selected in each phase. Finally, purple rectangles are decision gates at which the engineers should pause and assess the output of the previous phase, only proceeding to the next phase when confident that settings and outputs are satisfactory. Red rectangles are the terminators of the process.

Mapped Manual Process for Topology Optimization



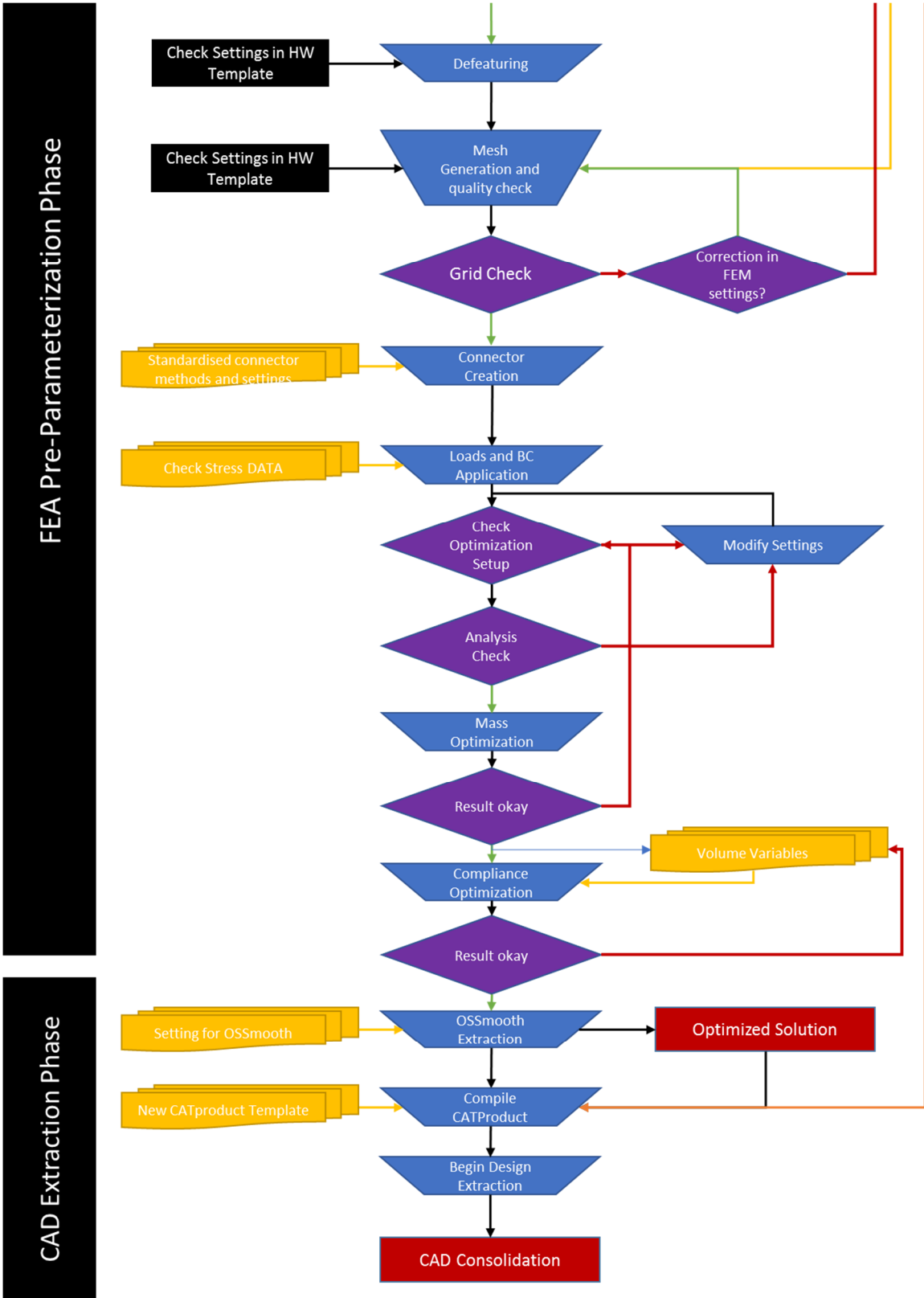


Figure 73 - Flow process for the MMP

5.5 Methodology for Testing the Effectiveness of the Mapped Manual Process

In order to determine the effectiveness of the MMP in both reducing NRC from design time and increasing processes robustness and repeatability between operators, a series of investigations were undertaken. Using the same candidate pool of Optistruct operators as was originally used to capture data pertaining to time consumed during optimization (section 3.3.1), the effectiveness of the MMP in these regards were tested. Each participant was again asked to undertake the optimization of one or more of the candidate parts, this time using the MMP and its inputs in place of their usual, experience derived methods for the application of TO. Whilst the same pool of candidates was used to test the MMP as was used in Section 3.3.1, care was taken to ensure that no operator was tasked with the optimization of the same geometry as previously optimized, so as to remove the possibility of familiarity.

5.6 Results of Using the Mapped Manual Process

The results of the analysis, overlaid against the original result of the investigation can be seen in Figure 74 and Figure 75. Figure 74 shows the results of both the original optimization tasks performed by the airbus operators and the repeat tasks performed by same operator pool, but using a standardised process and toolset.

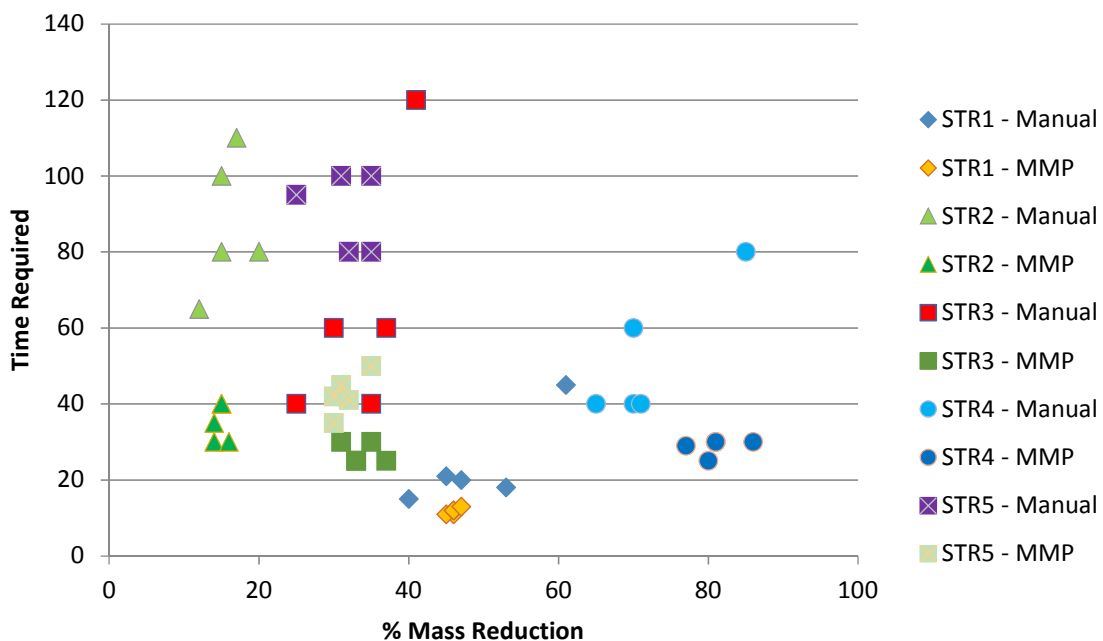


Figure 74 - Results of using the MMP when compared to the original approach

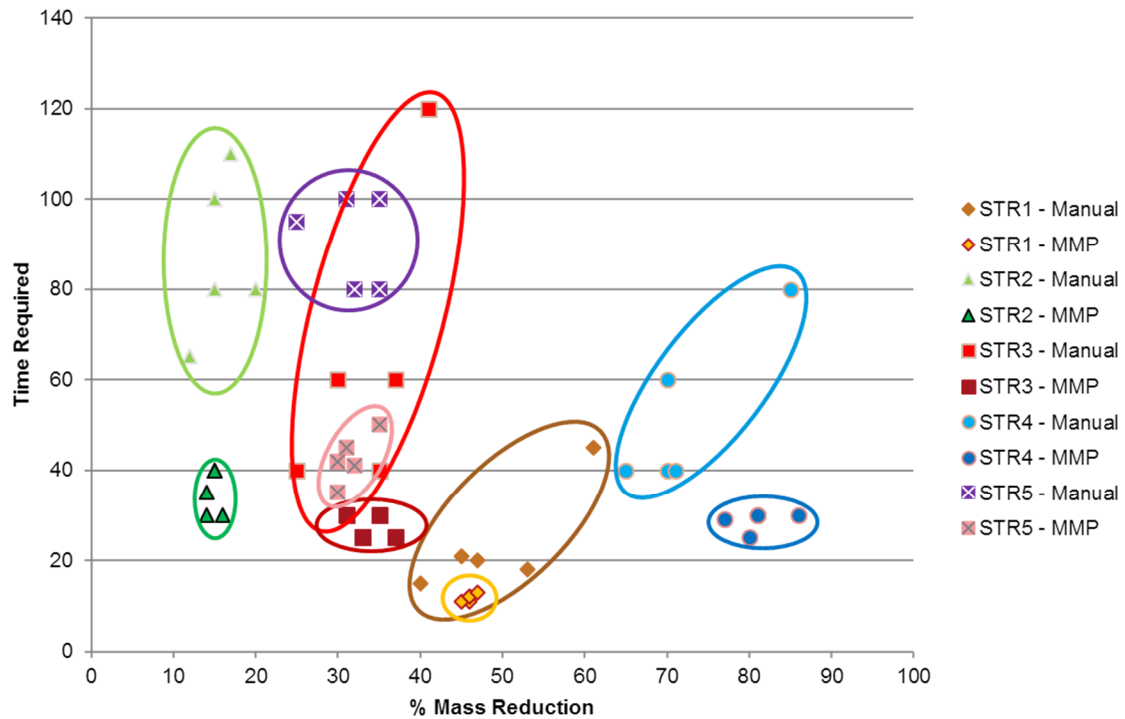


Figure 75 - Comparison of the variation between operators before and after implementation of the MMP

Table 16 - Showing the average mass reduction and stress value for each structure optimized manually and using the MMP

	STR1	STR2	STR3	STR4	STR5
Average Mass (kg)	0.135	1.312	0.651	0.652	0.967
Average Stress (MPa)	565	731	336	610	365
MMP Average Mass (kg)	0.135	1.356	0.601	0.45	0.979
MMP Average Stress (MPa)	501	605	351	752	365

5.7 Discussion of Results for the Mapped Manual Process

When clustered as in Figure 75, the results show the dramatic difference made by use of the Mapped Manual Process. For each structure (STR4 in blue for example) the data points are much more tightly clustered demonstrating a much more robust process with high levels of accuracy even when using a candidate pool of operators with wildly vary skill levels.

The effects of the Mapped Manual Process on process robustness and repeatability are clear to see, with each component, regardless of the individual performing the operation yielding a similar result to others charged with an identical optimization task. For each component optimized by each of the four participants (20 in total), the grouping for time vs mass saved are incredibly tight when compared to their previous results on similar tasks which're widely spread and highly varied for both mass and time. What is also evident from the application of the MMP

is its effects on those with extreme skill with TO processes. By forcing their adherence to a standardised process, their insight into specific parameterization and optimization strategies which may work well for a given design are lost, along with significant savings. Conversely, the Mapped Manual Process also improves those operators with less skill or that use more time during parameterization, bringing them up to an above average level of capability.

The results in Table 16 show that on average, mass reduction is either maintained or further reduced through use of the MMP, but an average value does reduce the effects of extraordinary performance in the results of STR1 and STR4. The results also show that on highly constrained parts such the manifold candidate (STR5), that due to the fact that the internal architecture cannot be varied, and that the principal stress is carried on these surfaces in the form of fatigue load, that the stress remains constant. Displacement values are not recorded as they are used as constraint values during the initial analysis of the component prior to optimization and material change. It is interesting to note that STR3 and STR5, both of which are sized by fatigue loading demonstrate little or no delta between stress values through use of the MMP.

5.8 Conclusions of the use of the Mapped Manual Process

Ultimately the Mapped Manual Process is an incredibly capable process for the removal of variation and increase in harmonization of the TO process whose drawbacks are more than outweighed by its benefits. The process sacrifices the upper 20% of potential weight savings by bringing the remaining 80% into a tightly controlled, easily repeatable process. Furthermore, the Mapped Manual Process can be applied easily by any engineer who has undergone the basic Airbus Hyperworks training course, allowing a vast increase in the potential list of operators, without an associated increase in variability through use of the process.

The Mapped Manual Process developed exclusively in this research was issued as an Airbus Approved Instruction Set under DOC REF 67894583 in December 15 and is in use by numerous Airbus staff and interns up until January 2017.

5.9 Application of Automation to Mapped Manual Process

Whilst the primary goal of the Mapped Manual Process was to terminate and complete the project in such a way as to be of use to Airbus, and was not specifically targeted to improving individual productivity, it seemed wasteful to not attempt to integrate the developed means of process automation and test their effectiveness against the newly established baseline. At this point, none of the automation code developed as part of this research project was linked or integrated either as a complete package or in terms of harmonised inputs, it was merely individual programs which could be potentially applied to sections of the MMP where deemed

appropriate. The advantage of the new Mapped Manual Process to the developed code was in the standardisation of inputs, outputs and requirements.

Five process automation phases were believed suitable for application to the MMP – These were: 1.) Feature Recognition, 2.) CAD Preparation, 3.) Design Space Separation, 4.) FEM generation and 5.) Load Perturbation. In each of these phases, the automation code was adapted and targeted, not just to the appropriate phase of the MMP, but also to the required process inputs for the next stage.

5.9.1 Feature Recognition and CAD Parameterization Automation in the Mapped Manual Process

In order to match the newly refined criteria of the Mapped Manual Process, the Python script for the analysis and modification of STEP files (CAD) was amended to allow for the recognition of bolt and mounting hole features with the specific details required to separate the design space. The scripts capability was increased to allow for the subsequent creation of adjacent features using lookup tables from the ADR. This was done by applying an additional circle creation code line into the feature recognition script. The code line will create an additional circle on the planar face where the bolt hole was recognised. The radius of this circle is 1x the diameter of the hole being recognised in accordance with airbus design rules for titanium components. Subsequent to this, a drafted surface using the vector of the surface normal on which the circle was created was swept. This swept surface would be used later as a separation surface in the separation of DS and NDS zones within the domain. These created sub-features were appended to the STEP file and when imported alongside their sister CAD, could be readily used in within Hyperworks for rapid design space separation using the modification tools of the software. Whilst not completely (end to end) automated, It was believed that by using this approach, hundreds of individual operations, usually required within Hyperworks for the separation of geometry/design space could be saved.

5.9.2 CAD De-Featuring in Preparation for Meshing

Utilising the tools developed in section 4.1.4, the Hyperworks template is updated with control features based on an analysis of the CAD data using the wall thickness analysis tool. Once the associated and analysed CAD has been imported into the template, and once design space separation has been completed, the operator can run the defeaturing tool with only 4 mouse clicks using the in-built features for geometry de-featuring within Hyperworks. All settings will be pre-adjusted and bespoke to the CAD being evaluated. The before and after shots of this phase can be seen in Figure 76.

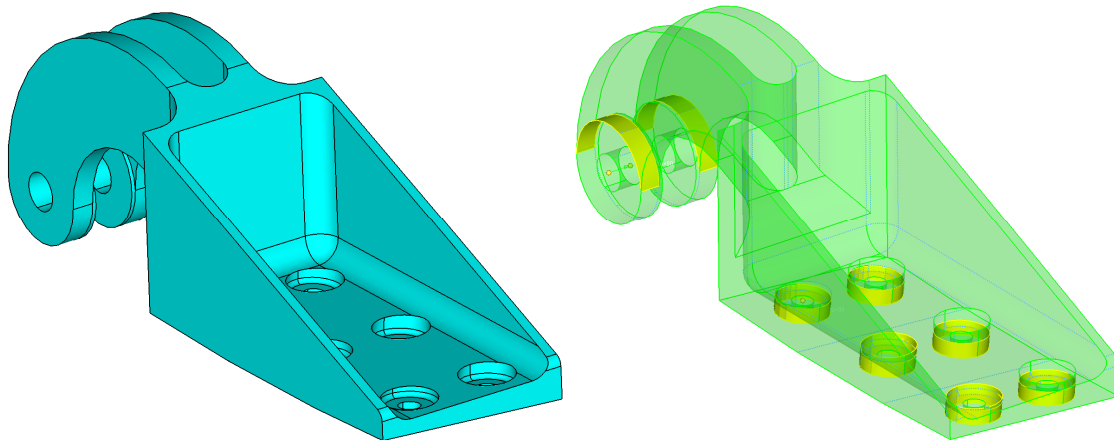


Figure 76 - Showing the before (left) and after (right) depiction of the automated defeaturing process on STR3.

5.9.3 Grid Generation for Analysis and Optimization

As previously discussed, the possibility of automated, iterative grid refinement proved too difficult to easily accomplish within the bounds of this research, but the application of automated meshing to the MMP using some of the developed techniques was deemed to be at least plausible. Again, using the minimum wall thickness determined earlier, the global element size was defined in accordance with the results. Subsequently, proximity and refinement, specified at angles greater than 35deg with element minimisation equal to 20% of the global size were applied to the template and grid generation was initiated. The grid then went through several stages of refinements and correction in order to ensure a high-quality index for the Tet10 Grid. Initially it was envisioned that the grid would be generated in accordance with the design space to which it was assigned in the Hyperworks Design Tree. Unfortunately, in both Hyperworks11 and Hyperworks12, technical glitches when generating grids in different collectors, in neighbouring zones persist, causing errors and system crashes. As such, the entire grid is created within the DS and elements created in CAD bodies of the NDS are moved after creation to enable easier optimization at a later date. The organisation of the elements makes no difference to their numbering or to their connectivity and from an analysis point of view, the presence in a different collector is irrelevant to the solution. Regardless of the wall thickness, the total maximum grid size is capped at 10m elements in order to allow for a relatively rapid solution on a single node of the GISEH computing cluster at Airbus UK. When tested on the candidate parts, none of the parts exceed this limit, but when examined on a large manifold candidate part, the predicted element count stopped the automated mesher due to the total number of cells being greater than 10m (16.8m). At this juncture, the automation loop would end asking for user intervention. Notably, even though an Expanded Design Space presents a significantly larger domain which must be filled with elements, its removal of many thin walled elements from the ancestor part

reduces the number of smaller elements required to represent them, thus stabilising the element count.

5.9.4 Load Application and Perturbation

For the majority of components, sizing and shaping of the part are performed using basic CAD coupled to hand calculations with significant reserve to ensure conformance. As such, the part design brief or stress documents rarely defines (by co-ordinates) the direct interaction of loads with the structure/CAD. As a result, there is no easily ascribable relationship between the part and its loads to which an automated process could be applied which might improve the speed of application of this step. It is only when considering the application perturbation to the loads that automation can be considered to be a potential time saver to the process. The perturbation is applied not to the Hyperworks file directly, but as an appendment to the FEM between the point of Hyperworks export and Optistruct solve. The user has no visual clue as to their application without a direct interrogation of the FEM deck prior to solve.

5.9.5 Summary of Automation for the Mapped Manual Process

The resulting automation phases of the Mapped Manual Process alter the earlier defined flow-process Figure 73 in the manner shown in Figure 77. Each of the automation aspects (new blue rectangles automated by green input scripts) must be ran individually using a python command line (under Python 3.6) with their specific instructions detailed directly within the Mapped Manual Process. A commentary on their application and use is covered in the user guide for the Mapped Manual Process under DOC REF 67894587. Of the stages automated in the process, it is the stages concerning geometry modification and grid preparation that yield the greatest time saved, and thus the greatest predicted NRC saving through use the Mapped Manual Process.

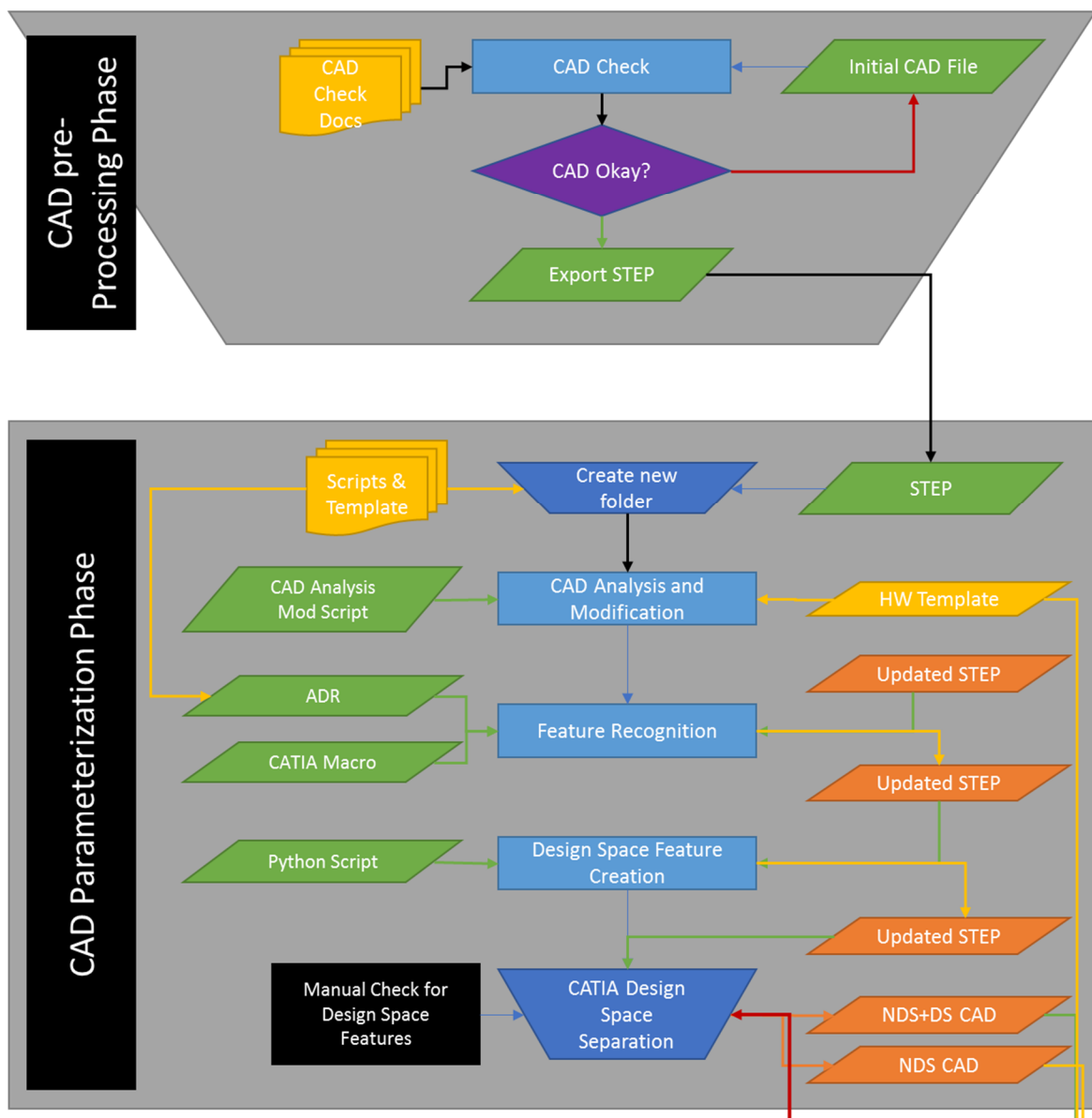
5.10 Methodology for Testing of the Semi-Automated Mapped Manual Process

As the automation of the MMP was not an Airbus requirement at this point, it was not supported and so could not be tested using the full candidate pool as in sections 3.3.1 and 5.3. Instead, and as STR1 and STR3 were previously optimised by myself, it was deemed appropriate to repeat the same optimisation using the semi-automated MMP as a baseline results were available to compare to. As such STR1 and STR3 were again optimised, this time using both the MMP and the scripts and codes required to automate each section in the parameterization phase. The time required to perform each section was then recorded and compared to the original data from section 3.3.1.

5.11 Results of Automation Implementation

Whilst not a direct requirement, the unautomated Mapped Manual Process did speed the process of optimization driven redesign for small metallic components. Problematically, a comparison between the unautomated MMP and the base process (in terms of time required for redesign using the Mapped Manual Process) was never undertaken. This was due to the limited time and budget available in the closing stages of the project and that the task would've required an additional ~800 work hours from Airbus staff (20 operators at 40 hours per person) equivalent to ~€85k. Thus, the application of automation to the Mapped Manual Process could only be graded against the original, totally manual, non-templatised variant of the process.

Semi-Automated Mapped Manual Process for Topology Optimization



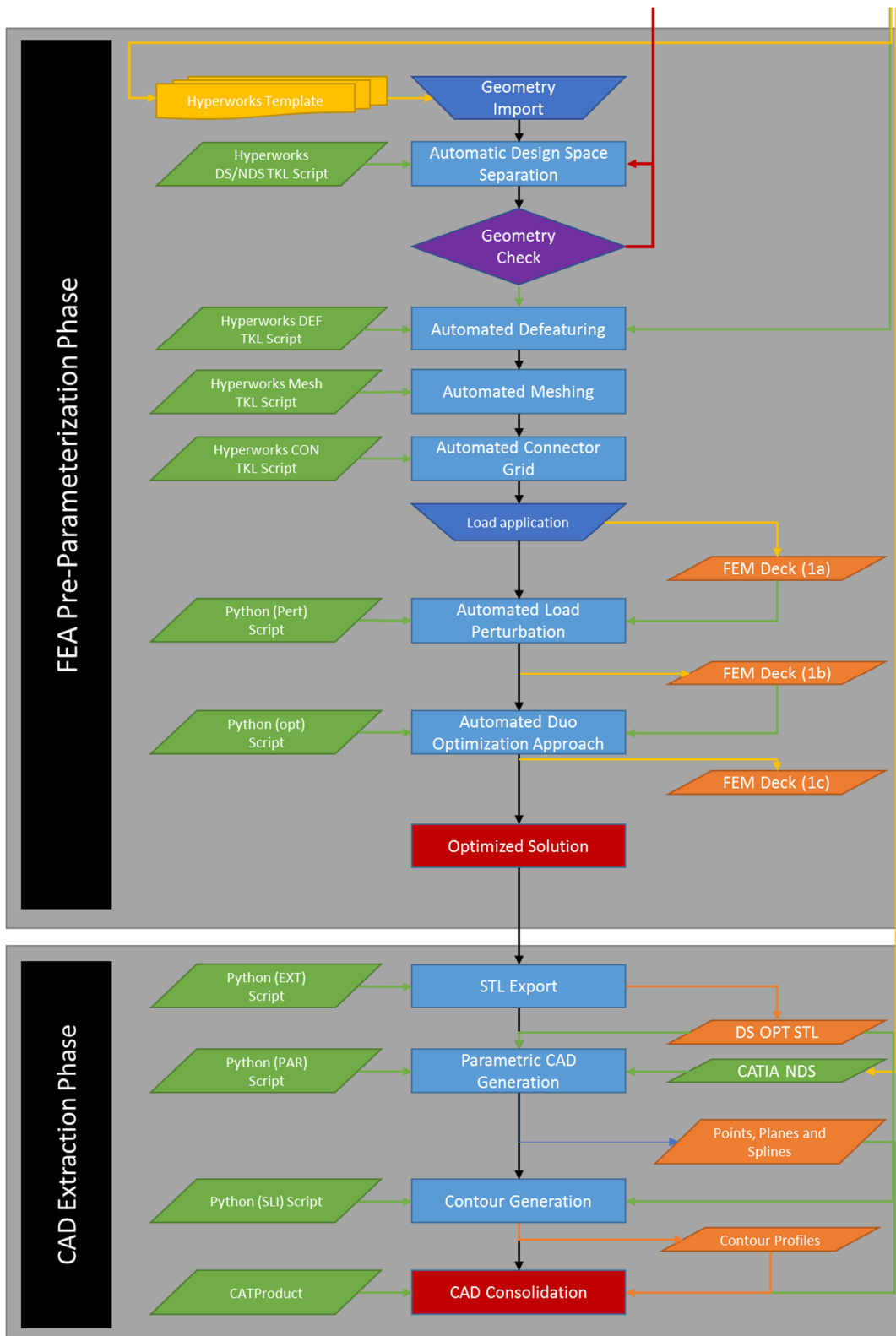


Figure 77 - Proposed design process after MMP and automation

When graphically compared (Figure 78) it can be clearly seen that significant time savings have been achieved through the application of the MMP and its stages of automation.

Furthermore It is known that from previous analysis, the MMP acts to deliver significant increases in process robustness and repeatability between operators (Section 0) and that the implementation of the MMP opens the use of optimization for concept design generation to a wider pool of potential candidate users within the Airbus community.

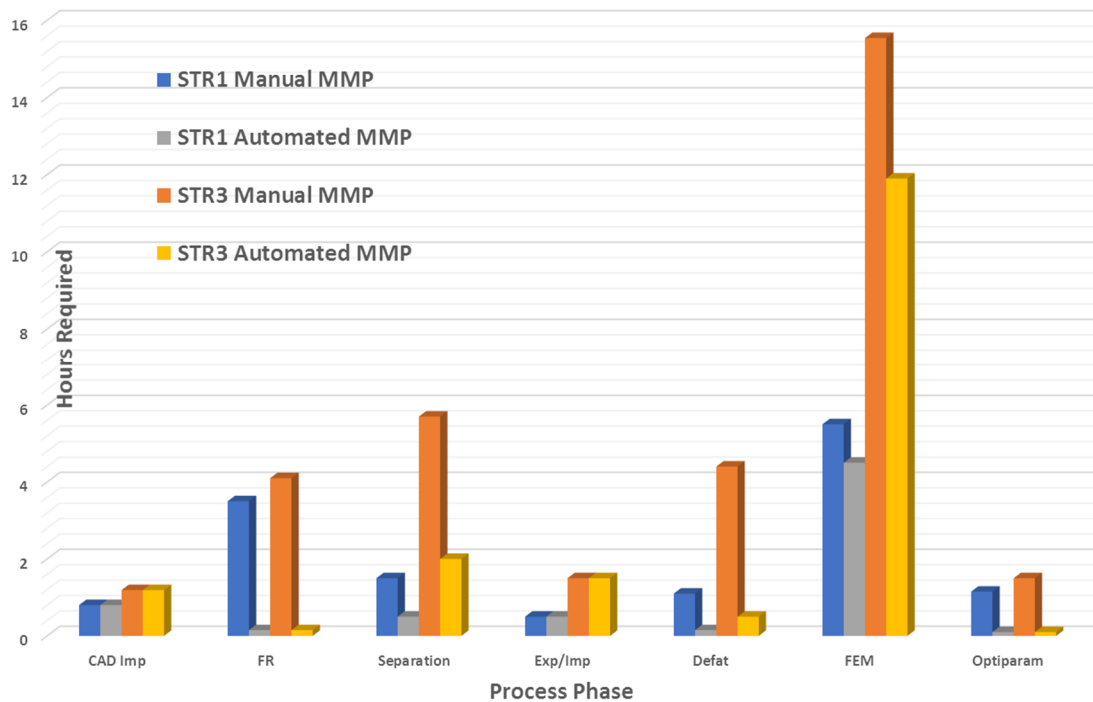


Figure 78 - Effectiveness of the partially automated Mapped Manual Process at reducing the required time for design optimization

From the original process as depicted in section 3.2.2, the average time required for the optimization of each of the components is shown in Figure 75. Using the partially automated MMP process and again optimising each component in turn, the time required to optimized each of the components up to the point of design extraction is shown is dramatically reduced. When graphically compared (Figure 78) it can be clearly seen that significant time savings have been achieved through the application of the MMP and its stages of automation. Furthermore It is known that from previous analysis, the MMP acts to deliver significant increases in process robustness and repeatability between operators (Figure 75) and that the implementation of the MMP opens the use of optimization for concept design generation to a wider pool of potential candidate users within the Airbus community.

5.12 Summary of The Effects of the Combined Automated Processes on the Time Required for Topology Optimization

Due to an internal Airbus reorganisation and refocussing on cost improvements, the project was deemed to be superfluous and future developments and funding terminated. Airbus requested

that the project be tied off, demonstrating what was accomplished and how it could be employed. A combination of a mapped, fully defined process for TO and the implementation of the developed automation for pre-processing and analysis was coupled. This was done in order to provide Airbus with a means of utilising the research in the short term to achieve their current strategic goals (Objectives 3 and 5). The effectiveness of the MMP and its associated automation was demonstrated using the same candidate pool originally used to determine targets for automation with dramatic effect (Objective 9). The process and programs demonstrate substantial savings and the capability for de-skilling the analysis and optimization process for small parts intended to be made using AM. As the software only targets the pre-processing phases, substantial quantities of skilled analysis, Methods and Process department and Design specialists are still required to perform the end-end part.

6 Automation of Parametric Design Extraction

Design extraction and its automation is possibly the most complex task within this research and has seemingly never been successfully accomplished in either research or commercial software. Going one step further, the research detailed in the following sections attempts not only to address this problem but to do so in a manner that allows for direct, parametric linking of the optimisation process to the design CAD.

6.1 Introduction to Design Extraction

The problems concerning the redesign for manufacture of topologically optimised components is well documented in literature (Muir, 2015, Gilbert et al., 2014) and has been explained in some depth in section 2.5. The noted and substantial dissatisfaction of TO users in undertaking this section of the optimization, with most describing it as one of their most onerous tasks. Section 2.6.4 noted the developments of several software vendors attempts aimed at addressing this particular aspect by use of both a single software environment and a simplified method of extraction using T-splines.

Problematically, these novel software packages are aimed toward enablement of designers through reduction of the expert process of design optimization (Orme et al., 2017). Whilst a laudable goal, this approach has been deemed by Airbus to be a precursor to detailed design (Section 2.6.4) and thus does not directly address the aim and objectives of this project (section 1.3). Again, the problem lies in the NRC associated with component redesign of existing aircraft structures and components. Currently, the process for component redesign looks like that shown in Figure 79. The new 3DX tools developed for Airbus by Dassault Systems will look like Figure 80 but will be targeted for the development of new component concepts, not for redesign. In both processes, the point at which analysis completes and design extraction begins represent a split in the digital chain. Up to this point, FE has been applied directly to the CAD and loads to the FE, thus creating a link. At the extraction point, the only link between the analysis and the new design is visual and thus at the discretion of the user performing the extraction. The developed process specifically targets and automates the final stages identified in section 3.6, and does so using parametric CAD linked to the FEA using node numbering. By creating a link between FEA and CAD, any subsequent minor modifications can be accomplished by shape optimisation in the FE and due to node linking, subsequently updates the CAD automatically. This linking coupled with pre-processing as automated in section 4, means that only the extraction task remains. When looking at both the original process and 3DX processes detailed in Figure 79 and Figure 80 respectively, it can be seen that the loop created between validation and optimization, a loop required in order to give a conformal part design, can still be potentially costly in terms of

time required. The principal reason for this cost stems from the iterative nature in which final, detailed/critical designs attain their status within Airbus and the larger aviation industry. The reason for this stems from two areas, one historic and the other systematic. The former is rooted in the specialized nature of roles within the industry, in that parts are designed by a series of specialists each working on common parts, but in a serial approach. As such it is rare that total component requirements fully captured (or even known) at the start of the design cycle. The aircraft loads and attachments will, of course be well known, but the assembly order, machining preparations, additional

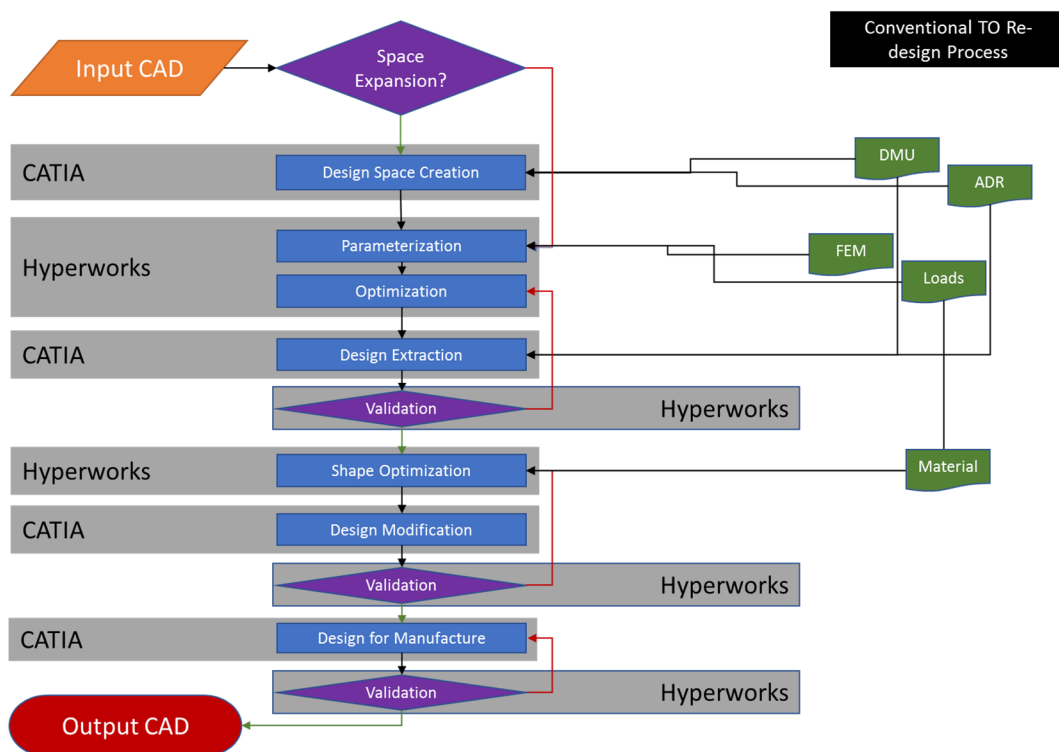


Figure 79 - Current Design Process in Airbus showing manual tasks (blue) validation phases (purple) input documents (green)

DFM and MRO requirements are often added later and thus, at each stage, the part changes, meaning the original design validation may now be invalid. If it is, this then places the design back with the stress authority who will analyse and request changes from the design authority. The cycle thus repeats, presenting the second, systematic problem. And so, unless the former (requirements) can be fully captured and parameterized at the start, the latter (systematic iteration) will continue. This process is one of the reasons why the new design and analysis tools have thus far been used only for AM concept generation. Whilst the desire to enact change on the Airbus process is powerful and would have the greatest effect, changing the direction of such a large body as Airbus is far outside the scope of this investigation. This leaves but one option,

the creation of a tool which makes the process of design iteration more fluidic, and perhaps more efficient

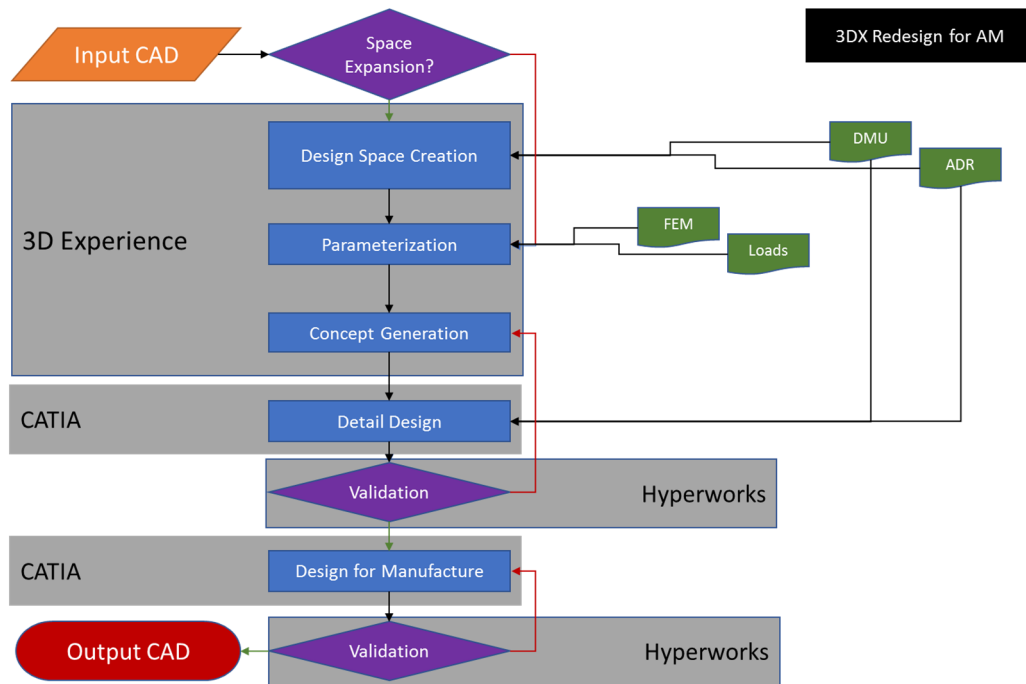


Figure 80 - New design process for AM concept generation showing how design space creation, parameterization and concept generation are now performed in a single software environment.

6.2 Establishment of Baseline Inputs and Benchmarks for Design Extraction

Before beginning any development work on automated extraction techniques, it was important to establish a suitable baseline against which other techniques could be gauged. As such, a single candidate part (STR1) was selected from the pool of five (Section 3.2.3.1) for progression with the trials and establishment of a baseline analysis. First a suitable topology optimization was performed using the semi-automated MMP under a high mesh density of 5-7m elements. The resulting topology is shown in Figure 81 with the STL extraction shown in Figure 82 and the OSSmooth output shown in Figure 82. The resulting topology was extracted manually (Figure 84) and then validated against design loads (Figure 85) demonstrating a reserve factor of 1.5. These outputs formed the basis for all subsequent extraction trials and the base for the comparison of the developed techniques. The extraction process took almost 20 hours to complete.

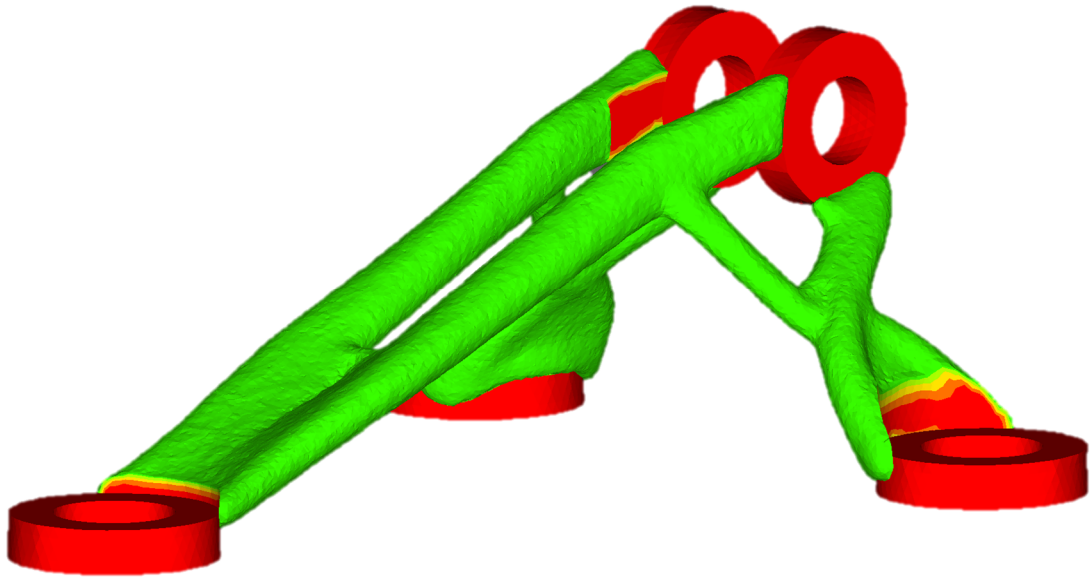


Figure 81 - Baseline topology output for extractions trials

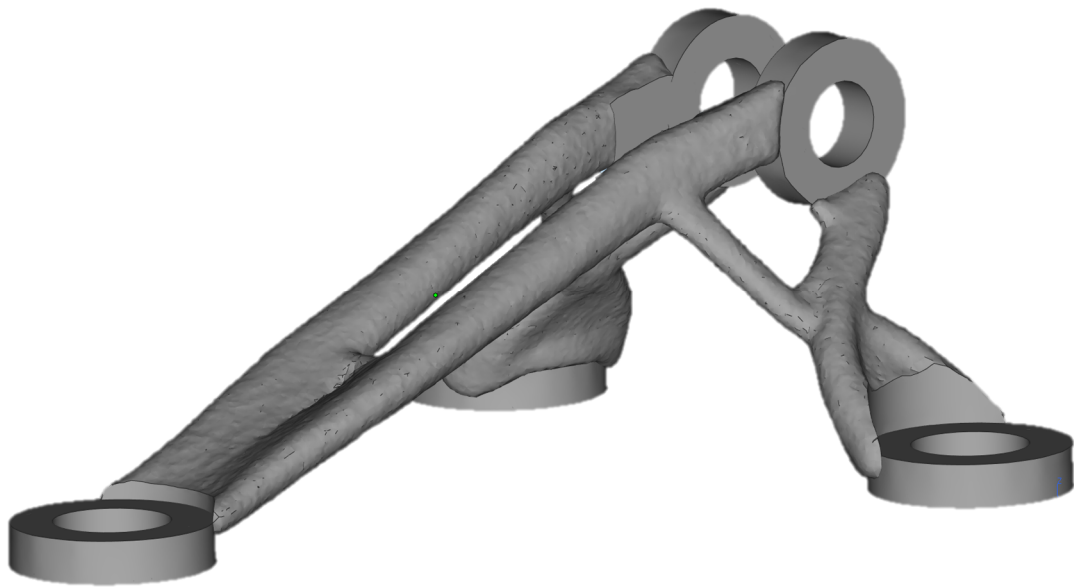


Figure 82 - Direct STL Output from the Optistruct via Hyperview

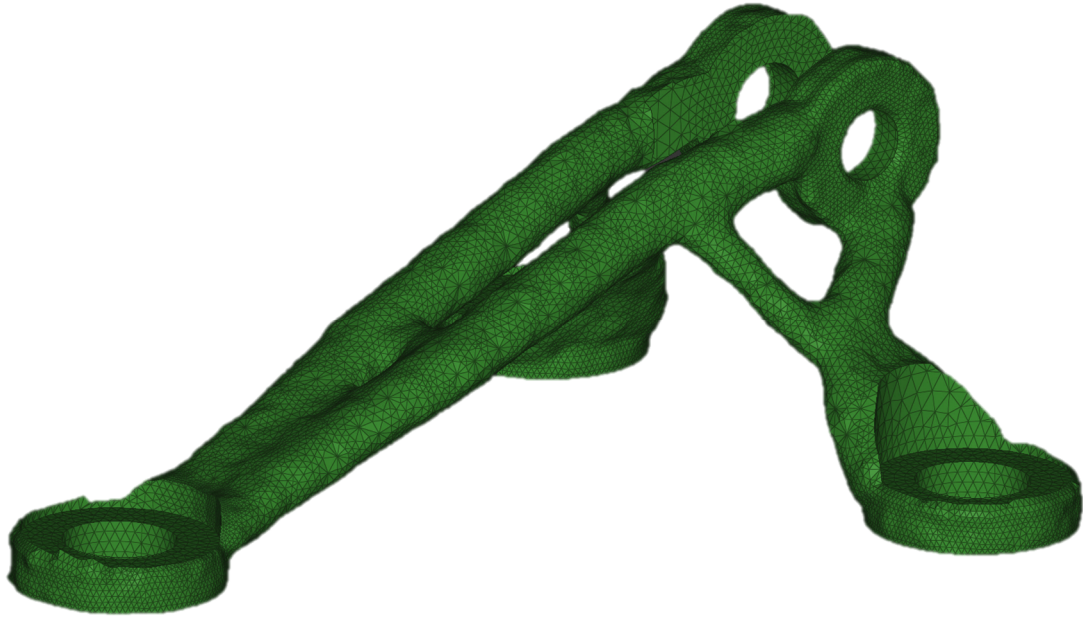


Figure 83 - STL output from Optistruct after completion of OSSmooth at fine limits.

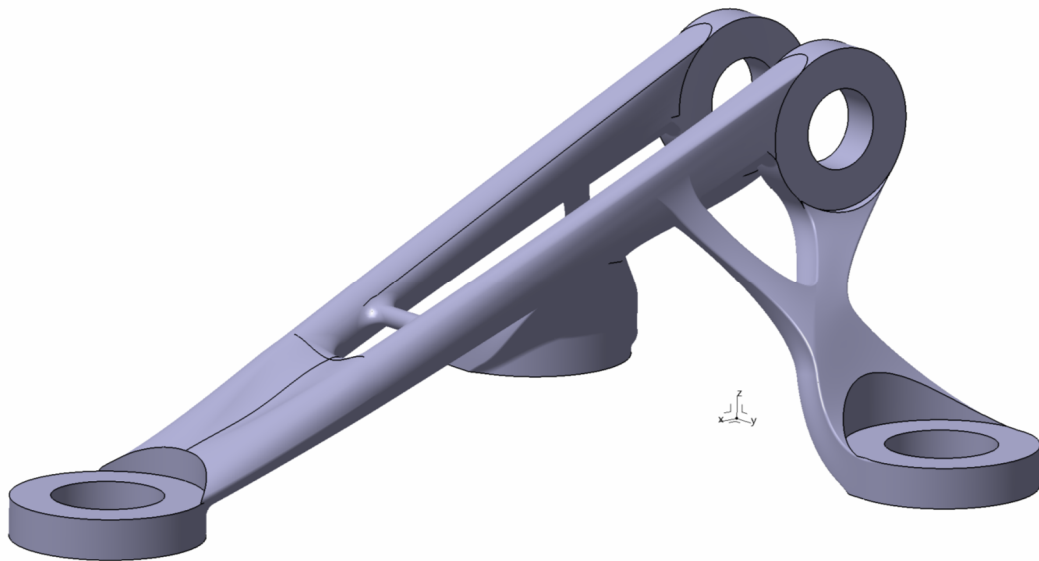


Figure 84 - design extraction from CATIA using advanced surfacing techniques

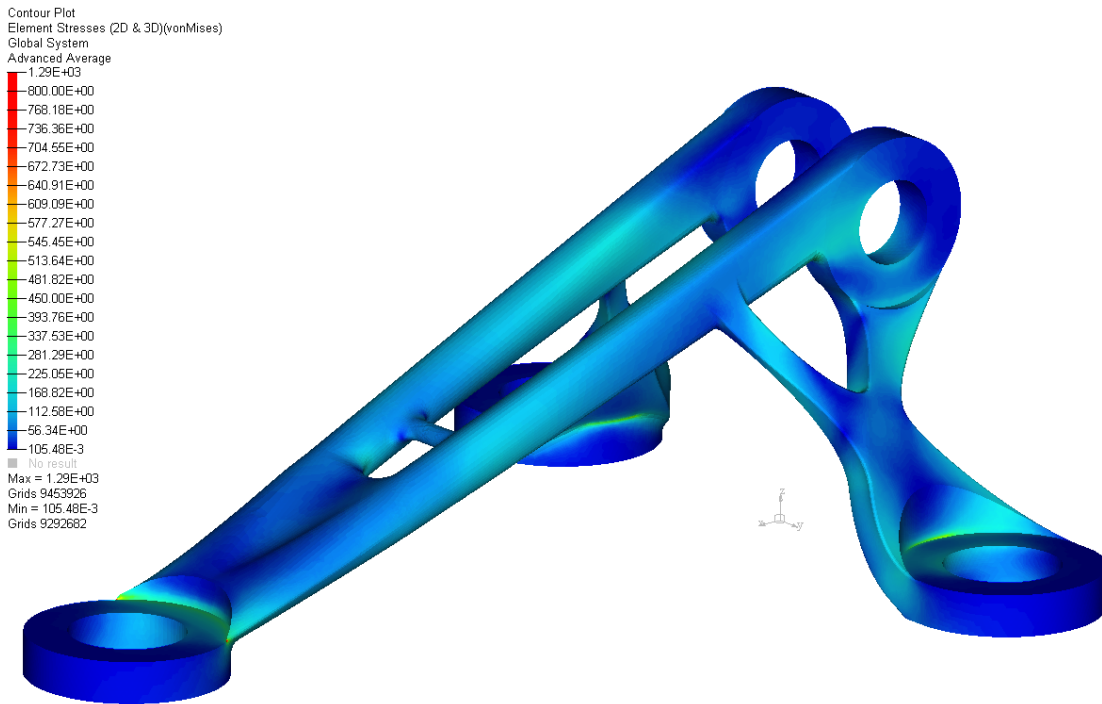


Figure 85 - Validation of final design showing a reserve factor >1.5

6.2.1 Baseline Results for Design Extraction

The majority of research in this chapter focuses initially on the most simple and smallest of the candidate parts – STR1 with additional activities tested on STR3. In determining the effectiveness of any developed means for enhanced design extraction, the baseline average extraction time and mass from the study in section 3.4 will be used. As such, the baseline mass for the optimised part is 135g and the time required for extraction based upon the research aim is ~8 hours.

6.3 Introduction to Attempted Methods of Design Extraction

During this section, four methods for expediting the design extraction of topology optimized components are attempted. In each, the aim is to reduce the time required to perform design extraction whilst maintaining compatibility with Airbus processes for design and analysis. The four methods attempted were:

1. Mesh Smoothing - Investigates the potential for the direct use of the output STL from Topology Optimization through various mesh smoothing techniques with the intention to produce and acceptable (to commercial aerospace) serial production parts with little to no user time for design re-creation after optimization.
2. Skeletal Modelling - Details efforts to advance methods of skeletal modelling (found in literature for 2d cases) into a more complex 3D environment and complex topology for rapid design re-creation.

3. Parametric CAD from FE - Borne out from the failures of the previous two attempts this approach was intended to provide a means by which design extraction can be parametrically accomplished within current toolsets to reduce time at the expense of completeness.
4. Skinned Point Cloud Method - Uses a combination of multi-axis AM slicing to determine smooth boundary profiles in the design space areas and reconstruct those smooth surfaces using CATIA's Quick Surface Reconstruction toolbox.

The aim in the development of these reconstruction methods is not to fully automate the design process, but to significantly reduce the engineering time required to extract complex designs from topology optimization solutions.

6.4 Mesh Smoothing for Design Extraction

6.4.1 Mesh Smoothing/Modification of the STL Output from Topology Optimization

From most commercial software it is known (and shown - Figure 82) that a direct export of the STL which defines the results of the TO is particularly coarse. Whilst such a design can be directly printed, it is highly unlikely that it ever would be. The highly tessellated surface would be likely to act as a crack initiator during operational loading for any serial production part, thus preventing its use in aerospace structures. However, many Rapid Prototyping (RP) applications often do not require the stringent operational and service requirements of production parts and so can tolerate the irregular (but softened) output of the smoothed/morphed STL so long as the production task is completed quickly. For RP activities, mesh smoothing (section 2.5.3.2) is perhaps the most widely used method of proceeding from TO designs to manufacture when using AM. There are several different techniques used to perform mesh smoothing on output STL (or any set of connected polygon) data (Belyaev and Ohtake, 2003, Wang et al., 2007a, Canann et al., 1993) and dependent upon their settings, can and have been used to great effect (Chen and Holst, 2010, Krishnamurthy and Levoy, 1996).

6.4.2 Methodology for the Testing of Mesh Smoothing Techniques for Extraction

The aim of the mesh smoothing task was to determine the base capabilities of mesh smoothing to create an acceptable design output in a cost/time effective manner. Rather than undertake an exhaustive search and test of mesh smoothing tools (there are literally hundreds of packages, both commercial and freeware in multiple different environments) the assessment was made using tools available and actively in use at Airbus Central Research in order to expedite the task. As such, three packages were assessed for capability: 1.) Geomagics, 2.) Materialise Magics/3Matics, and 3.) Altair Optistruct. None of these packages are specifically designed for

mesh smoothing, but do contain mesh smoothing tools in order to perform their primary functions of shape reconstruction, STL preparation (for printing) and optimised design validation respectively. In this phase, each package was given the same input STL (Figure 86) and allowed the same number of smoothing operations (up to 90) under similar settings.

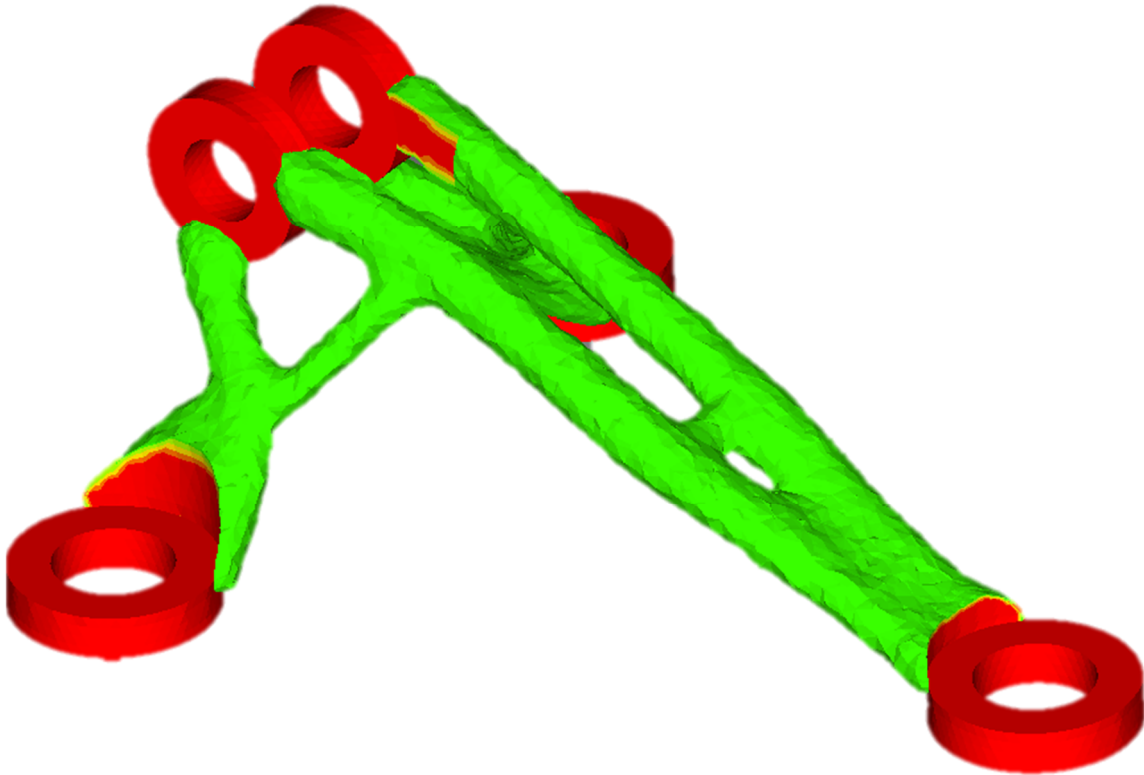


Figure 86 - Baseline topology output using the unperturbed result of STR1 at moderate mesh density

Initially, and in an attempt to address the primary objective, each package was employed, and where possible to determine, the type of smoothing algorithm was assessed, varied and cross compared. In order to assess the capabilities of mesh smoothing as a means of design extraction, several software packages were lightly assessed for their capabilities at both global and local levels looking to determine if such approaches could provide for a means of smooth CAD, which could be interacted with and interrogated using existing tools such as CATIA.

6.4.3 Inputs to Mesh Smoothing and Its Effects

In combination with the type of smoothing technique used, the success or failure of mesh smoothing is highly dependent upon the quality of the both the optimization setup and the density of the FEM grid upon which it is to be applied. In the case of the former, an example of insufficient definition can be seen in Figure 87.

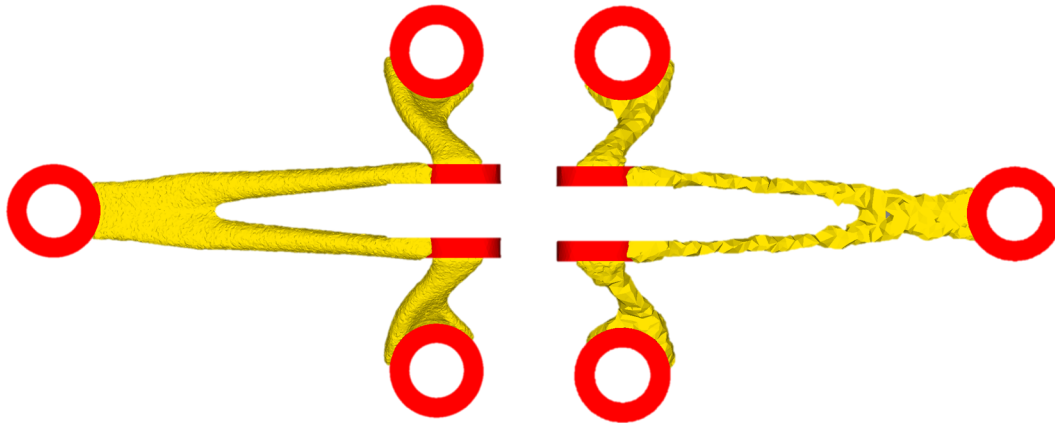


Figure 87 - Comparison of a well-defined optimization result (left) to a poorly defined one (right)

In this example, the optimization was defined without a minimum dimension parameter and so the resulting output is, in some locations, only 1-2 elements thick. As the grid is an unstructured tetrahedral mesh, the resulting structure is highly tessellated and only extremely aggressive smoothing techniques will have any effect on the output. In the case of the latter, a similar, highly tessellated result is seen on a TO result achieved using a coarse grid definition (Figure 88). In such a result, the optimiser will have achieved convergence using a high number of cells at partial densities. The effect of these partial densities are mainly encountered in the selection of an appropriate density threshold for design extraction. During this phase and in direct response to the coarse mesh, even small changes in density threshold result in dramatic changes to the topology due to removal of elements from the final representation. As each element is large, its removal (and prior to smoothing) results in a highly notched surface which is difficult to uniformly smooth without aggressive parameters which can have dramatic consequences to the resulting topology (Stanford, 2012).

The baseline TO STL output has a number of features which are important to the design (Figure 89) and have been specifically parameterized in order that they be retained during optimization. These design features must be similarly retained, unaltered, during the smoothing phase for later adaptation of the STL is commonly difficult to achieve. Once assessed, the secondary objective was to assess each packages capability for advanced reconstruction/reformulation of STL data using different smoothing techniques and methods (Mallenpre and Bergers, 2008).

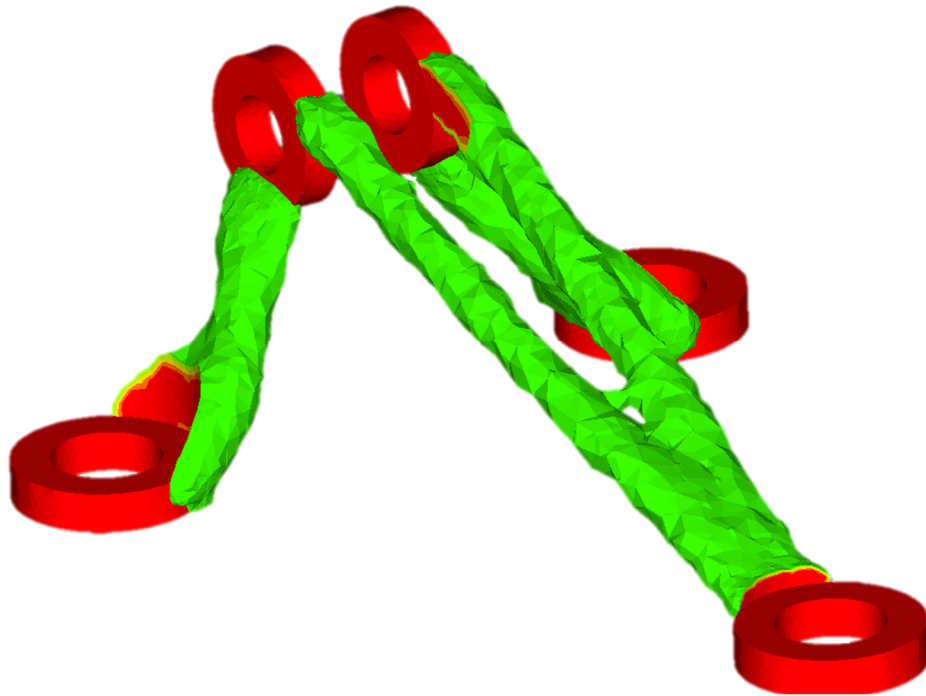


Figure 88 - A coarse grid definition has revealed a highly tessellated structure

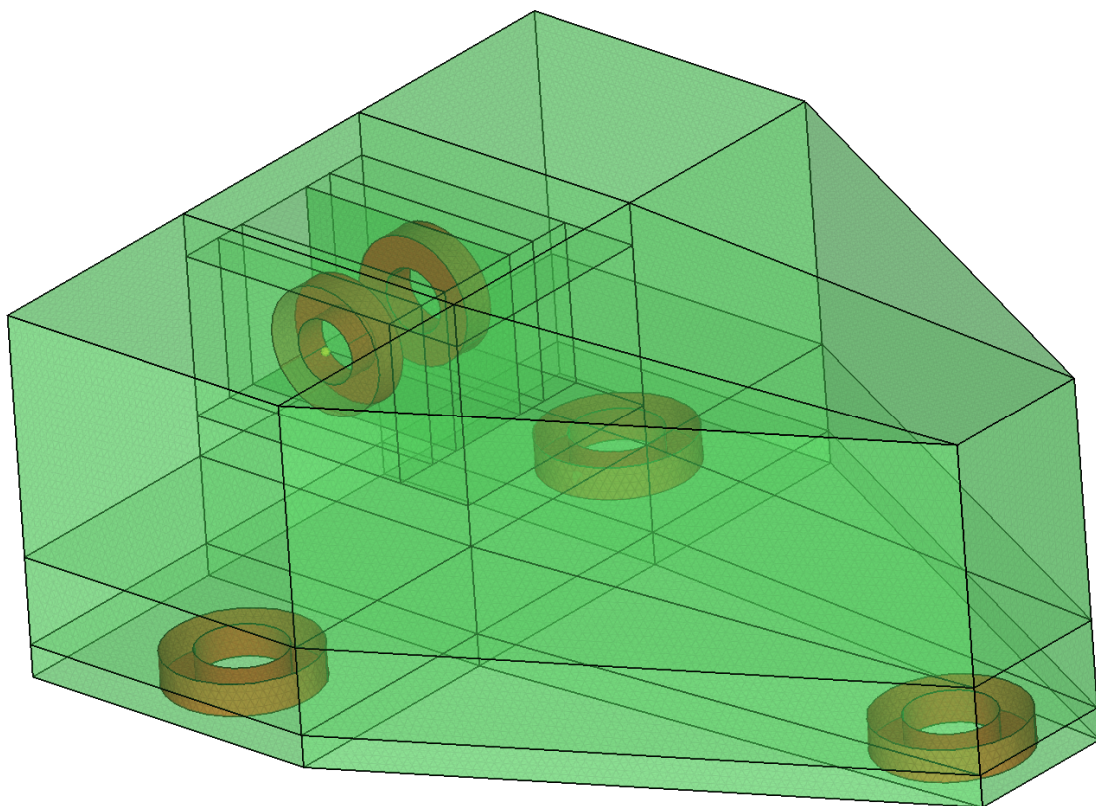


Figure 89 - Non-design space of STR1 indicating feature which must be preserved intact and in conformance with the Airbus Design Rules.

6.4.4 Investigation and results of Mesh Smoothing as an Approach to Design Extraction.

6.4.4.1 Geomagics Assessment

Geomagics (European Commission, 2013) is a software provided by 3DS and is primarily used in conjunction with a laser scanner (made by FARO) for metrology and reverse engineering. As such, the software is designed specifically for the removal of noise from scan data in order to allow for the efficient reconstruction (or alignment, depending upon whether metrology or reverse engineering is being performed) to allow for the efficient recognition and/or reconstruction of surface data from clouds of scan points. Whilst initially appearing dissimilar to requirements for STL smoothing, the software (unlike CATIA QSR) reconstructs its surfaces directly from the point data into series of connected triangles, thus making an STL.

The smoothing within the software is both powerful and highly adaptable and is designed specifically with the intention of STL manipulation ready for use in CAD assemblies or manufacturing. There are several smoothing algorithms available, but the default is based on an adapted form of Laplacian smoothing (Belyaev and Ohtake, 2003) designed to minimise the negative effects of shrinkage and detail loss. In use the software allows for tailoring of the aggression of smoothing along with control of the number of iterations and the means by which irregular detail is recognised by the smoother. Applied globally, the best response was found to be to use a single medium pass to remove the high spots and then several (10+ iterations of weak smoothing to remove the low spots and smooth the peaks. With the results shown in Figure 90.



Figure 90 - Results of best practice methods for mesh smoothing of STR2 within Geomagics.

Even so, the results are a long way from replicating the smooth surfaces of the advanced surfacing design extraction showcased in Figure 84 with significant pitting and protrusions still present. In addition, some loss of detail is incurred during smoothing even with careful experimentation and application. Indeed if more aggressive settings are used, the resulting damage to the STL can be significant, both in terms of detail loss and total volumetric area.

6.4.4.2 Materialise Magics/3-Matics Assessment

Magics by Materialise (Altair Engineering, 2017) is the primary AM pre-processor used for build setup by Airbus Central R&T. It is used primarily for STL repair, size reduction and support generation in preparation for the AM build. At the time of undertaking this research, Magics had within its structure, a useful set of tools for STL manipulation including advanced smoothing and surface reconstruction. Over time these functions have been gradually transitioned out of Magics and into the more expensive, optional tools contained within 3-matics (Siemens, 2012), but for the purposes of this investigation, they will be examined as part of the package known as Magics.

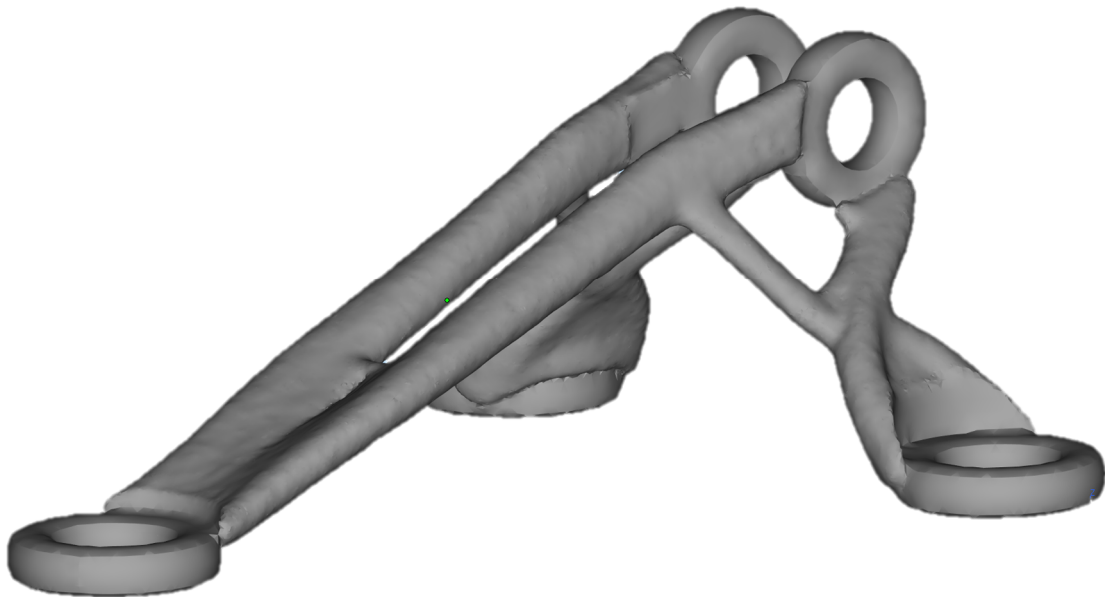


Figure 91 - Showing the significant loss of detail through use of aggressive smoothing techniques and poor application.

The primary function of smoothing within Magics is not for the purpose of extracting TO designs, but is instead like Geomagic, designed to repair/prepare SLT data for another function. Unlike Geomagic however whose primary purpose is to prepare point data for further CAD work, Magics is design to repair and prepare STL data from a variety of sources for manufacture via AM.

Like other packages, direct smoothing of the STL at a global level produces unsatisfactory results which are similar to the results seen in Figure 91. However, Magics has the ability to both locally smooth and to preserve geometric detail based upon angles of deviation between elements/triangles. The effect of these combined features is impressive and results in significant improvement in STL quality as shown in Figure 92. Sadly, whilst quite effective at smoothing areas in which the smoother has the ability to sample large number of similar surrounding cells in order to create a norm, the software and smoother struggles in both areas of convergence and highly complex areas. In these environments, the software tends to create deep pits in the STL in an attempt to satisfy several objectives from each converging member (Figure 93). Whilst the pits can be manually removed in the software, the triangle creation tool is painfully slow and relies heavily upon the surrounding grid. As such, it can be difficult to create smooth intersections.

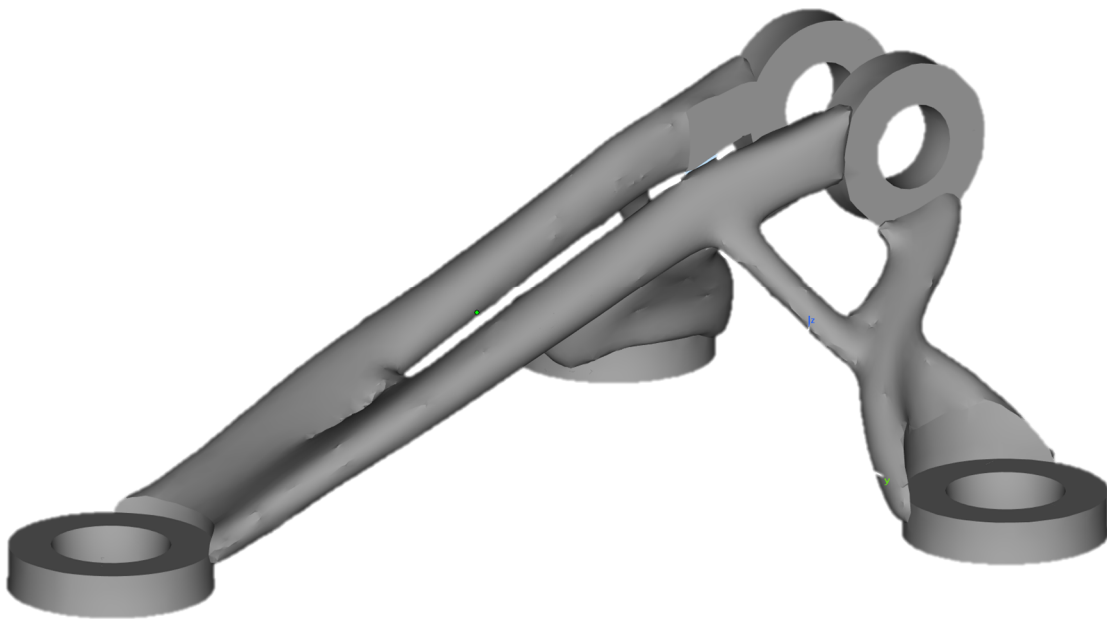


Figure 92 - Showing the effects of Magics local smoothing with combined feature preservation at bespoke settings

Regrettably, whilst Magics does provide for excellent smoothing and refinement and 3-matics provides (with the correct modules) for surface reconstruction using similar proximity averaging to that described earlier, the problems at intersections and in areas where non-design space and design space meet, cannot be easily addressed within the software. In these areas a blend or fillet would be carefully applied to control stress. This cannot be done simply within the STL and significantly limits the application of the software as a design tool which would be acceptable to Airbus.

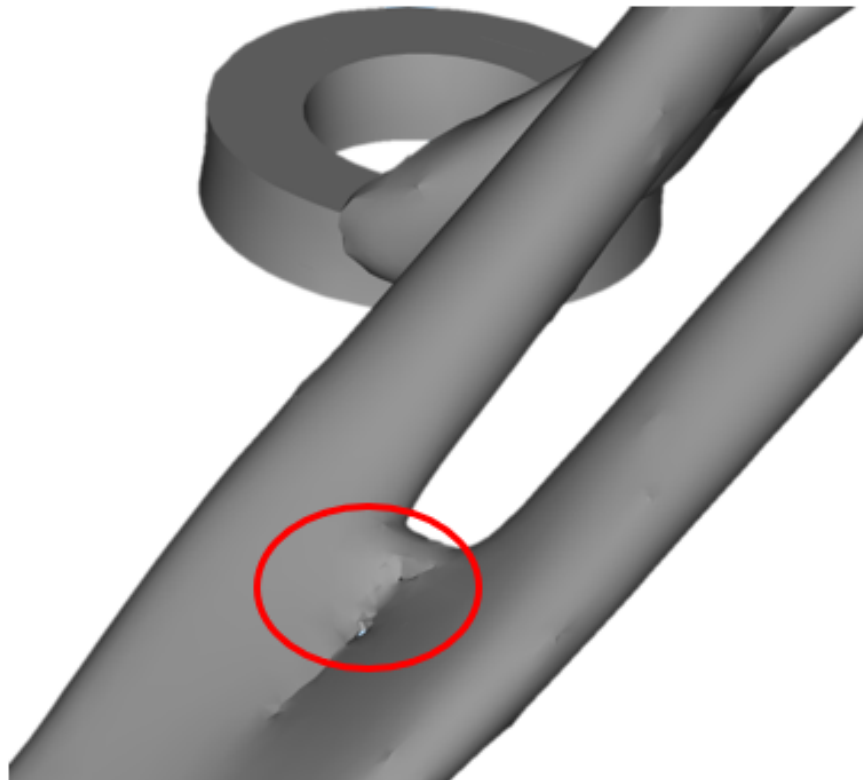


Figure 93 - Showing damage to converging areas during STL repair/smoothing.to size topology directly off the resul

6.4.4.3 Altair Optistruct and OSSmooth

Of all the tools tested here, the OSSmooth function within Optistruct (European Commission, 2017) is both the least adaptable and, in some respects, most usable. Its functionality is limited as it is designed purely to facilitate the extraction of a smooth surface mesh, either back into the Hypermesh/Optistruct environment as a 3F FEM comprised of 2D (tri3) elements or into an STL for export. The settings for the smoothing are mostly pre-defined with no options to select a smoothing type and variability allowed only for the number of iterations and the search angle. The resulting mesh and its reformulation for reanalysis can be seen in Figure 83 (Page 178). OSSmooth is an almost essential part of the design process and is commonly used prior to STL export and in advance of other STL smoothers such as Magics and Geomagics. Its simplicity coupled with the fact that it is already within the Optistruct package, means that whilst it is not, in and of itself, a solution to design extraction, it can and does form a vital link between the TO and the eventual CAD.

6.4.5 Automation of Mesh Smoothing.

Whilst assessing each of the techniques and software packages details earlier, consideration was also given to their ease of automation and their eventual inclusion into the design approach. Ultimately, both OSSmooth and Geomagics have a global, easily definable, and largely ordered approach to mesh extraction and smoothing making them easy to automate via Python command line coupled with either macro (Geomagics) or TKL (Optistruct) scripting. Magics and 3-Matics (surface reconstruction) are more problematic to automate, their smoothing and surface reconstruction methods require manual identification of local elements and split lines to achieve successful results. It is difficult to conceive of how such a process could be automated beyond use of the NDS for some elements. As the TO output is unknown during the parameterization and the STL is essentially a dumb (usually) watertight boundary upon exit, there is no means of identifying and carrying data through the optimization process in a way that can be recognised by Magics.

6.4.6 Conclusions of Mesh Smoothing as a Means of Design Extraction

Of the tools investigated (and latterly, observed) each method seems to have a number of problems which hinder its application to automated design extraction. The use of global mesh smoothing removes required sharp edged detail from the NDS as equally as it does from the tessellated highs and lows of the TO surface topology, meaning the resulting part no longer represents the level of detail required for manufacturing. This loss of detail cannot be easily restored within the STL file and doing so would require reconstruction of the STL back into original CAD formatting, thus destroying many of the purported benefits (expedience/simplicity) of using mesh smoothing to begin with. Local mesh smoothing provides for some ability to control specific areas for smoothing, but in doing so creates a hard boundary between the NDS and the DS resulting in high stress and poor connectivity. Furthermore, the ability to automate the process is limited due to the unknown nature of the continuum topology at the start of the problem, and thus the ability to pre-define transferrable parameters for it is limited. OSSmooth provides for the greatest benefit with the greatest applicability coupled with the least complex method of automation. Whilst not suitable from a geometric capability standpoint, the potential of the mesh smoothing approach from a speed perspective is undeniable. Even when multiple serial applications of smoothing parameters are required, the total operation are completed in minutes, vs. hours for the conventional methods. the Whilst it doesn't provide for a true means of full cycle design extraction, the smoothed output from FEA/TO is invaluable to more comprehensive methods for design extraction. OSSmooth also has the benefit of not introducing yet another piece of software within the chain process, thus removing further likelihood of error

when swapping between file types and versions. OSSmooth will be included as part of the automated design extraction methods.

6.5 Skeletal Modelling Approach - Introduction

The first approach undertaken was based on the work of Laszlo and Karoly (Laszlo and Karoly, 2011) using 2D topology optimization with a combination of BESO and SIMP to demonstrate a Mitchell Truss based proof of concept. The method utilised the resulting 2D mesh of a TO problem, analysing the primary confluence locations where members in the structure came together and subsequently placing a node at these locations. Connections were then made between the nodes of the resulting structure using a vector plot, thus giving a layout as shown in Figure 94. The 2D validation using the Mitchell truss is where the research terminates, with no follow-up information, nor subsequent research despite listing the potential for future work in 3D. The idea of creating a skeletal framework has significant merit and has historically been used under the name of the topological skeleton (Blum, 1967) or later, medial axis transformation (Leymarie and Kimia, 2008) using either image based recognition or computed boundaries for the data inputs. The methods can be used to size a new structure directly from the TO result, but by including parametry for sizing as a CAD post-process presents a number of options for sizing of the member and modelling of the connections between them (Gilbert et al., 2014). The difficulty comes when attempting to move into a 3D domain. The method and its required follow-up activities means unless significant manual intervention is applied, the entire structure must be comprised of trusses. This type of layout whilst common in 2D optimisation is far less likely to occur (unless forced) in a 3D domain. Examples of this can be seen in section 4.5.



Figure 94 - 2D Optimization problem with representative skeletal approach.

6.5.1 2D Skeletal Modelling Methodology

Despite no supporting evidence of its functionality in 3D (Daroczy and Jarmai, 2011), it was initially believed that this method could be quickly adopted and advanced in order to create a solution to the TO extraction problem. Focussing initially on 2D problems, the research undertaken by Laszlo was quickly approximated using Python working on an STL output from Optistruct. First, and distinct from the previous techniques, the output STL created from the FEM

is sliced (coloured contours in Figure 95) in a similar way to that of a file prepared for manufacture using AM. Each slice is then assessed determining the surface normal vectors of the edge elements along with the centroid location of each sub-section within the slice. The centroid location data from each slice is then compiled and a line of best fit computed (Figure 96) from the summated slice profile centroids thus giving a series of bi-directional vectors whose magnitudes can be capped by the design domain limits. As can be seen in Figure 95, the resulting planform is not ideal with multiple interconnecting vectors, thus at the points of intersection between the projected curves, the nodal connections for skeletal structure are established and fixed giving each curve a full vector description. These resulting structural nodes are of course, dependent upon the grid density, objective and constraints, but the approach proved viable even at extreme mesh densities (Figure 95) though with significantly increased levels of complexity and error.

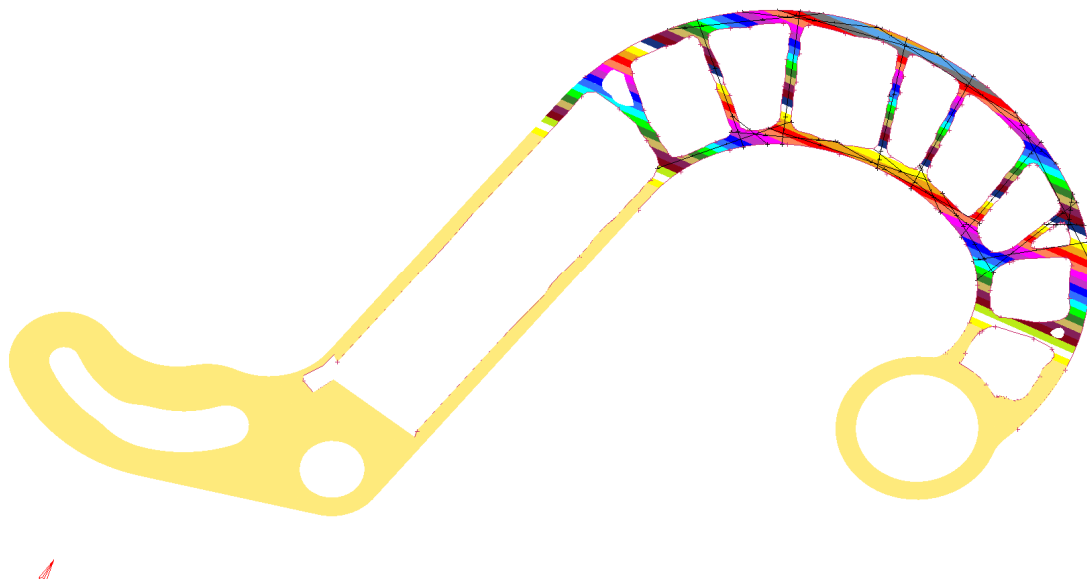


Figure 95 – Optimised and sliced 2D representation of STR 2 with vector plots based upon slice zone averaged centroid locations

With the skeletal modelling approach now at least primarily complete, the next step was to add thickness to the members, by imparting sizing to the 1D profiles developed for the code and interrogation. Initially it was considered whether some form of parametric CAD optimization could provide for a solution in this regard, with Optistruct/Hyperstudy providing sizing solutions to a parametric CATIA database. This approach was quickly discounted due to it being superficially similar to what the work of Gilbert (Gilbert et al., 2014) does with Discontinuity Layout Optimization (DLO). Whilst an extremely effective technique for quickly determining an optimal layout, the DLO approach had shown that when moving to 3D, this approach would

predominantly reveal an almost lattice type truss structure which (due to failure modes (Noviello, 2016)) would be difficult for Airbus to certify at the current maturity level of AM and the required inspection techniques. As such, a means of more accurately representing the topology output through a combination of the analysis of its exported STL/grid, and the parametric CAD recreation driven by those metrics as gained from that STL was needed. The average thickness of the struts are thus computed based upon the sum average distance of the surface normal in each slice from the vector line computed (respectively) in the skeletal modelling approach described above. This is performed by projection of a line parallel to a proximate skeletal member at a distance calculated from the average of each surface normal position from the same skeletal member. Only surface normal within 10° of perpendicular to the original skeletal member are included in the average distance calculation in order to aid with corner profile creation. The lines which form these results are again extrapolated, intersected and trimmed at their first intersection point in a similar method to that used for computing the skeletal layout.

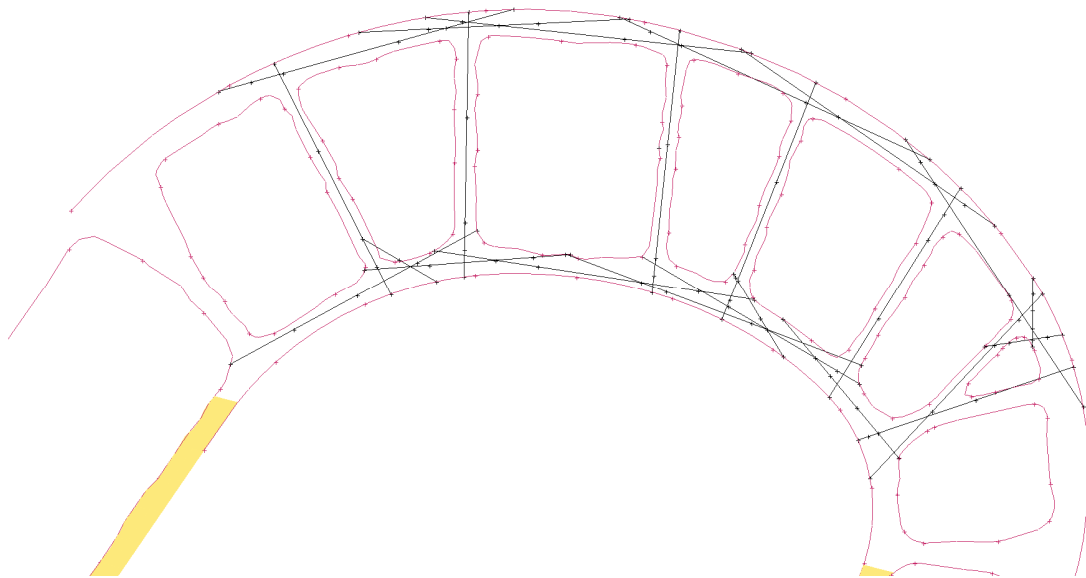


Figure 96 - Confusing pattern of vector intersections in areas of complex geometry even after boundary trimming

The resulting grid specific structure is shown in Figure 97. In order to map vector change, a confluence/divergence identification was required within the code. Thusly, the coding includes a break angle formulation where a normal vector change greater than 15° (to a neighbouring cell, indicates the presence of a divergence and thus the potential formation of distinct vector line. The 15° value was chosen as this is the standard value in Optistruct and Magics used to detect surface discontinuity.

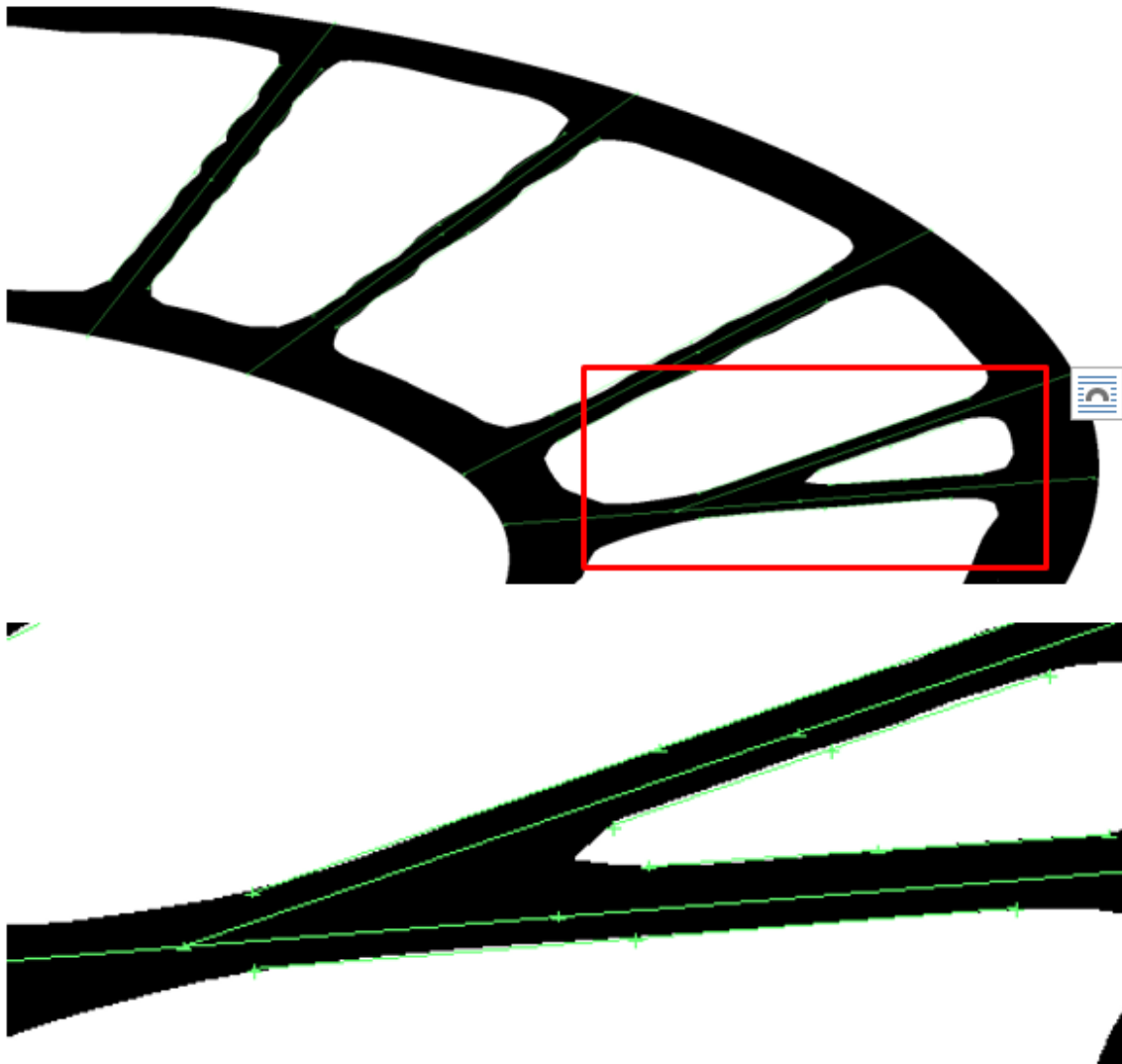


Figure 97 - Showing the offset line profiles designed to impart thickness to the trusses resulting from the optimization

6.5.2 Conclusions of the 2D Skeletal Approach

This approach works well on STL outputs defined with OSSmooth (Optistruct) but can perform poorly on a direct export without application of Laplacian smoothing. On more complex structures it can be seen that, dependent upon the grid, too many vector lines were identified/created as they attempted to map smooth curves around nodal connects (Figure 96). It was determined that greater grid densities and coarser slicing could, in a crude manner, prevent this occurrence. However, a more elegant solution was to alter the code to prevent the formation of small lines in proximity to nodes. These omitted small lines can be recreated later using radii. This approach was intended to be completed later, but was instead terminated in favour of progression to a 3D technique.

6.5.3 Introduction to 3D Skeletal Based Modelling

With promising 2D, the difficulty of performing this approximation in 3D quickly became apparent. A 2D structure can be represented in CAD by connected lines on a single plane exactly as shown above, but in 3D, the solution has a high degree of complexity. In 2D, a truss type member can, almost always, be represented by a series of rectangles (created from 3 parallel lines) trimmed (with other rectangles) to create a final structure. In 3D, connecting trusses are rarely so easily defined especially when not cylindrical. Indeed, when looking at the resulting TO output in Figure 98, it can be seen that whilst some trusses are cylindrical, many are not. As such, each truss/connection would thus require use of complex surfacing tools such as multi-sections and sweeps in order to accurately map to the TO results. Complex CAD operations such as surfacing rarely perform well in automated approaches where large variations in input parametry are expected. Furthermore, when considering vertex positions and formulations, the confluence/divergence of multiple truss members into/from a single vertex is difficult to describe and thus difficult to code for. Regardless, a 3D approach was required in order to provide for process improvement within Airbus.

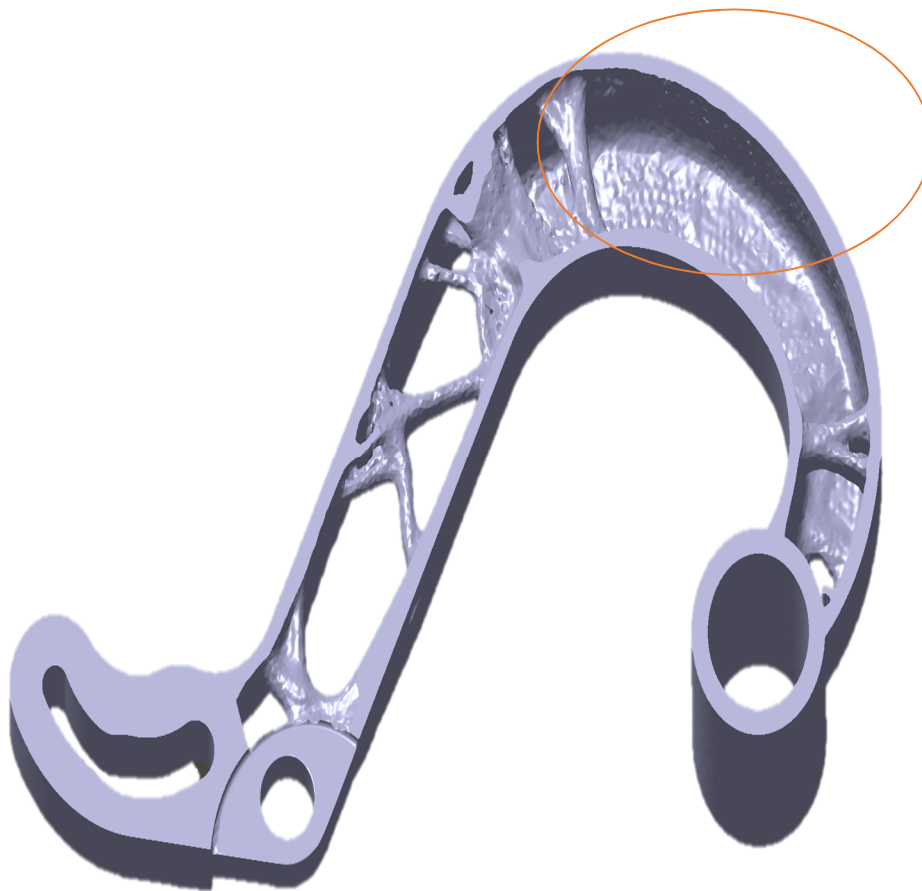


Figure 98 - Output of STR2 showing complex geometry and shape of irregular truss members

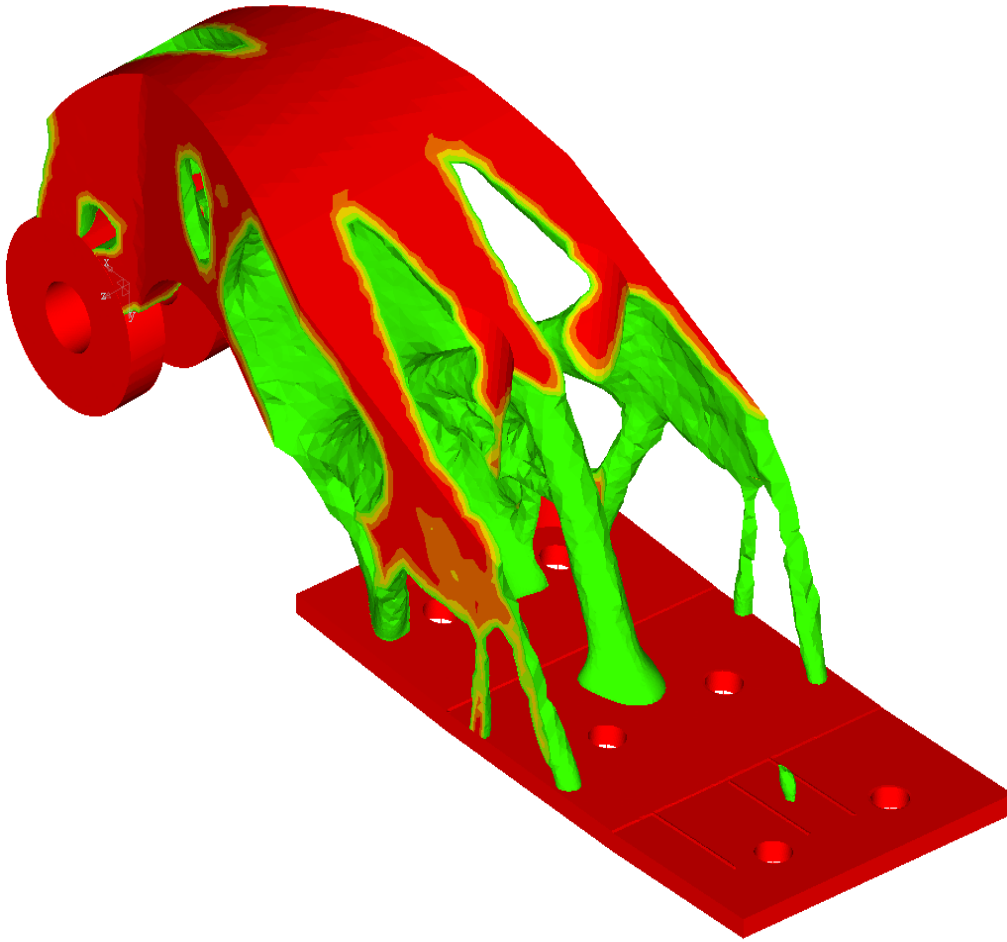
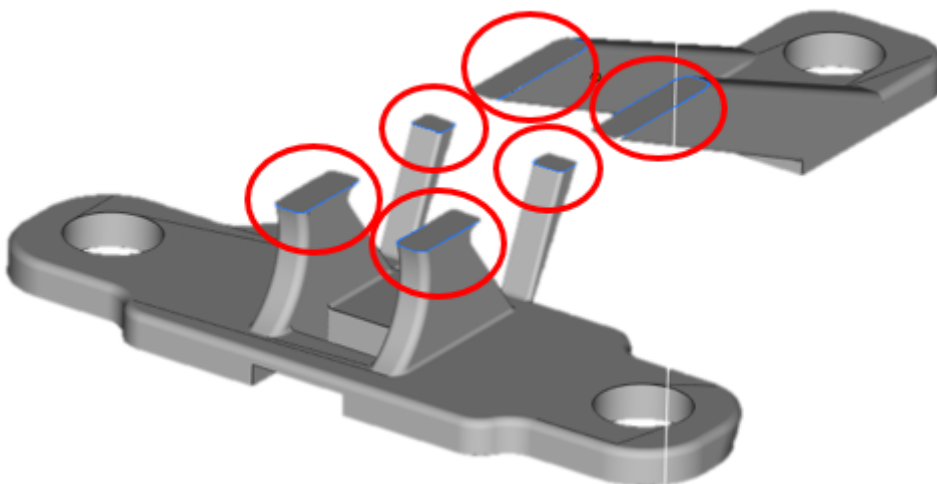


Figure 99 - TO output of STR3 showing truss style connections in some locations



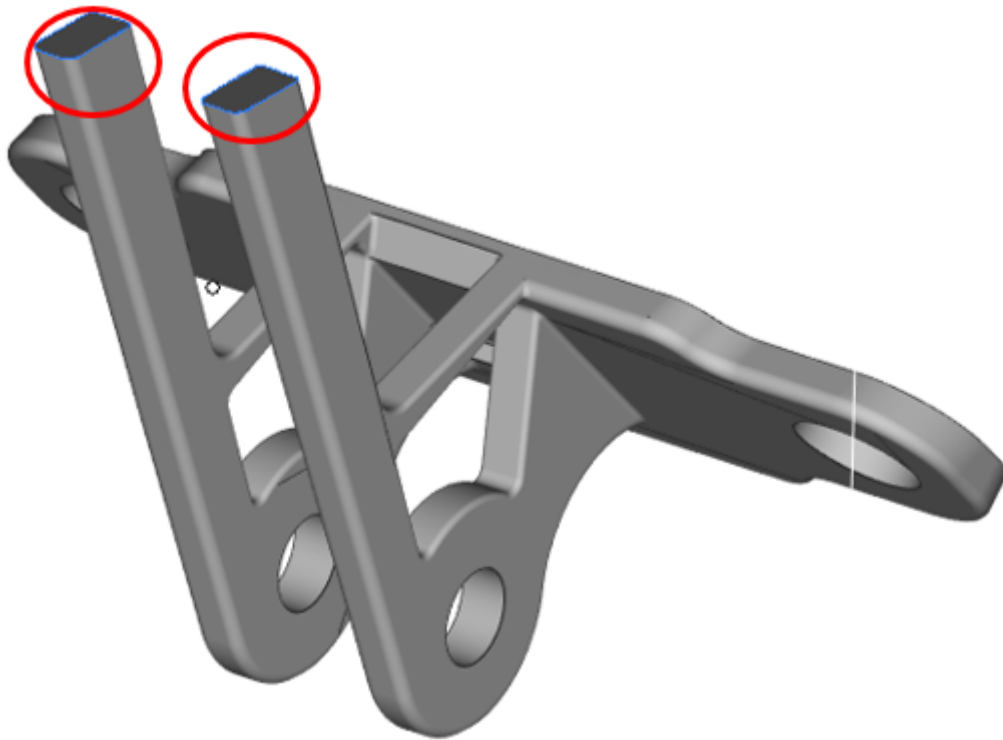


Figure 100 - Differences in centroid location determination based upon two different slice directions

6.5.4 Methodology for Development of the 3D Skeletal Modelling Approach

To start the 3D process, the STL (Figure 101) was this time sliced from the XY plane using the developed slice code. For each distinct area within the sliced CAD (Figure 102), the code then extracted and measured the difference between the extremum points in the other two axes (X and later Y) subsequently creating a mid-point between the two (Figure 103). Thus, for each area within each slice, an approximate centroid location was established and tabulated. The points at each midpoint were then defined in cartesian space and used to plot a spline curve (Figure 104).

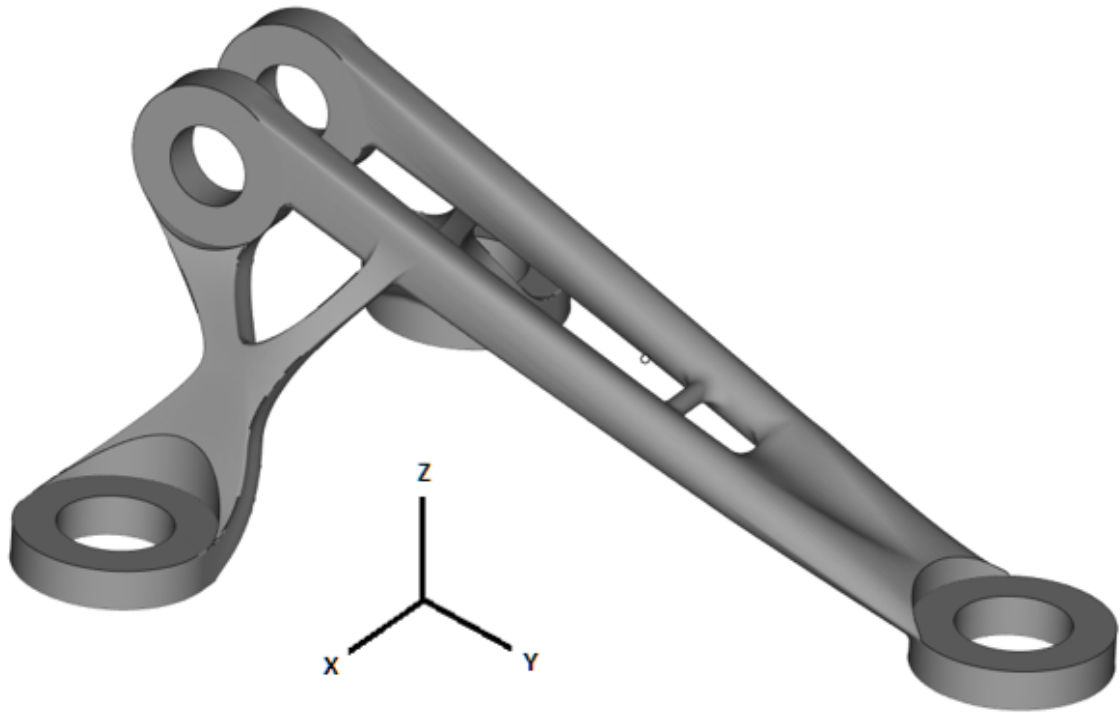


Figure 101 - Advanced surfacing extracted design of STR1

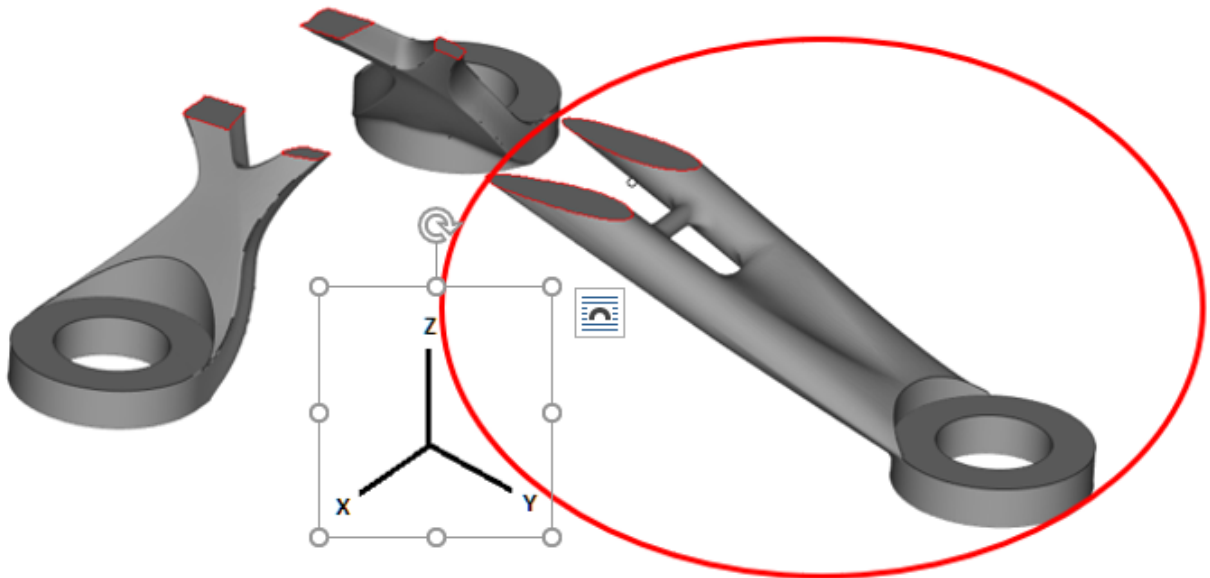


Figure 102 - Sliced STL of STR 1 Design Extraction showing individual areas within the slice

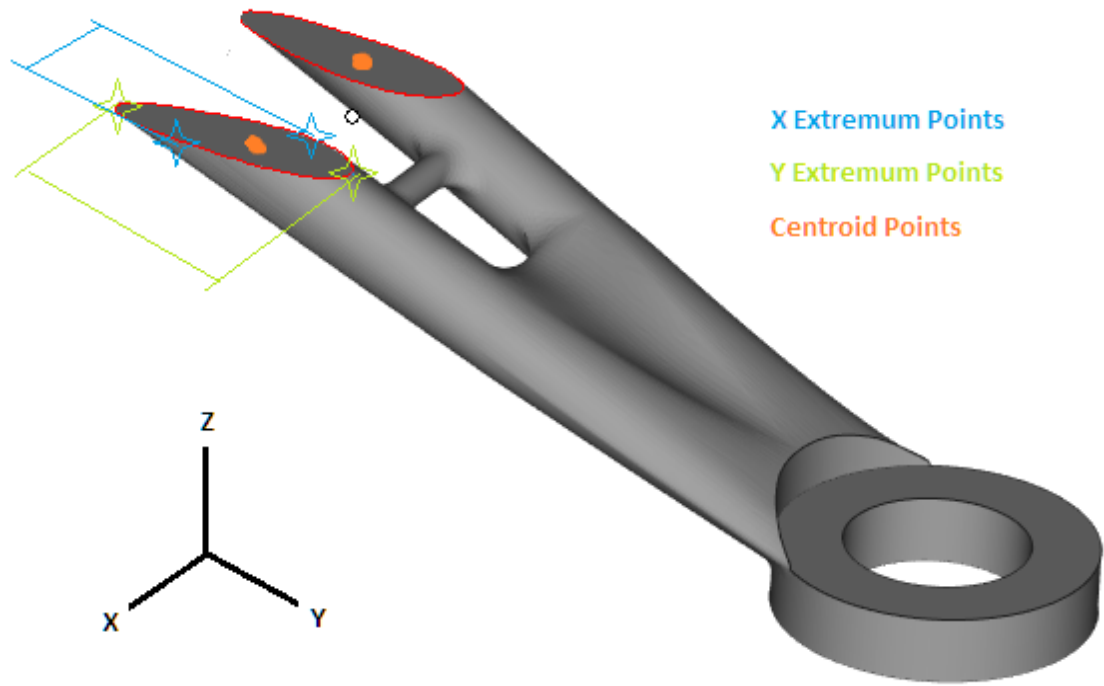


Figure 103 - Showing the sliced profile of STR1 along with the extracted extremum points of one contour and their axial (along X or y axis) measurements

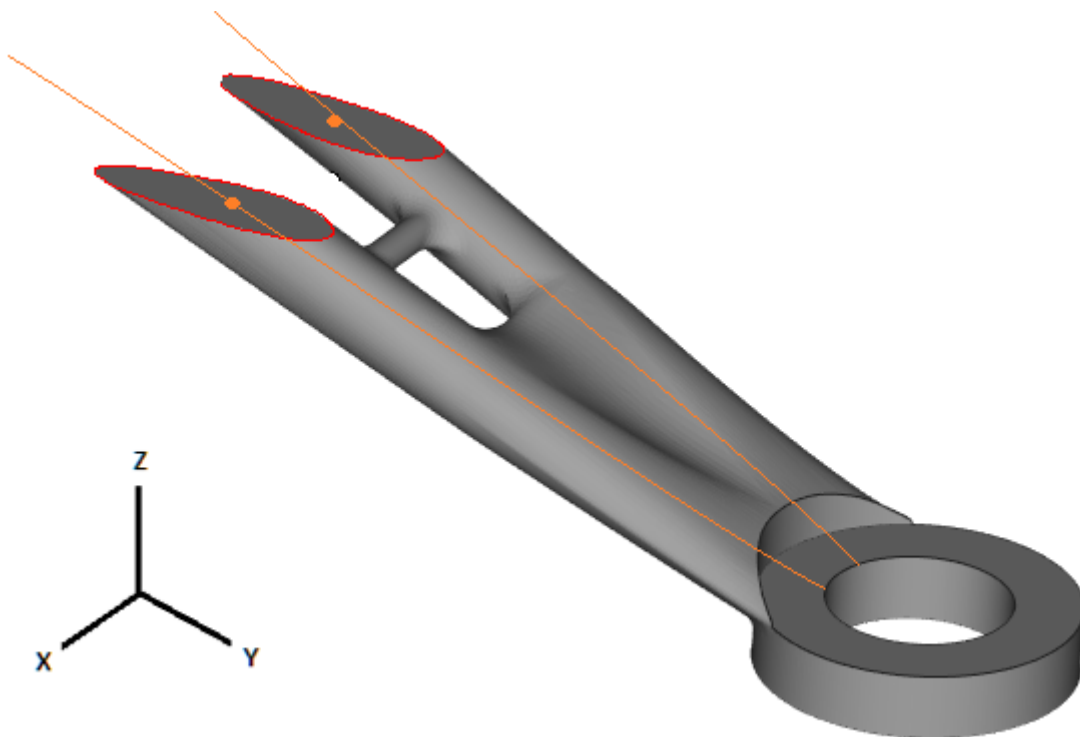


Figure 104 - Showing the computed centroid locations and the spline curves created through them and their previous slice profile centroid locations

For each centroid location established within each slice, a circular profile was then created with its central location centred on the prior determined point. The circle was computed based upon the 3-point method with each point defined by 2 of the 4 planer extremum points extracted earlier from the slice plane coupled with the calculated centre point. The planer extremums were extracted from the nodal co-ordinates of boundary nodes for each contour within the slice taking care to extract the points which demonstrate the largest separation distance so as not to undersize the strut. The centroid, points (extremums) and circle profiles were then imported into CATIA and used as the basis for a series of multi section surfaces based upon a guide curve which passes through the centroid of each zone. The resulting import of the developed profiles and reconstruction of a truss (in isolation) is shown in Figure 105

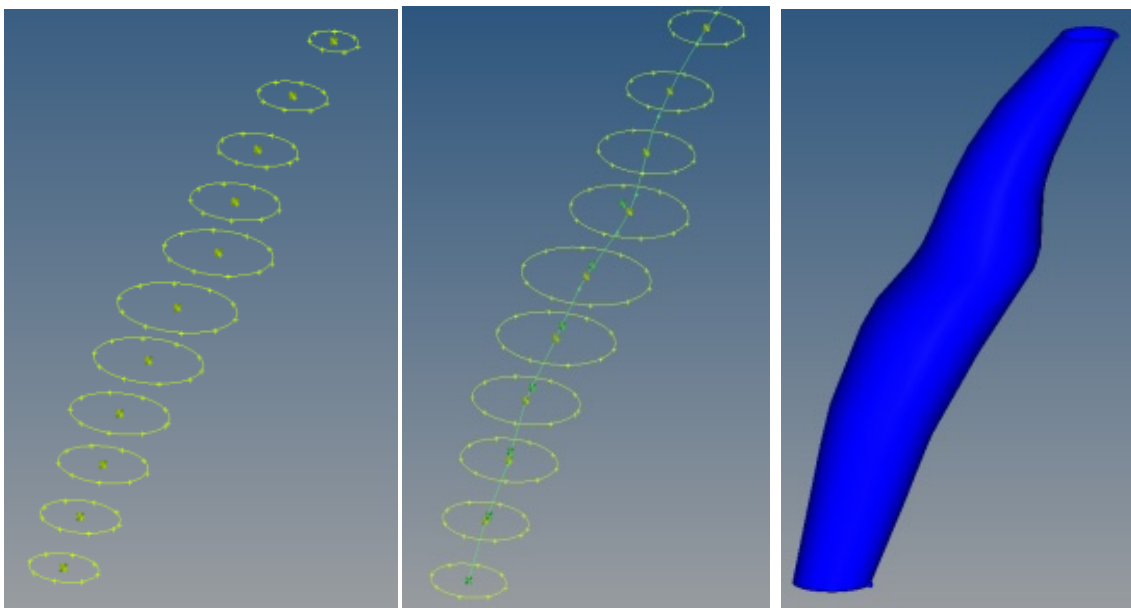


Figure 105 - Surface reconstruction using sliced FEM for profile sizing and centroid locations - note the bump/discontinuity in the structure due to the tessellated attributes of the underlying FEM TO.

The resulting designs, although smoother than a direct output from STO were still clunky when compared to true CAD design (Figure 101) and as such were in dire need of smoothing – This could not be applied within CATIA/CAD as a post-process activity, thus presenting further difficulties.

A better approach was to work on the reconstruction CAD directly, thus ensuring a smooth output. As such, a line of best fit between points (whose search separation was no greater than 1.9x the slice thickness) was created prior to circle creation. This 1.9 number was determined to be the optimal size to find nearest neighbours regardless of profile aspect change due to slicing. The tabulated points are then translated on their slice plane until they intersection with the line of best fit. Once intersected, the (spline and point) data was transferred directly to

CATIA where a default CATIA MACRO initiates the points and planes repetition function. At each point location, a plane is placed normal to the line of best fit. The STL is then intersected at each of these planer locations and searches for the four planer extremum co-ordinates of the slice. The sum average of these four is then used as the radius variable for a circular profile applied to the slice plane and centred on the co-ordinate which intersects the plane and the line of best fit. The result is a series of smooth curves with identical spine locations and start locations, thus making them ideal for multi-section surface creation. The result of this process is shown in Figure 106.

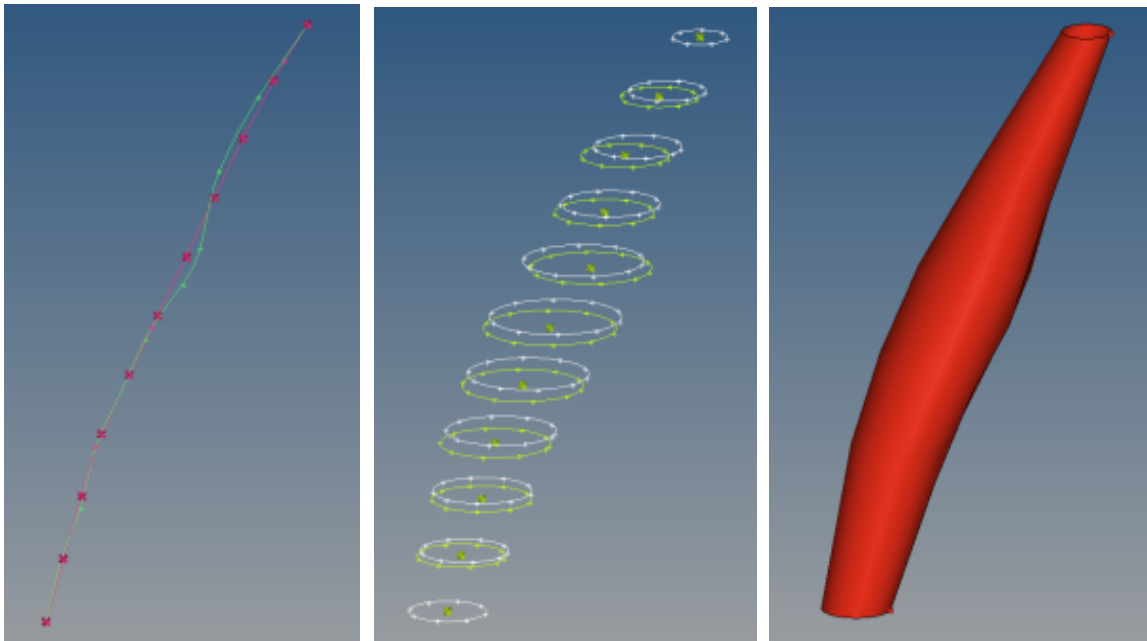


Figure 106 - Modified spine for control of discontinuities within the structure

The process performs extremely well for linear truss examples, but due to the use of a line of best fit, cannot curve properly around a corner. This is in stark contrast to the previous, unsmoothed result, which functioned well in this regard due to its use of a computed spline (Figure 107). A spline smoothing cannot function correct in the presences of a continuous complex spline in 3D space. The limitations of the methodology naturally presented similar problems to that of the 2D approach when considering intersections and a similar approach to solving them was undertaken.

6.5.5 Results of the 3D Skeletal Modelling Method

Perhaps predictably, 3D intersections present significant problems at points of structural intersection which occur within the sliced layers. If the slicing is too coarse, insufficient detail is available to capture the details of the convergence/divergence and the resulting lines of best fit do not meet at appropriate locations to match the TO result. If the slicing is too fine and the

break angle not carefully controlled the number of resulting lines are too small and too numerous creating difficulties for the CATIA parametry to intersect the structures to one-another.

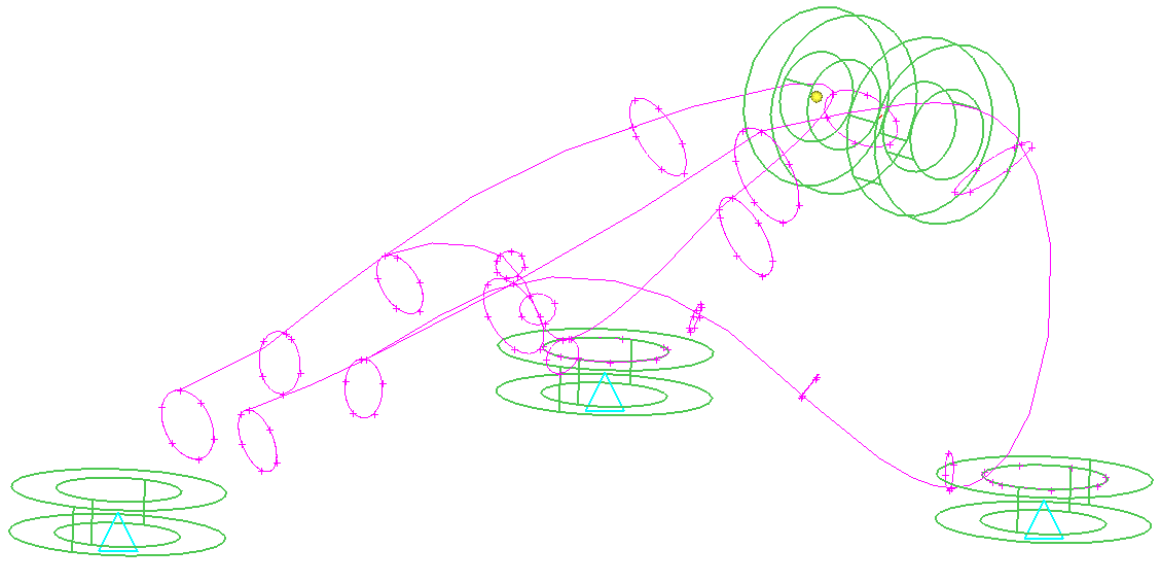


Figure 107 - Computed spline curve for surface reconstruction

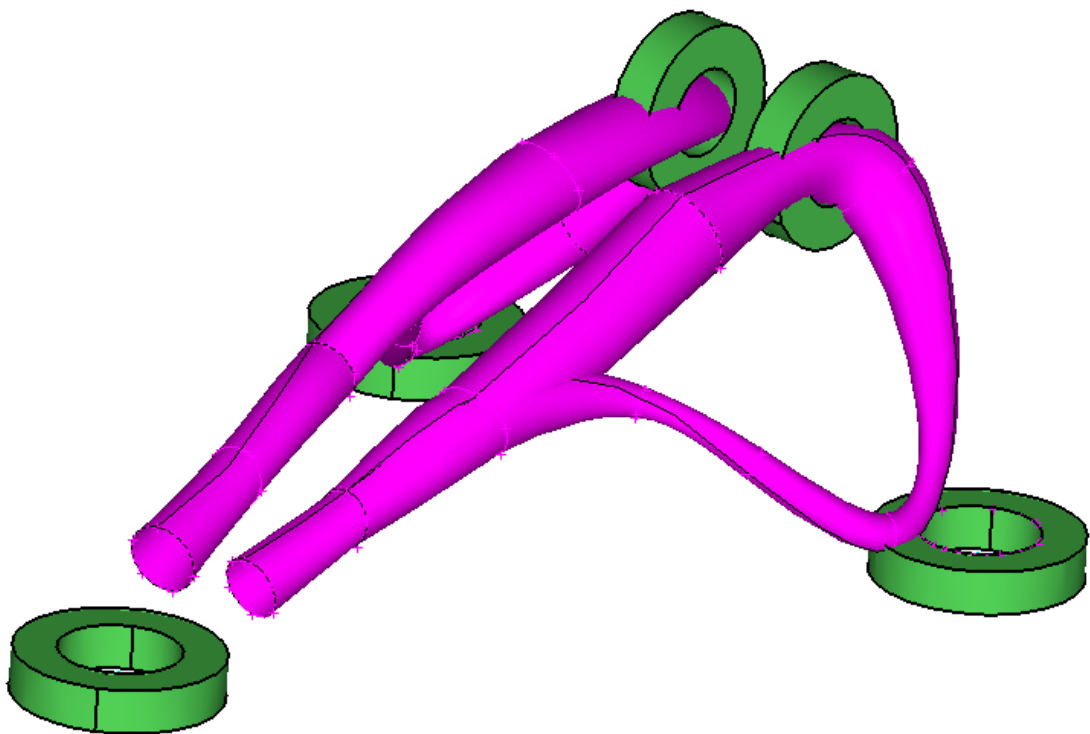


Figure 108 - Full Surface reconstruction using parametric CATIA functions fed by interrogation of the STL

The problem compounds further when the optimiser is subject to a component with challenging geometry such as that seen in STR5 (Section 3.4.2 - Table 4).

When STR1 is optimised and extracted using the 3D Unsmoothed Skeletal Method the resulting output looks something like that seen in Figure 108. Whilst the result of the automated extraction does not resemble a conventional manual design extraction (Figure 84), the geometry which defines the surface reconstruction is parametric and is thus manipulable. This means the design could be manually iterated toward a more conventional approach with comparative ease.

6.5.6 Discussion of 3D Skeletal Modelling

In testing the methodology, the code written for the extraction process (which can be found in 10.3 Appendix C – Coding and Scripting) proceeds well in structures whose continuum topology result can be potentially represented by interconnected truss structures. Problematically, for many optimization problems, a compliance-based optimization objective will be targeting the total stiffness of the structure for a defined volume fraction. In such circumstances and dependent upon the geometry and the loads, total truss-based connections will only appear on extremely refined grids. In coarser grids or less constrained optimization problems, pure truss-based solutions are less likely to occur, with thinner webs instead providing connection between the main trusses as opposed to more, cross linked truss structures. The result is that the contour areas for each sliced output STL layer are no longer approximately circular (similar to if only a single, slice direction were used to extract circles – at certain angles, the resulting profiles are ellipses, not circles) and thus cannot be represented by reconstructed cylinders based upon parametric (due to the requirements for parametric CAD) relationships with CAD. When confronted with complex shapes and using the same extremum based circular profile creation approach, the result of prior coding would be a truss of enormous diameter for that section. The presence of these irregular cross sections can be clearly seen in Figure 109.

By default, the slice file will automatically return irregular structural profiles in each layer (these are normally discarded in favour of reconstruction techniques based upon the extremum of those profiles) and so can be used directly, or preferably with profile smoothing for each contour for the recreation of the surfaces. Problematically, whilst it is still possible during the extraction phase to create multi-section surfaces which link irregular profiles to one another, significant construction geometry (scaffolding through guide curves) is required in order to have any chance of success. Due to the unknown shape of any resulting topology output in advance of the optimization, this is impossible to predict and thus cannot be automated as part of the extraction process. This limits the shape of extracted struts to largely tubular constructs based upon circular profiles of varying cross section and is only applicable to the results of 3 of the 5 test structures

and of those only partially to 2 of them. After several attempts to modify the method to allow for the extraction/reconstruction of geometry based upon contour profiles, the research reached an impasse and was halted during the period of which the research for Airbus was halted.

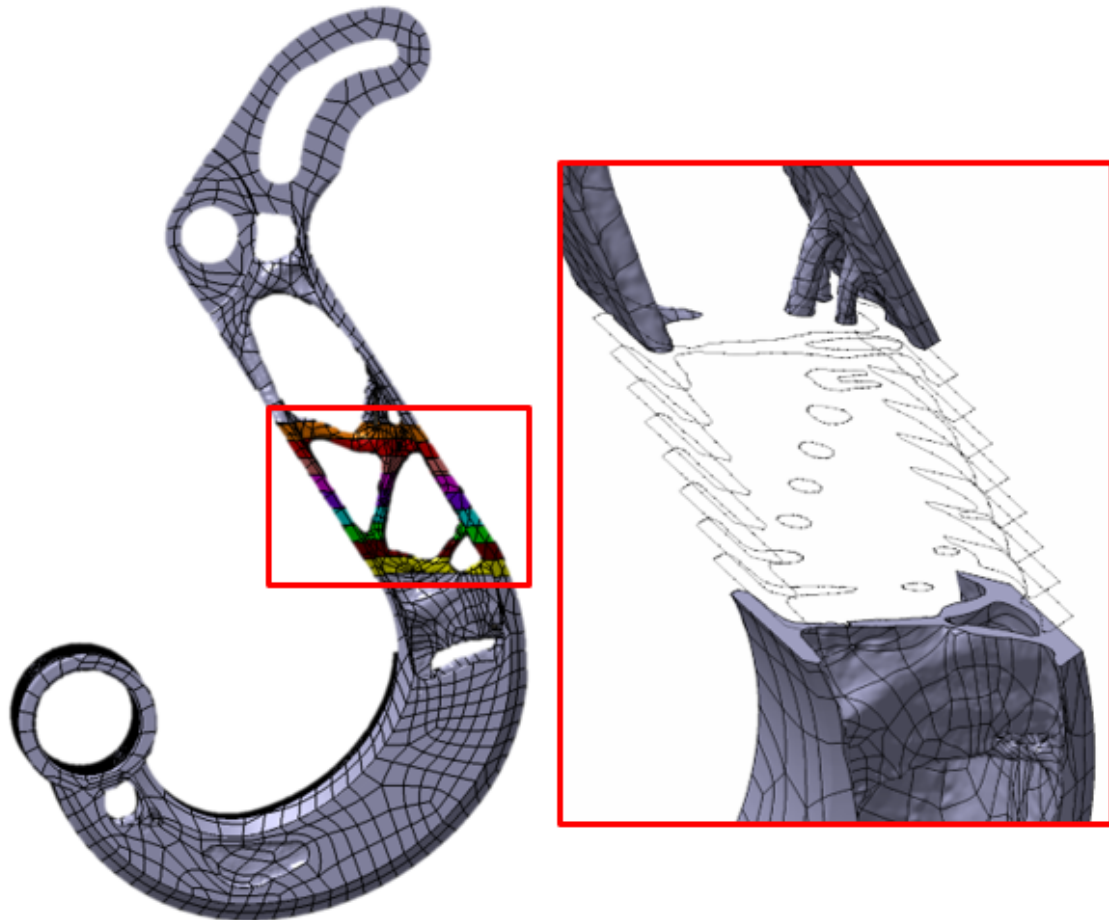


Figure 109 - Presence of non-cylindrical cross sections in the output from the slicer from the optimisation of STR2

6.5.7 Conclusions of the Skeletal Modelling Approach

Whilst the problems with this approach may be solvable for some component geometries, there will always be a substantial proportion for which the approach cannot help, or worse, simply wastes the time it was intended to save. Despite this, there are several positives to be taken from the research. The first is the ability of the software to not only interrogate the resulting output FEM (in the form of an STL), but also to link that FEM (via STL) to parametric geometry items created in an open source STEP format. The second is the ability to automatically recreate features which mimic the TO output within CATIA using a combination of parameter sets and enabled macros. As a major focus of this research is in the potential for time reductions and increases in process robustness. Direct linking of the FEM through optimization to the recreation CAD in a semi-automated process provides for substantial benefits and completes (in a limited

form) one of the major objectives of this research. The means of parametric linking will be re-used in further methods of automated design extraction.

6.6 Problems with Investigated Methods for Design Extraction

Two prevalent problems exist with the methods developed for automatic TO extraction. Problem 1.) Certification of Design and Analysis - relates to the resulting design extraction and its acceptability for use in commercial aerospace. Problem 2.) Design Traceability relates to the derived topology, the means by which it was achieved, and the resulting CAD used to represent that topology including how the data is traced/interacted.

Mesh smoothing struggles with both of these problems due largely to its total use of STL based file formats by prioritising simplicity and expedience, over flexibility and design detail. Commonly the TO result is not a perfect result, particularly if chasing extremely lightweight structures with a reserve factor (how much structural redundancy is present in any component – 1=none) close to 1. The TO software will allow infringement of the global stress constraint if the percentage of those element which exceeds the limit is less than .05% of the continuum. As a result, even the best techniques for direct STL extraction and smoothing tend to reveal the presence of stress hotspots at the boundaries between NDS and DS zones (Figure 110) where the TO solver has failed to implement a full stress constraint. Caused by small notches in the surface topology they are/could be a significant contributing factor to the premature failure of a part due to fatigue cycling (Tong et al., 2017). The presence of these hotspots would usually be mitigated by the application of fillets or additional material in areas of stress in the CAD environment, but modification of the STL to add these features is a laborious process and rarely proceeds either fast or well. Therefore, the stress hotspots cannot be easily mitigated against without reliance on unacceptable global smoothing techniques which would blend the boundary of the NDS and DS.

Of greater interest during the mesh smoothing task was the capability for rapid re-validation (Optistruct) and even of certain software's ability to reconstruct smooth surface data based upon adjacent surfaces, even in complex domains. Even so, the lack of direct control of STL derived CAD relegates mesh morphing and adaptation techniques (at least at this stage of development) to an RP role which is not one suited for repeat production of high value, tightly controlled components in commercial aerospace. Problem 1 is not found in skeletal modelling as reconstruction occurs in a CAD environment and thus allows for modification with ease. Relating to the second problem of FEM>CAD traceability and linking, thus far, almost all of the techniques investigated for the extraction of TO designs have shared one significant thing in common with one another (beyond their topologically derived nature) – they all, without

exception, sever the digital link between original CAD and the new design during the analysis (FEM) phase. Commonly this occurs when the FEM replaces the true CAD as the digital representation of the component. Without a link between FEA and the new CAD, any subsequent analysis/optimization requires the process to begin almost from scratch.

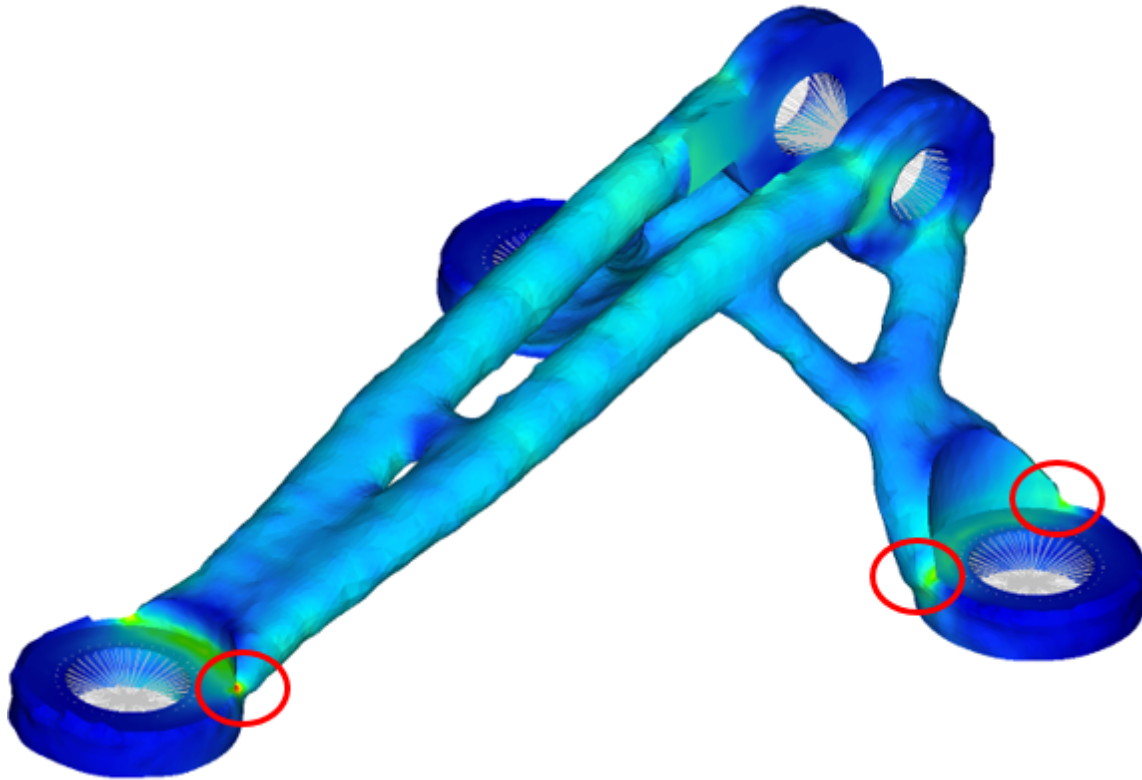


Figure 110 - Stress hotspots in the extracted design after local smoothing whilst attempting to maintain Non-modifiable design features.

As such, parametrically linking the FEA to the CAD is beneficial from a reduced NRC point of view. In the case of mesh smoothing and many other techniques, the process starts with CAD and ends with CAD/FEA in the form of an STL, and whilst a link between the original and the new could be forged using python and CATIA, STL is a dead-end format and cannot be manipulated within CATIA, and thus cannot be integrated into the Airbus DMU. This significant limitation practically discounts the use of STL as a method for design extraction unless it can be linked parametrically to CATIA QSR. In contrast, skeletal modelling uses the output of the optimization (the STL/FEA) to create a series of parametric profiles within the CAD environment supported by Airbus. Whilst not an industry first, it is an Airbus first and certainly a first which also include some of the constraints applicable to AM. Whilst the technique has limits, this means of reading the output FEM/STL and linking it to parametric features in the CAD is both powerful and adaptable, both reducing the NRC and expediting any future optimization and analysis process.

6.7 Problem Formulation for New Extraction Method

The primary focus of this research has been to develop a means of significantly expediting the optimization of small parts intended for production via AM. Problematically, the research undertaken thus far has demonstrated that significant proportions of work within the optimization and design process occur within functional loops. Within these loops a concept design is generated and iterated until a convergent design, compatible with all fields is achieved. As much as any other time sink, it is these requirements, inherent to this looped (design > assess > optimise > extract and validate) process which significantly slow the work. One of the primary reasons for this loss of time is incurred within program switching and the subsequent requirement for CAD clean-up and accurate remeshing/pre-processing. Whilst mesh smoothing the skeletal modelling were both (for different reasons) failures in terms of their usefulness for expeditious design extraction, they did have a number of notable achievements in minimising design loops through either removal of software steps or the restoration of links between packages.

As this research progressed and the results were fed to Airbus, it became apparent that whilst the desire for a simpler method of optimised design extraction existed, an appetite for new tools to perform this function did not. As such, it was deemed likely that a furtherment of the skeletal modelling approach to enable rapid CAD development within CATIA would be the most palatable and acceptable to Airbus perimeter. The skeletal approach failed largely due to problems in areas of convergence/divergence and the limited ability of the written software to capture elements/cross sections of a non-circular nature, but a means of linking to CATIA was at least partially established; it is this CATIA link that was selected for further development.

Complex geometry is often best extracted within CATIA GSD (Generative Shape Design) advanced surfacing, rather than the more common Part Design (solid modelling approach) as it allows more control during surface intersections and less likelihood of poor CAD (Section 2.5.3). Problematically, advanced surfacing requires substantially more construction elements in order to create the surfaces required to replicate the topology extraction. This is especially true when the optimised design output (STL) cannot be interacted with inside of CATIA CAD environment as there is no foundation for the new structure, the result is that more time is lost in complex design, than in conventional design. This is not only due to the nature of the topology, but more a combination of the topology and the complex tools and methods needed to extract it. The difficulty in extracting complex designs automatically has been aptly proven in research (Section 2.6.4) and development (Section 6.5.3) and is largely complicated by the unknown nature of the resulting and the methods available to seamlessly link aspects of that topology. This complex

task easily handled by design engineers once they see the problem and consider the effects of the multiple structure or connections, but to get to that point takes excessive time. However, if we are again to look at a further detailed breakdown of the design extraction task specific to a CATIA environment, it can be seen (Figure 111) that there are a number of common steps relating to the creation of construction geometry which occur regardless of the component type.

Thus, a new method of automation application, designed to aid the design engineers, by providing the vast majority of the required support and connection geometry automatically was developed. In doing so, the aim was to leave only the intersections and specific intricacies for each unique design to be dealt with by the engineer. This geometry was to be provided parametrically within CATIA to enable simple interaction, and, if required, modification. By targeting these initial steps, it was believed that not only would a significant amount of time per design be saved, but also that the commonality between designs made by different engineers would be substantially increased, thus providing robustness to the process.

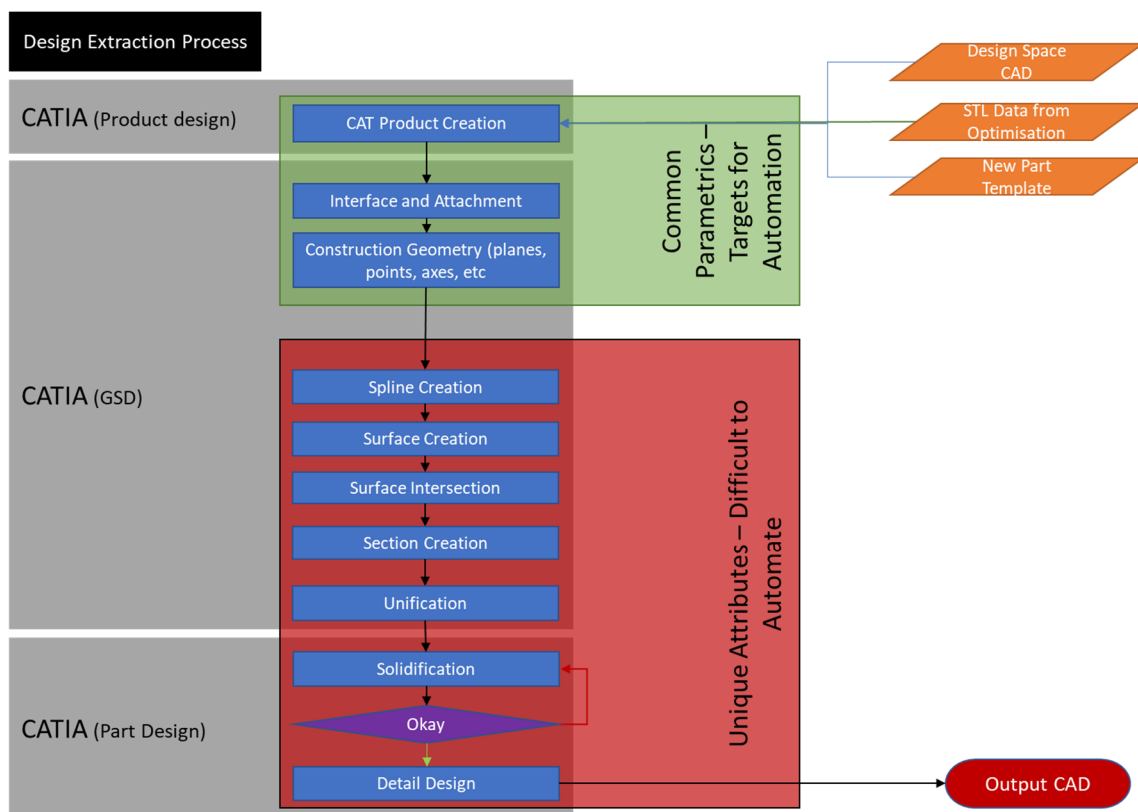


Figure 111 - Detailed extraction process showing common steps in design extraction and those which're unique to the design being extracted.

6.8 Parametric Linking of the CAD to the FEM

In almost all well framed optimization problems, loads and constraints are applied to the structure via areas of non-design space which is connected to the remainder of the structure (design space) via connected surfaces and, in the FEM, via shared elemental boundaries. These areas of NDS are inviolate and thus remain constant throughout the optimization process, whilst in contrast the design space varies continually. As the NDS remains constant, the data pertaining to co-ordinates on its boundaries are also constant and thus can be directly copied/transferred from the input CAD ready for analysis. The next stage was to target the creation of a series of construction elements connected to, and based off, the NDS elements already present in the CAD. It was postulated that whilst it could not be guaranteed to work 100% of the time it was highly probable that all areas of NDS would be connected to the final TO design in any compliance optimization and thus provided good foundations for the creation of the elements.

A distinct advantage of this approach is in any situation that might require a re-analysis and optimization of the structure under investigation due to a change in load, materials of optimization objective. In such a situation and assuming the geometry remains constant, the fact that the parametric NDS remains means that only the DS will vary and when converged, the intersection between the DS and NDS will automatically update, maintain the link back to the CAD and into the future CAD.

6.8.1 Creation of Key Parametric CAD based on Recognised Commonality between the Input CAD and the TO Results

In order to create a spline in 3D space, several features must first be present to allow for the creation and control of the connectivity of that spline. Firstly, a spline must pass through or be proximate to a number of points which control its shape. Each of these points must somehow be defined using either cartesian co-ordinates or proximity to another feature. Next, control over the attachment of that spline (usually via tangency) is required. There are many methods of doing this, but perhaps the most flexible is to point a direction based upon a planer reference. And so, to create a spline, the very minimum one would require is for a pair of points and planes.

Tackling these in order, Problem 1.) Control Points - the location of the initial control points is critical as the base for the splines intended to function as the primary driving curves for the creation of bridging surfaces between the various areas of NDS. The first approach was the locating of primary control points at the boundaries at which the NDS and DS, intersect. When previously defining and using the skeletal methodology, a smoothed (via OSSmooth) STL output was used as the basis for extraction. Problematically for the new method, a smoothed STL means that identifying control points on the DS which also exist on the NDS will require additional

computation (due to nodal displacement caused during smoothing) which could be avoided through use of an exact extracted mesh. A non-smoothed STL is much larger file, comprised of thousands more surfaces than a smoothed STL and will be difficult to later interpret smoothly and so a compromised had to be reached. During the early stages a non-smoothed output would be used to determine construction geometry and a smoothed mesh was to be used for final extraction.

To find the initial control points present on the boundary between the DS and NDS zones, a script was written which automatically imported and compared the STL described NDS (from Hyperworks) with the resulting non-smoothed DS topology output from Hyperview. The comparison simultaneously assessed both files looking for identical co-ordinate locations common to both files. These co-ordinates are only found in locations in which the DS and NDS bridge and are almost always located coincident with the surfaces and splines of the NDS, providing an excellent basis for further geometry creation. Once identified, the script analyses the resulting point clusters (Figure 112) and determines the four most extreme co-ordinates on a planar function and outputs the tabulated cartesian points (in the form of a CSV file) ready for import into CATIA using the point importing function native to the program. When complete, the result is a series of parametric surfaces (the NDS) and a series of complementary parametric points which define the locations in which the primary curves of the new topology would connect to the NDS. All of these features are fully interactive within CATIA and thus can be used and manipulated by the design engineer.

6.8.2 Automation of Common Reconstruction Features - Planes, Control Points and Curve Reconstruction

6.8.2.1 Points – the Automation of FEM Linked Primary Construction Geometry

Whilst creation of the intersection points and the transfer of the NDS zones to the new part are a start and will save several hours per part in terms of NRC design time, significantly more can be done to aid the extraction process. Whilst remaining within the common parameters identified (Figure 111), additional structural elements based, at least partially upon the created intersections were required in order to provide framework for the derivative CAD. Problematically, the method used for extracting the intersection points between the NDS and DS created significantly more points than are actually required for the creation of surface curve functions. As such, and without any prior filtering, almost any subsequent function reaction (which is based off/from those points) will exponentially multiply the problem, creating too many confusing and unrequired CAD Artefacts.

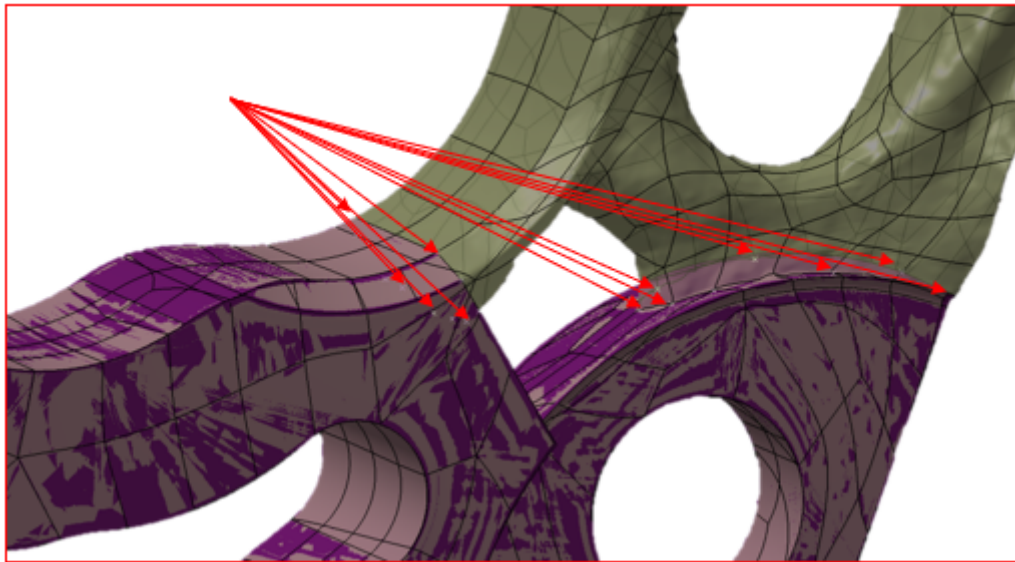
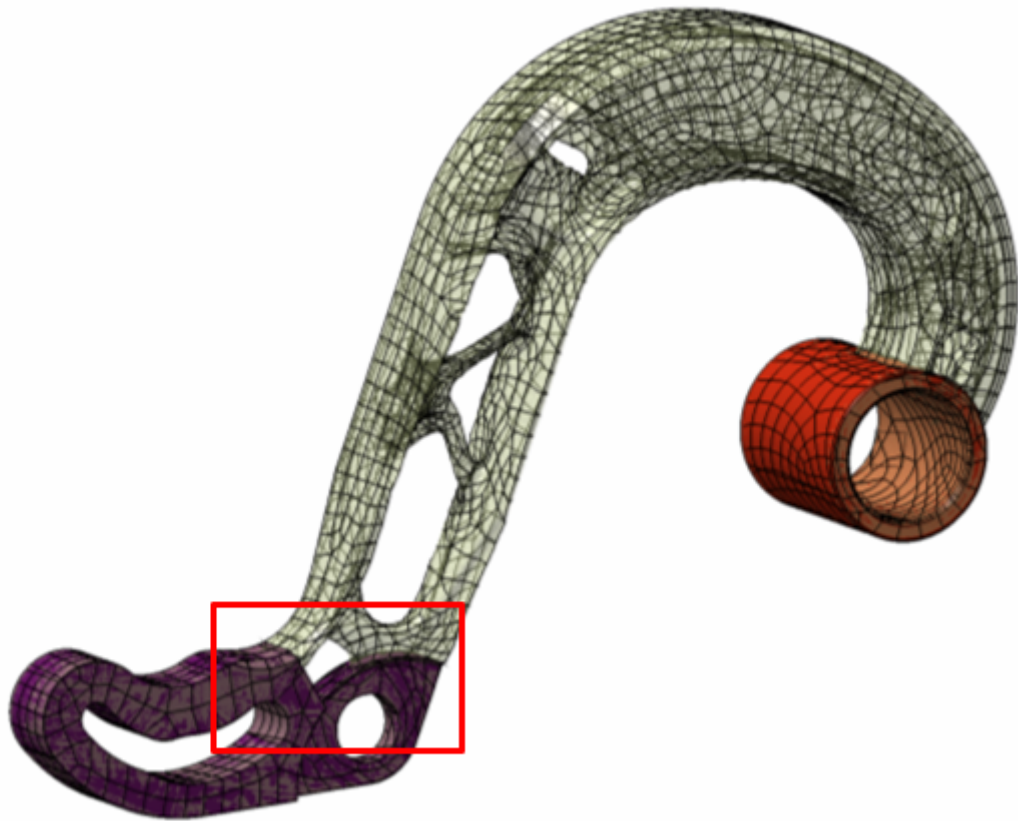


Figure 112 - Point clusters where DS and NDS meet as identified by scripting

This propensity highlighted the need for some form of point filtering in order to reduce the total amount of unrequired CAD generation. Filtering of the points of intersection is currently performed manually through the sequential selection of points and their eventual transfer to a points collector within the construction geometry. Ideally, this process would be automated, but

without significant assumption as to the shape of resulting truss members (this shape information is not determined by TO, only the vector and thickness), the appropriate control points cannot be down-selected. Thus, all points must remain available for manual filtering and progression to the next phase of design. Full, but limited scope automation of this phase could be completed but would require more time than is currently available within the project.

6.8.2.2 Automated Plane and Axis Creation for FEM Linked CAD

Planes and axes represent two of the most fundamental aspects of design creation in any CAD software. Their presence is required for almost any geometry creation and can be used to great effect for more advanced features such as curvature control and sweep tangency. Due to the nature of the components selected for this investigation and the unconstrained methods of manufacture and design, it was deemed to be highly unlikely that any of the primary construction planes (other than the major part axis) would be of any use to the future design. Furthermore, it was determined that the likelihood of using complex curves in 2D space was low and thus the majority of curves created would be of the 3D, (non-planar) complex variety. In such an environment, planes and axes tend to have less functionality than they would in 3D parts designed with many lofted, extruded and pocketed features, but can be used transversally in other areas. In this context, it was decided to use orthogonal planes to define tangency, intersection and, where appropriate, point placement on both the DS and NDS areas. Again, starting at the points of intersection, planes, normal to the surface at the filtered points of intersection were automatically created using a CATIA points/planes creation within a CATIA macro. Once created, the macro then parameterized a series of further planes rotated on an automatically created axis drawn parallel to the NDS extrude and projected from the intersection point. This plane allows for full control of the curve tangency at the intersection location through modification of the rotation parameter created with the plane. The resulting construction geometry looks like that seen in Figure 113 and can be used, to a certain degree, to directly extract back to CAD, the geometry exported from the TO solver. However, the generated curves used to create the surfaces would be VERY simplistic in nature, controlled only by 2 points and planar tangency at the termination points, thus failing to capture all of the required nuances of the topology, particularly on detailed structures. In addition to the orthogonal planes used to project curves and their attachment in 3D space, additional planes were generated on the planar boundaries of NDS elements. In many structures, these additional control points do little as the planes can be rapidly created, but in some structures (Such as STR3), the tightly controlled design space means that much of the existing parts boundary systems are used in the final TO design making design extraction on those planer surfaces much more simplistic.

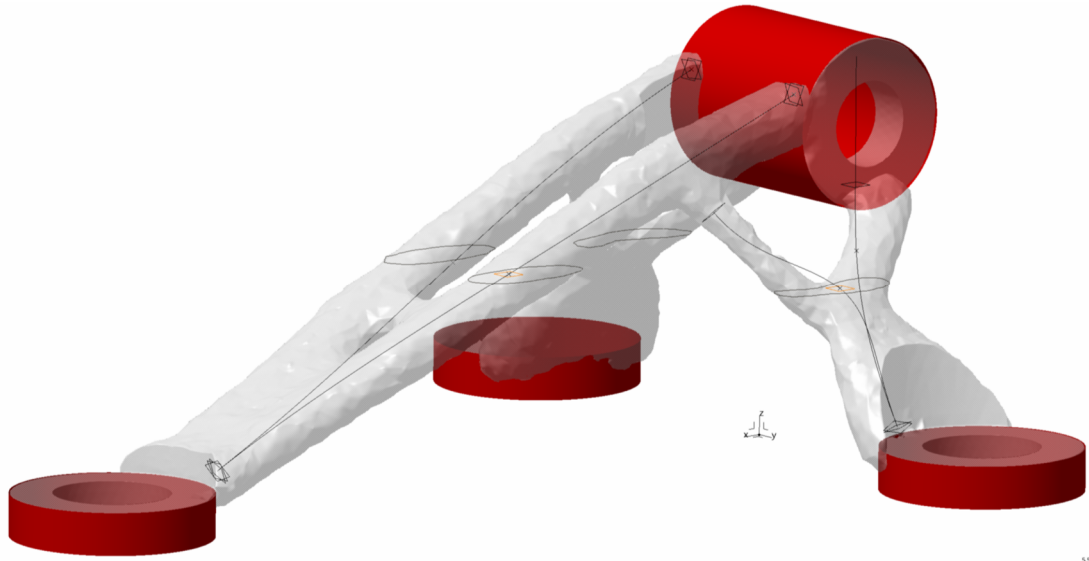


Figure 113 - Intermediate slice plane (orange) and contours (black) for use in spline drafting

The resulting geometric features for STR1 and STR3 along with the proposed manual next steps are shown in Figure 114 and Figure 115.

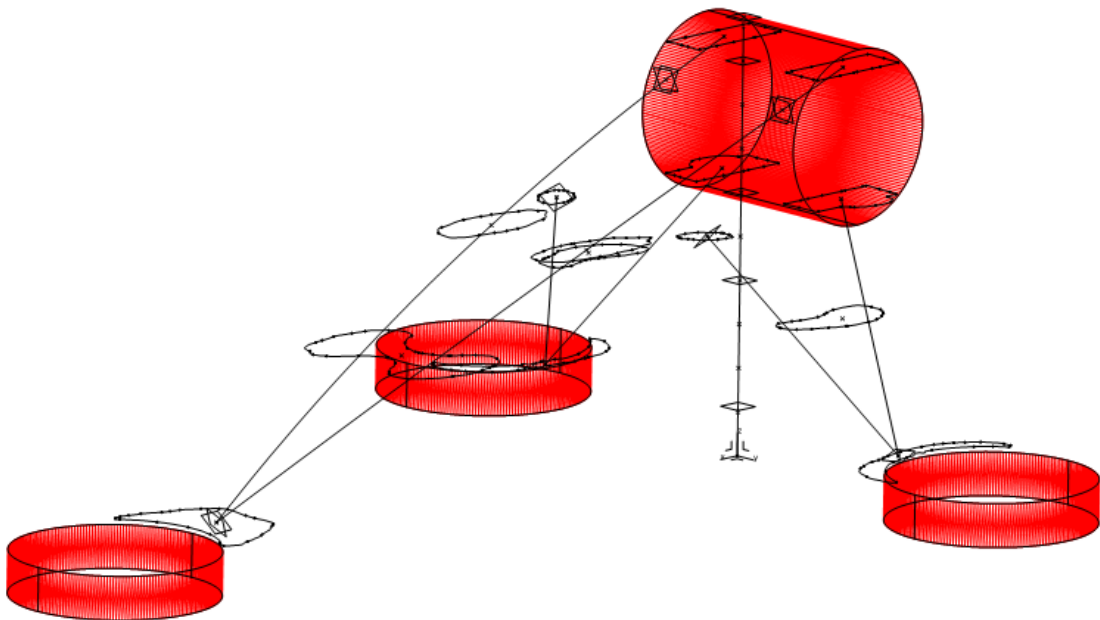


Figure 114 - STR1 and STR3 at the end of automated transfer of DS (top) and creation of parametric construction geometry (bottom)

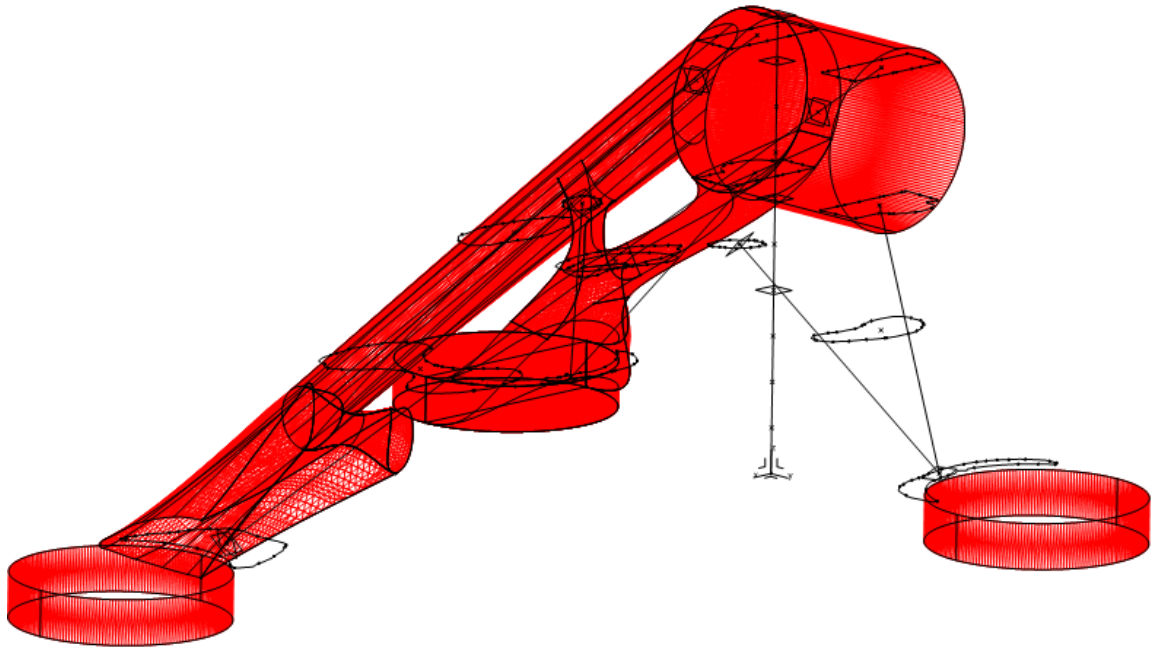


Figure 115 - Manually demonstrated next steps for design extraction on STR 1

6.8.2.3 The Use of Complex Curves in Design Extraction – Why Are They Required? How to Automate?

Almost any stress engineer will correctly state that stress tends to travel in straight lines and as such, there should be no need for complex curves in 3D space.

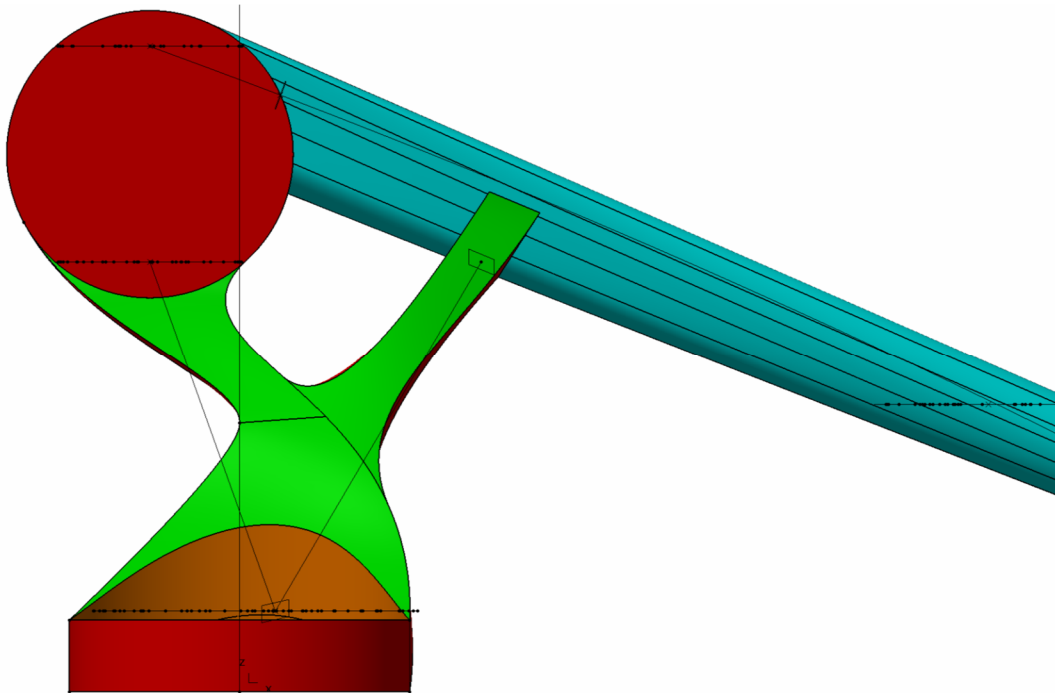


Figure 116 - Showing the effects of kinematic factors included as NDS (tool access – orange) on the load paths (Black) of TO results (Green).

However, complex design problems are rarely solved by simple solutions. It is true that in an idealized world, the linear supposition of stress holds true, but under complex loading or when subject to kinematic considerations, the result can quite substantially skew this supposition, as shown in Figure 116. In such an environment and with an outcome as shown in Figure 83, the resulting TO pattern is not completely linearized and has a complex shape between the attachment points. Though the result is visually *close* to a series of cross connected beams, when examined in detail, the connectivity is far more complex. The extraction of such a design using a linear function curve is difficult and could not be performed correctly when attempts were made for the design extraction shown in Figure 84 (page 172). Similar complex features can and do occur quite regularly in TO problems and can take substantial time to correctly detail during extraction, particularly for a CAD engineer without substantial advanced surfacing experience. As such, whilst automating the parameterization of complex curves was not within the identified Common Features for ALL CAD extraction (Figure 111), it is a significant potential time saver and is (based on examination of the compiled Airbus small part library) applicable to a significant number of components, thus making it an ideal target for enhanced automation.

Whilst the curve functions defined earlier are, technically, complex curves, they are simple constructs, using only tangency to add complexity and shape; for full control of a curve in 3D space additional parametric points are required. As the geometry result of any TO problem is unknown, a generalized approach for where and how to create those points was a difficult question to answer. Ultimately, several methods of point placement for this problem were considered with two versions making the final cut to full development.

6.8.2.3.1 Profile Centred Point Development

The idea behind the Profile Centred Point (PCP) method was supposed to be the simple application of a centre point to derived curves based upon simplistic projection of vectors in a similar way to the Skeletal approach. Unfortunately, in 3D and based upon a series of point clusters and planes, there is no simplistic way of computationally linking one set of points to another in a method which is faster than that of an engineer visually checking and connecting the areas. Regardless, it was deemed important to progress and a means of creating a connection was eventually devised. Using the four points captured earlier, a centre point was calculated for each captured intersection. Once created, each point was connected to each other point within the domain and the total length of the connection measured. For each, the shortest two lines were retained and a central point (parameterized by cartesian co-ordinates) was created on those lines (Figure 117). In addition, and based upon noted results from STR 1 and STR4, an

additional step was performed in which the shortest perpendicular length from any generated line to any intersection area was also created as a line connection.

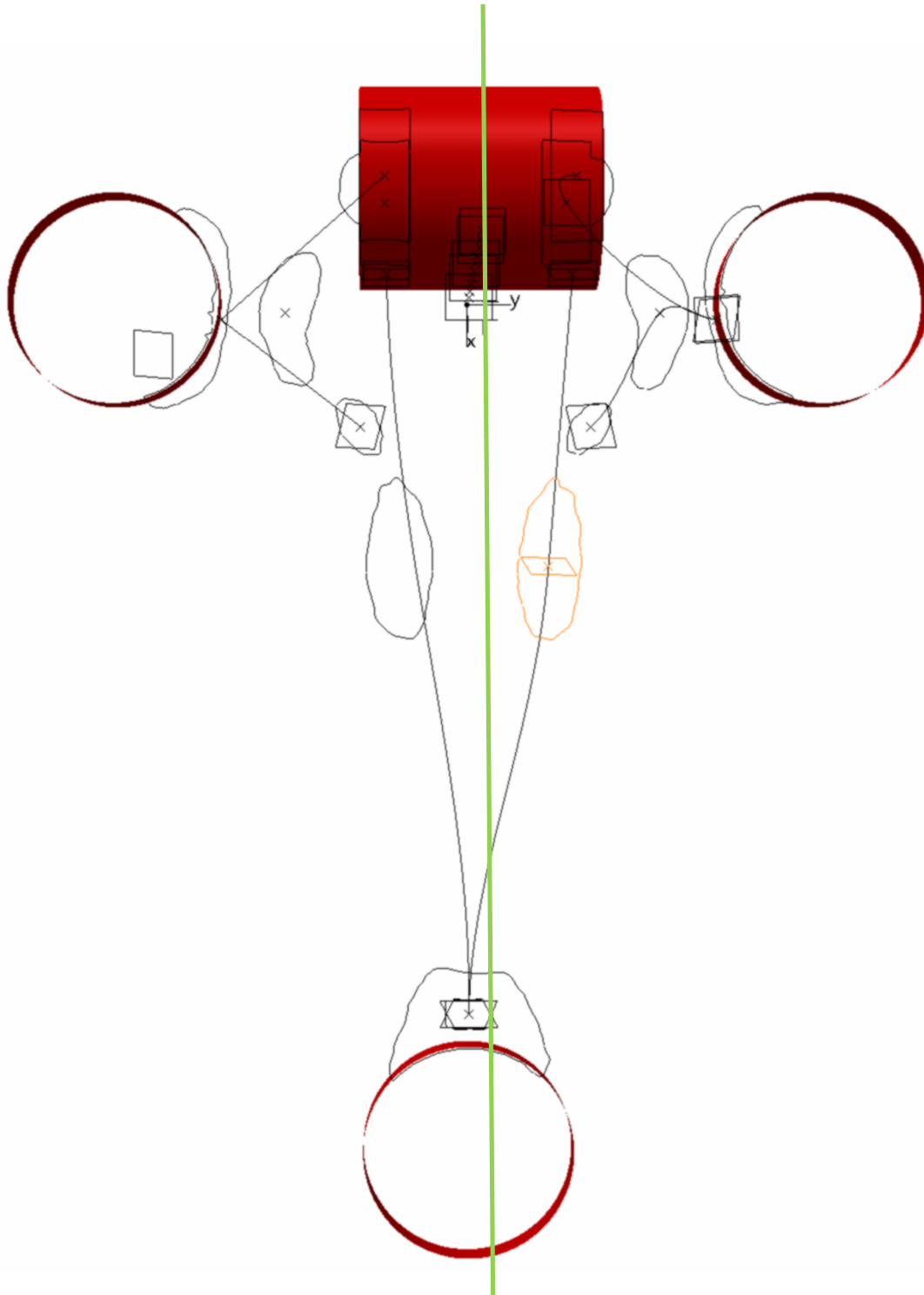


Figure 117 – Showing changes in spline curves (left original, right new) as a result of additional mapped sections and planes at centre profiles (orange)

6.8.2.3.2 Direct STL Derived Control Points

In application, extraction of control points directly from the STL was intended as a fall-back position, due to difficulties with the PCP method which were eventually overcome. Regardless, the direct method was determined to have some significant advantages over the PCP method once research had been completed. The direct method, as the name implies, functions through direct interrogation of the output STL within the CATIA Environment. To do this, it was necessary to first overcome CATIA's unwillingness to work with STL files. Initially methods of importing the STL as a series of disconnected surfaces and combining them into a single surface within the environment was investigated. This works well for small files, but as the order of connection is important to the surface creation and as the size and complexity of the file increases, it becomes almost impossible to maintain the ordering and connectivity without system errors within the program. It was determined that interrogation of the STL was best accomplished outside of CATIA and that functional CAD be imported directly for the investigation. In this manner, a new 3D slicer code was created in Python and the smoothed STL output from Optistruct was then passed through it. The files are sliced at 0.5mm increments starting at 0mm on the XY plane. For parts whose primary axis does not lie on the XY plane, the parts are re-orientated and translated so that their largest areas of attachment are in contact with the XY plane. The slicer creates a series of 2D curve profiles, calculating their total area as it does so. The program then analyses neighbouring profiles (within 0.6mm) and assesses whether their total area is comparable (within 10% total). If verified the slicer extracts the centroid of that area and adds it to the table of centroids presumed to be from a single truss. The process continues until a believed truss length is measured. The code then extracts what it believes to be the mid-point of each truss along with the profile for that point and writes them to an IGES file for export. The IGES line file is subsequently imported to CATIA thus providing an engineer with not only the centre point of each truss but also its presumed profile too (Figure 118)

This method of application does not provide for a direct link between areas, nor does it create the curves required for construction; it simply provides the centre points and profiles to the engineer, ready for implementation. Whilst not as thorough as the PCP, it is more effective for more of the time, is more robust when in operation and is easier to both code and implement. Although the method bears superficial similarity to the Skeletal approach, the code is substantially different and does maintain direct links to the FEM results, thus fulfilling one of the primary criteria for the research.

6.8.3 Automated Surface Generation and Intersection Computation

Automated CAD based surface regeneration is the ultimate objective of design extraction techniques, not only for myriad industries, but also as a potentially lucrative product for the software providers themselves. If a means of accurately and smoothly reconstructing CAD, based entirely upon, or ideally in concert with, global design rules could be created and demonstrated to be effective, it would be leapt upon by most aircraft and automotive programmes as a means of cost reduction and performance enhancement.

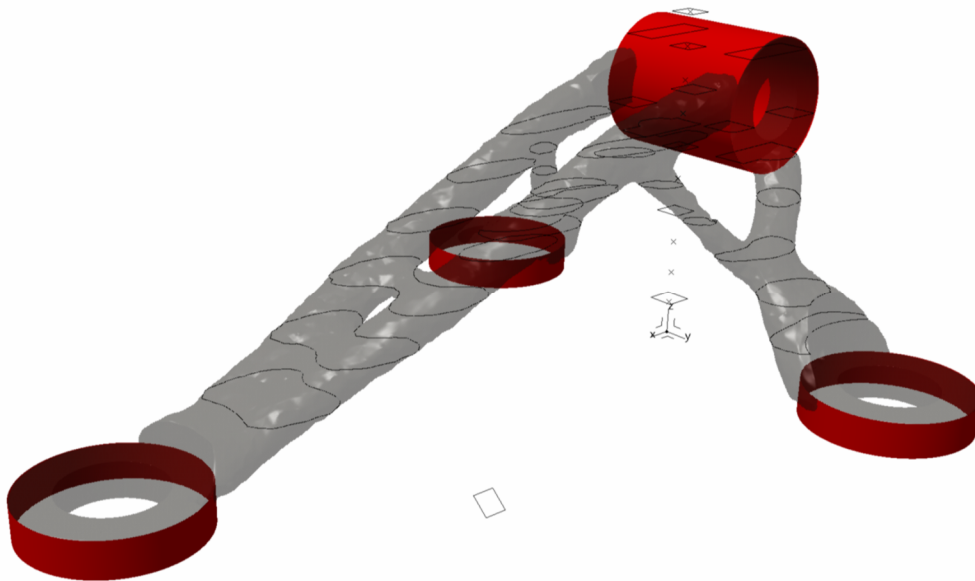


Figure 118 – Imported IGES slice/line data (black contours) for CATIA based upon slicing and analysis

Automated surface re-generation can and has been attempted from a number of standpoints over the years, with the only commonality being that no methods attempted (published or otherwise) have been shown to give sufficient advantage worthy of commercial development in such a potentially lucrative field. Of the methods academically demonstrated but not further, there are two which are believed to have enough potential to be worthy of future study. The first is to consider the automation the T-spline process for surface reconstruction through some form of backwards link to the FEM which in turn feeds a parametric front end for the T-spline software. The second is to build upon the methods developed during this research for the recreation of parametric CAD and to determine how to propagate those surfaces. There is also another potential direction, which is to base new surfaces directly off parameters extracted from the resulting FEM in an ordered and precise manner, later intersecting them to provide a structure.

6.8.3.1 Automated T-Spline Surface Reconstruction

In recent years, T-splines have been used extensively by software vendors to enable rapid design space creation and extraction of TO designs for manufacture via AM. T-splines implementation was previously limited by manufacturing technologies which could not recreate the organic features which typify T-spline use, nor could they be easily adapted to conventional manufacturing methods. AM and more specifically, metallic PB AM, removed this constraint and thus enabled T-splines development and commercialization. T-splines are now present in all major software packages aimed at TO and AM, but in the four years since their appearance, no automated process for implementation and extraction has been released by either the providers, of the academic community. Given the level of effort being placed into T-splines by Dassault, Altair and Autodesk and having spoken at length with all of them during the Airbus review process, it is clear that if this were an easy task, one of the vendors would have completed it and used it to leverage their position with industries such as Airbus and Ferrari. Regardless, no supplier could provide information (one way or another) about their attempts to automate T-splines, but merely expressed the difficulties in doing so and that it was an area of active investigation. Based upon these conversations and personal experience of T-splines, it was believed the major stumbling block would be the parametrics surrounding the iterative definition of control-points for the NURBS which drive the surfaces. T-splines work from a single location and spread outwards to cover the required design space, the growth is iterative and the interactions complex with ancestor points both affecting and being affected by their progeny as the design progresses. Parametrically controlling the available parameters (translation, rotation, affinity etc) at each point location whilst also considering symmetry and connectivity is complicated enough to comprehend and spell out, never mind to code. Ultimately, it was decided that within the time-frame remaining in this research, that a suitably effective development which would satisfy the Airbus criteria could not be produced. Furthermore, it was determined that if indeed the software providers are addressing this topic as they allude to, that they, with their substantial time advantage and their level of available resource, would reach an answer far quicker than if attempted during this research.

6.8.3.2 Automated Parametric CAD Linked Surface Reconstruction

It was initially believed that only minor modifications and additions to the points, planes and curves methods developed earlier, would be required to begin the generation of surfaces based off the construction CAD; this was woefully optimistic and dramatically underestimated the scale of the problem. Through manual experimentation and small stages of attempted automation through parametry, it was determined (based upon evidence from the skeletal process and

repeat manual trials) that advancement of the automated surface generation for extraction would require substantial redevelopment of the already established code. To be effective, points, planes and especially curves would have to be regimentally numbered and clustered during creation in order that they could be robustly referenced for later surface creation. In the early trials, this proved to be a solvable problem using a macro on the CATIA Tree to organize elements without changing their order in the tree. The method relied upon the curve profiles developed in section 6.8.2.3, these curves were then mapped into pairs and swept along their length, creating a series of connected surfaces which can represent a truss in a complex profile shape of between 4 and 8 surfaces.

Though moderately successful, the limitations of the surface function in CATIA coupled with differences in the geometry of the guide curves, meant that on any piece of geometry recreation, fully 50% of the curves might fail to complete (Figure 119). Furthermore, of the curves which did complete, the end points of the curves were not uniform making secondary intersection computation and design VERY difficult, even when performed manually afterwards. Ultimately, the problems encountered with this method were only partially based upon written code, with the other aspect being relate to limitations with CATIA; the former might be solvable with time and effort, the latter would not. Though it is substantially beyond the scope of this research, it is believed that a solution for the robustness issues could be achieved. Even so, the remaining problems at points of intersection would be made more complex to solve and thus would and save little in terms of NRC over a totally manual approach based upon the automated construction geometry already established.

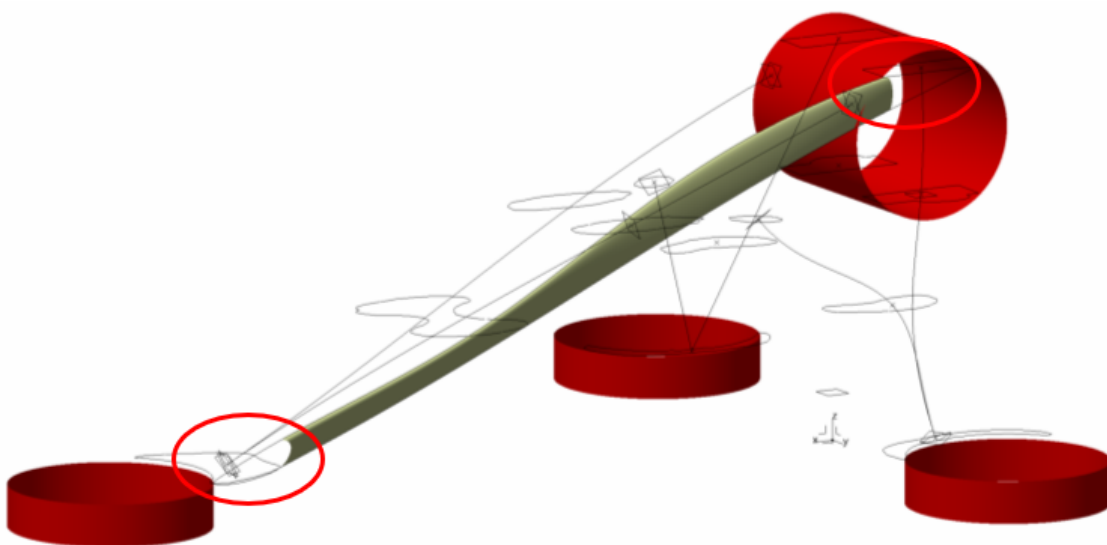


Figure 119 - Failure of manual sweep operations due to complex curvature (Red)

6.9 Skinned Point Cloud Surface Reconstruction

The final method identified was to base new surfaces off the resulting topology output of the FEM and to have those surfaces be created, parametrically in CATIA. Surface reconstruction based point cloud data is not new, and is actually performed in both GEOMAGICs and CATIA (using Quick Surface Reconstruction (QSR)) (Dassault Systems, 2017) but is applied in very different ways. Geomagics works almost identically to how it does when smoothing a topology output. Minor variance is identified and removed and an STL is created over the resulting smoothing cloud. QSR works much more methodically, using the advanced algorithms to visually filter the point cloud data in order to allow an engineer to quickly draft new geometry, it also allows for the total reconstruction of surfaces from cloud data, with varying levels of success. The method investigated as part of this research has greater similarity to aspects of CATIA QSR than it does to Geomagics, but in this method NO smoothing of data is required.

Throughout this project, STL slicing has been performed for a number of reasons but has always been applied in a simple, planar direction at any one time. In this method, the STL is sliced in all 3 major planes, at 0.25mm (this can be altered later) increments. The effect is similar to the image shown in Figure 120 but on a highly refined level and resembles a series of interconnected cubes, like a Lego structure.

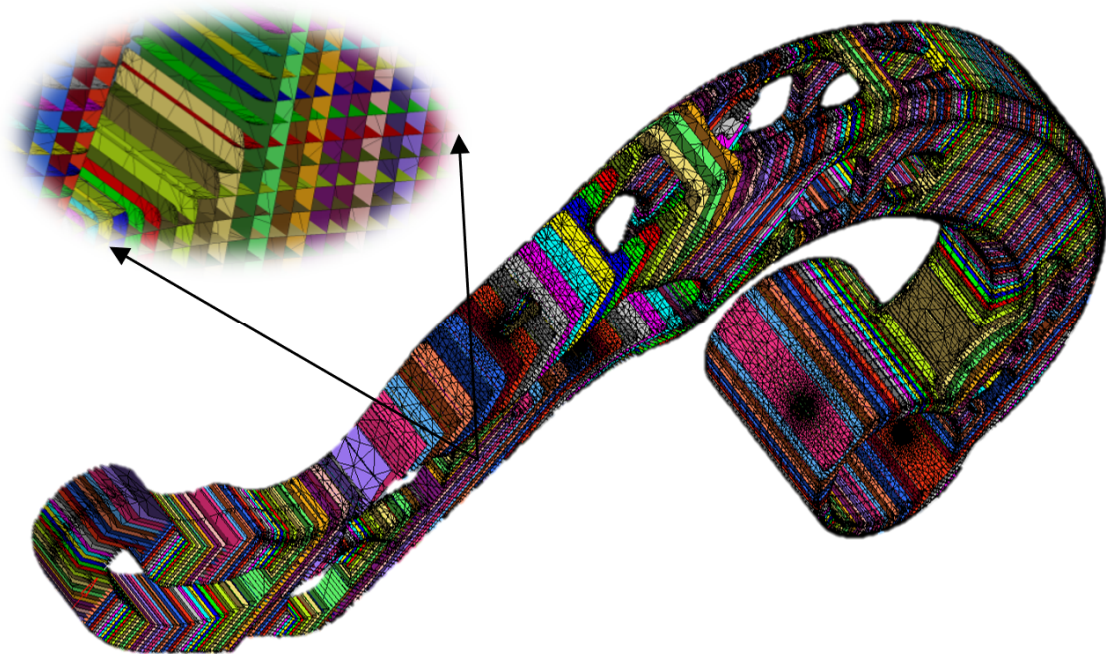


Figure 120 - Effects of multiplane slicing of STR2

The next step was to analyse the resulting data and determine which of the points in each connection in the design space was referenced by less than the full 6 connections of internal neighbouring cells. Cells identified as having fewer than 6 connections were determined to be on the exterior of the design space and were removed, like a peeling a carrot. The resulting topology grid is very smooth with most gradation occurring with linear increments approximate to the thickness of the slice multiplied by the angle to the plane. Once complete the process again scans the STL for node which possess more than 3 connections but less than the full 6, this identifies useful, patterned nodes on the boundary whilst disregarding aberrant elements left during the process. The resulting cloud of points is then imported into CATIA QSR and extremely smooth surfaces for the topology optimised areas are then manually created. The results are both remarkable and fully interactive within CATIA and, when coupled with both the construction geometry and the NDS imported earlier into the CATProduct template allow for rapid extraction with a direct link to CAD (Figure 121). Thus far, no automation of the CATIA reconstruction process has been attempted as there are pressing time constraints within the project and work is already outside the self-imposed scope of the design extraction limits

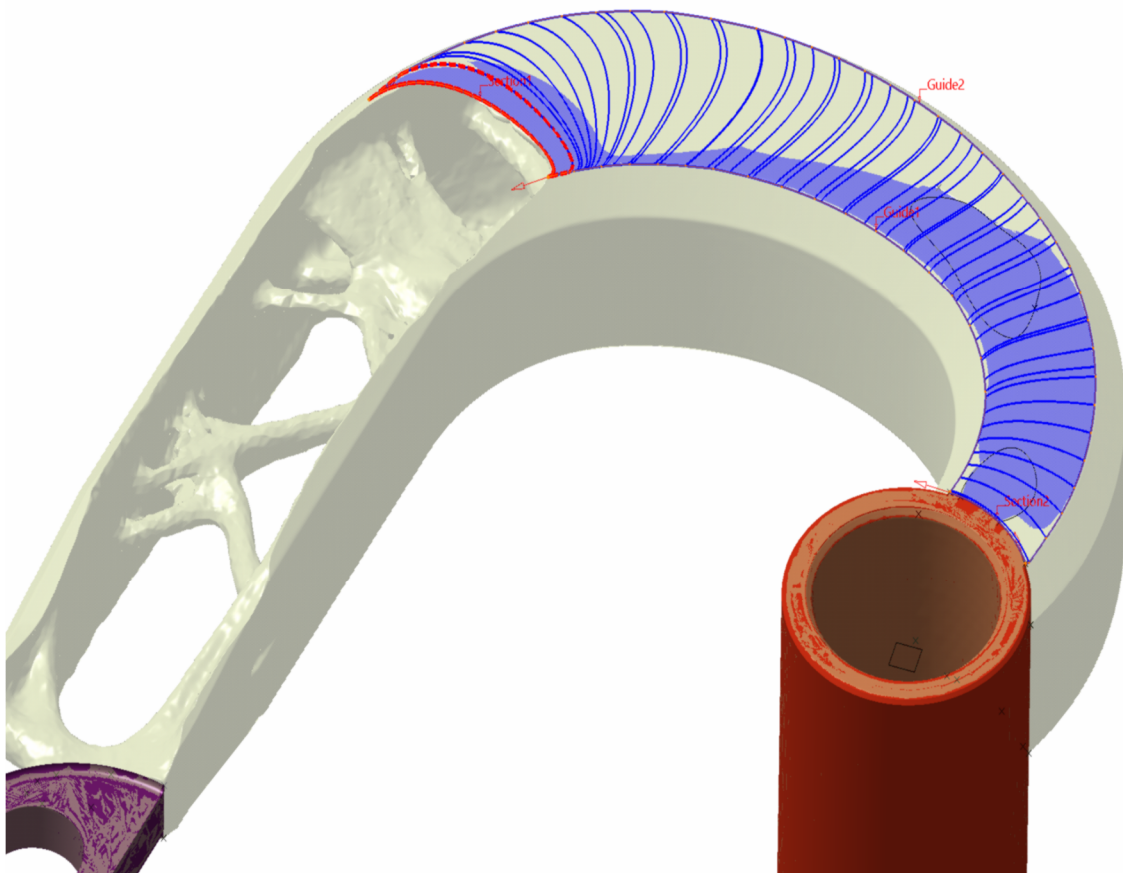


Figure 121 - Results of the skinned point cloud method of surface reconstruction method using CATIA QSR on STR3 the creation of the new surface (blue) can be seen to almost perfectly overlap the output topology

6.10 Results of Design Extraction Methodology on the 5 Candidate Parts

Addressing each of the five candidate parts in sequence and subjecting them to the methods of design extraction specified under sections 6.8.1, 6.8.2, 6.9, the following results were obtained. In each of the linked images below, the resulting automated topology optimization results and the output of the extraction methods are shown side by side (left and right respectively) in Figures (122-126) along with the calculated mass reduction and the averaged time reduction for design process – non-recurring design cost (NRDC).

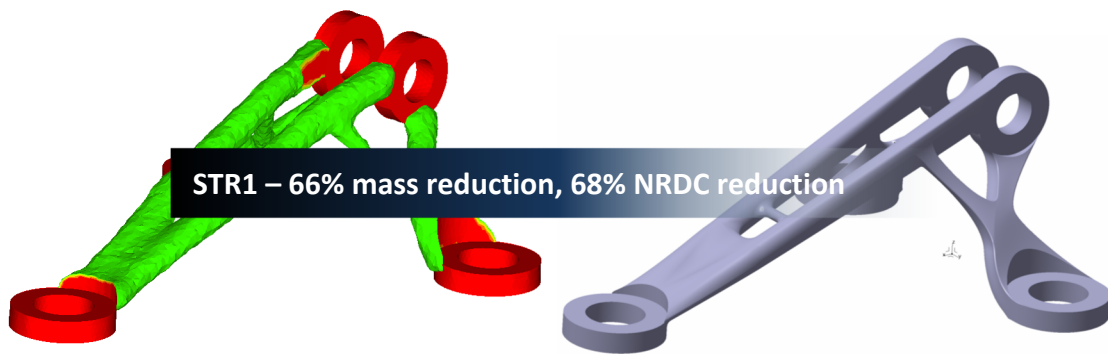


Figure 122 - STR1 TO output (left) and Design extraction enabled by research (right)

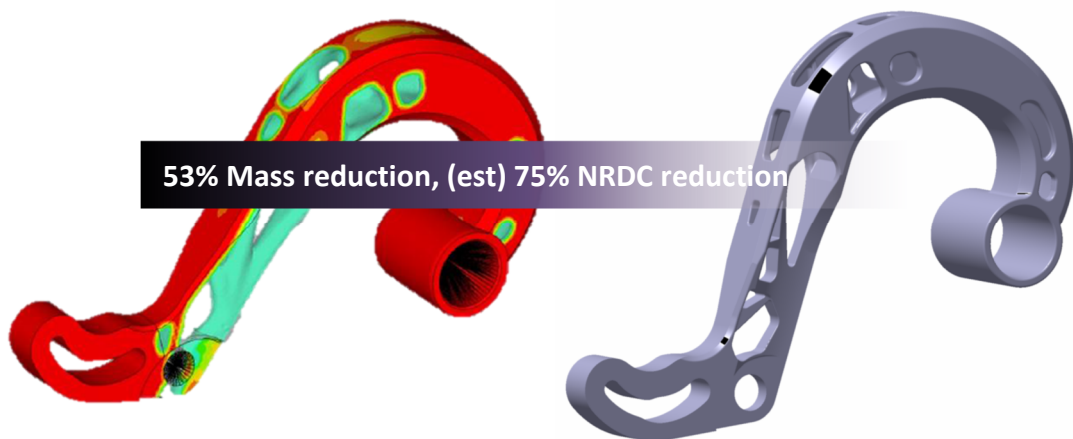


Figure 123 - STR2 TO output (left) and Design extraction (penalised for AM) (right)

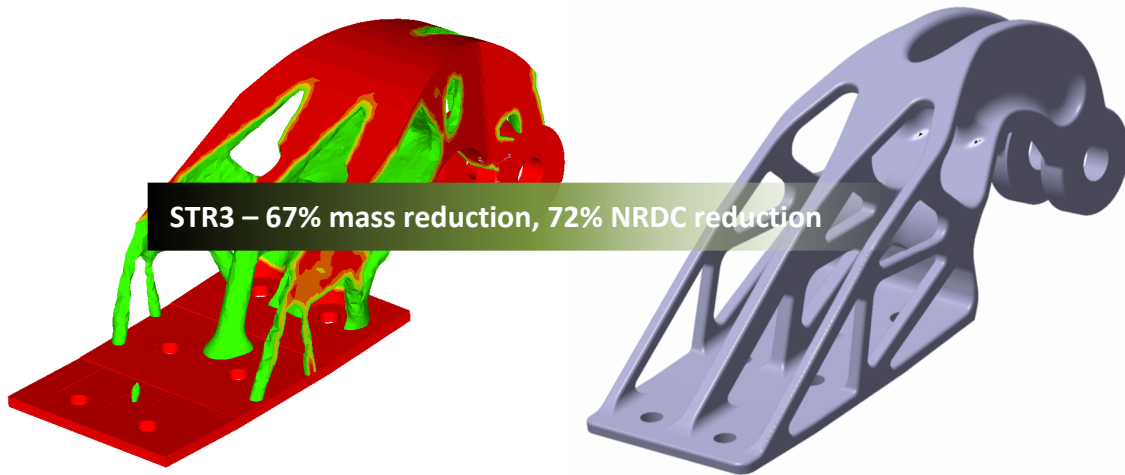


Figure 124 – STR3 TO output (left) and Design extraction without intersection (right)

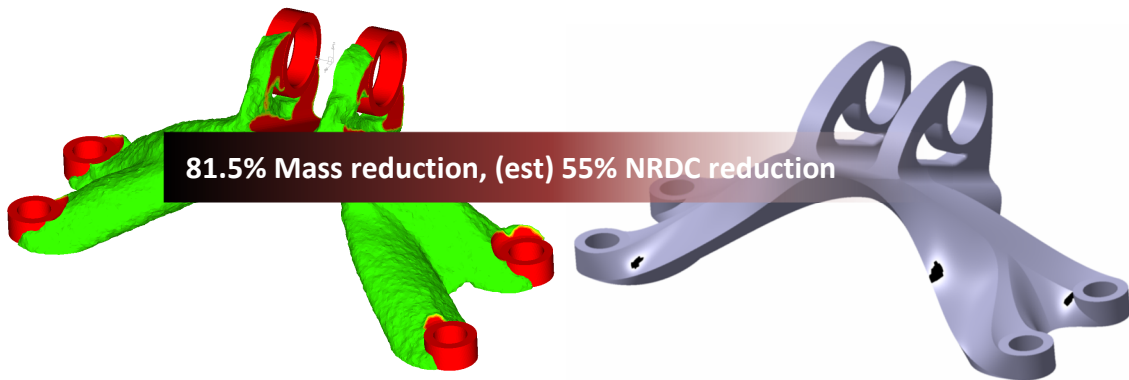


Figure 125 – STR4 TO output (left) and Design extraction without intersection (right)

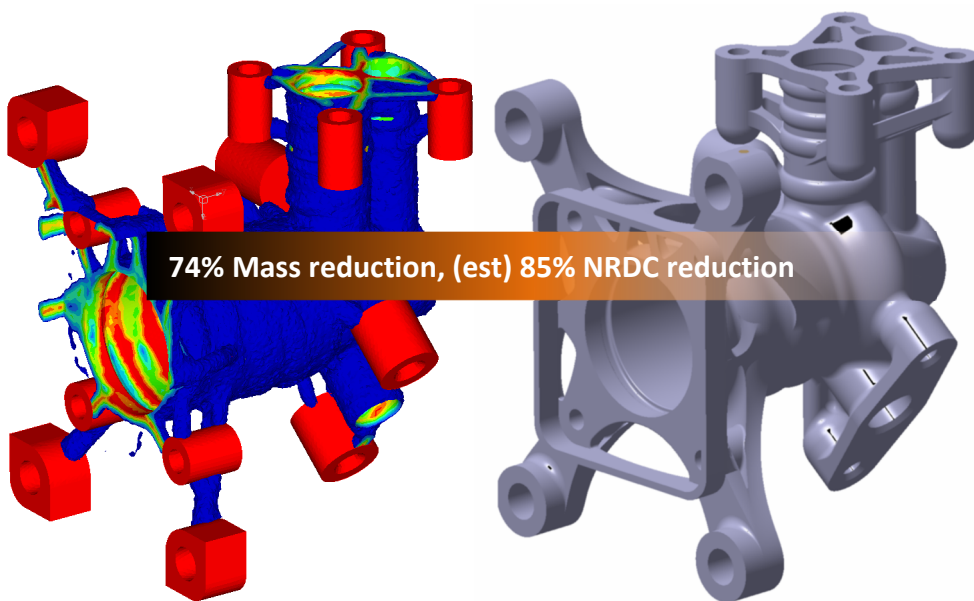


Figure 126 – STR5 TO output (left) and Design extraction without intersection (right)

In addition to the material layouts and progression of design extraction, the time taken to reach the current phase of extraction was also tabulated and cross compared (Table 17) to the time taken for the original extraction. Whilst the results are not directly comparable, they are close and some information relating to the success of the automation for extraction can be gleaned. As the project was at this point no longer funded by Airbus, the ability to assess the previous pool of engineers to determine the effects of automation on a moderately unbiased sample was no longer available. Unfortunately this means that it was impossible to draw direct comparisons to the work undertaken earlier in the research and thus any percentage savings are based upon a single viewpoint with intimate familiarity of all components under investigation, thus (unintentionally) giving way to highly biased assessment of the benefits.

Table 17 – Results of Design Extraction in respect of time taken to complete the task vs manual methods for each structure

Structure	Time Required for Manual Design Extraction (Hours)	Time Required for Automated Design Extraction (Hours)
1	29	10
2	45	30
3	35	9
4	23	5
5	65	31

6.11 Discussion of the Design Extraction Results

As predicted, one of the most complex technical issues was related to extraction of the TO design back to CAD (Section 1.6) using commercially acceptable tools. The extraction task was challenging, and due to the effort involved and time constraints present, remains somewhat incomplete when considering the wording of the Aims and Objectives. Part of this complexity stems (again predictably) from the Airbus driven requirement to achieve CAD parity with the ancestor design, thus significantly limiting the potential for adoption of modern methods or relaxation of the CAD requirement link. The remaining complexity was self-imposed, driven by frustration with the current, iterative design process and the broken analysis/CAD link during the optimization process. Combined, the requirements created an environment with little research guidance available upon which to build and develop. Conversely, the restrictions imposed by Airbus and the requirements to link the FEM to the CAD, did help to focus a potentially sprawling research topic into a number of potential research philosophies.

Initially the research attempted to achieve a quick and easy win using mesh smoothing and direct extraction. It had been suggested (and indeed is still suggested by new software providers such as ParaMatters) that these methods represent the most realistic solution to automated

extraction of CAD for manufacture by AM. Unfortunately, in each of the methods tested, the resulting smoothed STL was either not smooth enough, or had oversmoothed the domain resulting in a loss of feature recognition. As such, the STL smoothing methods were not seen as a practicable solution to the problem of simplified design extraction. Knowing in advance that STL based CAD would be difficult for Airbus to integrate into the design framework, research on the Skeletal approach proceeded in parallel. The Skeletal approach was initially intended to be a small step back from the direct approach, using the STL to develop circular parametric CAD profiles and then using multi-sections to link those surfaces together. Envisioned as an easy step from 2D to 3D, the application fully underestimated the problems of complex 3D geometry in a design space largely based upon pre-formed, projected 2D elements. Whilst successful in delivering results in STR 1 and STR3, the approach was a complete failure on the remaining candidate parts. However, what the approach did succeed in, was to prove that a means of intelligently interrogating the STL output from TO and converting that into data for the formation of parametric CAD, was both possible and practicable as a means of progression. Evaluating the feedback of Airbus and the successes/failures of the skeletal approach, a more systematic method for parametric design extraction was formulated around the premise of aiding the designer, rather than replacing them.

From the breakdown and the results, it can be seen that by targeting common features for all extraction problems and doing so in a means which provided (within the CATIA environment) modifiable construction CAD to the designer, significant savings in NRC design time have been found along with a dramatic increase in process robustness. Currently the tools for extraction are based upon sequential activation of a series of Python based scripts for slicing, analysis and intelligence gathering and then CATIA macros for parametric CAD creation. They are not linked and must be ran individually and sequentially after the STL file has been output from TO, fixed in MAGICS and exported again as an ASCII STL. Whilst each step ultimately saves time in the design cycle, the finding, modifying and running of each code batch adds time and complexity which would deter their use. Were more time available, linking of the code through either Python or model centre would be undertaken, thus providing a smoother interface.

Of additional note are the latter developments surrounding the Skinned Point Cloud Method (SPCM). Whilst still in their infancy at the time of completion, these methods have the potential to accomplish exactly what was attempted in the early stage using the 2D skeletal approach, but in 3D and with significant increases in applicability and, potentially robustness. There are a number of predicted limitations to the SCPM, most notably that it has similar problems to the mesh smoothing in that the design volume will decrease as the model is skinned.

It is believed that this can be somewhat overcome by extracting a lower density threshold STL from the optimiser (~30% rather than the usual 50%) thus compensating for lost volume. A further problem relates to the combination of grid size, minimum member control within the optimiser and the slice layer thickness. A smooth output is more beneficial, but requires a fine grid, which in turn requires high density slicing to achieve the required tolerance. All combine to make for a complex and costly post-processing operation, particularly when in the CATIA reconstruction environment. It is also worth considering that the QSR toolbox within CATIA is only available on the advanced license (AL3) package at Airbus for which there are few licenses due to cost. Use of the AL3 is prohibited except for advanced CATIA users. Regardless, it is believed that the SPCM could achieve as high as 70-90% automated extraction using the methods defined, leaving only small interfaces and intersections to be completed manually on CAD that is fully interactive with the design environment.

6.12 Summary of Automated Design Extraction

As predicted, design extraction proved to be the most technical and difficult task of the whole research project. Balancing Airbus' requirements for all design work to be undertaken within the CATIA environment with the self-imposed goal of parametrically bridging the gap between FEM and CAD, the research was complex. After several partial successes looking to recreate generic truss based geometric connections in 3D space, a more fundamental approach looking to aid rather than replace the designer was undertaken. The developed automation processes function via direct interrogation of the STL output of TO, gathering information on common features to create construction geometry to enable rapid regeneration of the TO output within the CATIA environment. The developed tools, automatically create points, planes and lines of intersection upon areas of the NDS, whilst extracting areas of profile data which can be used as further seed points for surface and line generation. The Surface reconstruction is NOT attempted automatically due to complexities in CATIA surface generation. In the latter stages of research, a new approach to surface reconstruction using a method which approximates the peeling of the outer skin from the part (to generate a smooth surface for reconstruction) is attempted and discussed with promising results.

In use, the combined tools (not including the latterly developed peeling model) generate significant time savings, but are currently an expert level process, requiring of further development before rollout to a wider community. (Objective 4)

7 The Effects of Full Automation Implementation into the Design Process.

As the work undertaken during this research project has been significantly affected by project politics within Airbus, there are several smaller results sections within it which are coincident with each completion point. These completion points are roughly centred around the pre-processing and post-processing elements of the complete design cycle and the development MMP. These sectional results are important, in and of themselves, but do not paint a full picture of what has been achieved within the project as a whole and whether the research successfully accomplishes the Aim to reduce the design time for optimization driven design process.

7.1 Introduction

By this point in the project, only the baselines established on STR1 and STR3 can be used for comparison to both the initial state-of-the-art and the effectiveness of the MMP as these are the only structures which were optimised by myself at each stage. As such, all economic analyses and conclusion will be based upon STR1 and STR3 with extrapolation drawn to the other components

7.2 Methodology for Establishing Baseline Costing for Conventional and Optimization Driven Design in Airbus

The aim of this research was to provide for a new means of cost effectively employing TO on small components intended for production via AM. Cost effectiveness in this context means that the mass/cost of material saved must be greater than the cost associated with the significant increase in design time for the use of optimization and advanced design. To establish a baseline against which to compare the developed process, STR1 and STR3 were shown to staff from Airbus Rapid Spares, who were then asked to provide (without bravado) an approximate time for design, assessment and design for manufacture for each of the two components. (Table 18).

To provide the TO baseline, each of the two components was also manually optimised by the researcher. This exercise was performed at the start of the project (thus without the MMP or template) in an effort to balance the numbers in the survey, but also has the effect of mimicking the interaction that someone unfamiliar with the component might have during the first encounter. This can be seen in Table 19. Together this gives two baseline numbers, a conventional design with cost (part cost + design cost) and weight and a manually optimised design with similar costing and mass fractions. For the purposes of this investigation the machining hourly rate are be calculated at €55/h for both machining and for AM and machines for production are assumed to be fully amortised at his point in service. Media cost is calculated

at €55/kg for billet and €150/kg for powder. These figures are consistent with Airbus purchasing in 2016.

7.3 Results – The cost of Design and Manufacturing without Automation

Table 18 - Breakdown of time required for the design, assessment and validation of ST1 and STR3 using manual methods and the most skilled CAD operators

Task	CAD Operator							
	MM	1	2	3	4	5	6	7
STR1 Design	29	15	22	18	31	35	14	11
STR3 Design	35	19	35	21	29	30	21	36
STR1 Assessment and Validation	3.5	8	7	3	6	3.5	7	6
STR3 Assessment and Validation	5.5	7	4	5.5	6	4.5	5	3

With a baseline for conventional design time (and thus cost) established, The time required

Table 19 - Showing the costing of each process using equations and base input costs found in Appendix D - Calculations

	STR1 Conventional Design and Manufacturing	STR1 Manual Design Optimisation and AM	STR3 Conventional Design and Manufacturing	STR3 Manual Design Optimisation and AM
Component Mass (Kg)	0.45	0.15	0.91	0.3
Buy 2 Fly	5	1.15	8	1.25
Raw Material Cost €	275	161	440	175
Machining time (hours)	3.5	0.5	6.25	1
AM Hours	NA	1.5	NA	9
Machining cost €	192.5	27.5	343.75	55
Total Design Time (hours)	7	51	8	65
Total Design Cost €	560	4080	640	5200
Total RC €	467.5	271	783.75	725
Total NRC €	560	4080	640	5200
Total Part cost (1000 aircraft) €	468.06	275.08	784.39	730.2

The results shown in table 19 clearly show the dramatic increase in NRC for design, but overall show a reduction in cost due to the use of AM for manufacture of the new lightweight component.

7.4 Discussion of Conventional Design Costs

Whilst design cost does increase almost 800% in both cases, the effects of those cost increases are somewhat negated by the high volume of aircraft over which the costs can be spread. In such circumstances, RCs are of far more importance than NRCs. Were that aircraft volume to drop, the NRC for design would have a much greater effect on the individual part cost than it does in table 19.

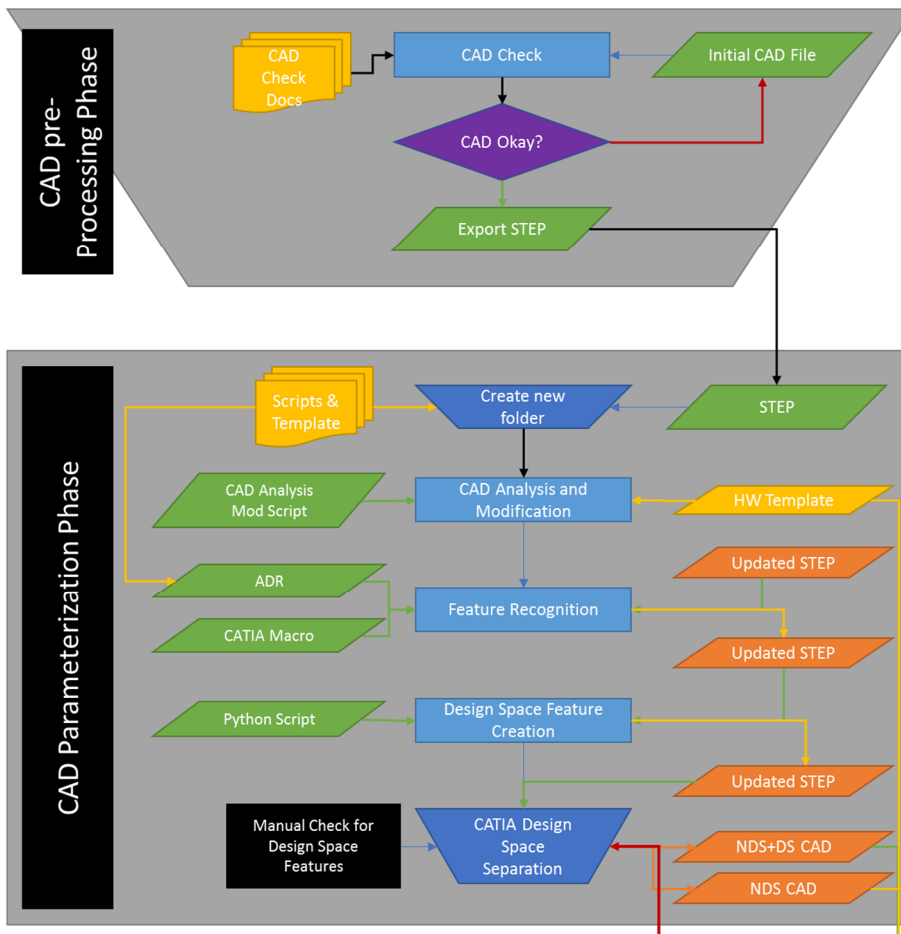
7.5 Does Automation Reduce the Cost of Optimization Driven Design?

The results shown in section 5.11 demonstrate that sequential automation of several pre-processing phases, coupled with adherence to a governed cycle for TO application and common template for optimization defaults, led to significant increases in robustness, efficiency and commonality between engineers. Earlier Sections also show the time savings attributed to the effects of automation on post-processing phases, particularly in the early stages of design extraction.

7.6 Methodology for Testing if Design Automation Reduces Component Cost

Whilst the results of the previous sections show the potential of the automation, for a number of reasons, it is difficult to summate the effectiveness of each section in order to provide an answer as to whether the aim was met. First, each of the sections test their results in different ways – this was due to Airbus cancelling internal funding and thus not being able to use Airbus staff to validate later work. The second relates to the manner in which each sample effectiveness – the automation does save time on each sub section, when running, but to get the automation running requires some manual editing and running of each automation script. Also, as the software is still effectively a prototype, and thus results must be carefully checked before acceptance. This time needs to be accounted for, even if it will later disappear in a full rollout version. As such, it was decided that STR1 and STR3 were to be assessed by the researcher using the methods of the automation processes as defined in Figure 127. Using the same calculation methods as earlier, this provides the total cost (time + manufacture) of design using the automated methods. The results of the process are shown in Table 20. In comparison to the earlier methods, there is a notable drop in design time vs. the manual approach for TO.

Semi-Automated Mapped Manual Process for Topology Optimization



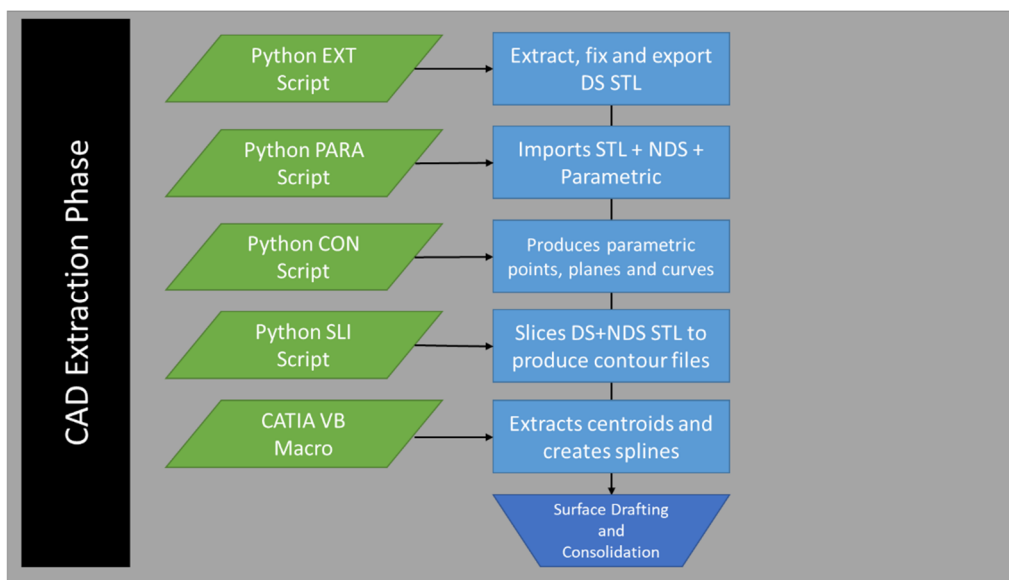
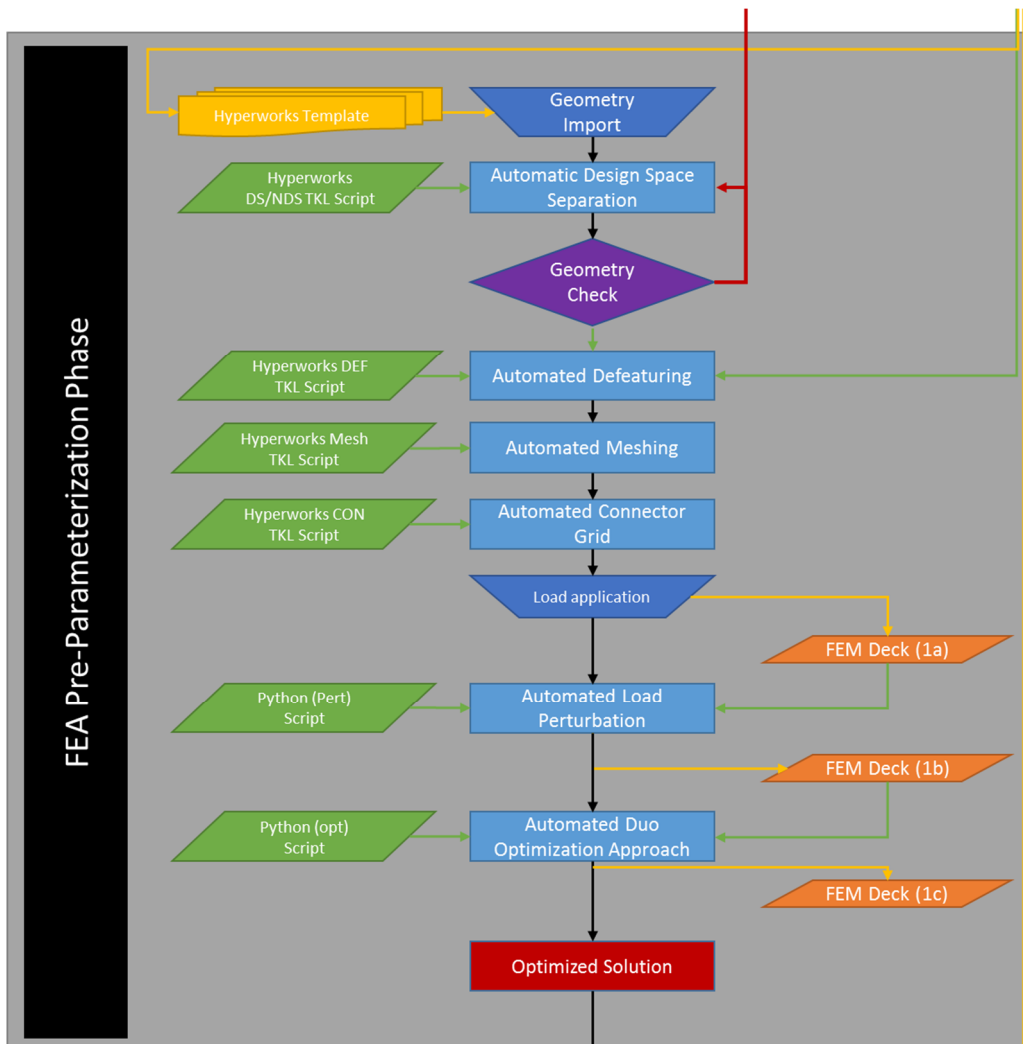


Figure 127 - Final flow-process showing the semi-automated approach to topology optimized design.

7.7 Results of Automated Design Processes

Table 20 - Final calculated costs and times of each of the 3 processes when tasked with optimization and design of STR1 and STR3 and showing the dramatic reduction in NRC stemming from optimisation and design.

	STR1 Conventional Design and Manufacturing	STR1 Manual Design Optimization and AM	STR1 Automated Design Optimization and AM	STR3 Conventional Design and Manufacturing	STR3 Manual Design Optimization and AM	STR3 Automated Design Optimization and AM
Component Mass (Kg)	0.45	0.15	0.17	0.91	0.3	0.3
Buy 2 Fly	5	1.15	1.15	8	1.25	1.25
Raw Material Cost €	275	161	161	440	175	175
Machining time (hours)	3.5	0.5	0.5	6.25	1	1
AM Hours		1.5	1.5		9	9
Machining cost €	192.5	27.5	27.5	343.75	55	55
Total Design Time (hours)	7	51	16	8	65	18
Total Design Cost €	560	4080	1280	640	5200	1440
Total RC €	467.5	271	271	783.75	725	725
Total NRC €	560	4080	1280	640	5200	1440
Total Part cost (1000 aircraft) €	468.06	275.08	272.28	784.39	730.2	726.44

The results shown in Table 20 show an almost 75% reducing in NRC design time as a result of the application of Automation to the process of optimization driven design, but on this volume of aircraft, do not dramatically alter the price due to the quantities involved. On a smaller number of orders (A380) the effects would be notable.

7.8 General Discussion

7.8.1 Introduction and Overview of Results

The results of this research span four distinct sections, one which considers the identification of appropriate targets for automation (Section **Error! Reference source not found.**). Two more concerning the development of strategies for the automation of TO (Section 5.11) and the extraction of its output back to CAD (Section 6.10) With the final section detailing the effectiveness of those automation processes at reducing the total cost of component development and production using AM (Section **Error! Reference source not found.**). There are also several smaller results sections concerning material properties, design allowables, etc (Sections 4.6.5, **Error! Reference source not found.**).

7.8.1.1 Results of Automation Target Selection

Addressing the major sections first, the results begin with a sample of UK based Airbus TO users. These staff members form the expert community, usually charged with the investigation of analysis driven design when corrective/innovative solutions to problems are required. Given their familiarity with the toolsets and the frequency with which they use them, this pool formed the perfect foil against which any automation software should be matched. Conveniently, they also the perfect population from which to determine areas of excessive time consumption during the TO process. This user pool was asked to assess the 5 candidate parts noting both where time was lost, and also where experienced staff were completing mundane/required tasks that require little skill or judgement. Once cross compared and summated, the research revealed the three ideal targets for automation: Parameterization (formulation of design space, vs non-design space, the definition of the loads, constraints, materials, additional forces etc); Extraction and FEM Generation.

7.8.1.2 Results of Parameterization and FEM (pre-processing) Automation

During this section the complete breakdown of the pre-process phases along with their inputs, outputs and relationships were accomplished. Performed through mapping of actions undertaken by members of the Airbus user pool, these individually identified phases were used to determine accurate automation targets in (those most appropriate) the pre-processing phase. Of these, the first was automated feature recognition as a pre-cursor to design space separation, with rules and measurement practice driven in accordance with Airbus global design rules. Next was the creation of a specific template for use in optimization tasks, complete with measured and verified material and process data for myriad AM platforms. The section completes with Automated design space separation, loading perturbation and attempts at constant mesh density

topology optimization. The combined outputs of this phase have significant effects on the time required for optimization parameterization and the robustness/uniformity of the final output.

7.8.1.3 Results of Design Extraction Automation

After investigating various approaches and strategies for design extraction, a method for executing partially automated design extraction with full iteration with Airbus tools and process was accomplished. Through an interrogation of the resulting FEM output from TO, a means of automatically creating CATIA based construction geometry was extracted from the grid and tested with good results. The scripts and macros developed in sections (4, 5 and 6 and listed in Appendix C – Coding and Scripting) allow for rapid recreation of TO designs within conventional CATIA design environments and thus allow for (with careful CATIA tree management) the complete automatic update of resulting CAD in response to a change in optimization requirements.

7.8.1.4 General Results

The purpose of the general results section was to determine if indeed the automation of various stages of analysis driven design had been effective in reducing the combined costs of advanced design and manufacture. The results demonstrate the dramatic difference that the new automation tools have on the total non-recurring cost (NRC) for the part. Compared to the original, manual approach to the design process for STR1 and STR3, a reduction in time (and thus cost) of almost 75% is shown (Table 20). Over 1000 aircraft the cost savings are dramatic for the combination of AM and automated TO on STR1 with a recurring cost (RC) saving of almost 40% and a mass saving of over 65%. For STR3 the results show a more modest saving in cost as the RC cost for the AM part is high (the part is large and so fewer can be built at the same time) but still, a saving of ~7% is demonstrated whilst reducing mass by over 65%. NRC is however always easier to distribute on a larger number of components for a higher volume of aircraft (A320), but the redesign of components for large, lower volume aircraft such as A380 has always been difficult to economically justify. The research shows that by dramatically reducing the cost of component redesign, a larger number of potential parts can now be designed reducing both aircraft mass and manufacturing cost. The demonstrated effectiveness of the developed automation tools and their application to the Airbus design process completes the primary research aim of this investigation along with Objectives 9 and 10 of the Secondary Research Objectives.

8 Discussion, Conclusions and Future Work

8.1 Technical Accomplishments

At the outset of this project a single aim, four primary and five secondary objectives were set. Of those, most could be considered technical and of those, all were met. In addition, there were several additional technical tasks which, whilst not objectives in their own right, were important to the final work. The details of these accomplishments are recorded below.

8.1.1 Introduction and Integration

In attempting to introduce a relatively automated form of design using a combinatorial application of two novel technologies, the research undertaken within this project is moderately complex when studied in isolation, but when studied in the notoriously stayed and risk-averse context of commercial aerospace, becomes substantially more difficult. In order to somewhat mitigate these factors, significant attempts have been made to develop these methods in a manner most suited to Airbus' current processes and their future development needs. As such, one of the greatest technical accomplishments of this project relates to its ability to use existing tools within the Airbus domain, thus achieving novel design methods within the existing framework allowing for near seamless integration.

Additionally, by including Airbus staff (both users and controllers) from the earliest phases of experimentation, Airbus have been aware of the software development for some time. Indeed, whilst the latter stages of the project are (technically) unsupported by Airbus, Super-users within both Optimization and Methods and Tools have continued to provide support and feedback on developments in order to ensure that they can, if wanted, be integrated into the roadmap for future projects.

8.1.2 Identification of Primary Targets for Optimization

By working with/for Airbus in the development of these automated processes, it was logical to base the targets for optimization off an assessment of those users who would eventually use the software. Identifying a pool of potential candidates, some 50 were approached with 30 eventually selected as participants. A detailed questionnaire was created which, after performing the optimization on a series of the candidate parts, was answered by the participants. By cross comparing the results of several questions, suitable targets for automation were mathematically selected.

8.1.3 Airbus Specific Feature Recognition and Design Space Separation

Feature recognition is available in many CAD packages, but does not commonly identify all features which would be of use to an optimization definition. During this research a means of

identifying features such as bolts holes, radii distance, flange thickness, etc were developed for use within CATIA. These elements then form the basis of the non-design space elements used in the optimization definition. After recognition and export from CATIA, the features are interpreted by a python script which calculates the correct application of Airbus Design Rules to the part, creating additional separation surfaces for later use. The resulting step file can be subsequently imported into back into CATIA (or Optistruct) and used for modification of a very simple EDS model, thus creating a simple DS/NDS domain for use in Optistruct and eventual extraction.

8.1.4 Forces Splitter and Loading Perturbation

Noting the propensity of structures optimised for a single or dominant driving load cases to deliver outputs which are potentially fragile under slight changes in load application, a system which automatically analyses, separates (into component forces) and then perturbs those loads into a series of concurrent load cases has been created. The process adds substantial robustness to the output design without significant effects on either solution time or mass reduction.

8.1.5 Hyperworks Optimization Template

Whilst sounding rather simple in description and requiring only the input of a series of numbers, the creation of the optimization template and the derivation/determination of those input values was one of the more time consuming and costly aspects of the project. Required not only to increase robustness, but also to ensure the validity of material properties throughout the domain by accurately and effectively controlling geometric sizing for AM, the values for the template were painstakingly generated. To determine these values an in depth understanding of both the material performance and the machine production capability was required. Problematically, Airbus has several component suppliers in multiple locations with access to myriad different AM platforms, thus to provide suitable numbers for material properties and geometric performance, multiple platforms were tested using a common build and analysis technique on a single material.

8.1.6 The Mapped Manual Process

Although rather simplistic in nature, the MMP is an invaluable tool, not only for the identification of relationships between phases, but also for the education of staff and for the later use of automation processes within the design loop. The MMP is now in active use with 3 BUs.

8.1.7 Automated FEA Linked Parametric CAD Extraction Methods

Believed to be a first in the field, the methods developed in this research provide for a full, parametric CAD link between the input geometry, TO output and the framework for the new design. By analysing co-ordinate geometry at common points between the DS and NDS areas,

parametric construction geometry to aid in the design extraction is automatically created. In addition, a series of sliced contour profile provide for a means of almost direct interaction with the STL within the CATIA environment. This is highly uncommon and has not been witnessed in operation by anyone in the Airbus CAD community.

8.1.8 Skinned Point Cloud Methodology

Using a multivariate slicing method at a high enough resolution so as to be below the minimum element sizing the method allows for the removal of the rough outer skin of a part by effectively gridding the total structure and removing boundary noise up to a level provided by the slice thickness. The effect is the creation of an almost uniformly smooth series of surfaces with exceptional resolution and full interactivity not found with either morphing or wrapping techniques. Though it requires further work, the initial results are extremely promising.

8.1.9 Material and Geometric capabilities for AM platforms

In order to create a template useable in all circumstances where a part is intended for production via AM, stable, homogeneous material properties which align with Airbus AIMS and API documentation were required. Though a bespoke build and testing arrangement, performed on multiple AM platforms, geometric capability and material properties for Titanium6Al4V Grade 5 were determined and included into the HW template in order to reduce variance and speed development.

8.2 Conclusions – Research Strengths and Limitations

8.2.1 Cost implications for Automation

When considering the general results and the effectiveness of the undertaken research in addressing the aim, it can be seen that whilst the steps undertaken to automate the process have achieved significant savings in required design time, the total cost of design is still higher than for the ancestor process when considering both components. However, this is perhaps an unfair comparison as several factors combine to skew the results in favour of the conventional design and manufacture approach. Firstly, by using Airbus Rapid Spares for conventional design assessment, the resulting design time estimate is extremely low. The reason for this is that the RS team are some of the most experienced designers within the Airbus perimeter. Secondly, the costing assumes that all sequential design processes are achieved seamlessly and with no loss of time, which is unrealistic at best. Thirdly, the automated process time for design currently takes into account the time required to find, modify, stage and execute each automation code. It also includes time required to check its output upon completion. In a full tool rollout, these aspects would be solved through the combined application of the tools through a single, linked interface. Finally, in comparing the original design to the newly optimised one, no consideration for mass

(other than the reduction of required powder for AM) is factored into the cost calculations due to Airbus' current focus on cost and not mass. Historically however, when a new aircraft variant is being introduced, mass reductions can be valuable and when considering that each component optimised as part of this research saves a minimum of 40%, those cumulative savings could well be hundreds of KG and thus millions of Euros.

8.2.2 Robustness and Variation

It was known from the literature that automation was often sought, not to reduce costs, but to either maintain them in the face of increasing labour, or, through standardisation of inputs, to reduce variation or process outputs. Whilst (at least initially) not actively sought as part of this research, the effects of automation on process robustness were considered for the first time when analysing participant optimization data (Section **Error! Reference source not found.**). The data showed an unexpectedly wide spread of optimization responses from a group of people who were ostensibly optimizing identical structures and were trained to use of optimization (by Airbus) in a very specific way. Airbus themselves were surprised by this data spread as it is something (variation between operators) which standardised tools and processes are designed to limit. The reason for this variation was ultimately determined to be human, related not to the tools themselves, but the methods and order in which they were used. The development of the MMP was performed in such a way as to mitigate these effects, by first standardising and then automating as many aspects of the process as possible. When the MMP was ultimately tested, it was tested in such a way as to replicate the original survey sampling methods. This time, it was ensured that each participant optimised different parts to their previous assessment, thus limiting the potential for skewed results through participant familiarity. The effects of the MMP and the application of pre-process automation were dramatic, substantially reducing variability between users from the optimization process. In some cases, variability was reduced by over 70% when compared to standard use within the Airbus community. These results were a notable strength of the research and something which Airbus were very happy to see and ultimately use in order to achieve commonality between staff and future programmes.

8.2.3 Structure Types

At the outset of the project an analysis of potential candidate parts was undertaken. In order to be considered, the parts had to be small enough for AM (Section 2.1.4.3.1), made from titanium or steel (with potential to shift to titanium) (Section 4.3), of low safety classification (Section 2.1.1.1) and of acceptable rate for production with AM. The vast majority of the down-selected components are directly structural in application (usually brackets) and thus are possessing of some degree of commonality in design features. The reason for this commonality stems from

the manner in which Airbus designs and manufactures its Aircraft and more specifically, how it engages with its suppliers and for certain aspects of design and manufacture. Airbus designs and manufactures (through risk sharing partners) almost all of the structure and thus the designs and attributes for all those items are readily available in the part catalogue. However, the vast majority of system components (including those with structural aspects) are designed and made by suppliers working to Airbus specifications. Component geometry for these parts is not directly accessible within the PRIMES (AIRBUS CAD Storage) database and thus were not acknowledged as potential candidates until much later in the project. Resultingly, the developed software for automation has been developed with predominantly structural type bracket components as the targets for development and verification. When attempting to run the developed pre-processing software on non-bracket components in early 2016 (AMALGaM Project), it was found that when given a small manifold to assess, the performance of the scripting was degraded due to significant quantities of additional cylinders (the internals of the manifold) being recognised as bolt holes. In an attempt to address this limitation, STR 5 was replaced (after the MMP creation) with a fictitious manifold candidate part and included in the AM design training course. Its inclusion in this material was an attempt to rapidly generate data to be compared to original sampling. The AM Design Training allows Airbus engineer to come to AGI to be trained in AM, Optimization and Design for AM. Over 20 design courses, 40 teams of engineers (4 people per team) have attempted to optimize and extract STR 5 within the 4 days of the course ready for manufacture on the 5th. The data provided by the staff on these courses has been invaluable in determining the effectiveness of the MMP and the automation tools for systems components without project budget from Airbus.

8.2.4 Software Limitations

At the outset of the project, the current/prolific versions of each software type, which allowed interface into Airbus were standardised and used for all testing and development (Section 0). Sadly, whilst CATIA has remained current, thus preserving all CATIA developed macro coding, the interfaces to other software will need to be further modified before rollout. The current Airbus Python codes are 2.7 and 3.4 and the allowed versions of Hyperworks are v13 and v14, thus differing significantly to the established version control within the project. This will be an ongoing problem with almost any developed software which interacts with commercial codes. Not only will compatibility have to be checked but the outputs of any linking will have to be verified as stable between those versions, thus ensuring continuity. Predicting these issues and where possible, file inputs and outputs have been abstracted from the software in which they were generated by using open source formats such as STL, IGS/IGES and STP/STEP formats. This not

only allows for continuity, but also, at least potentially, for the use of codes/packages other than those specified. Doing so however would significantly degrade the parametric capability of the final design extraction automation as it is specific to the CATIA means for parametric design.

8.2.5 Automated Meshing

A major limitation of the research and one which significantly affects either the speed of solution or the performance of the TO process, is that related to automated meshing. The automation and control of meshing within Hyperworks is relatively straightforward so long as an (relatively) uncontrolled tetrahedral volume mesh is sufficient for analysis purposes. The only things required to create the grid are a link between minimal geometric features and values for Min/Maximum element size as completed in Section 5.3.3.1. Within this research, the two values are near identical with max set at the minimum element size (as determined by thickness analysis) +20%. This is hugely computationally inefficient with grids for small part routinely in excess of 8m cells thus taking a long time to solve. The proposed solution to this was through use of constant mesh density topology optimization. Unfortunately, the automation of this approach was never completed as the process was difficult to enough to perform manually due to the nature of the re-analysis mesh quality. Had this element been completed as part of the project, it is believed that solution time would have been reduced by ~70% vs more conventional methods. This aspect was not part of the original objectives, but was investigated as a potential avenue for future research.

8.2.6 Material and Production Data for Hyperworks Template

Having investigated the wealth of published material data on AM, along with the data emerging from AM testing and qualification as pursued by Airbus, it was determined that there was insufficient evidence across multiple platforms to provide for generic inputs into the HW template. In order to allow for the introduction of this research into the Airbus community and to further the acceptance of parallel projects using AM and optimization, a decision was made to eliminate as many variables as possible and test material performance across a range of platforms using standardized material, builds and, where possible, melt themes. The resulting data proved not only that AM could be used reliably, but that it was also valid in multiple orientations with only fractional anisotropy which could be mitigated easily by accepting the lowest data points from each testing environment after outliers were eliminated. When complete, this research (in combination with the geometric testing) was vastly in advance of any published research and indeed any internal work within Airbus, thus helping to aid in the acceptance of AM for the manufacture of TO components. The samples used/manufactured/tested in the research are common with Airbus test specimens and thus the data produced during testing was able to be

cross compared to Airbus QTP (Qualification Test Plan) data as it later became available in 2016/2017. The results were near identical with design allowables in the 0, 90 directions within 1% of those achieved as part of this research. To this date, no other study has directly compared the build qualities of three different types of AM platform using common media, themes and build data.

8.2.7 Expert Level Process

The research in its current state requires not only the MMP, but also a user guide to implementation, access to Python and CATIA Scripting (only allowed for power users) front ends. This makes the software something of an expert user process only, as it requires a certain level of skill and comfort with code modification in order to target the correct folders and files.

8.3 Impact - Applicability and Use

8.3.1 Direct use on Aerospace Componentry

From the outset the research has always been intended for implementation within Airbus and thus has been developed with Airbus foremost in mind throughout. To this end, many aspects of the research have seamlessly found their way into use within Airbus and its business units for the use of TO and AM. Within Airbus Group Innovations (AGI) many aspects of the research are used continuously on task requiring optimization and design for AM. These include: 1.) automated feature recognition, 2.) design defeaturing, 3.) loading perturbation, 4.) design space separation and 5.) design extraction. Only automated meshing is not in direct use as there are more computationally efficient methods available if time is taken to mesh manually. In addition to Airbus, these methods have been used on components for BAE systems, PALL Aerospace, Aerosud, Israeli Aircraft Industries, Mercedes Formula 1, Ferrari Formula 1, MBDA, Airbus, Airbus Military, Airbus Defence and Space and Airbus Apworks. Together their use has saved thousands of hours of engineer's time and helped junior users to perform optimization at advanced levels which was part of the primary aim of the project.

8.3.2 Use in on-going and Future Research

In addition to direct use on the optimization of aerospace componentry, aspects of the research have made their way into several active research projects within Airbus Central R&T. AMALGaM (Additive Manufacture of Airbus Main Landing Gear Manifolds) is one such project – aiming to both reduce the costs and increase the performance of existing manifolds through optimization driven redesign and additive manufacturing. AMALGaM uses the research developed in this PhD (predominantly the feature recognition and parametric design interface) to form the basis of an MDO toolbox for systems components such as hydraulic manifolds. Started in mid-2016 with a

specific focus on the ATA32 package of A350s main landing gear manifolds, the project, enabled via MDO promises to save almost €80m over 600 aircraft with each aircraft also benefitting from a mass saving close to 40kg. When considering that the projected cost and mass savings apply only to a single aircraft programme and then only to a small work package (11 parts), the potential savings if applied globally are tremendous. The automated design methodology developed in both the PhD and AMALGaM are now being used to develop methods for the design of spacecraft systems in the same/similar way to that of manifolds, but for electromagnetics rather than fluidics.

8.3.3 Indirect use in Training and Development

The tools for Automated parameterization and particularly the MMP are now in regular use both in Airbus Defence and Space and Central R&T. Whilst the MMP is easy to transfer and easy to update in response to new software, the developed coding is not quite so simple, particularly without funding to develop it. Regardless, using funding available in AMAZE, AMALGaM and soon, DigiSat, the advancement of the tools into working and distributable packages, usable by power users will commence within the coming year (2018) with a first rollout (beyond beta test) predicted for late quarter 3 of 2018.

For training purposes, staff coming to Central R&T for training utilise equipment on our independent network and thus have access to all the tools developed as part of the research. During this training, they are tasked with the analysis and optimization (completed in advance) of a component (SRT5) and the extraction of that design within the CAD environment. The tools for design extraction (CAT Product, STL manipulation and Construction geometry) developed during this research are used to provide that data to the trainees in order to speed their attempts at complex design. These tools and methods also the users to complete in a day and a half what took the researcher over a week to complete manually upon the first attempt. These tools are frequently asked for and distributed to the trainees upon their departure from the training.

8.4 Future work

The presented research demonstrates an applied method for dramatically reducing the time required to introduce analysis driven design approaches and does this through the use of staged automation. Whilst the research was effective in introducing automation to the TO process, it also highlighted a number of additional research opportunities which would either expedite the existing research, or would provide for future cost savings from parallel streams of integrated research.

8.4.1 Constant Mesh Density Topology Iteration

As previously discussed, a significant limitation of the automated process is created by constraints of balancing grid parameters to competing requirements for computational efficiency and highly refined design outputs. The proposed and partially investigated method for constant mesh density iteration provides for a potential solution to this problem.

Problematically, and as the research showed, the time required for this start-stop-extract-remesh approach is significant and difficult to automate, even with detailed steps and settings. Compounding the problem is process robustness when concerning the re-meshing and re-application of applied loads to geometry (as the geometry, so far as the software is concerned, no longer exists). The unknown topology, particularly around areas of NDS and DS interaction can cause holes in the extracted surface mesh making re-meshing without shrink wrapping difficult if not impossible. Whilst shrink wrapping does present a solution for the meshing, it does so at the expense of load application as nodal positions are now slightly out of alignment with existing geometry position and thus cannot be equivalenced without mesh distortion. Again, whilst solvable, it is achieved at the expense of something else – mesh quality, which can be somewhat automatically improved, but can displace loads and connectors creating further difficulties. The development of this process would cap the computational requirement at a known level and then provide the best possible solution for that problem within those computational limits.

8.4.2 Integration of Toolsets

The research completed thus far would be akin to achieving TRL2 moving toward TRL3 for most technologies in the aerospace environment. This means that the basic aspects of the process have been identified and, in this case, automated, thus demonstrating that a proof of concept has been within a sterile environment has been achieved. The next step in development would be the industrialisation of the software in preparation for its rollout and use by the business units for actual component development. For this to happen a full integration of the individual codes into a harmonised and simple to apply process is required. The individual codes could be linked together using another piece of software which would control the calling and running of codes and commercial packages, handling the data between solvers and CAD and thus providing a single, accessible GUI for the user. Initial conversations have been held with both Modefrontier (Enginesoft) and Pheonix Software (ModelCentre) looking to determine the best potential provider for such code linking. ModelCentre (for which we already have a license and for which the researcher already has experience) would be a good candidate for such software.

8.4.3 Skinned Point Cloud Surface Reconstruction

Whilst design extraction was assessed during the course of this research, it remains, due to constraints at Airbus, one of the most underdeveloped aspects of research and the one that would benefit the most from a future research project. The SPC methods presented in section 6.9 are possessing of perhaps the greatest potential for full automation of this phase. The results already presented show that on a pair of structures, that the resulting surfaces are exceptionally well defined and that that their intersection are easily reconstructed from extracted data. The challenge in conducting this research would be balancing mass lost through outer boundaries with the significantly increased computational requirements demanded by high density slicing and the subsequent analysis of the slice data to determine boundary information. The successful implementation of such an approach would finally close the loop back to CAD for the analysis driven design approach.

8.4.4 Multi-Disciplinary Optimization Research

As previously mentioned in section 8.3, use of some aspects of the research undertaken have already found their way into additional research projects concerned with the MDO of systems components to be made via AM. Should the above methods be completed, their integration into the MDO research would be invaluable, particularly for complex problems such as manifolds and waveguide filters which're computationally heavy during simulation and design heavy during extraction.

8.5 Concluding Statement

In summary, this thesis, in accomplishing all of its primary objectives, demonstrated that through substantial use of automation, that dramatic increases in process efficiency could be achieved. Moreover, the research shows that the established increase in process efficiency, in turn, yielded substantial reductions in component design time and thus component cost when compared to conventionally applied TO. Furthermore, when applied for design and enabled through relatively unconstrained production via AM, the work shows that substantial reductions in mass could also be found and used to further reduce component cost. In addition to the achievements in automation and cost reduction, the application of process instructions and serially applied, robust automation led to substantial increases in process robustness and commonality between process users which was highlighted as being absent from current methods within Airbus. Beyond direct automation, the analysis of material properties and geometric capabilities spanning multiple AM platforms using common builds and feedstock was notable. Through careful build design and testing it was established that in multiple orientations at multiple locations within each build chamber of each machine, the concerns surrounding material anisotropy and

chamber location which abound in literature are ill founded. This positive result definitively unlocks the use of topology optimization for AM production as no notable material knockdown factors are required in compound orientations within the build. Finally, whilst the current phase of this research completes with this project, the developments of this research have been included in several current research projects which aim to build upon the developed methods and potentially exploit the rich veins of research still available through investigation of the avenues presented in the future research in section 8.4. Combined consideration of the aspects of research and development presented within this thesis undoubtedly proves that the use of automation can act as a substantial enabler to the combined application of topology optimization design and additive manufacturing for future aerospace components and systems.

9 References

- ADARSH, K. R., AKSHAY, S., ASISH, R., ATHISH, S. U. & KURIAKOSE, M. 2017. *Optimized Brake Disc Design using Topology Optimization*.
- ADELI, H. 2003. *Advances in design optimization*, Taylor & Francis.
- AGGARANGSI, P. & L BEUTH, J. 2006. *Localized Preheating Approaches for Reducing Residual Stress in Additive Manufacturing*.
- AHSAN, M. N., PINKERTON, A. J., MOAT, R. J. & SHACKLETON, J. 2011. A comparative study of laser direct metal deposition characteristics using gas and plasma-atomized Ti-6Al-4V powders. *Materials Science and Engineering: A*, 528, 7648-7657.
- AIAA. 2015. *History of Flight - Timeline* [Online]. Available: <https://www.aiaa.org/historytimeline/> [Accessed October 2015].
- AIRBUS 2014. Functional Classification of Structure and System Installation Parts. *M2396.1*. Airbus: Airbus.
- AL-BERMANI, S. S., BLACKMORE, M. L., ZHANG, W. & TODD, I. 2010. The Origin of Microstructural Diversity, Texture, and Mechanical Properties in Electron Beam Melted Ti-6Al-4V. *Metallurgical and Materials Transactions A*, 41, 3422-3434.
- ALEXA, M. 2002. Recent Advances in Mesh Morphing. *Computer Graphics Forum*, 21, 173-198.
- ALI, F., CHOWDARY, B. V. & GONZALES, L. 2013. An integrated design approach for rapid product development. *Journal of Engineering, Design and Technology*, 11, 178-189.
- ALLAIRE, G., JOUVE, F. & TOADER, A.-M. 2004. Structural optimization using sensitivity analysis and a level-set method. *Journal of Computational Physics*, 194, 363-393.
- ALLEN, J. 2006. An Investigation into the Comparative Costs of Additive Manufacture vs. Machine from Solid for Aero Engine Parts Rolls Royce.
- ALMEIDA, P. 2015. AMAZE WP3D - Wire Fed Deposition Report. In: ESA (ed.). AMAZE: ESA.
- ALTAIR. 2006. Optimizaing Aircraft Structures. *Altair C2R* [Online], 2006. Available: [http://www.google.co.uk/url?sa=t&rct=j&q=&esrc=s&frm=1&source=web&cd=2&ved=0CDkQFjAB&url=http%3A%2F%2Fwww.altairproductdesign.com%2F\(S\(v2hrnr3g0ptjgqzrcdycomb3\)\)%2FResLibDownload.aspx%3Ffile_id%3D119%26%26resource_id%3D191&ei=woviUeXzDLH54QSC-4DwAg&usg=AFQjCNE-NKqFleuE6rkZOX7fhWC8TayHOW&sig2=De9FkOgSHp5M-TkQLPwARw](http://www.google.co.uk/url?sa=t&rct=j&q=&esrc=s&frm=1&source=web&cd=2&ved=0CDkQFjAB&url=http%3A%2F%2Fwww.altairproductdesign.com%2F(S(v2hrnr3g0ptjgqzrcdycomb3))%2FResLibDownload.aspx%3Ffile_id%3D119%26%26resource_id%3D191&ei=woviUeXzDLH54QSC-4DwAg&usg=AFQjCNE-NKqFleuE6rkZOX7fhWC8TayHOW&sig2=De9FkOgSHp5M-TkQLPwARw).
- ALTAIR ENGINEERING 2012. Hyperview. HW12 ed.: Altair Engineering.
- ALTAIR ENGINEERING 2017. Optistruct. HW14 ed.
- ANDERSON, W. J., SPIERS, R. P. & DINSMOOR, W. B. 1927. *The Architecture of Ancient Greece: An Account of Its Historic Development : Being the First Part of The Architecture of Greece and Rome*, B.T. Batsford, Limited.
- ANTONYSAMY, A. A. 2012. *Microstructure, Texture and Mechanical Property Evolution during Additive Manufacturing of Ti6Al4V Alloy for Aerospace Applications*, Manchester, School of Materials.
- ANTONYSAMY, A. A., MEYER, J. & PRANGNELL, P. B. 2013. Effect of build geometry on the β -grain structure and texture in additive manufacture of Ti6Al4V by selective electron beam melting. *Materials Characterization*, 84, 153-168.
- ARGYRIS, J. 1954. Energy Theorems and Structural Analysis: A Generalized Discourse with Applications on Energy Principles of Structural Analysis Including the Effects of Temperature and Non-Linear Stress-Strain Relations. *Aircraft Engineering and Aerospace Technology*, 26, 383-394.
- ASTM 2011. ASTM F2792 - 12a Standard Terminology for Additive Manufacturing Technologies,. West Conshohocken: ASTM.
- ASTM 2013. Additive Manufacturing Technology Standards. *ASTM F2924 - 12a Standard Specification for Additive Manufacturing Titanium-6 Aluminum-4 Vanadium with Powder Bed Fusion*. ASTM International, West Conshohocken, PA.

- AUTODESK 2012. Fusion 360. 1.1022 ed.
- BABIC, B., NESIC, N. & MILJKOVIC, Z. 2008. A review of automated feature recognition with rule-based pattern recognition. *Computers in Industry*, 59, 321-337.
- BANERJEE, A. & CHAUDHURY, S. 2010. Statistics without tears: Populations and samples. *Industrial Psychiatry Journal*, 19, 60-65.
- BAUFELD, B., BIEST, O. V. D. & GAULT, R. 2010. Additive manufacturing of Ti-6Al-4V components by shaped metal deposition: Microstructure and mechanical properties. *Materials & Design*, 31, Supplement 1, S106-S111.
- BAUM, J. D. 1964. *Elements of Point Set Topology*, Dover Publications.
- BAUMERS, M., TUCK, C., WILDMAN, R., ASHCROFT, I. & HAGUE, R. 2016. Shape Complexity and Process Energy Consumption in Electron Beam Melting: A Case of Something for Nothing in Additive Manufacturing? *Journal of Industrial Ecology*, n/a-n/a.
- BELYAEV, A. & OHTAKE, Y. A comparison of mesh smoothing methods. the Israel-Korea BiNational Conference on Geometric Modeling and Computer Graphics, 2003 2003. 83-87.
- BENDSØE, M. P. 1989. Optimal shape design as a material distribution problem. *Structural optimization*, 1, 193-202.
- BENDSØE, M. P., BEN-TAL, A. & ZOWE, J. 1994. Optimization methods for truss geometry and topology design. *Structural optimization*, 7, 141-159.
- BENDSOE, M. P. & SIGMUND, O. 2003. *Topology optimization: theory, methods and applications*, Springer.
- BENDSØE, M. P. & SIGMUND, O. 1999. Material interpolation schemes in topology optimization. *Archive of Applied Mechanics*, 69, 635-654.
- BERKE, L. & KHOT, N. S. 1987. Structural Optimization Using Optimality Criteria. In: MOTA SOARES, C. A. (ed.) *Computer Aided Optimal Design: Structural and Mechanical Systems*. Berlin, Heidelberg: Springer Berlin Heidelberg.
- BEYER, H.-G. & SENDHOFF, B. 2007. Robust optimization – A comprehensive survey. *Computer Methods in Applied Mechanics and Engineering*, 196, 3190-3218.
- BHAVAR, V., KATTIRE, P., PATIL, V., KHOT, S., GUJAR, K. & SINGH, R. 2014. *A review on powder bed fusion technology of metal additive manufacturing*.
- BI, G., SUN, C. N. & GASSER, A. 2013. Study on influential factors for process monitoring and control in laser aided additive manufacturing. *Journal of Materials Processing Technology*, 213, 463-468.
- BISHOP, K. C. & HANSMAN, J. R. 2012. *ASSESSMENT OF THE ABILITY OF EXISTING AIRPORT GATE INFRASTRUCTURE TO ACCOMMODATE TRANSPORT CATEGORY AIRCRAFT WITH INCREASED WINGSPAN FOR IMPROVED FUEL EFFICIENCY*. Masters Degree Individual Masters, Massachusetts Institute of Technology
Cambridge, MA 02139 USA.
- BLACKLAY, E. H. 2016. Materials and Process Update In: AUTHORITY, C. A. (ed.) *2016 Airworthiness Standards Seminar*. London, England: CAA.
- BLUM, H. 1967. A Transformation for Extracting New Descriptors of Form. *Models for the Perception of Speech and Visual Form*, 362-380.
- BOEING 1997. Aircraft Structural Repair. In: BOEING (ed.).
http://www.boeing.com/resources/boeingdotcom/commercial/services/flight-operations-solutions/training-and-resourcing/maintenance-training/assets/pdf/Boeing_Structures_Training_Courses.pdf.
- BOOTH, P., GILMORE, J., VALLES LLUCH, E. & HARVEY, M. 2016. *Enhancements to satellite feed chain performance, testing and lead-times using additive manufacturing*.
- BOYD, S. P. & VANDENBERGHE, L. 2004. *Convex optimization*, Cambridge university press.
- BOYER, R. R. 1996. An overview on the use of titanium in the aerospace industry. *Materials Science and Engineering: A*, 213, 103-114.

- BOYER, R. R. 2010. Attributes, characteristics, and applications of titanium and its alloys. *JOM*, 62, 21-24.
- BRACKETT, D., ASHCROFT, I. & HAGUE, R. 2011. *Topology optimization for additive manufacturing*.
- BRAJLIH, T., VALENTAN, B., BALIC, J. & DRSTVENSEK, I. 2011. Speed and accuracy evaluation of additive manufacturing machines. *Rapid Prototyping Journal*, 17, 64-75.
- BRANDL, E., HECKENBERGER, U., HOLZINGER, V. & BUCHBINDER, D. 2012. *Additive manufactured AlSi10Mg samples using Selective Laser Melting (SLM): Microstructure, high cycle fatigue, and fracture behavior*.
- BRENNER, S. & SCOTT, R. 2007. *The Mathematical Theory of Finite Element Methods*, Springer New York.
- BRUNS, T. E. 2005. A reevaluation of the SIMP method with filtering and an alternative formulation for solid-void topology optimization. *Structural and Multidisciplinary Optimization*, 30, 428-436.
- BUCHBINDER, D., SCHLEIFENBAUM, H., HEIDRICH, S., MEINERS, W. & BÜLTMANN, J. 2011. High Power Selective Laser Melting (HP SLM) of Aluminum Parts. *Physics Procedia*, 12, 271-278.
- BULMAN, S., SIENZ, J. & HINTON, E. 2001. Comparisons between algorithms for structural topology optimization using a series of benchmark studies. *Computers & Structures*, 79, 1203-1218.
- BURDEKIN, F. M. 2006. *The Early Pioneers – Bridges, Canals, Railways and Ships*. Manchester MAE.
- CAI, S., ZHANG, W., ZHU, J. & GAO, T. 2014. Stress constrained shape and topology optimization with fixed mesh: A B-spline finite cell method combined with level set function. *Computer Methods in Applied Mechanics and Engineering*, 278, 361-387.
- CAMPBELL, I., BOURELL, D. & GIBSON, I. 2012. Additive manufacturing: rapid prototyping comes of age. *Rapid Prototyping Journal*, 18, 255-258.
- CANANN, S. A., STEPHENSON, M. B. & BLACKER, T. 1993. Optismoothing: An optimization-driven approach to mesh smoothing. *Finite Elements in Analysis and Design*, 13, 185-190.
- CANDEL-RUIZ, A., KAUFMANN, S. & MÜLLERSCHÖN, O. 2015. Strategies for high deposition rate additive manufacturing by Laser Metal Deposition. *Lasers in Manufacturing Conference* Munich, Germany: LIM.
- CAUTLEY, R. V. & MAZET, H. S. 1932. Aero-Engine Development: A Review of the Basic Trends in Design During the Past Thirty Years. *Aircraft Engineering and Aerospace Technology*, 4, 221-225.
- CAVAZZUTI, M., BALDINI, A., BERTOCCHI, E., COSTI, D., TORRICELLI, E. & MORUZZI, P. 2011. High performance automotive chassis design: a topology optimization based approach. *Structural and Multidisciplinary Optimization*, 44, 45-56.
- CHANG, K. H. & TANG, P. S. 2001. Integration of design and manufacturing for structural shape optimization. *Advances in Engineering Software*, 32, 555-567.
- CHEN, L. & HOLST, M. 2010. *Efficient mesh optimization schemes based on Optimal Delaunay Triangulations*.
- CHENY, A. 2016. A Low Density Lattice Structure for the Earth Re-entry Capsule. Bloodhound Technical Centre.
- CHIANDUSSI, G., GAVIGLIO, I. & IBBA, A. 2004. Topology optimisation of an automotive component without final volume constraint specification. *Advances in Engineering Software*, 35, 609-617.
- COTTON, J., D BOYER, R., WEBER, G. & T SLATTERY, K. 2008. *Titanium Alloy Development Needs for Commercial Airframes*

- COURANT, R. 1943. Variational methods for the solution of problems of equilibrium and vibrations. *Bull. Amer. Math. Soc*, 49, 23.
- CRUMP, S. S. 1992. Apparatus and method for creating three-dimensional objects. Google Patents.
- CUILLIÈRE, J.-C., FRANCOIS, V. & DROUET, J.-M. 2014. Towards the Integration of Topology Optimization into the CAD Process. *Computer-Aided Design and Applications*, 11, 120-140.
- CUNNINGHAM, C. R., WIKSHÅLAND, S., XU, F., KEMAKOLAM, N., SHOKRANI, A., DHOKIA, V. & NEWMAN, S. T. 2017. Cost Modelling and Sensitivity Analysis of Wire and Arc Additive Manufacturing. *Procedia Manufacturing*, 11, 650-657.
- DA SILVA, R. B., MACHADO, Á. R., EZUGWU, E. O., BONNEY, J. & SALES, W. F. 2013. Tool life and wear mechanisms in high speed machining of Ti-6Al-4V alloy with PCD tools under various coolant pressures. *Journal of Materials Processing Technology*, 213, 1459-1464.
- DAJANI, S. 2016. The Future of Engine Technology. Airfinance Journal Roundtable Summit: GE Aviation.
- DAROCZY, L. & JARMAI, K. 2011. Topology optimization: On the automatization of design of truss structures based on results of topology optimizations. Parallel Multi-level Filter-Centered Ridge Detection for Topology Optimization. Structural and Multidisciplinary Optimization.
- DAS, P., CHANDRAN, R., SAMANT, R. & ANAND, S. 2015. Optimum Part Build Orientation in Additive Manufacturing for Minimizing Part Errors and Support Structures. *Procedia Manufacturing*, 1, 343-354.
- DASSAULT SYSTEMS 2012a. CATIA V5 R21 ed.
- DASSAULT SYSTEMS 2012b. Imagine and Shape 2. V2.0 ed.
- DASSAULT SYSTEMS 2017. CATIA Quick Surface Reconstruction V5 R21 ed.
- DE FLORIO, F. 2011. Chapter 5 - Type Certification. *Airworthiness (Second Edition)*. Oxford: Butterworth-Heinemann.
- DEATON, J. & GRANDHI, R. 2013. A survey of structural and multidisciplinary continuum topology optimization: post 2000. *Structural and Multidisciplinary Optimization*, 1-38.
- DECKARD, C. R. 1988. Method and apparatus for producing parts by selective sintering. Google Patents.
- DELGADO, G. 2014. *Optimization of composite structures: A shape and topology sensitivity analysis*. Masters, Ecole Polytechnique.
- DENLINGER, E. R., HEIGEL, J. C., MICHALERIS, P. & PALMER, T. A. 2015. Effect of inter-layer dwell time on distortion and residual stress in additive manufacturing of titanium and nickel alloys. *Journal of Materials Processing Technology*, 215, 123-131.
- DIETRICH, S., WUNDERER, M., HUISSEL, A. & ZAEH, M. F. 2016. A New Approach for a Flexible Powder Production for Additive Manufacturing. *Procedia Manufacturing*, 6, 88-95.
- DING, J., COLEGROVE, P., MEHNEN, J., GANGULY, S., SEQUEIRA ALMEIDA, P. M., WANG, F. & WILLIAMS, S. 2011. Thermo-mechanical analysis of Wire and Arc Additive Layer Manufacturing process on large multi-layer parts. *Computational Materials Science*, 50, 3315-3322.
- DINWIDDIE, R., DEHOFF, R., LLOYD, P., LOWE, L. & B. ULRICH, J. 2013. *Thermographic In-Situ Process Monitoring of the Electron Beam Melting Technology used in Additive Manufacturing*.
- DOD, D. O. D. 2004. Aircraft Structural Integrity Program. 1530b. www.everyspec.com: DOD.
- DONG, G., TANG, Y. & FIONA ZHAO, Y. 2017. *A Survey of Modeling of Lattice Structures Fabricated by Additive Manufacturing*.
- DUNNING, P. D. & KIM, A. H. 2013. A new hole insertion method for level set based structural topology optimization. *International Journal for Numerical Methods in Engineering*, 93, 118-134.

- DUNNING, P. D. & KIM, H. A. 2015. Introducing the sequential linear programming level-set method for topology optimization. *Structural and Multidisciplinary Optimization*, 51, 631-643.
- EGERLAND, M., ROOS, D. & WILL, J. 2007. *Optimization of a fan shroud by ANSYS/DesignModeler and optiSLang*.
- EUROPEAN COMMISSION. 2013. AMAZE [Online]. www.amaze.eu. Available: <http://amazeproject.eu/> [Accessed June 2015].
- EUROPEAN COMMISSION. 2017. Cleansky [Online]. Available: <http://www.cleansky.eu/> [Accessed 2015].
- EVERTON, S. K., HIRSCH, M., STRAVROULAKIS, P., LEACH, R. K. & CLARE, A. T. 2016. Review of in-situ process monitoring and in-situ metrology for metal additive manufacturing. *Materials & Design*, 95, 431-445.
- EZUGWU, E. & WANG, M. Z. 1997. *Titanium alloys and their machinability—a review*.
- EZUGWU, E. O. 2005. Key improvements in the machining of difficult-to-cut aerospace superalloys. *International Journal of Machine Tools and Manufacture*, 45, 1353-1367.
- FAA, F. A. A. 2013. *Aviation Maintenance Technician Handbook for General Aviation*.
- FADEL, G. M. & KIRSCHMAN, C. 1996. Accuracy issues in CAD to RP translations. *Rapid Prototyping Journal*, 2, 4-17.
- FERNHOLZ, K. D. 2013. Quantifying the Visibility of Surface Distortions in Class “A” Automotive Exterior Body Panels. *Journal of Manufacturing Science and Engineering*, 135, 011001-011001-11.
- FLOWER, H. M. 2012. *High Performance Materials in Aerospace*, Springer Science & Business Media.
- FORD, S. & DESPEISSE, M. 2016. Additive manufacturing and sustainability: an exploratory study of the advantages and challenges. *Journal of Cleaner Production*, 137, 1573-1587.
- FRAZIER, W. E. 2014. Metal Additive Manufacturing: A Review. *Journal of Materials Engineering and Performance*, 23, 1917-1928.
- GAO, W., ZHANG, Y., RAMANUJAN, D., RAMANI, K., CHEN, Y., WILLIAMS, C. B., WANG, C. C. L., SHIN, Y. C., ZHANG, S. & ZAVATTIERI, P. D. 2015. The status, challenges, and future of additive manufacturing in engineering. *Computer-Aided Design*, 69, 65-89.
- GAUL, W. A. & RITTER, G. 2012. *Classification, Automation, and New Media: Proceedings of the 24th Annual Conference of the Gesellschaft für Klassifikation e.V., University of Passau, March 15—17, 2000*, Springer Berlin Heidelberg.
- GEORGIADIS, S., GUNNION, A. J., THOMSON, R. S. & CARTWRIGHT, B. K. 2008. Bird-strike simulation for certification of the Boeing 787 composite moveable trailing edge. *Composite Structures*, 86, 258-268.
- GIBSON, I. R., D, W; STUCKER, B; 2010. *Additive Manufacturing Technologies*, Germany, Springer Verlag.
- GILBERT, M., SMITH, C. C., HAWKSBEER, S. J. & TYAS, A. 2014. Use of Layout Optimization to Solve Large-Scale Limit Analysis and Design Problems. In: SPILIOPOULOS, K. & WEICHERT, D. (eds.) *Direct Methods for Limit States in Structures and Materials*. Dordrecht: Springer Netherlands.
- GRABCAD. 2013. *GE Engine Bracket Challenge* [Online]. [www.Grabcad.com](http://www.grabcad.com). Available: <https://grabcad.com/challenges/ge-jet-engine-bracket-challenge> [Accessed March 2013 2013].
- GREENHALGH, E. & HILEY, M. 2003. The assessment of novel materials and processes for the impact tolerant design of stiffened composite aerospace structures. *Composites Part A: Applied Science and Manufacturing*, 34, 151-161.
- GU, D. D., MEINERS, W., WISSENBACH, K. & POPRAWE, R. 2012. Laser additive manufacturing of metallic components: materials, processes and mechanisms. *International Materials Reviews*, 57, 133-164.

- GUESS, T., KOČVARA, M., STINGL, M., WEIN, D. & HUBNER, D. 2016. Material Optimization using Lattice Structures. Applied Mathematics, 2015 Manchester, England. Turing Institute.
- GUIASSA, R., MAYER, J. R. R., BALAZINSKI, M., ENGIN, S. & DELORME, F. E. 2014. Closed door machining error compensation of complex surfaces using the cutting compliance coefficient and on-machine measurement for a milling process. *International Journal of Computer Integrated Manufacturing*, 27, 1022-1030.
- GUO, N. & LEU, M. C. 2013. Additive manufacturing: technology, applications and research needs. *Frontiers of Mechanical Engineering*, 8, 215-243.
- HAFTKA, R. T., GÜRDAL, Z. & KAMAT, M. 1992. Elements of structural optimization. . Kluwer Academic Publishers, Dordrecht.
- HAGUE, R., CAMPBELL, R. I. & DICKENS, P. 2003. *Implications on design of rapid manufacturing*.
- HAGUE, R., MANSOUR, S. & SALEH, N. 2004. Material and design considerations for rapid manufacturing. *International Journal of Production Research*, 42, 4691-4708.
- HARDEE, E., CHANG, K.-H., TU, J., CHOI, K. K., GRINDEANU, I. & YU, X. 1999. A CAD-based design parameterization for shape optimization of elastic solids. *Advances in Engineering Software*, 30, 185-199.
- HARIA, R. 2014. The A350 Charge: Batch By Batch. *Things with Wings* [Online]. Available from: <http://aviationweek.com/blog/a350-charge-batch-batch> 2016].
- HASLINGER, J., KOČVARA, M., LEUGERING, G. & STINGL, M. 2010. Multidisciplinary Free Material Optimization. *SIAM Journal on Applied Mathematics*, 70, 2709-2728.
- HAWRELIAK, A. J., LIND, J., MADDOX, B., BARHAM, M., MESSNER, M., BARTON, N., JENSEN, J. B. & KUMAR, M. 2016. *Dynamic Behavior of Engineered Lattice Materials*.
- HERNÁNDEZ-NAVA, E., SMITH, C. J., DERGUTI, F., TAMMAS-WILLIAMS, S., LEONARD, F., WITHERS, P. J., TODD, I. & GOODALL, R. 2016. The effect of defects on the mechanical response of Ti-6Al-4V cubic lattice structures fabricated by electron beam melting. *Acta Materialia*, 108, 279-292.
- HERNANDEZ, D. 2017. Artificial Intelligence Still Needs a Human Touch. *The Wall Street Journal*, March 12th
- HINTON, E. & SIENZ, J. 1995. Fully stressed topological design of structures using an evolutionary procedure. *Engineering Computations*, 12, 229-244.
- HOLMBERG, E., TORSTENFELT, B. & KLARBRING, A. 2013. Stress constrained topology optimization. *Structural and Multidisciplinary Optimization*, 48, 33-47.
- HOLMSTRÖM, J., PARTANEN, J., TUOMI, J. & WALTER, M. 2010. Rapid manufacturing in the spare parts supply chain: Alternative approaches to capacity deployment. *Journal of Manufacturing Technology Management*, 21, 687-697.
- HOLTZAPPLE, M. T. & REECE, W. D. 2000. *Foundations of engineering*, McGraw-Hill.
- HOWARD, R. W. 2016. Planning for super safety: the fail-safe dimension. *The Aeronautical Journal (1968)*, 104, 517-555.
- HRENNIKOFF, A. 1941. Solution of problems of elasticity by the framework method. *Journal of applied mechanics*, 8, 169-175.
- HUI, Z., HEPING, C. & NING, X. 2006. Automated robot programming based on sensor fusion. *Industrial Robot: An International Journal*, 33, 451-459.
- HULL, C. W. 1986. Apparatus for production of three-dimensional objects by stereolithography. Google Patents.
- ICAO, I. C. A. O. 2014. Safety Report. ICAO Webset: ICAO.
- JÄRVINEN, J.-P., MATILAINEN, V., LI, X., PIILI, H., SALMINEN, A., MÄKELÄ, I. & NYRHILÄ, O. 2014. Characterization of Effect of Support Structures in Laser Additive Manufacturing of Stainless Steel. *Physics Procedia*, 56, 72-81.
- JOHN, R., JATA, K. V. & SADANANDA, K. 2003. Residual stress effects on near-threshold fatigue crack growth in friction stir welds in aerospace alloys. *International Journal of Fatigue*, 25, 939-948.

- JOHNSON, R. E., KORDING, K. P., HARGROVE, L. J. & SENSINGER, J. W. 2017. Adaptation to random and systematic errors: Comparison of amputee and non-amputee control interfaces with varying levels of process noise. *PLoS ONE*, 12, e0170473.
- JOOSUNG, L. & JEONGHOON, M. 2011. Analysis of Technological Innovation and Environmental Performance Improvement in Aviation Sector. *International Journal of Environmental Research and Public Health*, 8, 3777-3795.
- KAI-MING, Y., YU, W. & CHARLIE, C. L. W. 2017. Smooth geometry generation in additive manufacturing file format: problem study and new formulation. *Rapid Prototyping Journal*, 23, 34-43.
- KAJI, F. & BARARI, A. 2015. Evaluation of the Surface Roughness of Additive Manufacturing Parts Based on the Modelling of Cusp Geometry. *IFAC-PapersOnLine*, 48, 658-663.
- KHAJAVI, S. H., PARTANEN, J. & HOLMSTRÖM, J. 2014. Additive manufacturing in the spare parts supply chain. *Computers in Industry*, 65, 50-63.
- KOCVARA, M. & STINGL, M. 2008. *Free material optimization: recent progress*.
- KÖRNER, C. 2016. Additive manufacturing of metallic components by selective electron beam melting — a review. *International Materials Reviews*, 61, 361-377.
- KÖRNER, C., HELMER, H., BAUEREIß, A. & SINGER, R. 2014. *Tailoring the grain structure of IN718 during selective electron beam melting*.
- KRISHNAMURTHY, V. & LEVOY, M. 1996. *Fitting Smooth Surfaces to Dense Polygon Meshes*.
- KROG, L., TUCKER, A., KEMP, M. & BOYD, R. 2004. Topology Optimisation of Aircraft Wing Box Ribs. *10th AIAA/ISSMO Multidisciplinary Analysis and Optimization Conference*. American Institute of Aeronautics and Astronautics.
- KROG, L., TUCKER, A. & ROLLEMA, G. Application of topology, sizing and shape optimization methods to optimal design of aircraft components. Proc. 3rd Altair UK HyperWorks Users Conference, 2002.
- KUMAR, L. J. & KRISHNADAS NAIR, C. G. 2017. Current Trends of Additive Manufacturing in the Aerospace Industry. In: WIMPENNY, D. I., PANDEY, P. M. & KUMAR, L. J. (eds.) *Advances in 3D Printing & Additive Manufacturing Technologies*. Singapore: Springer Singapore.
- KUO, Y.-H., CHENG, C.-C., LIN, Y.-S. & SAN, C.-H. 2017. *Support structure design in additive manufacturing based on topology optimization*.
- LAGAROS, N. D., PAPADRAKAKIS, M. & KOKOSSALAKIS, G. 2002. Structural optimization using evolutionary algorithms. *Computers & Structures*, 80, 571-589.
- LANE, S. D. & CHEREK, D. R. 2000. Risk Aversion in Human Subjects under Conditions of Probabilistic Reward. *The Psychological Record*, 50, 221-234.
- LASZLO, D. & KAROLY, J. 2011. On the Automation of Design of Truss Structures Based on the Results of Topology Optimizations. *Structural and Multidisciplinary Optimization*.
- LEYMARIE, F. F. & KIMIA, B. B. 2008. From the Infinitely Large to the Infinitely Small. In: SIDDIQI, K. & PIZER, S. M. (eds.) *Medial Representations: Mathematics, Algorithms and Applications*. Dordrecht: Springer Netherlands.
- LIN, W.-S., STARR, T., HARRIS, B., ZANDINEJAD, A. & MORTON, D. 2013. *Additive Manufacturing Technology (Direct Metal Laser Sintering) as a Novel Approach to Fabricate Functionally Graded Titanium Implants: Preliminary Investigation of Fabrication Parameters*.
- LÖBER, L., BIAMINO, S., ACKELID, U., SABBADINI, S., EPICOCO, P., FINO, P. & ECKERT, J. 2011. *Comparison of selective laser and electron beam melted titanium aluminides*.
- LOBORG, P. 1993. *Error Recovery in Automation - An Overview*.
- LONDON BUSINESS SCHOOL 2003. GM and the great automation solution. *Business Strategy Review*, 14, 18-24.
- MACHRY, T., EATOCK, D., MEYER, J., ANTONYSAMY, A., HO, A. & PRANGNELL, P. 2016. Effect of microstructure on the tensile strength of Ti6Al4V specimens manufactured using additive manufacturing electron beam process. *Powder Metallurgy*, 59, 41-50.

- MACHUNZE, W. Topology design of a metallic load introduction bracket manufactured by ALM. Altair EATC, April 2013 2013 Turin, Italy.
- MAHALE, T., CORMIER, D., HARRYSSON, O. & ERVIN, K. 2007. *Advances In electron beam melting of aluminum alloys*.
- MAHASHABDE, A., WOLFE, P., ASHOK, A., DORBIAN, C., HE, Q., FAN, A., LUKACHKO, S., MOZDZANOWSKA, A., WOLLERSHEIM, C., BARRETT, S. R. H., LOCKE, M. & WAITZ, I. A. 2011. Assessing the environmental impacts of aircraft noise and emissions. *Progress in Aerospace Sciences*, 47, 15-52.
- MALLENPREE, T. & BERGERS, D. Complex Anatomies in Medical Rapid Prototyping. In: LIM, C. T. & HONG, J. G. C., eds. 13th International Conference on Biomedical Engineering: ICBME 2008, 3-6 December 2008 2008 Singapore. Springer Berlin Heidelberg, 3.
- MANVATKAR, V., DE, A. & DEBROY, T. 2015. Spatial variation of melt pool geometry, peak temperature and solidification parameters during laser assisted additive manufacturing process. *Materials Science and Technology*, 31, 924-930.
- MARTINA, F. Wire + Arc Additive Manufacturing: properties, cost, parts. 2nd Mexican Workshop on Additive Manufacturing, 2015 Queretaro, Mexico.
- MASOOD, A., SIDDIQUI, R., PINTO, M., REHMAN, H. & KHAN, M. A. 2015. Tool Path Generation, for Complex Surface Machining, Using Point Cloud Data. *Procedia CIRP*, 26, 397-402.
- MATTHEWS, G. & WELLS, A. 2016. *Attention and Emotion: A Clinical Perspective*, Taylor & Francis.
- MERRULA, A. Developing Ferrari's Next Generation Architecture with the C123 Concept Process. 10th UK Altair Technology Conference, September 2017 2017 Gaydon, UK. Altair.
- MERTENS, A., DELAHAYE, J. & LECOMTE-BECKERS, J. 2017. *Fusion-Based Additive Manufacturing for Processing Aluminum Alloys: State-of-the-Art and Challenges: Fusion-Based Additive Manufacturing for Processing Aluminum Alloys*.
- MINDT, H. W., MEGAHED, M., LAVERY, N. P., HOLMES, M. A. & BROWN, S. G. R. 2016. Powder Bed Layer Characteristics: The Overseen First-Order Process Input. *Metallurgical and Materials Transactions A*, 47, 3811-3822.
- MOWER, T. M. & LONG, M. J. 2016. Mechanical behavior of additive manufactured, powder-bed laser-fused materials. *Materials Science and Engineering: A*, 651, 198-213.
- MUIR, M. Civil Aerospace Mass Reduction Through Automated Topology Optimization and Advanced Manufacturing. . 9th ASMO UK/ISSMO Conference on Engineering Design Optimization, 2012a Cork, Ireland.
- MUIR, M. 2012. Topology Optimization and Advanced Manufacturing for Civil Aerospace Applications. In: SHAHPAR, S., ed. Automated Design Optimisation Seminar, September 2012 2012b Derby, England. Rolls Royce.
- MUIR, M. Multidisciplinary Optimisation of Business Jet MED Hinge for Production by Additive Manufacturing 2013 European Altair Technology Conference, 2013 Lingotto, Turin, Italy. Altair Engineering.
- MUIR, M., MULDAL, C., KOLB, E., ROBERTSON, G., PARKINSON, A., QUERIN, O. M., HEWSON, R. W. & TOROPOV, V. V. The use of MDO and Advanced Manufacturing to Demonstrate Rapid, Agile Construction of a Mission Optimized UAV. 54th AIAA/ASME/ASCE/AHS/ASC Structures, Structural Dynamics, and Materials Conference
- 9th AIAA Multidisciplinary Design Optimization Specialist Conference, 04, 2013 2013 Boston, Ma, USA. AIAA.
- MUIR, M., QUERIN, O. & TOROPOV, V. 2014. Rules, precursors and parameterization methodologies for topology optimized structural designs realized through additive manufacturing. *10th AiAA*. Washington DC.

- MUIR, M. J. Civil Aerospace Mass Reduction through Automated Topology Optimization and Advanced Manufacturing. 2012c Cork, Ireland. 9th ASMO UK Conference Engineering Design Optimization.
- MUIR, M. J. Additive Manufacture of Multi-Disciplinary Optimised Aero-Structures and Systems. Altair ATCx, 27 10 2015 2015 MTC Coventry. Altair Engineering.
- MUIR, M. J. 2016. AMAZE - Overview Report. Airbus: Airbus.
- MUIR, M. J. Multi-Disciplinary Optimization and Additive Manufacture of Airbus Main Landing Gear Manifolds Aircraft System Technologies, 22 02 2017 2017 Hamburg Germany. TUHH.
- MUSTAFA, K. & CHENG, K. 2017. Improving Production Changeovers and the Optimization: A Simulation Based Virtual Process Approach and Its Application Perspectives. *Procedia Manufacturing*, 11, 2042-2050.
- NABHANI, F. 2001. Machining of aerospace titanium alloys. *Robotics and Computer-Integrated Manufacturing*, 17, 99-106.
- NEILL, D. J., JOHNSON, E. N. & CANFIELD, R. 1990. *ASTROS - A multidisciplinary automated structural design tool*.
- NEUGEBAUER, F., KELLER, N., PLOSHIKHIN, V., FEUERHAHN, F. & KOEHLER, H. 2014. *Multi Scale FEM Simulation for Distortion Calculation in Additive Manufacturing of Hardening Stainless Steel*.
- NISONGER, T. E. 2008. The "80/20 Rule" and Core Journals. *The Serials Librarian*, 55, 62-84.
- NOOR, A. K., VENNERI, S. L., PAUL, D. B. & HOPKINS, M. A. 2000. Structures technology for future aerospace systems. *Computers & Structures*, 74, 507-519.
- NORSK TITANIUM. 2018. *The Future of Manufacturing - Raid Plasma Deposition* [Online]. <http://www.norsktitanium.com/>. Available: <http://www.norsktitanium.com/> [Accessed January 2018].
- NOVIELLO, D. 2016. Understanding the Mechanical Properties of Additively Manufactured Lattice Structures with Testing and Simulation. Autodesk University.
- OATES, C. J., WEN, W. & HAMILTON, D. W. 2011. Role of Titanium Surface Topography and Surface Wettability on Focal Adhesion Kinase Mediated Signaling in Fibroblasts. *Materials*, 4, 893.
- ÖCHSNER, A. & ALTENBACH, H. 2015. *Mechanical and Materials Engineering of Modern Structure and Component Design*, Springer.
- ONWUBIKO, C. O. 2000. *Introduction to engineering design optimization*, Prentice-Hall New Jersey.
- ORME, M. E., GSCHWEITL, M., FERRARI, M., VERNON, R., MADERA, I. J., YANCEY, R. & MOURIAUX, F. 2017. Additive Manufacturing of Lightweight, Optimized, Metallic Components Suitable for Space Flight. *Journal of Spacecraft and Rockets*, 54, 1050-1059.
- OSTROM, L. T. & WILHELMSSEN, C. A. 2008. Developing Risk Models for Aviation Maintenance and Inspection. *The International Journal of Aviation Psychology*, 18, 30-42.
- PARKES, P. N., BUTLER, R. & ALMOND, D. 2013. Fatigue of Metal-Composite Joints with Penetrative Reinforcement. *54th AIAA/ASME/ASCE/AHS/ASC Structures, Structural Dynamics, and Materials Conference*. American Institute of Aeronautics and Astronautics.
- PATEL, M. H. 1978. On the linear superposition of aerodynamic forces on wings in periodic gusts. *The Aeronautical Journal (1968)*, 82, 267-272.
- PETERSSON, J. 1996. *On stiffness maximization of variable thickness sheet with unilateral contact*.
- PIER DAVIDE, C., ZILL, T. & BJOERN, N. 2012. Aeroelastic Design and Optimization of Unconventional Aircraft Configurations in a Distributed Design Environment. *53rd*

- AIAA/ASME/ASCE/AHS/ASC Structures, Structural Dynamics and Materials Conference. American Institute of Aeronautics and Astronautics.
- PINKERTON, A. J. 2016. [INVITED] Lasers in additive manufacturing. *Optics & Laser Technology*, 78, 25-32.
- POLISHETTY, A., GOLDBERG, M., LITTLEFAIR, G., PUTTARAJU, M., PATIL, P. & KALRA, A. 2014. A Preliminary Assessment of Machinability of Titanium Alloy Ti 6AL 4V During thin Wall Machining Using Trochoidal Milling. *Procedia Engineering*, 97, 357-364.
- PRABHAKAR, P., SAMES, W. J., DEHOFF, R. & BABU, S. S. 2015. Computational modeling of residual stress formation during the electron beam melting process for Inconel 718. *Additive Manufacturing*, 7, 83-91.
- PRAMANIK, A. 2014. Problems and solutions in machining of titanium alloys. *The International Journal of Advanced Manufacturing Technology*, 70, 919-928.
- QUERIN, O. M., STEVEN, G. P. & XIE, Y. M. 1998. Evolutionary structural optimisation (ESO) using a bidirectional algorithm. *Engineering Computations*, 15, 1031-1048.
- RAMAKRISHNAN, C. V. & FRANCAVILLA, A. 1974. Structural Shape Optimization Using Penalty Functions. *Journal of Structural Mechanics*, 3, 403-422.
- RAO, S. S. 1996. *Engineering Optimization: Theory and Practice*, Wiley.
- RAZANI, R. 1965. Behavior of fully stressed design of structures and its relationship to minimum-weight design. *AIAA Journal*, 3, 2262-2268.
- RHINOCEROS 2012. Rhino 4ed.
- RIDGWAY, S. L. & SHANGYOU, Z. 1990. Finite element interpolation of nonsmooth functions satisfying boundary conditions. *Mathematics of Computation*, 54, 483-493.
- RIESENFELD, R. F., HAIMES, R. & COHEN, E. 2015. Initiating a CAD renaissance: Multidisciplinary analysis driven design: Framework for a new generation of advanced computational design, engineering and manufacturing environments. *Computer Methods in Applied Mechanics and Engineering*, 284, 1054-1072.
- ROSEN, D. 2014. *What are Principles for Design for Additive Manufacturing?*
- ROSSOW, M. P. & TAYLOR, J. E. 1973. A Finite Element Method for the Optimal Design of Variable Thickness Sheets. *AIAA Journal*, 11, 1566-1569.
- ROZVANY, G. 2001. Aims, scope, methods, history and unified terminology of computer-aided topology optimization in structural mechanics. *Structural and Multidisciplinary Optimization*, 21, 90-108.
- ROZVANY, G. I. N. 2009. A critical review of established methods of structural topology optimization. *Structural and Multidisciplinary Optimization*, 37, 217-237.
- RUFFO, M., TUCK, C. & HAGUE, R. 2006. *Cost estimation for rapid manufacturing - Laser sintering production for low to medium volumes*.
- SACHS, E., CIMA, M., CORNIE, J., BRANCAZIO, D., BREDT, J., CURODEAU, A., FAN, T., KHANUJA, S., LAUDER, A., LEE, J. & MICHAELS, S. 1993. Three-Dimensional Printing: The Physics and Implications of Additive Manufacturing. *CIRP Annals - Manufacturing Technology*, 42, 257-260.
- SAFFARZADEH, M. & MASOUMI, G. 2004. *An optimum analysis and design model for airport aprons*.
- SCHILLINGER, D., DEDÈ, L., SCOTT, M. A., EVANS, J. A., BORDEN, M. J., RANK, E. & HUGHES, T. J. R. 2012. An isogeometric design-through-analysis methodology based on adaptive hierarchical refinement of NURBS, immersed boundary methods, and T-spline CAD surfaces. *Computer Methods in Applied Mechanics and Engineering*, 249, 116-150.
- SCHULTZ, R. L. & ZAGALSKY, N. R. 1972. Aircraft performance optimization. *Journal of Aircraft*, 9, 108-114.
- SEDERBERG, T. W. 2007. System and method for defining T-spline and T-NURCC surfaces using local refinements. Google Patents.

- SEDERBERG, T. W., CARDON, D. L., FINNIGAN, G. T., NORTH, N. S., ZHENG, J. & LYCHE, T. 2004. T-spline simplification and local refinement. *ACM Trans. Graph.*, 23, 276-283.
- SEDERBERG, T. W., ZHENG, J., BAKENOV, A. & NASRI, A. 2003. T-splines and T-NURCCs. *ACM Trans. Graph.*, 22, 477-484.
- SHAO, S. & MUROTSU, Y. 1999. Approach to failure mode analysis of large structures. *Probabilistic Engineering Mechanics*, 14, 169-177.
- SHOJAEI, S. & MOHAMMADIAN, M. 2012. Structural topology optimization using an enhanced level set method. *Scientia Iranica*, 19, 1157-1167.
- SIEMENS 2012. NX. 8.022 ed.
- SILLARS, S. A., SUTCLIFFE, C. J., PHILO, A. M., BROWN, S. G. R., SIENZ, J. & LAVERY, N. P. 2018. The three-prong method: a novel assessment of residual stress in laser powder bed fusion. *Virtual and Physical Prototyping*, 13, 20-25.
- SIVAPURAM, R. & KIM, H. A. Level-Set Topology Optimization for Additive Manufacturing. 12th World Congress on Computational Mechanics, July 2016 2016 Seoul, Korea. ICAM.
- SLOTWINSKI, J. A., GARBOCZI, E. J., STUTZMAN, P., F. FERRARIS, C., WATSON, S. & PELTZ, M. 2014. *Characterization of Metal Powders Used for Additive Manufacturing*.
- SMITH, C. J., TAMMAS-WILLIAMS, S., HERNANDEZ-NAVA, E. & TODD, I. 2017. Tailoring the thermal conductivity of the powder bed in Electron Beam Melting (EBM) Additive Manufacturing. *Scientific Reports*, 7, 10514.
- SMITHSONIAN. 1999. *Inventing a Flying Machine - Engine* [Online].
<https://airandspace.si.edu/exhibitions/wright-brothers/online/fly/1903/engine.cfm>.
 Available: <https://airandspace.si.edu/exhibitions/wright-brothers/online/fly/1903/engine.cfm> [Accessed 06/12 2015].
- SOBIESZCZANSKI-SOBIESKI, J. & HAFTKA, R. T. 1997. Multidisciplinary aerospace design optimization: survey of recent developments. *Structural optimization*, 14, 1-23.
- SONG, B., ZHAO, X., LI, S., HAN, C., WEI, Q., WEN, S., LIU, J. & SHI, Y. 2015. Differences in microstructure and properties between selective laser melting and traditional manufacturing for fabrication of metal parts: A review. *Frontiers of Mechanical Engineering*, 10, 111-125.
- SPALL, J. C. 2005. *Introduction to stochastic search and optimization: estimation, simulation, and control*, Wiley. com.
- SPIERINGS, A. B., VOEGTLIN, M., BAUER, T. & WEGENER, K. 2016. Powder flowability characterisation methodology for powder-bed-based metal additive manufacturing. *Progress in Additive Manufacturing*, 1, 9-20.
- STANFORD 2012. Mesh Smoothing. *Mesh Smoothing*. Graphics Department: Stanford
- STATEN, M. L., OWEN, S. J., SHONTZ, S. M., SALINGER, A. G. & COFFEY, T. S. 2012. A Comparison of Mesh Morphing Methods for 3D Shape Optimization. In: QUADROS, W. R. (ed.) *Proceedings of the 20th International Meshing Roundtable*. Berlin, Heidelberg: Springer Berlin Heidelberg.
- STAVINOHA, J. N. 2012. *Investigation of plasma arc welding as a method for the additive manufacturing of titanium-(6)aluminum-(4)vanadium alloy components*. PhD PnD, The University of Montana.
- STOLPE, M. & SVANBERG, K. 2001. On the trajectories of penalization methods for topology optimization. *Structural and Multidisciplinary Optimization*, 21, 128-139.
- STORN, R. & PRICE, K. 1997. Differential Evolution – A Simple and Efficient Heuristic for global Optimization over Continuous Spaces. *Journal of Global Optimization*, 11, 341-359.
- STRANO, G., HAO, L., EVERSON, R. M. & EVANS, K. E. 2013. A new approach to the design and optimisation of support structures in additive manufacturing. *The International Journal of Advanced Manufacturing Technology*, 66, 1247-1254.

- STRÜBER, H. 2014. THE AERODYNAMIC DESIGN OF THE A350 XWB-900 HIGH LIFT SYSTEM. 29th Congress of the International Council of the Aeronautical Sciences, 2014 St Petersburg, Russia. ICAS, 1-10.
- SUH, S.-H. & LEE, J.-J. 1998. Five-Axis Part Machining With Three-Axis CNC Machine and Indexing Table. *Journal of Manufacturing Science and Engineering*, 120, 120-128.
- SURESH, K., THOMAS, S. V. & SURESH, G. 2011. Design, data analysis and sampling techniques for clinical research. *Annals of Indian Academy of Neurology*, 14, 287-290.
- SUSSKIND, R. & SUSSKIND, D. 2015. *The Future of the Professions: How Technology Will Transform the Work of Human Experts*, Oxford University Press.
- SZYKIEDANS, K. & CREDO, W. 2016. Mechanical Properties of FDM and SLA Low-cost 3-D Prints. *Procedia Engineering*, 136, 257-262.
- TAMMAS-WILLIAMS, S., WITHERS, P. J., TODD, I. & PRANGNELL, P. B. 2016. The Effectiveness of Hot Isostatic Pressing for Closing Porosity in Titanium Parts Manufactured by Selective Electron Beam Melting. *Metallurgical and Materials Transactions A*, 47, 1939-1946.
- TANSKANEN, P. 2002. The evolutionary structural optimization method: theoretical aspects. *Computer Methods in Applied Mechanics and Engineering*, 191, 5485-5498.
- TAPIA, G. & ELWANY, A. 2014. *A Review on Process Monitoring and Control in Metal-Based Additive Manufacturing*.
- TAYLOR, A. 2016. The future of the professions: how technology will transform the work of human experts. *Social Work Education*, 35, 371-372.
- TERWILLIGER, T. C. & BERENDZEN, J. 1999. Automated MAD and MIR structure solution. *Acta Crystallographica Section D: Biological Crystallography*, 55, 849-861.
- THIGALE, S. & SHAH, C. 2016. WEIGHT REDUCTION IN BRAKE DISC USING TOPOLOGY OPTIMIZATION. *International Journal of Research in Engineering and Technology*, 5, 3.
- THOMPSON, K. 2015. 5 Reasons Surface Modeling Is A Needed Skill. *TriMech Blog* [Online]. Available from: <https://blog.trimech.com/5-reasons-surface-modeling-is-still-a-needed-skill>.
- TOBI, A. L. M. & ISMAIL, A. E. 2016. Development in Geared Turbofan Aeroengine. *IOP Conference Series: Materials Science and Engineering*, 131, 012019.
- TOMLIN, M. & MEYER, J. Topology Optimization of an Additive Layer Manufactured (ALM) Aerospace Part. The 7th Altair CAE Technology Conference, Gaydon, UK, 10th May, 2011.
- TONG, J., BOWEN, C. R., PERSSON, J. & PLUMMER, A. 2017. Mechanical properties of titanium-based Ti-6Al-4V alloys manufactured by powder bed additive manufacture. *Materials Science and Technology*, 33, 138-148.
- TORENBEEK, E. 2007. BLENDED WING BODY AND ALL-WING AIRLINERS. European Workshop on Aircraft Design Education, May 2007 2007 Samara, Russia,. HAW Hamburg: EWAD.
- TUMBLESTON, J. R., SHIRVANYANTS, D., ERMOSHKIN, N., JANUSZIEWICZ, R., JOHNSON, A. R., KELLY, D., CHEN, K., PINSCHMIDT, R., ROLLAND, J. P., ERMOSHKIN, A., SAMULSKI, E. T. & DESIMONE, J. M. 2015. Continuous liquid interface production of 3D objects. *Science*, 347, 1349.
- TURNER, M. J., CLOUGH, R. W., MARTIN, H. C. & TOPP, L. J. 1956. Stiffness and Deflection Analysis of Complex Structures. *Journal of the Aeronautical Sciences (Institute of the Aeronautical Sciences)*, 23, 805-823.
- UHLMANN, E., KERSTING, R., KLEIN, T. B., CRUZ, M. F. & BORILLE, A. V. 2015. Additive Manufacturing of Titanium Alloy for Aircraft Components. *Procedia CIRP*, 35, 55-60.
- VAN DIJK, N. P., MAUTE, K., LANGELAAR, M. & VAN KEULEN, F. 2013. Level-set methods for structural topology optimization: a review. *Structural and Multidisciplinary Optimization*, 48, 437-472.

- VANDERPLOEG, A., LEE, S.-E. & MAMP, M. 2017. The application of 3D printing technology in the fashion industry. *International Journal of Fashion Design, Technology and Education*, 10, 170-179.
- VANEKER, T. H. J. 2017. The Role of Design for Additive Manufacturing in the Successful Economical Introduction of AM. *Procedia CIRP*, 60, 181-186.
- VAYRE, B., VIGNAT, F. & VILLENEUVE, F. 2012. Designing for Additive Manufacturing. *Procedia CIRP*, 3, 632-637.
- VENKATESH, B. D., CHEN, D. & BHOLE, S. D. 2009. *Effect of heat treatment on mechanical properties of Ti-6Al-4V ELI alloy*.
- WAIKER, A. & NICHOLS, P. 1997. Aviation safety: a quality perspective. *Disaster Prevention and Management: An International Journal*, 6, 87-93.
- WANG, D., HASSAN, O., MORGAN, K. & WEATHERILL, N. 2007a. Enhanced remeshing from STL files with applications to surface grid generation. *Communications in Numerical Methods in Engineering*, 23, 227-239.
- WANG, M. Y., WANG, X. & GUO, D. 2003. A level set method for structural topology optimization. *Computer Methods in Applied Mechanics and Engineering*, 192, 227-246.
- WANG, P., NAI, M. L. S., TAN, X., SIN, W. J., TOR, S. & WEI, J. 2016. *Anisotropic Mechanical Properties in a Big-Sized Ti-6Al-4V Plate Fabricated by Electron Beam Melting*.
- WANG, S. Y., LIM, K. M., KHOO, B. C. & WANG, M. Y. 2007b. An extended level set method for shape and topology optimization. *Journal of Computational Physics*, 221, 395-421.
- WILLIAMS, S. W., MARTINA, F., ADDISON, A. C., DING, J., PARDAL, G. & COLEGROVE, P. 2015. *Wire+Arc Additive Manufacturing*.
- WOHLERS, T. T., ASSOCIATES, W., CAMPBELL, R. I. & CAFFREY, T. 2016. *Wohlers Report 2016: 3D Printing and Additive Manufacturing State of the Industry : Annual Worldwide Progress Report*, Wohlers Associates.
- WOHLERS, T. T. & CAFFREY, T. 2015. *Wohlers report 2015 : 3D printing and additive manufacturing state of the industry annual worldwide progress report*, Fort Collins, Colo., Wohlers Associates.
- WOLSEY, L. A. 2000. Integer programming. *IIE Transactions*, 32, 2-58.
- WONG, K. V. & HERNANDEZ, A. 2012. A Review of Additive Manufacturing. *ISRN Mechanical Engineering*, 2012, 10.
- WRIGHT, S. 1921. Correlation and Causation. *Journal of Agricultural Research*, 20, 557-585.
- WRIGHT, S. 2015. 3D printing titanium and the bin of broken dreams. Available: <http://pencerw.com/feed/2015/3/15/3d-printing-titanium-and-the-bin-of-broken-dreams> [Accessed May 2015].
- WU, Y. T. 1994. Computational methods for efficient structural reliability and reliability sensitivity analysis. *AIAA Journal*, 32, 1717-1723.
- WYCISK, E., SOLBACH, A., SIDDIQUE, S., HERZOG, D., WALTHER, F. & EMMELMANN, C. 2014. Effects of Defects in Laser Additive Manufactured Ti-6Al-4V on Fatigue Properties. *Physics Procedia*, 56, 371-378.
- XIE, Y. M. & STEVEN, G. P. 1993. A simple evolutionary procedure for structural optimization. *Computers & Structures*, 49, 885-896.
- XIE, Y. M. & STEVEN, G. P. 1997. Basic Evolutionary Structural Optimization. In: XIE, Y. M. & STEVEN, G. P. (eds.) *Evolutionary Structural Optimization*. London: Springer London.
- YADROITSEV, I., KRAKHMALOV, P., YADROITSAVA, I., JOHANSSON, S. & SMUROV, I. 2013. Energy input effect on morphology and microstructure of selective laser melting single track from metallic powder. *Journal of Materials Processing Technology*, 213, 606-613.
- YAN, C., HAO, L., HUSSEIN, A. & RAYMONT, D. 2012. *Evaluations of cellular lattice structures manufactured using selective laser melting*.

- YAN, M., XU, W., DARGUSCH, M. S., TANG, H. P., BRANDT, M. & QIAN, M. 2014. Review of effect of oxygen on room temperature ductility of titanium and titanium alloys. *Powder Metallurgy*, 57, 251-257.
- YANG, R. J. & CHAHANDE, A. I. 1995. Automotive applications of topology optimization. *Structural optimization*, 9, 245-249.
- YANG, S., TANG, Y. & ZHAO, Y. F. 2015. A new part consolidation method to embrace the design freedom of additive manufacturing. *Journal of Manufacturing Processes*, 20, 444-449.
- ZHANG, B. 2016. Boeing's most turbulent saga of the past decade is finally over. *Business Insider UK* [Online]. Available: <http://uk.businessinsider.com/boeing-787-dreamliner-terrible-teens-2016-7> [Accessed May 2017].
- ZHANG, J. 2017. *Additive Manufacturing of Metallic Materials: A Review*.
- ZHONG, C., CHEN, J., LINNENBRINK, S., GASSER, A., SUI, S. & POPRAWA, R. 2016. A comparative study of Inconel 718 formed by High Deposition Rate Laser Metal Deposition with GA powder and PREP powder. *Materials & Design*, 107, 386-392.
- ZHOU, M., SHYY, Y. K. & THOMAS, H. L. 2001. Checkerboard and minimum member size control in topology optimization. *Structural and Multidisciplinary Optimization*, 21, 152-158.
- ZHU, B., ZHANG, X. & FATIKOW, S. 2015. Structural topology and shape optimization using a level set method with distance-suppression scheme. *Computer Methods in Applied Mechanics and Engineering*, 283, 1214-1239.

10 Appendices

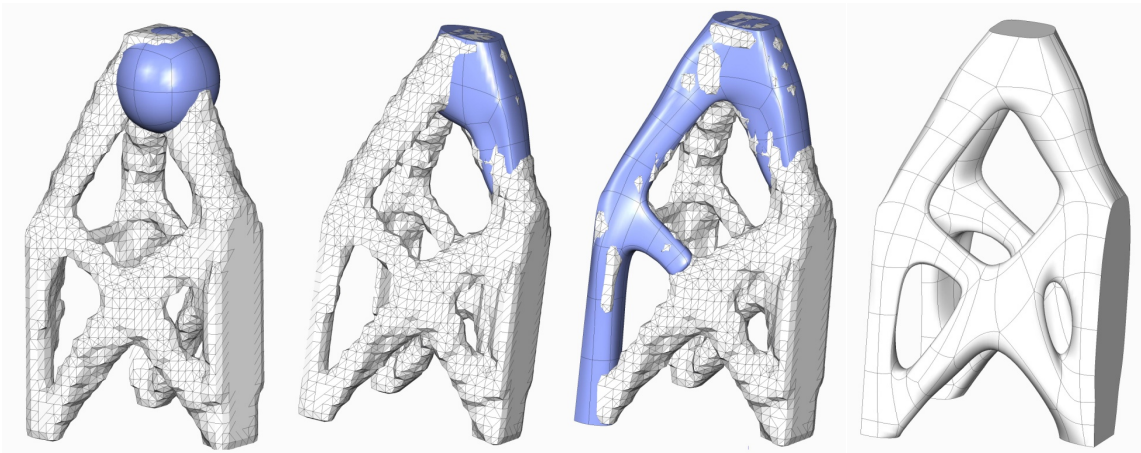
10.1 Appendix A – Background Material

10.1.1 Additive Manufacturing Standards

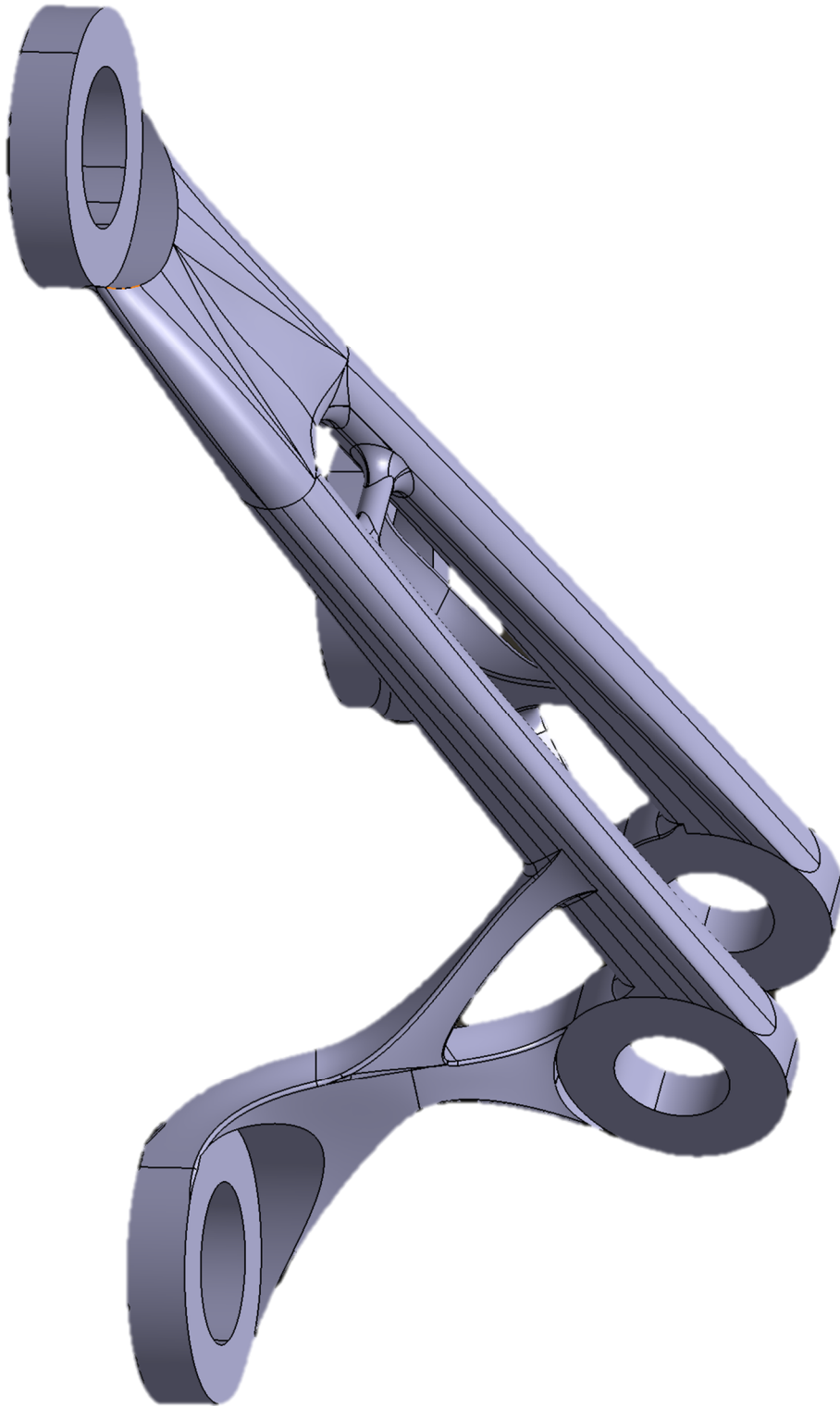
- SO / ASTM52915 – 16 Standard Specification for Additive Manufacturing File Format (AMF) Version 1.2
- ISO / ASTM52910 – 17 Standard Guidelines for Design for Additive Manufacturing
- ASTM F2924 - 14 Standard Specification for Additive Manufacturing Titanium-6 Aluminum-4 Vanadium with Powder Bed Fusion
- ASTM F3301 - 18 Standard for Additive Manufacturing – Post Processing Methods – Standard Specification for Thermal Post-Processing Metal Parts Made Via Powder Bed Fusion
- ASTM F3302 - 18 Standard for Additive Manufacturing – Finished Part Properties – Standard Specification for Titanium Alloys via Powder Bed Fusion
- ASTM F3187 - 16 Standard Guide for Directed Energy Deposition of Metals

10.2 Appendix B – Design Work

10.2.1 T-spline Modelling Trials



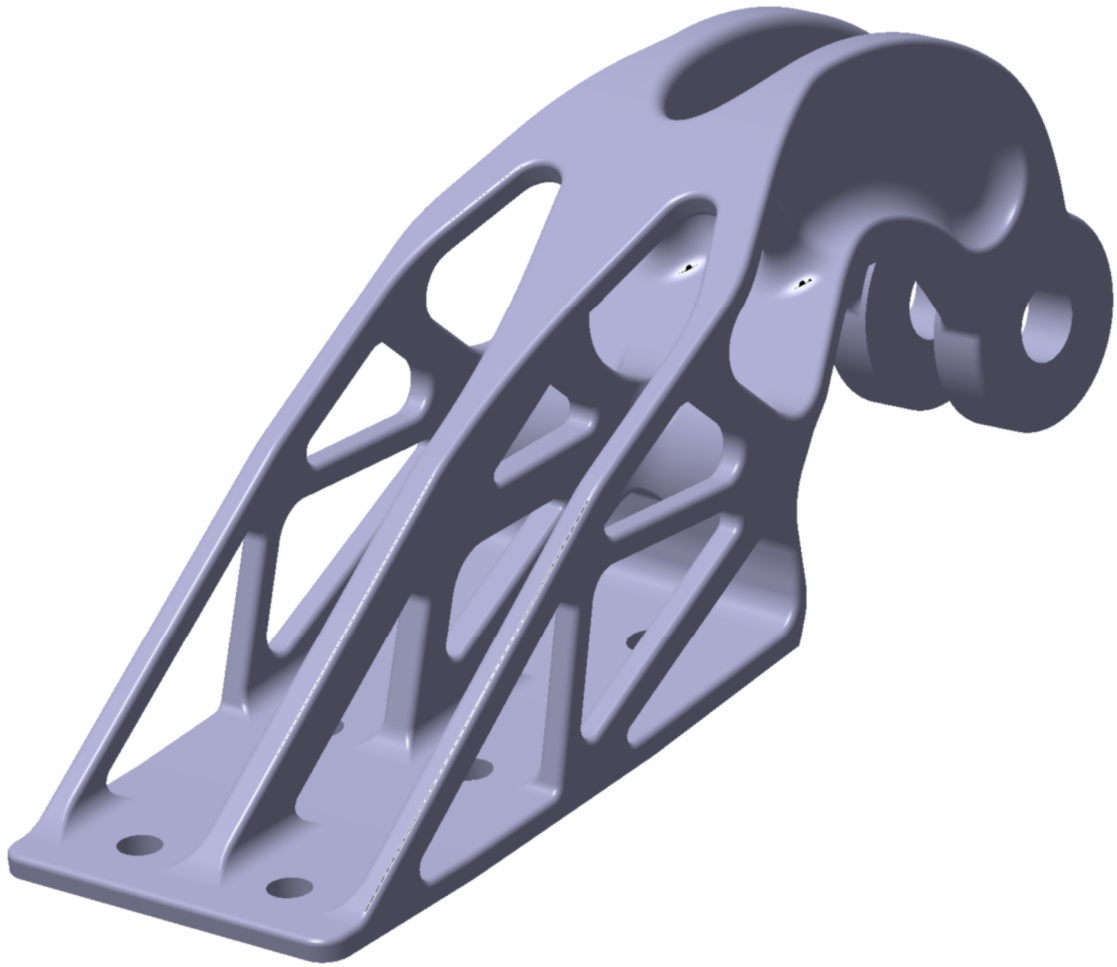
10.2.2 STR1 Design Extraction



10.2.3 STR2 Design Extraction



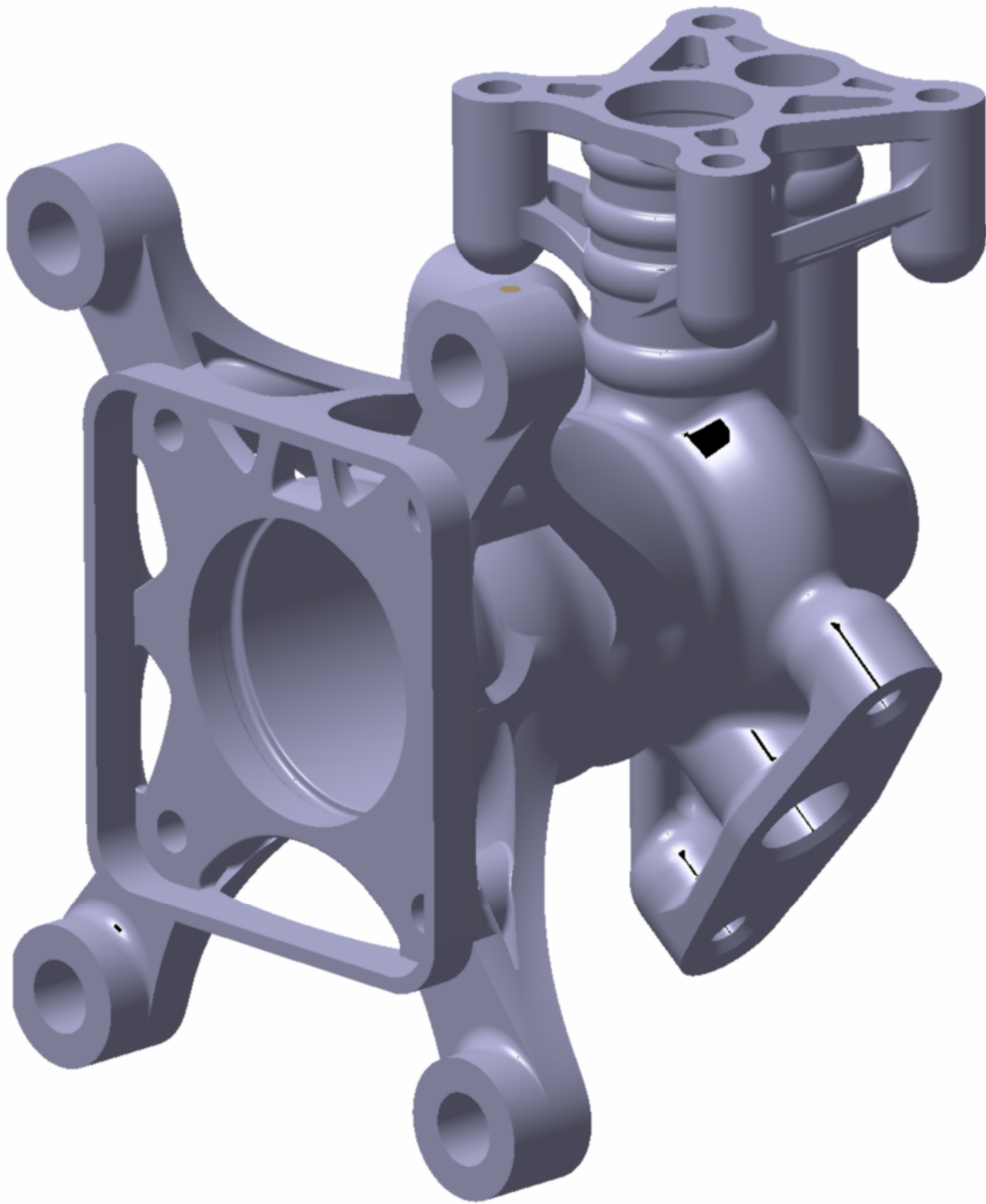
10.2.4 STR3 Design Extraction



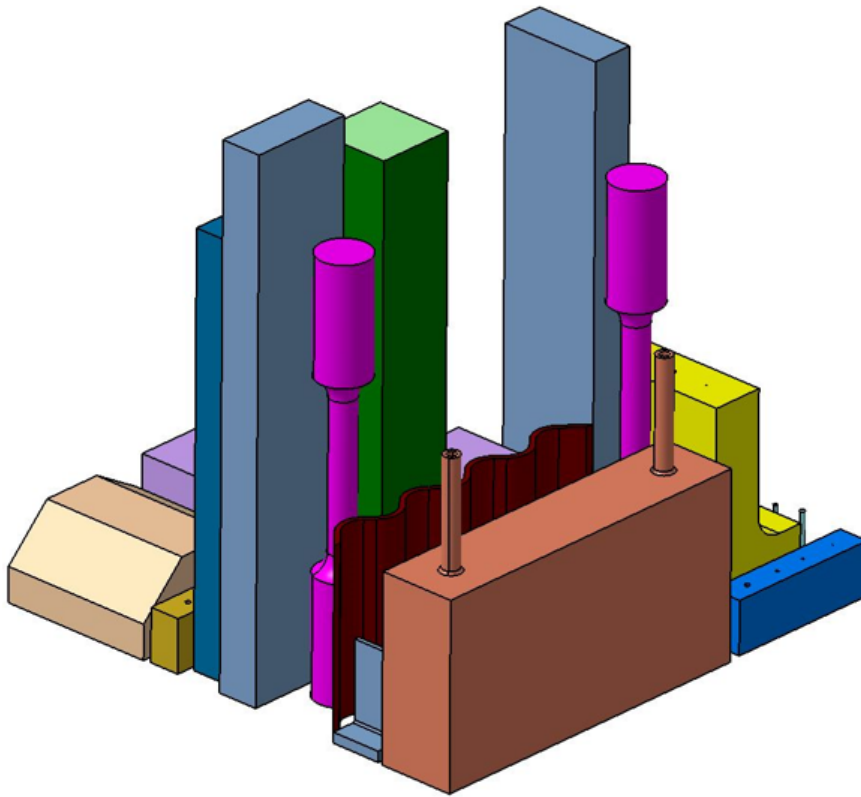
10.2.5 STR4 Design Extraction



10.2.6 STR5 Design Extraction



10.2.7 Geometric Sample Build Setup



Build contains:

- Vertical holes
- 90 degree channels
- Tortuous path
 - Pins
- Stepped holes
 - Walls
 - Tank
- Solid test piece
- Test piece with centre lattice
- 3 different lattice pieces
 - Cavity
 - Corrugated
- Solid plate with attached lattice
- Solid reference / test blocks
 - Tube stubs

10.3 Appendix C – Coding and Scripting

10.3.1 Feature Recognition and Domain Segregation Script

```
07_stp_extract_v4_with_comments.py - K:\Projects\R21\Martin_Data\AMALGaM\Amr\05_Python\07_stp_extract_v4_with_comments.py (2.7.10)
File Edit Format Run Options Window Help

from math import *

def TripleSplit( myString ):
    return myString.split("(")[-1].split(")") [0].split(",")

def SearchAndSplit( ref, listoflists ):
    for line in listoflists:
        if line[0] == ref:
            #print line
            return TripleSplit( line[1] )

#globals
data = []
pSets = []

# first we create a class with the name point3f
class Point3f:
    # In this class we define a method "__init__" which allows us to assign the existed objects (in this case the coordinates of a point and then the normals)
    # That means the when we capture the x coordinate of a point python run the method __init__ and assign the captured value to a.

    #x y z are three member variables of the class
    def __init__(self,a,b,c):
        self.x=a
        self.y=b
        self.z=c

    #MEMBER FUNCTIONS OF THE CLASS
    # if we request string using function like print, it knows how to display
    def __str__(self):
        return "["+str(self.x)+", "+str(self.y)+", "+str(self.z)+"]"

    #operator overloading for basic maths with vectors
    #subtraction
    def __sub__(self,p):
        return Point3f(self.x-p.x, self.y-p.y, self.z-p.z)

    #division of vectors
    def __div__(self,s):
        return Point3f(self.x/s, self.y/s, self.z/s)
    #equality test for vectors
    def __eq__(self,p):
        if ( self.x==p.x and self.y==p.y and self.z==p.z):
            return True
        else:
            return False

#OTHER UTILITY FUNCTIONS NOT IN CLASS BUT USE WITH POINT3F
#here we calculate the magnitude of the vector
def mag( pt ):
    return sqrt( pt.x*pt.x + pt.y*pt.y + pt.z*pt.z )

#Unit normal vector
def normalise( pt ):
    return pt/mag(pt) #USES MAG FUNCTION FOR LENGTH AND THEN VECTOR DIVISION BY SCALAR

#Dot product of a vector I.E. A POINT3F, TWO POINT3F NEEDED AS INFUT
def dot( A, B ):
    return A.x*B.x + A.y*B.y + A.z*B.z

# Here we define the global class PointSet
# In the global class we have sets and each set has a property.
# That means when python capture first point. it will normalise THE AXIS DIRECTION and ALSO addS the point into the plist.
# then it will add the radius of this point into the r.list
# delta list contains the real distance between the points IN THIS SET. FIRST POINT IS THE ORIGIN SO =0
#
class PointSet:
    def __init__( self, a, b, c, d, e, f, g ):
        self.dirac = normalise(Point3f(a,b,c))
        self.pList = [ Point3f(d,e,f) ]
        self.rList = [ g ]
        self.delta = [ 0 ]

    #FOR NEW POINT IN SAME SET (AXIS SAME AND COLINEAR)
    # MUST PROVIDE POINT3F, RADIUS OF CIRCLE AND DISTANCE FROM ORIGIN POINT (FIRST POINT IN LIST)
    def Add_Point( self, pt, rad, delta ):
        self.pList.append( pt )
        self.rList.append( rad )
        self.delta.append( delta )
```

Ln: 9 Col: 30

```

07_stp_extract_v4_with_comments.py - K:\Projects\R21\Martin_Data\AMALGaM\Amr\05_Python\07_stp_extract_v4_with_comments.py (2.7.10)
File Edit Format Run Options Window Help

def WriteOutput( n, p, z ):
    # -----
    # mathworld.wolfram.com/SphericalCoordinates
    # -----

    # ANGLES OF THE VECTOR FROM THE NORTH-POLE OF EARTH
    theta = atan2( n.y, n.x )
    phi = atan2( sqrt(n.x*n.x + n.y*n.y), n.z )

    # two perpendicular & tangential unit vectors
    u_theta_vec = [-sin(theta), cos(theta), 0]
    u_phi_vec = [cos(theta)*cos(phi), sin(theta)*cos(phi), -sin(phi)]

    # scale vector by some amount... WE CHOOSE TO PUT THE TWO EXTRA POINTS ON THE RADIUS
    scalar = r
    theta_vec = [ scalar * i for i in u_theta_vec ]
    phi_vec = [ scalar * i for i in u_phi_vec ]

    # CONSTRUCT THE THREE POINTS THAT WE WILL OUTPUT... 1ST IS JUST THE CENTRE
    p0 = [ p.x, p.y, p.z ]
    p1 = [ p.x+theta_vec[0], p.y+theta_vec[1], p.z+theta_vec[2] ]
    p2 = [ p.x+phi_vec[0], p.y+phi_vec[1], p.z+phi_vec[2] ]

    # CONVERT EACH POINT TO CORRECT FORMAT FOR CSV FILE

    # EXAMPLE: p0= [1,2,3]
    # STR(p0) = "[1,2,3]"
    # SLICE THE STRING TO REMOVE THE "[" AND THE "]"
    # ADD THE CARRIAGE RETURN (COMMAND FOR CREATE A LEW LINE) ONTO END OF STRING

    outfile.write( str(p)[1:-1]+"\\n" )
    outfile.write( str(p1)[1:-1]+"\\n" )
    outfile.write( str(p2)[1:-1]+"\\n" )

#-----
#-----
#-----

# THIS IS WHERE WE REALLY START ANY WORK...

#-----
#-----
#-----

infile = open("./example.stp", "r")
infile = open("./AM Training Part.stp", "r")

# Python starts to read the file from line to line
# it splits only lines starting with hashtag and split the line at the first equal sign.
# the split lines it appends into a list names data
# the split looks like: [ "#104" | "CIRCLE('generated circle',#103,2.6)\\n" ] (the | describes the split)
# = sign disappears
for line in infile.readlines():
    if line[0]=="#":
        data.append( line.split("=",1) )

infile.close()

# now it reads from line to line the data list
# if the first six characters of the item[1] are not "circle" continue to next line
# if it is circle then split the item[1] of the line at the first open bracket and close bracket. Besides it should split the line at the commas - line[1] =
# [ "" | "generated circle" | "#103" | "2.6" | "" ]
# At the same moment save " the referencenr.=#103 into axis_id" and " the radius=2.6 into radius_str"
# change the radius output from string into float.
# if the radius of the circle is bigger than 3.6 then continue to next line as not interested
# Search in the data list from line to line after the "axis_id with the referencenr." if it find a match then split at the first open and close bracket and
# At the same moment save the "referencenr.=#101 into centre_id" and "referencenr.=#102 into normal_id"
# After that search in the data list after centre_id and save into temp and change into float.
# After that search in the data list after normal_id and save into temp and change into float.

# Create Sets
N=0
for line in data:

```

```

07_stp_extract_v4_with_comments.py - K:\Projects\R21\Martin_Data\AMALGaM\Amv05_Python\07_stp_extract_v4_with_comments.py (2.7.10)
File Edit Format Run Options Window Help
-----
N=0
for line in data:
    if line[1][:6]!="CIRCLE":
        continue

    axis_id,radius_str = TripleSplit( line[1] )[1:3] # FIRST TIME WE USE FUNCTINO FROM TOP
    radius = float(radius_str)

    if( radius<=9.6 ):
        continue

    centre_id,normal_id = SearchAndSplit( axis_id, data ) [1:3] # SECOND TIME WE USE FUNCTION FROM TOP

    temp = SearchAndSplit( centre_id, data )
    cx,cy,cz = [float(s) for s in temp]

    temp = SearchAndSplit( normal_id, data ) #overwrites temp
    nx,ny,nz = [float(s) for s in temp]

    #FIRST TIME WE USE OUR OWN CLASS
    # Here we create TWO INSTANCES OF THE class POINT3F. 1 for the point and 1 for the normal (SEE ABOVE)
    #ONLY USES THE __INIT__ FUNCTION == INITIALISATION
    p = Point3f(cx,cy,cz)
    n = Point3f(nx,ny,nz)

    # check all sets to FIND A MATCH FOR OUT NEW CIRCLE
    #IF WE FIND A SET THAT HAS THE SAME AXIS AND OUT NEW CIRCLE IS COLINEAR, WE ADD
    #OTHERWISE WE CREATE A NEW POINTSET

    matched=False #MUST ALWAYS START THIS ALGO WITH FALSE
    for ps in pSets:

        pRef = ps.pList[0] # WE USE THE FIRST POINT IN FLIST (OF CURRENT POINTSET) AS OUR REFERENCE
        nRef = ps.dirac # normalised on construction

        cosTheta = dot(nRef, n) / ( 1*mag(n) ) #ANGLE IN RADIANS BETWEEN AXIS OF CURRENT CIRCLE AND POINTSET

        if( cosTheta>0.999999 and cosTheta<0.999999 ):
            continue # to next set as norms OF AXIS not aligned

        if( p==pRef ): #coincident (SPECIAL CASE, IF SO DELTA=0)
            dp=0
        else: #IS IT colinear?
            vec=p-pRef # VECTOR SUBTRACTION, STORE IN TEMP VECTOR CALLED VEC
            dp = dot(nRef, vec) #projecction OF VEC ONTO unit vector nRef, GIVE MAGNITUDE OF DELTA AND DIRECTION
            cosTheta = dp / ( 1*mag(vec) ) # USE DP RESULT TO FIND ANGLE BETWEEN VEC AND THE NORMAL
            if( cosTheta>0.999999 and cosTheta<0.999999 ): #IF 0 OR 180 THEN PARALLEL AND THUS THEY ARE COLINEAR
                continue # goto next set as point not colinear

        ps.Add_Point( p, radius, dp ) #HOLE AXIS IS ALIGNED AND THE POINT IS COLINEAR SO ADD TO THIS POINTSET :)
        matched=True #WE ONLY CHANGE IF WE FIND A POINTSET FOR OUR POINT
        N+=1
        break

    # if set found, broken out... go to next
    if( matched ):
        continue

    # WE HAVE NOW TESTED ALL SETS AND NO MATCH FOUND SO CREATE NEW POINTSET AND ADD TO pSet LIST
    pSets.append( PointSet(nx,ny,nz,cx,cy,cz,radius) )
    N+=1

print "PointSets (Lines)\t", len(pSets)
print "Total Circles\t",N

#-----
#-----
#-----

#been thru all circles
outfile = open("./extracted_points.csv", "w")
outfile.write("StartLoft\nStartCurve\n")

# write just the centre points for debugging...

```

```

07_stp_extract_v4_with_comments.py - K:\Projects\R21\Martin_Data\AMALGA\Amr\05_Python\07_stp_extract_v4_with_comments.py (2.7.10)
File Edit Format Run Options Window Help

#been thru all circles
outfile = open("../extracted_points.csv", "w")
outfile.write("StartLoft\nStartCurve\n")

# write just the centre points for debugging...
# also groups the geo sets based on point set

# for ps in pSets:
#     # for i,p in enumerate(ps.pList):
#         # outfile.write( str(p)[1:-1]+",")
#         # outfile.write( str(ps.delta[i])+"\n")
#     # outfile.write( "EndSet\n" )

# ONLY KEEP POINTS IF THERE IS AT LEAST ONE DUPLICATE
#OTHERWISE THE ASSUMPTION IS THAT THE CIRCLE FORS A FILLET RAD

#TEST ALL POINTSETS IN ORDER
for ps in pSets:
    removals=[]
    for i,p in enumerate(ps.pList):
        if(ps.pList.count(p)==1): #COUNT OCCURENCES OF EACH POINT, IF ONLY 1 THEN NO DUPLICATE SO ADD TO REMOVALS LIST
            removals.append(i)

    # IF NUMBER OF POINTS IN FLIST IS SAME AS NUMBER OF POINTS IN REMOVALS LIST THEN THERE WILL BE NOTHING LEFT
    #THEREFORE DONT BOTHER REMOVING THEM, JUST IGNORE THIS POINTSET AND GO TO NEXT
    if( len(removals)==len(ps.pList) ):
        continue

    #MUST REMOVE THE NON-DUPLICATE POINTS IN REVERSE ORDER SO DONT GO OUT OF BOUNDS
    #I.E. DONT TRY TO ACCESS AN ELEMENT THAT NO LONGER EXISTS BECAUSE THE LIST IS SHORTER EVERYTIME ELEMENT REMOVED
    removals.sort(reverse=True)

    #NOW REMOVE THE DUPLICATES FROM FLIST AND ALSO EXTRA INFO ABOUT THE POINT (ITS RAD AND ITS DELTA)
    #THIS ENSURES ALL LISTS REMAIN THE SAME LENGTH
    for i in removals:
        del ps.pList[i]
        del ps.rList[i]
        del ps.delta[i]

    min_elem = ps.delta.index( min(ps.delta) ) #FIND MIN AND MAX DELTAS AND THE LOCATION OF THESE ELEMENTS
    max_elem = ps.delta.index( max(ps.delta) )

    #WRITE THE OUTPUT USING FUNCTION AT TOP OF SCRIPT,
    #THIS FUNCTION NEEDS TO KNOW THE DIRECTION OF THE HOLE AXIS, LOCATION OF CENTRE FROM FLIST AND THE RADIUS
    WriteOutput( ps.dirac, ps.pList[min_elem], ps.rList[min_elem] )

    #SPECIAL CASE, IF MIN AND MAX THE SAME ONLY OUTPUT THE MIN, SECOND POINT NOT NEEDED
    if( min_elem==max_elem ):
        WriteOutput( ps.dirac, ps.pList[max_elem], ps.rList[max_elem] )

# outfile.write("EndCurve\nEndLoft\nEnd\n")
outfile.close()
Ln: 9 Col: 30

```

10.3.2 Thickness Calculation Script

```
File Edit Format Run Options Window Help
import sys
import numpy as np
from visual import *
import math
from numpy.linalg import norm
from mpl_toolkits.mplot3d import Axes3D
from matplotlib import cm
from matplotlib.ticker import LinearLocator, FormatStrFormatter
import matplotlib.pyplot as plt
from struct import unpack
from struct import pack
from Tkinter import Tk
from tkFileDialog import askopenfilename
import time
BINARY_HEADER = "80sI"
BINARY_FACET = "12fH"

start = time.time()

def area(a, b, c) :
    return 0.5 * norm(np.cross( b-a, c-a ) )
def __init__(self, x = 0, y = 0, z = 0):
    self.x, self.y, self.z = float(x), float(y), float(z)
def rotateX(X,Y,Z, angle):
    """ Rotates the point around the X axis by the given angle in degrees. """
    rad = angle * math.pi / 180
    cosa = math.cos(rad)
    sina = math.sin(rad)
    y = Y * cosa - Z * sina
    z = Y * sina + Z * cosa
    return [X,y,z]

def rotateY(X,Y,Z, angle):
    """ Rotates the point around the Y axis by the given angle in degrees. """
    rad = angle * math.pi / 180
    cosa = math.cos(rad)
    sina = math.sin(rad)
    z = Z * cosa - X * sina
    x = Z * sina + X * cosa
    return [x,Y,z]

x = []
y = []
z = []
normals3 = []
normals = []
triaPos = []
areas = []
cred = (1,0,0)
cgreen = (0,1,0)
ccyan = (0,1,1)
startvector = vector(0,0,-1)
colors = []
limitAngle = 40
limitAngleTolerance = 0.1
limitAnglerad = radians(40-limitAngleTolerance)
startErrorArea = 0
errorArea = float("inf")
minimalErrorAngle010 = 0
minimalErrorAngle100 = 0
degStepIncrement = 10
ErrorArray = []

Tk().withdraw()
fileName = askopenfilename(filetypes=(("Txt file", "*.txt"), ("STL File", "*.stl;*.STL")))
fileinfo = open(fileName, mode='rb')

####read the STL file###
if isinstance(fileinfo, str):
    fd = open(fileinfo, mode='rb')
elif isinstance(fileinfo, file):
    if fileinfo.mode != 'rb':
        filename = fileinfo.name
        fileinfo.close()
        fd = open(filename, mode='rb')
    else:
        fd = fileinfo
else:
    fd = fileinfo
```

Ln: 1 Col: 0

```

text = fd.read()
if chr(0) in text: # if binary file

    print("Reading STL Data...")
    fp = open(fileName, 'rb')
    Header = fp.read(80)
    nn = fp.read(4)
    Numtri = unpack('i', nn)[0]
    #print nn
    record_dtype = np.dtype([
        ('normals', np.float32, (3,)),
        ('Vertex1', np.float32, (3,)),
        ('Vertex2', np.float32, (3,)),
        ('Vertex3', np.float32, (3,)),
        ('attrr', '<i2', (1,))
    ])
    data = np.fromfile(fp, dtype = record_dtype, count = Numtri)
    fp.close()

    Normals = data['normals']
    Vertex1= data['Vertex1']
    Vertex2= data['Vertex2']
    Vertex3= data['Vertex3']

    # text = text[84:]
    # L = len(text)
    # N = 2*(L//25) # 25/2 floats per point: 4*3 float32's + 1 uint16
    # normals3 = zeros((N,3), dtype=float32)
    # triaPos = zeros((N,3), dtype=float32)
    # n = i = 0
    # while n < L:
    #     if n % 200000 == 0:
    #         print ("%d" % (100*n/L))+"%",
    #         normals3[i] = fromstring(text[n:n+12], float32)
    #         triaPos[i] = fromstring(text[n+12:n+24], float32)
    #         triaPos[i+1] = fromstring(text[n+24:n+36], float32)
    #         triaPos[i+2] = fromstring(text[n+36:n+48], float32)
    #         if normals3[i].any():
    #             normals3[i] = normals3[i+1] = normals3[i+2] = norm(vector(normals3[i]))
    #         else:
    #             normals3[i] = normals3[i+1] = normals3[i+2] = \
    #                 norm(cross(triaPos[i+1]-triaPos[i], triaPos[i+2]-triaPos[i]))
    #         n += 50
    #         i += 3
    #     for k in xrange(0, len(normals3), 3):
    #         normals.append(normals3[k])
    #
    #     for e in xrange(0, len(triaPos)):
    #         x.append(triaPos[e][0])
    #         y.append(triaPos[e][1])
    #         z.append(triaPos[e][2])
    #     for u in xrange(0, len(x)):
    #         print(x[u])

    for r in xrange(0, len(Vertex1)):
        triaPos.append(Vertex1[r])
        triaPos.append(Vertex2[r])
        triaPos.append(Vertex3[r])
        normals.append(vector(Normals[r][0], Normals[r][1], Normals[r][2]))
        for n in range(3):
            normals3.append(vector(Normals[r][0], Normals[r][1], Normals[r][2]))
            x.append(Vertex1[r][0])
            y.append(Vertex1[r][1])
            z.append(Vertex1[r][2])
            x.append(Vertex2[r][0])
            y.append(Vertex2[r][1])
            z.append(Vertex2[r][2])
            x.append(Vertex3[r][0])
            y.append(Vertex3[r][1])
            z.append(Vertex3[r][2])

    print("Count of Triangles: " + repr(len(Vertex1)))

else:
    fd.seek(0)
    Inhalt = fd.readlines()
    for zeile in Inhalt:
        feld = zeile.split(" ")
        anzahlNix = feld.count("")
        for i in range(0, anzahlNix):
            feld.remove("")

```

Ln: 1 Col: 1

```

        if feld[0]=="facet":
            normals.append(vector(float(feld[2]), float(feld[3]), float(feld[4])))
            for n in range(3):
                normals3.append(vector(float(feld[2]), float(feld[3]), float(feld[4])))
    print("Count of Triangles: " + repr(len(normals)))

###calculate areas of triangle surfaces###

for i in xrange(0,len(triaPos),3):
    #areas.append(area(vector(x[i],y[i],z[i]),vector(x[i+1],y[i+1],z[i+1]),vector(x[i+2],y[i+2],z[i+2])))
    areas.append(area(vector(x[i],y[i],z[i]),vector(x[i+1],y[i+1],z[i+1]),vector(x[i+2],y[i+2],z[i+2])))

###graphics###

for i in xrange(0,len(normals)):
    if degrees(diff_angle(startvector,vector(normals[i]))) < (limitAngle-limitAngleTolerance):

        for n in range(3):
            colors.append(cred)
        else:
            for n in range(3):
                colors.append(cgreen)

scene = display(x=0, y=0, width=500, height=500, center=(0,0,0), background=(0.5,0.5,0.5))
scene.title = "Orientator - Original Orientation"

f = frame()
f.axis = (1,0,0)
pointer = arrow(pos=(-20,0,0), axis=(0,0,20), shaftwidth=10, color = ccyan)

triaPos = array(triaPos)
normals3 = array(normals3)
colors = array(colors)
model = faces( pos = triaPos,normal = normals3,frame = f,color = colors )

#model = faces( pos = triaPos,normal = normals3, color = colors )
#f.rotate(angle = radians(minimalErrorAngle010),axis = (0,1,0),origin = (0,0,0))
#f.rotate(angle = radians(minimalErrorAngle100),axis = (1,0,0),origin = (0,0,0))

###compute trias which need a support###
for n in xrange(0,len(normals)):
    normals[n]=normals[n].norm()

tmpVector010 = startvector
for degStep in xrange(0,360,degStepIncrement):
    if(degStep % 10 == 0):
        print("Progress of orientating the part: " + repr(degStep*100/360) + "%")
        tmpVector010 = startvector.rotate(radians(degStep), (0,1,0))
        #arrow(pos=(-20,0,0), axis=tmpVector010, shaftwidth=5, color = (1,0,1))

    for degStep100 in xrange(0,360,degStepIncrement):
        tmpErrorArea = 0
        tmpVector100 = tmpVector010.rotate(radians(degStep100), (1,0,0))
        #arrow(pos=(-20,0,0), axis=tmpVector100, shaftwidth=5, color = (1,0,1))
        for i in xrange(0,len(normals)):
            #if dot(tmpVector100,normals[i])<limitAnglerad: #
            #print(visual.dot(tmpVector100,normals[i]))
            if diff_angle(tmpVector100,normals[i]) < limitAnglerad:#if diff_angle(tmpVector100,ve
                tmpErrorArea += areas[i]

        if degStep == 0 and degStep100 == 0:
            startErrorArea = tmpErrorArea
            #ErrorArray.append(tmpErrorArea)
            #print("Angle Y-Axis: " + repr(degStep) + " Angle X-Axis: " + repr(degStep100) + " Error: " + repr(tmpErrorArea))

        if tmpErrorArea < errorArea:
            errorArea = tmpErrorArea
            minimalErrorAngle010 = degStep
            minimalErrorAngle100 = degStep100

        tmpErrorArea = 0

print("Progress of orientating the part: 100%")

###printOutput###

```

Ln: 1 Col: 0

10.3.3 Design Extraction Script

```
File Edit Format Run Options Window Help
# coding=utf-8
from __future__ import print_function, division

import vis
import numpy as np
import visual
from visual import *
import math
from numpy.linalg import norm

from struct import unpack
from struct import pack
from Tkinter import Tk
from tkinterFileDialog import askopenfilename
import time

BINARY_HEADER = "80sI"
BINARY_FACET = "12fH"

import wx

def area(a, b, c) :
    return 0.5 * norm(np.cross( b-a, c-a ) )
def __init__(self, x = 0, y = 0, z = 0):
    self.x, self.y, self.z = float(x), float(y), float(z)
def rotateX(X,Y,Z, angle):
    """ Rotates the point around the X axis by the given angle in degrees. """
    rad = angle * math.pi / 180
    cosa = math.cos(rad)
    sina = math.sin(rad)
    y = Y * cosa - Z * sina
    z = Y * sina + Z * cosa
    return [X,y,z]

def rotateY(X,Y,Z, angle):
    """ Rotates the point around the Y axis by the given angle in degrees. """
    rad = angle * math.pi / 180
    cosa = math.cos(rad)
    sina = math.sin(rad)
    z = Z * cosa - X * sina
    x = Z * sina + X * cosa
    return [x,Y,z]

def unit_vector(vector):
    return vector / np.linalg.norm(vector)

def angle_between(v1, v2):
    v1_u = unit_vector(v1)
    v2_u = unit_vector(v2)
    normalvector = unit_vector(vector(0,0,1))
    angle = np.arccos(np.dot(v1_u, v2_u))
    if np.isnan(angle):
        if (v1_u == v2_u).all():
            return 0.0
        else:
            return np.pi
    w = np.cross(v1_u,v2_u)
    if np.dot(w,normalvector)< 0:
        angle = 2 * np.pi - angle
    return angle

x = []
y = []
z = []
rotationOption = 0
Ln: 882 Col: 0
```

```

File Edit Format Run Options Window Help
def rotateX(X,Y,Z, angle):
    rad = angle * math.pi / 180
    cosa = math.cos(rad)
    sina = math.sin(rad)
    y = Y * cosa - Z * sina
    z = Y * sina + Z * cosa
    return [X,y,z]

def rotateY(X,Y,Z, angle):
    """ Rotates the point around the Y axis by the given angle in degrees. """
    rad = angle * math.pi / 180
    cosa = math.cos(rad)
    sina = math.sin(rad)
    z = Z * cosa - X * sina
    x = Z * sina + X * cosa
    return [x,Y,z]

def unit_vector(vector):
    return vector / np.linalg.norm(vector)

def angle_between(v1, v2):
    v1_u = unit_vector(v1)
    v2_u = unit_vector(v2)
    normalvector = unit_vector(vector(0,0,1))
    angle = np.arccos(np.dot(v1_u, v2_u))
    if np.isnan(angle):
        if (v1_u == v2_u).all():
            return 0.0
        else:
            return np.pi
    w = np.cross(v1_u,v2_u)
    if np.dot(w,normalvector)< 0:
        angle = 2 * np.pi - angle
    return angle

x = []
y = []
z = []
rotationOption = 0
normals3 = []
normals = []
triaPos = []
areas = []
cred = (1,0,0)
cgreen = (0,1,0)
ccyan = (0,1,1)
cyellow = (1,1,0)
startvector = vector(0,0,-1)
colors = []
limitAngle = 44
limitAngleTolerance = 0.1
limitAnglerad = radians(limitAngle-limitAngleTolerance)
startErrorArea = 0
errorArea = float("inf")
minimalErrorAngle010 = 0
minimalErrorAngle100 = 0
degStepIncrement = 5
ErrorArray = []
check2Times = 0
sliceHeight = 1
currentSliceDistance = 0
sliceZPlane = None
sliceXPlane = None
sliceYPlane = None
plottedPoints = None
plottedLines = []

scriptString = "Language= \"VBSCRIPT\" \nSub CATMain()\nSet partDocument1 = CATIA.

#####
#
#           ***Open the file and read it***
#
#####

Ln: 882 Col: 0

```

```

file edit format run options window help
percentageOfError = givenAngle / limitAngle
return (1*percentageOfError + (1-percentageOfError),percentageOfError,0)
def openfile(evt):
    global w
    global x
    global y
    global z
    global normals3
    global normals
    global triaPos
    global areas
    cred = (1,0,0)
    cgreen = (0,1,0)
    ccyan = (0,1,1)
    cdarkorange = (1,0.55,0)
    global startvector
    global colors
    global limitAngle
    global limitAngleTolerance
    global limitAnglerad
    global startErrorArea
    global errorArea
    global minimalErrorAngle010
    global minimalErrorAngle100
    global degStepIncrement
    global ErrorArray
    global cyellow
    x = []
    y = []
    z = []
    normals3 = []
    normals = []
    triaPos = []
    areas = []
    colors = []
    minimalErrorAngle010 = 0
    minimalErrorAngle100 = 0
    Tk().withdraw()
    fileName = askopenfilename(filetypes=(("Supported file types", "*.stl;*.STL;*.t
    fileinfo = open(fileName, mode='rb')

    if isinstance(fileinfo, str):
        fd = open(fileinfo, mode='rb')
    elif isinstance(fileinfo, file):
        if fileinfo.mode != 'rb':
            filename = fileinfo.name
            fileinfo.close()
            fd = open(filename, mode='rb')
        else:
            fd = fileinfo
    else:
        raise TypeError, "Specify a file"
    text = fd.read()
    if chr(0) in text: # if binary file

        #print("Reading STL data...")
        tc.AppendText("Reading STL Data...")
        tc.AppendText("\n")
        fp = open(fileName, 'rb')
        Header = fp.read(80)
        nn = fp.read(4)
        Numtri = unpack('i', nn)[0]
        #print nn
        record_dtype = np.dtype([
            ('normals', np.float32, (3,)),
            ('Vertex1', np.float32, (3,)),
            ('Vertex2', np.float32, (3,)),
            ('Vertex3', np.float32, (3,)),
            ('attrr', '<i2', (1,))
        ])
    ]

```

Ln: 882 Col: 0

```

Normals = data['normals']
Vertex1= data['Vertex1']
Vertex2= data['Vertex2']
Vertex3= data['Vertex3']

for r in xrange(0,len(Vertex1)):
    triaPos.append(Vertex1[r])
    triaPos.append(Vertex2[r])
    triaPos.append(Vertex3[r])
    normals.append(vector(Normals[r][0],Normals[r][1],Normals[r][2]))
    for n in range(3):
        normals3.append(vector(Normals[r][0],Normals[r][1],Normals[r][2]))
    x.append(Vertex1[r][0])
    y.append(Vertex1[r][1])
    z.append(Vertex1[r][2])
    x.append(Vertex2[r][0])
    y.append(Vertex2[r][1])
    z.append(Vertex2[r][2])
    x.append(Vertex3[r][0])
    y.append(Vertex3[r][1])
    z.append(Vertex3[r][2])

#print("Count of Triangles: " + repr(len(Vertex1)))
tc.AppendText("Number of Triangles: " + repr(len(Vertex1)))
tc.AppendText("\n")
else:
    fd.seek(0)
    Inhalt = fd.readlines()
    for zeile in Inhalt:
        feld = zeile.split(" ")
        anzahlNix = feld.count("")
        for i in range(0,anzahlNix):
            feld.remove("")
        if feld[0]=="vertex":
            x.append(float(feld[1]))
            y.append(float(feld[2]))
            z.append(float(feld[3]))
            triaPos.append( [ float(feld[1]), float(feld[2]), float(feld[3]) ]

        if feld[0]=="facet":
            normals.append(vector(float(feld[2]), float(feld[3]), float(feld[4])
            for n in range(3):
                normals3.append(vector(float(feld[2]), float(feld[3]), float(fe)
#print("Count of Triangles: " + repr(len(normals)))
tc.AppendText("Number of Triangles: " + repr(len(normals)))
tc.AppendText("\n")

global xmin
global xmax
global ymin
global ymax
global zmin
global zmax

xmin = float("inf")
xmax = -float("inf")
ymin = float("inf")
ymax = -float("inf")
zmin = float("inf")
zmax = -float("inf")

for pos in xrange(0,len(triaPos)):
    x = triaPos[pos][0]
    y = triaPos[pos][1]
    z = triaPos[pos][2]
    if (x < xmin): xmin = x
    if (x > xmax): xmax = x
    if (y < ymin): ymin = y
    if (y > ymax): ymax = y
    if (z < zmin): zmin = z
    if (z > zmax): zmax = z

```

```

File Edit Format Run Options Window Help
    if (z > zmax): zmax = z
print ("xMin: %0.2f "%xmin,"xMax: %0.2f "%xmax)
print ("yMin: %0.2f "%ymin,"yMax: %0.2f "%ymax)
print ("zMin: %0.2f "%zmin,"zMax: %0.2f "%zmax)
print ("Bounding box (x,y,z): (%0.2f,%0.2f,%0.2f)"%( (xmax-xmin), (ymax-ymin), (zr
####graphics####

global scene
global d
d = 20
scene = display(title='Input Geometry',x=0, y=450, width=500, height=500,cente
scene.select()

pointer = arrow(pos=(-20,0,0), axis=(0,0,10), shaftwidth=10, color = ccyan)
label(pos=(-20,0,11), text='Z-Axis')
pointer = arrow(pos=(-20,0,0), axis=(10,0,0), shaftwidth=10, color = ccyan)
label(pos=(-9,0,0), text='X-Axis')
pointer = arrow(pos=(-20,0,0), axis=(0,10,0), shaftwidth=10, color = ccyan)
label(pos=(-20,11,0), text='Y-Axis')

#for n in xrange(0,len(normals3),3):
#    arrow(pos=((x[n]+x[n+1]+x[n+2])/3, (y[n+1]+y[n+1]+y[n+1])/3, (z[n+2]+z[n+2]+z[n-
global f
f = frame()
f.axis = (1,0,0)

triaPos = array(triaPos)
normals3 = array(normals3)

#calculateCrossSection()
global model
scene.select()
model = faces( pos = triaPos,normal = normals3, display = scene,frame = f )
global currentSliceDistance
currentSliceDistance = 0
global sliceZPlane
sliceZPlane = faces(pos=[vector(xmin*1.1,ymin*1.1,currentSliceDistance),vector
sliceZPlane.make_twosided()

scene.autocenter = True

####draw sectionCut####
global scene2
scene2 = display(title='Section Geometry',x=540, y=450, width=500, height=500,

scene2.select()
scene2.userspin = True#edit#
scene2.autocenter = True
calculateSectioninZAtHeight("z",0)

return (x,y,z,normals,triaPos,areas)

#####
#
#             ***Calculate crosssections***             #
#
#####
def xrange(start, stop, step):
    while start < stop:
        yield start
        start += step

def double_max( a, b): return a if a >= b else b
def double_min( a, b): return a if a <= b else b
def calculateSectioninZAtHeight(direction,height):

```

Ln: 882 Col: 0

```

File Edit Format Run Options Window Help
sliceVector = np.array([1,0,0])
layerVector = np.array([height,0,0])
scene2.forward=-vector(1,0,0)
elif direction == "y":
    sliceVector = np.array([0,1,0])
    layerVector = np.array([0,height,0])
    scene2.forward=-vector(0,1,0)
elif direction == "z":
    sliceVector = np.array([0,0,1])
    layerVector = np.array([0,0,height])
    scene2.forward=-vector(0,0,1)
global calculatedLinesDict
calculatedLinesDict = {}
tmpLines = []
##### *****Calculate intersection points and create lines****
startTime = time.time()
layer = height
if layer not in calculatedLinesDict:
    calculatedLinesDict[layer] = list()
for pos in range(0,len(triaPos),3):

    if direction == "x":
        v0z = triaPos[pos][0]
        v1z = triaPos[pos+1][0]
        v2z = triaPos[pos+2][0]
        V0 = np.array(triaPos[pos])
        V1 = np.array(triaPos[pos+1])
        V2 = np.array(triaPos[pos+2])
        minTria = double_min(triaPos[pos][0],double_min(triaPos[pos+1][0],tria
        maxTria = double_max(triaPos[pos][0],double_max(triaPos[pos+1][0],tria
    elif direction == "y":
        v0z = triaPos[pos][1]
        v1z = triaPos[pos+1][1]
        v2z = triaPos[pos+2][1]
        V0 = np.array(triaPos[pos])
        V1 = np.array(triaPos[pos+1])
        V2 = np.array(triaPos[pos+2])
        minTria = double_min(triaPos[pos][1],double_min(triaPos[pos+1][1],tria
        maxTria = double_max(triaPos[pos][1],double_max(triaPos[pos+1][1],tria
    elif direction == "z":
        v0z = triaPos[pos][2]
        v1z = triaPos[pos+1][2]
        v2z = triaPos[pos+2][2]
        V0 = np.array(triaPos[pos])
        V1 = np.array(triaPos[pos+1])
        V2 = np.array(triaPos[pos+2])
        minTria = double_min(triaPos[pos][2],double_min(triaPos[pos+1][2],tria
        maxTria = double_max(triaPos[pos][2],double_max(triaPos[pos+1][2],tria
    if minTria <= layer <= maxTria:
        intersectionPoint1 = None
        intersectionPoint2 = None
        intersectionPoint3 = None

        if (v0z < layer and (v1z>layer and v2z>layer)) or (v0z > layer and (v1
            #store intersection points and z as -1
            intersectionPoint1 = V0 + ((np.dot(sliceVector, (layerVector-V0)))/
            intersectionPoint2 = V0+ ((np.dot(sliceVector, (layerVector-V0)))/
            tmpzValue = -1000
        elif (v1z < layer and (v0z>layer and v2z>layer)) or (v1z > layer and (
            #store intersection points and z as -1
            intersectionPoint1 = V1+ ((np.dot(sliceVector, (layerVector-V1)))/
            intersectionPoint2 = V1+ ((np.dot(sliceVector, (layerVector-V1)))/
            tmpzValue = -1000
        elif (v2z < layer and (v0z>layer and v1z>layer)) or (v2z > layer and (
            #store intersection points and z as -1
            intersectionPoint1 = V2+ ((np.dot(sliceVector, (layerVector-V2)))/
            intersectionPoint2 = V2+ ((np.dot(sliceVector, (layerVector-V2)))/
            tmpzValue = -1000
        elif v0z == layer and v1z == layer and (v2z < layer or v2z > layer): #
            intersectionPoint1 = V0
            intersectionPoint2 = V1
            tmpzValue = v2z

```

Ln: 882 Col: 0

```

File Edit Format Run Options Window Help
tmpzValue v2z
elif v1z == layer and v2z == layer and (v0z < layer or v0z > layer): #c
    intersectionPoint1 = V1
    intersectionPoint2 = V2
    tmpzValue = v0z
elif v0z == layer and ((v1z < layer and v2z > layer) or (v1z > layer ar
    intersectionPoint1 = V0
    intersectionPoint2 = V1+ ((np.dot(sliceVector, (layerVector-V1)))/(r
    tmpzValue = -1000
elif v1z == layer and ((v0z < layer and v2z > layer) or (v0z > layer ar
    intersectionPoint1 = V1
    intersectionPoint2 = V0+ ((np.dot(sliceVector, (layerVector-V0)))/(r
    tmpzValue = -1000
elif v2z == layer and ((v0z < layer and v1z > layer) or (v0z > layer ar
    intersectionPoint1 = V2
    intersectionPoint2 = V0+ ((np.dot(sliceVector, (layerVector-V0)))/(r
    tmpzValue = -1000
elif v0z == layer and v1z == layer and v2z == layer:
    intersectionPoint1 = V0
    intersectionPoint2 = V1
    intersectionPoint3 = V2
    tmpzValue = layer

if intersectionPoint1 is not None:

    if tmpzValue == -1000:
        calculatedLinesDict[layer].append( ((intersectionPoint1[0],inte
    elif tmpzValue==layer:
        tmpLines.append(((intersectionPoint1[0],intersectionPoint1[1],i

    else:
        tmpLines.append(((intersectionPoint1[0],intersectionPoint1[1],i

    if intersectionPoint3 is not None:

        tmpLines.append( ((intersectionPoint1[0],intersectionPoint1[1],
        tmpLines.append( ((intersectionPoint2[0],intersectionPoint2[1],

print("Length calculatedLines: "+repr(len(calculatedLinesDict[layer]))+" Lengtl
#####deleting double lines#####
for i in xrange(len(tmpLines)):
    for j in xrange(len(tmpLines)):
        if i is not j:
            if (tmpLines[i][0] == tmpLines[j][0] and tmpLines[i][1] == tmpLines
                if (tmpLines[i][2]==-2000 and tmpLines[j][2] != -2000)or(tmpLir
                    calculatedLinesDict[layer].append(((tmpLines[i][0][0],tmpLi
                elif (tmpLines[i][2]<layer and tmpLines[j][2] > layer)or(tmpLir
                    calculatedLinesDict[layer].append(((tmpLines[i][0][0],tmpLi
print("Time for cross section calculation: "+repr(time.time()-startTime))
'''
#####Line grouping#####

tmpContourlines = calculatedLinesDict[layer]
#tmpContourlines.sort()
contourDict = {}
contourCounter = 0

if len(tmpContourlines)>0:
    while len(tmpContourlines)>0:
        startedge = tmpContourlines[0]
        endcontour = False
        contourDict[contourCounter] = list()
        contourDict[contourCounter].append(startedge)

        tmpContourlines.remove(startedge)

        breakCounter = len(tmpContourlines)
        counteri = 0
        currentedge = startedge
        while len(tmpContourlines)>0:
            if tmpContourlines[counteri][0] == currentedge[1]:

```

Ln: 882 Col: 0

```

File Edit Format Run Options Window Help

    currentedge = tmpContourlines[counteri]

    if startedge[0]==tmpContourlines[counteri][1]:
        contourCounter = contourCounter + 1
        print("contour closed")
        endcontour = True
        tmpContourlines.remove(tmpContourlines[counteri])

    if endcontour or breakCounter == 0:
        break
    if counteri >= len(tmpContourlines)-1:
        counteri = 0
    else:
        counteri = counteri + 1
print("Count of contours: " +repr(len(contourDict)))

...
startTime2 = time.time()

global ccyan
ft = frame()
if layer in calculatedLinesDict:
    linestoplot = []
    for k in xrange(0,len(calculatedLinesDict[layer])):
        linestoplot.append(calculatedLinesDict[layer][k])
    global plottedLines
    if len(plottedLines) > 0:
        for line in plottedLines:
            line.visible = False
            del line
        for i in xrange(0,len(linestoplot)):
            plottedLines.append(curve(pos =[linestoplot[i][0],linestoplot[i][1]], :
scene2.visible = True
print("Time for deleting and creating points: "+repr(time.time()-startTime2))
def calculateCrossSection():

    startTime = time.time()
    global triaPos
    minZvalue = 0
    maxZvalue = 0
    global sliceHeight

    sliceVector = np.array([0,0,1])
    global xmin
    global xmax
    global ymin
    global ymax
    global zmin
    global zmax

    global intersectionPointsDict
    intersectionPointsDict = {}
    calculatedLinesDict = {}
    nlayers = 4+abs(int((zmax-zmin)/sliceHeight))
    print("Number of slices: " + repr(nlayers))

    #####      *****Calculate intersection points and create lines****

    for pos in range(0,len(triaPos),3):

        zminTria = double_min(triaPos[pos][2],double_min(triaPos[pos+1][2],triaPos[
zmaxTria = double_max(triaPos[pos][2],double_max(triaPos[pos+1][2],triaPos[
        triaSliceStart = zmin + int((zminTria-zmin)/sliceHeight) * sliceHeight
        v0z = triaPos[pos][2]
        v1z = triaPos[pos+1][2]
        v2z = triaPos[pos+2][2]
        V0 = np.array(triaPos[pos])
        V1 = np.array(triaPos[pos+1])
        V2 = np.array(triaPos[pos+2])

```

Ln: 882 Col: 0

```

File Edit Format Run Options Window Help
while layer <= zmaxifia:

    intersectionPoint1 = None
    intersectionPoint2 = None
    intersectionPoint3 = None
    layerVector = np.array([0,0,layer])
    if (v0z < layer and (v1z>layer and v2z>layer)) or (v0z > layer and (v1z
        #store intersection points and z as -1
        intersectionPoint1 = V0 + ((np.dot(sliceVector, (layerVector-V0)))/
        intersectionPoint2 = V0+ ((np.dot(sliceVector, (layerVector-V0)))/
        tmpzValue = -1
    elif (v1z < layer and (v0z>layer and v2z>layer)) or (v1z > layer and (v
        #store intersection points and z as -1
        intersectionPoint1 = V1+ ((np.dot(sliceVector, (layerVector-V1)))/
        intersectionPoint2 = V1+ ((np.dot(sliceVector, (layerVector-V1)))/
        tmpzValue = -1
    elif (v2z < layer and (v0z>layer and v1z>layer)) or (v2z > layer and (v
        #store intersection points and z as -1
        intersectionPoint1 = V2+ ((np.dot(sliceVector, (layerVector-V2)))/
        intersectionPoint2 = V2+ ((np.dot(sliceVector, (layerVector-V2)))/
        tmpzValue = -1
    elif v0z == layer and v1z == layer and (v2z < layer or v2z > layer): #c
        intersectionPoint1 = V0
        intersectionPoint2 = V1
        tmpzValue = v2z
    elif v0z == layer and v2z == layer and (v1z < layer or v1z > layer): #c
        intersectionPoint1 = V0
        intersectionPoint2 = V2
        tmpzValue = v1z
    elif v1z == layer and v2z == layer and (v0z < layer or v0z > layer): #c
        intersectionPoint1 = V1
        intersectionPoint2 = V2
        tmpzValue = v0z
    elif v0z == layer and ((v1z < layer and v2z > layer) or (v1z > layer ar
        intersectionPoint1 = V0
        intersectionPoint2 = V1+ ((np.dot(sliceVector, (layerVector-V1)))/r
        tmpzValue = -1
    elif v1z == layer and ((v0z < layer and v2z > layer) or (v0z > layer ar
        intersectionPoint1 = V1
        intersectionPoint2 = V0+ ((np.dot(sliceVector, (layerVector-V0)))/r
        tmpzValue = -1
    elif v2z == layer and ((v0z < layer and v1z > layer) or (v0z > layer ar
        intersectionPoint1 = V2
        intersectionPoint2 = V0+ ((np.dot(sliceVector, (layerVector-V0)))/r
        tmpzValue = -1
    elif v0z == layer and v1z == layer and v2z == layer:
        intersectionPoint1 = V0
        intersectionPoint2 = V1
        intersectionPoint3 = V2
        tmpzValue = layer

    if intersectionPoint1 is not None:
        '''
        if layer not in calculatedLinesDict:
            calculatedLinesDict[layer] = list()
            calculatedLinesDict[layer].append( ((intersectionPoint1[0],interse
            '''
        if layer not in intersectionPointsDict:
            intersectionPointsDict[layer] = list()
            intersectionPointsDict[layer].append((intersectionPoint1[0],interse
            intersectionPointsDict[layer].append((intersectionPoint2[0],interse
            if intersectionPoint3 is not None:
                '''
                if layer not in calculatedLinesDict:
                    calculatedLinesDict[layer] = list()
                    calculatedLinesDict[layer].append( ((intersectionPoint3[0],inte
                    calculatedLinesDict[layer].append( ((intersectionPoint3[0],inte
                    '''
                if layer not in intersectionPointsDict:
                    intersectionPointsDict[layer] = list()
                    intersectionPointsDict[layer].append((intersectionPoint3[0],int
            layer += sliceHeight.
Ln: 882 Col: 0

```

```

File Edit Format Run Options Window Help
#####
#                                     #
#                               ***Export BinarySTL***                       #
#                                     #
#####

class Binary_STL_Writer:
    """ Export 3D objects build of 3 or 4 vertices as binary STL file.
    """
    def __init__(self, stream):
        self.counter = 0
        self.fp = stream
        self._write_header()

    def close(self):
        self._write_header()

    def _write_header(self):
        self.fp.seek(0)
        self.fp.write(pack(BINARY_HEADER, b'Python Binary STL Writer', self.counter))

    def _write(self, normal, triaPos1, triaPos2, triaPos3, color):
        self.counter += 1

        data = [
            np.float(normal[0]), np.float(normal[1]), np.float(normal[2]),
            np.float(triaPos1[0]), np.float(triaPos1[1]), np.float(triaPos1[2]),
            np.float(triaPos2[0]), np.float(triaPos2[1]), np.float(triaPos2[2]),
            np.float(triaPos3[0]), np.float(triaPos3[1]), np.float(triaPos3[2]),
            color
        ]
        self.fp.write(pack(BINARY_FACET, *data))

#####
#                                     #
#                               ***GUI Functions***                           #
#                                     #
#####

def scene1PlanarViewLeft (evt):
    global scene
    scene.forward = (1,0,0)
    scene.up = (0,0,1)
def scene1PlanarViewTop (evt):
    global scene
    scene.forward = (0,0,-1)
    scene.up = (0,0,1)
def scene1PlanarViewFront (evt):
    global scene
    scene.forward = (0,1,0)
    scene.up = (0,0,1)
def scene1PlanarViewRight (evt):
    global scene
    scene.forward = (-1,0,0)
    scene.up = (0,0,1)
def scene1PlanarViewBottom (evt):
    global scene
    scene.forward = (0,0,1)
    scene.up = (0,0,1)
def scene1PlanarViewBack (evt):
    global scene
    scene.forward = (0,-1,0)
    scene.up = (0,0,1)

def leftSliderButtonEvt (evt):

    global currentSliceDistance

Ln: 882 Col: 0

```

```

File Edit Format Run Options Window Help
global combol
if combol.GetValue() == "Slice x-axis":
    currentdirection = "x"
elif combol.GetValue() == "Slice y-axis":
    currentdirection = "y"
elif combol.GetValue() == "Slice z-axis":
    currentdirection = "z"

calculateSectioninZAtHeight(currentdirection,currentSliceDistance)
updateSlicePlane(currentdirection)
def rightSliderButtonEvt (evt):
    global currentSliceDistance
    global sliceHeight
    global currentSliceheightTextCtrl
    currentSliceDistance = currentSliceDistance + sliceHeight
    currentSliceheightTextCtrl.SetValue(repr(currentSliceDistance))
    global combol
    if combol.GetValue() == "Slice x-axis":
        currentdirection = "x"
    elif combol.GetValue() == "Slice y-axis":
        currentdirection = "y"
    elif combol.GetValue() == "Slice z-axis":
        currentdirection = "z"

calculateSectioninZAtHeight(currentdirection,currentSliceDistance)
updateSlicePlane(currentdirection)
def writeBinarySTL(evt):
    global normalsRot3
    global triaPosRot
    global colorsRot
    with open('OrientatorOutput.stl', 'wb') as fp:
        writer = Binary_STL_Writer(fp)
        for i in xrange(0,len(triaPos),3):
            color = 0
            if colorsRot[i] == (0,1,0):
                color = 0
            else:
                color = 1
            writer.write(normalsRot3[i],triaPosRot[i],triaPosRot[i+1],triaPosRot[i+2],color)
        writer.close()
    global saveSTLFileBtn
    saveSTLFileBtn.Disable()
def currentSliceheightTextCtrlSetText (evt):
    global currentSliceDistance

    global currentSliceheightTextCtrl
    currentSliceDistance = float(currentSliceheightTextCtrl.GetValue())
    currentSliceheightTextCtrl.SetValue(repr(currentSliceDistance))
    global combol
    if combol.GetValue() == "Slice x-axis":
        currentdirection = "x"
    elif combol.GetValue() == "Slice y-axis":
        currentdirection = "y"
    elif combol.GetValue() == "Slice z-axis":
        currentdirection = "z"

calculateSectioninZAtHeight(currentdirection,currentSliceDistance)
updateSlicePlane(currentdirection)
def updateSlicePlane(direction):
    global xmin
    global xmax
    global ymin
    global ymax
    global zmin
    global zmax
    global sliceXPlane
    global sliceYPlane
    global sliceZPlane
    global scene
    global combol
    global cyellow
    global currentSliceheightTextCtrl

```

Ln: 882 Col: 0

```

File Edit Format Run Options Window Help
global currentSliceheightTextCtrl
currentSliceDistance = float(currentSliceheightTextCtrl.GetValue())
if 'sliceXPlane' in globals():
    if sliceXPlane is not None:
        sliceXPlane.visible = False
        del sliceXPlane
if 'sliceYPlane' in globals():
    if sliceYPlane is not None:
        sliceYPlane.visible = False
        del sliceYPlane
if 'sliceZPlane' in globals():
    if sliceZPlane is not None:
        sliceZPlane.visible = False
        del sliceZPlane

if direction == "x":
    sliceXPlane = faces(pos=[vector(currentSliceDistance, ymin*1.1, zmin*1.1), vec
    sliceXPlane.make_twosided()
    sliceXPlane.visible = True
elif direction == "y":
    sliceYPlane = faces(pos=[vector(xmin*1.1, currentSliceDistance, zmin*1.1), vec
    sliceYPlane.make_twosided()
    sliceYPlane.visible = True
elif direction == "z":
    sliceZPlane = faces(pos=[vector(xmin*1.1, ymin*1.1, currentSliceDistance), vec
    sliceZPlane.make_twosided()
    sliceZPlane.visible = True

def addToSelection(evt):
    print("Add to selection")
    global currentSliceDistance
    global calculatedLinesDict
    global scriptString
    scriptString = scriptString + "\nSet body1=bodies2.Add()\nbody1.Name=\"zSlice:
    if combol.GetValue() == "Slice x-axis":
        scriptString = scriptString + "\nSet hybridShapePlaneExplicit1 = part1.Ori
    elif combol.GetValue() == "Slice y-axis":
        scriptString = scriptString + "\nSet hybridShapePlaneExplicit1 = part1.Ori
    elif combol.GetValue() == "Slice z-axis":
        scriptString = scriptString + "\nSet hybridShapePlaneExplicit1 = part1.Ori

    scriptString = scriptString + "\nSet PlaneXYref = part1.CreateReferenceFromObj
    scriptString = scriptString + "\nSet planeZ = ShFactory.AddNewPlaneOffset(Plane
    scriptString = scriptString + "\nbody1.AppendHybridShape planeZ\n"
    for line in calculatedLinesDict[currentSliceDistance]:

        scriptString = scriptString + "\nSet point0=ShFactory.AddNewPointCoord({},
        #scriptString = scriptString + "\npart1.Update()\n"
        scriptString = scriptString + "\nSet point1=ShFactory.AddNewPointCoord({},
        #scriptString = scriptString + "\npart1.Update()\n"
        if not np.allclose(line[0], line[1], 0.005):
            scriptString = scriptString + "\nSet reference1 = part1.CreateReferenc
            scriptString = scriptString + "\nSet reference2 = part1.CreateReferenc
            scriptString = scriptString + "\nSet line1 = ShFactory.AddNewLinePtPt(
            scriptString = scriptString + "\nbody1.AppendHybridShape line1\n"
            #scriptString = scriptString + "\npart1.Update()\n"

def saveSelectedContoursAsCatiaScript(evt):
    print("save")
    global scriptString
    scriptString = scriptString + "\npart1.Update()\n"
    scriptString = scriptString + "\nEnd Sub\n"
    text_file = open("ContourMacro.catvbs", "w")
    text_file.write(scriptString)
    text_file.close()
#####
#
Ln: 882 Col: 0

```

```

File Edit Format Run Options Window Help
#app = wx.App(redirect=False)

#app.MainLoop()

w = window(width=1060, height=450, menus=True, title='Contour Extraction')

p = w.panel
p.Hide()
p.Show()

openFileBtn = wx.Button(p, label='Open file', pos=(20,20))
openFileBtn.Bind(wx.EVT_BUTTON, openfile)

global tc
tc = wx.TextCtrl(p, pos=(20,70),size=(1000,180), style=wx.TE_MULTILINE)
tc.SetInsertionPoint(len(tc.GetValue())+1) # position cursor at end of text
tc.AppendText("Please select a STL file to extract cotours")
tc.AppendText("\n")

leftView = wx.Button(p, label='Left', pos=(20,280))
leftView.Bind(wx.EVT_BUTTON, scene1PlanarViewLeft)

frontView = wx.Button(p, label='Front', pos=(140,280))
frontView.Bind(wx.EVT_BUTTON, scene1PlanarViewFront)

topView = wx.Button(p, label='Top', pos=(260,280))
topView.Bind(wx.EVT_BUTTON, scene1PlanarViewTop)

rightView = wx.Button(p, label='Right', pos=(20,320))
rightView.Bind(wx.EVT_BUTTON, scene1PlanarViewRight)

backView = wx.Button(p, label='Back', pos=(140,320))
backView.Bind(wx.EVT_BUTTON, scene1PlanarViewBack)
|
bottomView = wx.Button(p, label='Bottom', pos=(260,320))
bottomView.Bind(wx.EVT_BUTTON, scene1PlanarViewBottom)

leftSliderButton = wx.Button(p, label='<', pos=(20,360))
leftSliderButton.Bind(wx.EVT_BUTTON, leftSliderButtonEvt)

rightSliderButton = wx.Button(p, label='>', pos=(260,360))
rightSliderButton.Bind(wx.EVT_BUTTON, rightSliderButtonEvt)

global currentSliceheightTextCtrl
currentSliceheightTextCtrl = wx.TextCtrl(p, pos=(140, 360),value = repr(0),size=(80,20))
currentSliceheightTextCtrl.Bind(wx.EVT_TEXT_ENTER, currentSliceheightTextCtrlSetText)

addToSelectionBtn = wx.Button(p, label='Add contour to selection', pos=(400,320))
addToSelectionBtn.Bind(wx.EVT_BUTTON, addToSelection)

saveSelectedContoursAsCatiaScriptBtn = wx.Button(p, label='Save selected contours as Catia script', pos=(400,360))
saveSelectedContoursAsCatiaScriptBtn.Bind(wx.EVT_BUTTON, saveSelectedContoursAsCatiaScript)

combo1 = wx.ComboBox(p, -1, value="Slice z-axis", pos=(400, 360), size=(120, 25), c

'''
noLog = wx.LogNull()
png = wx.Image('K:\Projects\R21\NGrafen_Data\Orientator\AGI Blue.png', wx.BITMAP_TYPE_PNG)
#wx.StaticBitmap(p, -1, png, (900, 10), (png.GetWidth(), png.GetHeight()))

bmp_withcolourmask = png
mask = wx.Mask(bmp_withcolourmask, wx.WHITE)
bmp_withcolourmask.SetMask(mask)

wx.StaticBitmap(p, -1, bmp_withcolourmask, (770, 20), (bmp_withcolourmask.GetWidth(), bmp_withcolourmask.GetHeight()))
Ln: 882 Col: 0

```

10.4 Appendix D – Calculations

10.4.1 Aircraft Small Part Numbers

Aircraft Type	Part Numbers
A330 all variants	1830
A320 all variants, all families	2187
A350 all variants	1382
A380	2446
A400M	1451
VIP	Similar to base aircraft

10.4.2 Forces Perturbation Calculations

Forces Splitter											
Angular Variation											
theta Delta	15	Req Delt		Component Forces (N)			Mag	Mag Check	SM	T1 (XZ)	T2 (XY)
		1	2	A (X)	B (Y)	C (Z)					
		0	0	-4032.000	0.000	3032.000	5044.804	5044.804	4032.000	36.943	0.000
		1	0	3109.874	0.000	3972.245	5044.804	5044.804	3109.874	51.943	0.000
		2	0.5	3570.937	470.123	3532.342	5044.804	5044.804	3601.750	44.443	7.500
		3	0	3894.613	1043.558	3032.000	5044.804	5044.804	4032.000	36.943	15.000
		4	-0.5	4355.676	573.436	2479.779	5044.804	5044.804	4393.261	29.443	7.500
		5	-1	4679.352	0.000	1885.129	5044.804	5044.804	4679.352	21.943	0.000
		6	-0.5	4355.676	573.436	2479.779	5044.804	5044.804	4393.261	29.443	-7.500
		7	0	3894.613	1043.558	3032.000	5044.804	5044.804	4032.000	36.943	-15.000
		8	0.5	3570.937	470.123	3532.342	5044.804	5044.804	3601.750	44.443	-7.500

Force Positions				
8	1	2		
7	0	3		
6	5	4		

0	X	Y	Z	MAG
1	V	K	V	K
2	V	V	V	K
3	V	V	K	K
4	V	V	V	K
5	V	K	V	K
6	V	V	V	K
7	V	V	K	K
8	V	V	V	K

Order or Calculation		Vector in 3D = A ² =I ² +J ² +K ²			
1	T1Delta				
2	C				
3	SM	Sin (theta)	Opp		
4	T2Delta		Hyp		
5	A	Cos (theta)	Adj	i	j
6	B		Hyp		k
			Opp		100
			Adj		
		Hyp=Mag			A ² -J ² =I ² +K ²)

10.4.3 Additional Material Data from Concept Laser

Concept Laser Tensile Testing	0	LL	620	695	6.5			
	0	UL						
	0	LR						
	0	UR						
	30	LL	895	991	16.7			
	30	UL						
	30	LR						
	30	UR					Mean	713.6
	45	LL	683	744	7.2		STDev	159.7178763
	45	UL					Upper	873.3178763
	45	LR					Lower	553.8821237
	45	UR					Outlier	234.4463712
	60	LL	515	568	5.6			
	60	UL						
	60	LR					Mean	785
	60	UR					STDev	172.8221629
	90	LL	855	927	16.4		Upper	957.8221629
	90	UL					Lower	612.1778371
90	LR					Outlier=	266.5335112	
90	UR							